Copyright is owned by the Author of the thesis. Permission is given for a copy to be downloaded by an individual for the purpose of research and private study only. The thesis may not be reproduced elsewhere without the permission of the Author.

Modelling sulphate dynamics in soils –

The effect of ion-pair adsorption

Rogerio Cichota

2007

MODELLING SULPHATE DYNAMICS IN SOILS –

THE EFFECT OF ION-PAIR ADSORPTION

A thesis presented in partial fulfilment of the
requirements for the degree of
Doctor of Philosophy in Soil Science
at Massey University

Rogerio Cichota

2007

ABSTRACT

Sulphur is an important nutrient to plants, and reports of its deficiency have been increasing worldwide. Sulphur starvation causes losses in both yield and quality, and it reduces nitrogen use efficiency of plants. As the timing for fertilisation can be decisive for avoiding deleterious effects, improvements in the description of the sulphur balance in fields are a valuable contribution for assisting fertiliser management. Sulphate is the most important inorganic form of sulphur in soils. Being the mobile form, sulphate is readily available for plants, and also prone to be leached. Therefore the description of the movement of sulphate is the key component of the sulphur balance.

Leaching of sulphate from the soil can be significantly delayed by its adsorption onto the soil particles. Soil type and pH are the main factors defining the sulphate adsorption capacity; although the presence of other ions in the soil solution can have a considerable effect. It has been reported that in some soils, typically volcanic and tropical soils with variable-charge characteristics, the co-presence of sulphate and calcium can substantially enhance their retention via ion-pair adsorption (IPA).

To determine the influence of cations on the movement of sulphate, series of batch and miscible displacement experiments were conducted using two New Zealand soils, of contrasting ion adsorption capacities: the Taupo sandy and Egmont loam soils. These experiments demonstrated the occurrence of cooperative adsorption of sulphate and calcium in the Egmont soil, but not in the Taupo soil. Batch experiments were conducted to examine the IPA adsorption process in the Egmont soil in more detail.

Based on the analyses of the results from these two series of experiments, plus the review of published data, three different mathematical

approaches for evaluating the amount of solute adsorbed as ion-pairs are proposed. A computer program was built for solving an adsorption model using these three approaches, and was used to compare the model's predictions and the observed adsorption data. An extension of this program, coupling the adsorption model with a solute transport description, was used to simulate the movement of sulphate and calcium. Comparisons between the data from the miscible displacements and the results from this model are used to demonstrate the applicability of the proposed IPA description for modelling the transport of these ions in the soil.

Finally, results from a pot trial with Egmont soil are used to examine the relevance of IPA for the movement of sulphate under non-equilibrium conditions, and with active plant growth. Although the results from this experiment regarding IPA were statistically non-significant, some insights could be obtained and are discussed. More studies involving IPA under non-equilibrium experiments are needed for a better understanding of the relevance of IPA in field conditions.

ACKNOWLEDGEMENTS

I would like to express my profound gratitude to my supervisors, Iris Vogeler, Nanthi Bolan, Brent Clothier, and David Scotter, for their advice, understanding, and encouragement.

Many thanks to Quirijn de Jong van Lier, for his advice and help when preparing my PhD application, as well as for his friendship.

Special thanks also to the scientists and technicians of the Sustainable Land Use group of HortResearch and of the Department of Soil Science of Massey University for their kindness, and help given when I needed.

I would like to also mention my gratefulness for all the scientists and students that, visiting HortResearch, have in any way helped in my work. In special, I would like to mention Thomas Rölke, Marijn van der Velde, François Hupet, and Marta Marmiroli, for their friendship.

I thank the Brazilian government that via CAPES (Federal Agency for Post-graduate Education) have made this work possible with the financial support (Contract no. 1516 027).

Finally I want to express my gratitude to my parents, Leonides and Terezinha, and my brother, Roberto. Their love and support, even from such a distance, have been invaluable.

Table of Contents

Abstract i

Acknowledgements iii

Table of Contents v

List of Tables xi

List of Figures xiii

List of Symbols and Abbreviations xxiii

Chapter 1 1

1. General introduction 1

1.1. Introduction 1

1.2. Outline of the thesis 3

1.3. Objectives of the study 6

Chapter 2 7

2. Modelling the movement of solutes in the soil 7

2.1. Introduction 7

2.2. Water movement 10

2.3. Solute movement – the convective-dispersive approach 13

2.4. Ion adsorption 20

2.5. Adsorption isotherms 24

2.6. Model fitting and parameterisation 29

Chapter 3 33

3. Sulphur in crop production 33

3.1. Introduction 33

3.2. Importance of sulphur for plants 35

3.3. Diagnosis of sulphur status 38
3.4. Sulphur in the soil 42

CHAPTER 4 47

4. Interactions between sulphate and cations in allophanic soils during miscible displacement experiments 47

4.1. Introduction 47
4.2. Cation influence on sulphate leaching in allophanic soils 49
4.2.1. Abstract 49
4.2.2. Introduction 50
4.2.3. Material and methods 52
4.2.3.1. *Soil* 52
4.2.3.2. *Miscible displacement experiments* 53
4.2.3.3. *Soil and leachate analyses* 55
4.2.4. Results and discussion 56
4.2.5. Conclusions 62

CHAPTER 5 65

5. An adsorption model with IPA - Description and parameterisation 65

5.1. Introduction 65
5.2. Describing solute equilibrium in the soil 66
5.2.1. Approach 1: Particle governed approach (PGA): 71
5.2.2. Approach 2: "Linear" solution governed approach (SGA1): 71
5.2.3. Approach 3: "Radical" solution governed approach (SGA2): 73
5.3. Adsorption data set 74
5.3.1. Methods 74
5.3.2. Results 77
5.4. Parameterisation of the adsorption model 80
5.4.1. Procedure 1 - Data Analysis 80
5.4.1.1. *Summary of the published data sets* 81
5.4.1.2. *Estimating the IPA factor – Literature data* 82
5.4.1.3. *Estimating the IPA factor – Present data set* 90

5.4.2. Procedure 2 – Least Squares 94
5.4.3. Procedure 3 – Inverse Modelling 98
5.4.3.1. Introduction 98
5.4.3.2. Maximum-likelihood method for inverse modelling 99
5.4.3.3. Objective function for the adsorption model 102
5.4.3.4. Estimation of the data variance 104
5.4.3.5. Fitting the adsorption model 107
5.5. Summary and conclusions 114
CHAPTER 6 117
6. Ion-pair adsorption and its effect on the movement of sulphate and calcium in an allophanic soil 117
6.1. Introduction 117
6.2. Simultaneous adsorption of calcium and sulphate and its effect on their movement 118
6.2.1. Abstract 118
6.2.2. Introduction 119
6.2.3. Material and methods 122
6.2.3.1. Soil 122
6.2.3.2. Batch experiments 122
6.2.3.3. Miscible displacement experiments 124
6.2.3.4. Partition of the soil solute concentrations considering IPA 125
6.2.3.5. Solute movement in the soil: 127
6.2.4. Results and discussion 128
6.2.4.1. Batch experiment 128
6.2.4.2. Miscible displacement experiments 132
6.2.5. Conclusions 136
6.3. BTC description using the SGA2 approach 137
CHAPTER 7 141
7. Sulphate and calcium movement in an allophanic soil – The relevance of ion-pair adsorption in the soil-plant system 141
7.1. Introduction 141

7.2. Materials and methods 143
7.2.1. Soil 143
7.2.2. Plant experiments 143
7.2.3. Plant and soil analyses 145
7.3. Results and discussion 145
7.3.1. Plant growth and nutrient uptake 145
7.3.2. Leachate 149
7.3.3. Soil ion concentration 151
7.4. Summary and conclusions 154

CHAPTER 8 157

8. Final summary and conclusions 157

REFERENCES 163

List of Symbols and Abbreviations of the Appendices 191

APPENDIX A 195

A. The miscible displacement experiments 195
A.1. Preliminary experiments 195
A.2. Main experiments 198

APPENDIX B 205

B. Solving the adsorption model with IPA 205
B.1. Presentation of the computer routines 205
B.2. Routine for solving the adsorption model 208
B.2.1. Partition of $Q_{S,i}$ without IPA – NR01 210
B.2.2. Partition of $Q_{S,i}$ with IPA – NR02 211
B.2.2.1. *Solution with PGA* 213
B.2.2.2. *Solution with SGA1* 214
B.2.2.3. *Solution with SGA2* 214
B.3. Routine for evaluating the objective function 215
B.4. Routines for the variation of the adsorption model parameters 216
B.4.1. Replication loop 217

B.4.2. Optimisation loop 219

B.4.2.1. *The optimisation loop at work* 221

B.4.2.2. *Computing the confidence intervals* 224

APPENDIX C 227

C. Describing sulphate and calcium BTCs with IPA 227

C.1. Introduction 227

C.2. Routine for evaluating the objective function 230

C.3. Routine for solving the solute movement - Simula_BTC 231

APPENDIX D 235

D. The Newton-Raphson method 235

D.1. Introduction 235

D.2. Method description with one variable 236

D.3. Newton-Raphson method for two variables 237

LIST OF TABLES

Table 4.1. Selected properties of the experimental soils. 53

Table 4.2. Concentration of the leaching solutes and some physical characteristics of the Egmont (E) and Taupo (T) soil columns used in the miscible displacement experiments (columns T_a, T_1 and T_3 were intact samples). 54

Table 4.3. Mass balance (%) for chloride (Cl^-), Calcium (Ca^{2+}) and sulphate (SO_4^{2-}) for all soil columns of the miscible displacement experiments on Egmont (E) and Taupo (T) soils. 57

Table 5.1. Selected chemical characteristics of Egmont soil, original soil and after leaching with magnesium and potassium solutions: 75

Table 1. Parameter k_s estimated using Equation [5.18] and its parameters as given by Bolan *et al.* (1993): 83

Table 5.2. Parameters of the adsorption model obtained by least squares fitting using the three proposed IPA approaches and two different response variables (as explained in the text) 96

Table 5.3. Parameters of the adsorption model obtained by inverse modelling procedure for the three proposed IPA approaches. Two objective function, Φ_C (Equation [5.30]) and Φ_S (Equation [5.31]), were used. The standard error and R^2 are calculated accordingly for $C_1 + C_2$ and $S_1 + S_2$. 108

Table 6.1. Selected properties of the Egmont soil used in the experiments. 123

Table 6.2. Concentration of the leaching solutions and some physical characteristics of the soil columns used in the miscible displacement experiments on Egmont soil. 124

Table 6.3. Adjusted parameters of Freundlich isotherms and the IPA (ion-pair adsorption) factor for sulphate and calcium. The adjustment was made using batch experiment data. Also presented are the agreement measures (contrasting measured against estimated values of S_{SO4} + S_{Ca})..... 131

Table 6.4. Adjusted parameters of Freundlich isotherms and the IPA (ion-pair adsorption) factor for sulphate and calcium. The adjustment was made using data from columns E_1 and E_2 of the miscible displacement (using $CaSO_4$ solution). Also presented are the agreement measures (measured vs. estimated values of the leachate concentration)..... 134

Table 6.5. Adjusted parameters of Freundlich isotherms and the IPA (ion-pair adsorption) factor for sulphate and calcium using SGA2 approach. The adjustment was made using data from columns E_1 and E_2 of the miscible displacement (using $CaSO_4$ solution). Also presented are the agreement measures (measured vs. estimated values of the leachate concentration)..... 138

Table 7.1. Sulphur concentration in the plants from the six treatments: no fertiliser (N), $CaSO_4$ (C), K_2SO_4 (K), low irrigation rate (L), and high irrigation rate (H). All values in mg g^{-1} dry mass..... 148

Table A.1. Selected characteristics of the soils columns and solutions used in the preliminary miscible displacement experiments..... 196

Table A.2. Selected characteristics of the soils columns and solutions of the main miscible displacement experiments..... 199

Table B.1. Upper and lower limits of the confidence interval for the optimisation of the Freundlich equation parameters (from B.4.2.1)..... 224

List of Figures

Figure 2.1. Simplified schematic of the water balance components. 10

Figure 2.2. Schematic of simplified models for describing the movement of water and solutes in the soil. The dark-grey colour represents the soil matrix, the white and light-grey represent the pores with different solution concentrations. In (a) pores are unconnected and the dispersion is scaled with depth, while in (b) the pore connections produce dispersion independent of depth. 14

Figure 2.3. Schematic of a miscible displacement experiment in a soil column and three hypothetical shapes for the BTC obtained by monitoring the concentration in the outflow solution over time. A is the piston flow BTC, B is a common BTC for a non-reactive solute, and C is a BTC delayed due to the effect of adsorption. The ordinate axis is the concentration relative to the input solution, and the initial concentration in the soil is assumed to be zero. 16

Figure 2.4. Schematic of the solid-solution interface and the main processes involving the ions present in this system. Also, in the detachment, it is a representation of the solid-solution interface in more detail, regarding the adsorption/desorption processes, with cations (⊕) and anions (⊖) retained in the particle's doubles layer. 20

Figure 2.5. Examples of the dynamics of phosphate adsorption: Relations between the fraction of solute adsorbed and equilibration time for two different soils. Adapted from Aharoni *et al.* (1991). 24

Figure 2.6. Examples of adsorption isotherm equations. For Freundlich equation, k_F = 1 L kg^{-1} and N = 0.5; for Langmuir equation, M_L = 2.8 mmol kg^{-1} and ϕ = 1.5 L mmol^{-1}. 27

Figure 3.1. Schematic of the quasi-equilibrium model for sulphur exchange between the organic and inorganic pools. Redrawn from Watkinson and Kear (1996a)..... 44

Figure 4.1. Schematic of the leaching apparatus used in the miscible displacement experiments. 55

Figure 4.2. Measured sulphate breakthrough curves (BTCs) for some columns with Taupo soil (a) and Egmont soil (b). Columns T_1, T_2, T_a, and E_2 were leached with 0.01 M $CaSO_4$, and E_3 with 0.01 M K_2SO_4. PV is the equivalent pore volumes of the columns. 57

Figure 4.3. Measured calcium breakthrough curves (BTCs) for some columns with Taupo soil (a) and Egmont soil (b). Columns T_1, T_2, T_a, and E_2 were leached with 0.01 M $CaSO_4$, and E_3 with 0.01 M K_2SO_4, and E_4 with 0.01 M $CaCL_2$. PV is the equivalent pore volumes of the columns. 58

Figure 4.4. Measure chloride breakthrough curves (BTCs) for some columns of Egmont soil. Column E_2 was leached with 0.013 $CaCl_2$, followed by 0.01 M $CaSO_4$, and E_3 with 0.03M KCl followed by 0.01 M K_2SO_4. PV is the equivalent pore volumes of the columns. 59

Figure 4.5. Measured pH of the leachate from three columns with Egmont soil. Column E_2 was leached with 0.01 M $CaSO_4$, and E_3 with 0.01 M K_2SO_4, and E_4 with 0.01 M $CaCL_2$. PV is the equivalent pore volumes of the columns. 60

Figure 4.6. Measured potassium breakthrough curve (BTC) of Egmont soil, column E_3 leached with 0.01 M K_2SO_4. PV is the equivalent pore volumes of the column. 61

Figure 5.1. Adsorption graph showing the diagonals corresponding to constant solute amounts and two different equilibrium conditions, represented by Freundlich isotherms (k_F = 12 L kg^{-1}, N = 0.5 for

continuous line and k_F = 22 L kg^{-1}, N = 0.5 for dashed line). The data point moves from ① to ② due to changes in the equilibrium conditions following the path constrained by Equation [5.3] (Q_S = 40 mmol kg^{-1}). All diagonals assume ϑ = 10 L kg^{-1} (from a batch experiment for example)..... 68

Figure 5.2. Adsorption graph showing the partition of S into S_s and S_{IP}. Point ① represents the initial condition, without IPA, and ② is the final equilibrium with IPA, after the addition of a counter ion. This results in a move from ① to ② following the diagonal described by Equation [5.3] (Q_S = 40 mmol kg^{-1}, ϑ = 10 L kg^{-1}). Point ③ represents the S_s value under IPA equilibrium. The Freundlich isotherm describes S_s (k_F = 12 L kg^{-1}, N = 0.5)..... 69

Figure 5.3. Schematic of the IPA model from Qafoku and Sumner (2002). The overlap of the double layer of two soil particles with opposite charge can trap ions as ion-pairs..... 72

Figure 5.4. Schematic of the combinations of solutions of sulphate and calcium used in the batch experiments. Cells marked with x represent the basic series of isotherms, and o denotes the additional combinations. Two or more symbols in a cell indicate multiple replicates and the symbols in bold specify combinations that did not exactly match the nominal value for at least one of the solutes..... 76

Figure 5.5. Measured adsorption data for sulphate (a) at different levels of calcium (Q_2, mmol kg^{-1}), and for calcium (b) at different levels of sulphate (Q_1, mmol kg^{-1}). The series labelled as zero level represents estimates of the adsorption values at the absence of the counter-ion. The procedure to estimate them is explained in the text..... 78

Figure 5.6. Measured adsorption data for sulphate (a) and calcium (b) determined with solutions of K_2SO_4 or $CaCl_2$ respectively, using either the original or the leached soil. 79

Figure 5.7. Variations in the pH of the solution after equilibration in the batch experiments plotted against the solutes' concentration..... 80

Figure 5.8. (a) Adsorption isotherms for sulphate with (black symbols) and without (white symbols) calcium in two tropical soils. In (b) the enhanced sulphate adsorption (S_1) at increasing amounts of calcium (S_2) in four soils presented by Bolan *et al.* (1993). 81

Figure 5.9. Freundlich adsorption isotherms for sulphate (a) and calcium (b) for two tropical soils. Data were obtained with the counter ion (continuous line) or without (dashed line) (adapted from Marcano-Martinez and McBride (1989))..... 82

Figure 5.10. IPA factors estimated at various concentrations of calcium (S_2) for Seqaqa (a) and Fagaga (b) soils (adapted from Bolan *et al.* (1993)). Isolated dots are estimates for data values and lines are estimates using the given Freundlich equations. 85

Figure 5.11. IPA factor estimated at various concentrations of sulphate and calcium, at equivalent amounts for two soils presented by Marcano-Martinez and McBride (1989). Dots represent estimates using sulphate (●) or calcium (○) values and their average (▣)..... 86

Figure 5.12. Estimates of IPA factor for the three proposed approaches of IPA. Relationship estimated using data or isotherms for two soils presented by Bolan *et al.* (1993). Dots represent S_{IP} estimates from data (▲) and from isotherms (○), and the line is from the linear regression. 88

Figure 5.13. Estimates of IPA factor for the three proposed approaches of IPA. Relationships estimated using isotherms from two soils

presented by Marcano-Martinez and McBride (1989). Dots represent estimates using sulphate (●) or calcium (○) values and their average (▣), and the line is the linear regression..... 89

Figure 5.14. Linear relationships for the enhanced adsorption of sulphate (a) and calcium (b), with increasing amounts of the counter ion..... 90

Figure 5.15. Estimated values of k_s using Equation [5.18] with parameters of the linear relationships for sulphate (◆) and calcium (◇)..... 91

Figure 5.16. Freundlich equations fitted to adsorption data of sulphate (a) and calcium (b). (◆) are results from equilibrations of $CaSO_4$ solutions, and (◇) are estimates of the adsorption without the counter ion..... 92

Figure 5.17. Estimates of the IPA factor for the three proposed IPA approaches determined at different concentrations (a, b, c). Linearised relationships of Equations [5.10], [5.11], and [5.13] for estimating a general IPA factor for each of the three IPA approaches (d, e, f). Dots represent estimates using sulphate (●) or calcium (○) values and their average (▣), and the line is the linear regression. 93

Figure 5.18. 3D representations of the fitting of the adsorption model with IPA using the least squares method. Results for the two response variables and the three proposed IPA approaches are shown..... 97

Figure 5.19. Representation of the information about the parameter estimate (p) contained in the objective function ($\Phi(p)$)..... 100

Figure 5.20. Example of a comparison between the variation of the three objective functions normalised to their minima with varying the parameter $k_{F,1}$, using the SGA2 approach..... 104

Figure 5.21. Relationships for the standard deviation of the measurements for sulphate (a) and calcium (b). Data comprises some samples of the batch experiment, and some solutions with a standard (known) concentration..... 105

Figure 5.22. Relationships between variation and the magnitude of the concentration in the batch experiment equilibration for sulphate (a) and calcium (b). Dots represent calculated values and the lines are the estimation using Equation [5.35]..... 107

Figure 5.23. Relationships between pairs of parameters of the adsorption model, using the PGA approach. The other parameters were set at optimum values..... 111

Figure 5.24. Relationships between pairs of parameters of the adsorption model, using the SGA1 approach. The other parameters were set at optimum values..... 112

Figure 5.25. Relationships between pairs of parameters of the adsorption model, using the SGA2 approach. The other parameters were set at optimum values..... 113

Figure 6.1. Observed adsorption isotherms for sulphate (a) and calcium (b) using three different amounts of the counter ion in the added solution. Lines show adjusted Freundlich isotherms without considering ion-pair adsorption (IPA)..... 129

Figure 6.2. Adsorption isotherms for sulphate and calcium, added in equimolar amounts. Dots show observed data, bold lines represent modelled S, and thin lines show S_S as estimated using the particle governed approach, PGA (a and b) or solution governed approach, SGA1 (c and d)..... 130

Figure 6.3. Measured breakthrough curves (BTCs) for sulphate (a) and calcium (b), for the four experimental columns. Columns E_1 and E_2

leached with $CaSO_4$, E_3 leached with K_2SO_4, and E_4 with $CaCl_2$ (see Table 6.2)..... 133

Figure 6.4. Measured chloride breakthrough curves (BTCs) for the four experimental columns, also is shown the adjusted model. Concentration is relative to the input solution. Columns E_1 and E_2 leached with $CaSO_4$, E_3 leached with K_2SO_4, and E_4 with $CaCl_2$ (see Table 6.2)..... 135

Figure 6.5. Measured (dots) and modelled (lines) breakthrough curves (BTCs) for sulphate and calcium from columns E_1 (a and b) and E_2 (c and d) (leached with $CaSO_4$). Ion-pair adsorption (IPA) was described using the particle governed approach, PGA (a and c) and solution governed approach, SGA1 (b and d). 136

Figure 6.6. Measured (dots) and modelled (lines) breakthrough curves (BTCs) for sulphate and calcium from columns E_1 (a) and E_2 (b) (leached with $CaSO_4$). Ion-pair adsorption (IPA) was described using the SGA2 approach. 139

Figure 7.1. Average of the water applied per pot for the two irrigation treatments, low irrigation rate (L) and high irrigation rate (H). 144

Figure 7.2. Average of the solution amount leached per pot for the two irrigation treatments, low irrigation rate (L) and high irrigation rate (H)..... 144

Figure 7.3. Development of the plants fresh weight and leaf area over the experimental time for the six treatments: no fertiliser (N), $CaSO_4$ (C), K_2SO_4 (K), low irrigation rate (L), and high irrigation rate (H). 146

Figure 7.4. Specific root length distribution in the soil profile for the six treatments: no fertiliser (N), $CaSO_4$ (C), K_2SO_4 (K), low irrigation rate (L), and high irrigation rate (H). 147

Figure 7.5. Averages of sulphur, calcium, and potassium uptake per pot for the six treatments: no fertiliser (N), $CaSO_4$ (C), K_2SO_4 (K), low irrigation rate (L), and high irrigation rate (H). Vertical lines represent the standard deviation. Columns with the same letter in the boxes, for each irrigation treatment, did not differ significantly (Tukey test at P<5%). 148

Figure 7.6. Average per pot of the leached amounts of sulphate, calcium, and potassium for the three treatments with high-rate irrigation: no fertiliser (N), $CaSO_4$ (C), K_2SO_4 (K). Vertical lines represent the standard deviation. Columns with the same letter in the boxes did not differ significantly (Tukey test at P<5%)..... 150

Figure 7.7. Concentration of sulphate and calcium in the leachate during the experimental time, for the three treatments with high-rate irrigation: no fertiliser (N), $CaSO_4$ (C), K_2SO_4 (K). 150

Figure 7.8. Average per pot of the final soil concentration of sulphate, calcium, and potassium for the six treatments: no fertiliser (N), $CaSO_4$ (C), K_2SO_4 (K), low irrigation rate (L), and high irrigation rate (H). Vertical lines represent the standard deviation. Columns with the same letter in the boxes, for each irrigation treatment, did not differ significantly (Tukey test at P<5%). 151

Figure 7.9. Concentration profile of sulphate, calcium, and potassium for the six treatments: no fertiliser (N), $CaSO_4$ (C), K_2SO_4 (K), low irrigation rate (L), and high irrigation rate (H)..... 153

Figure 7.10. Comparison between the final soil concentrations of calcium and sulphate measured in five different depths of each pot of all treatments..... 154

Figure A.1. Measured sulphate breakthrough curves for Egmont soil (a) and Taupo soil (b) for the preliminary experiments. PV is the

number of water filled pore volumes leached. Vertical bold dashed lines represent the change from pre-leaching to leaching stages..... 197

Figure A.2. Leachate pH from the preliminary experiments. (a) Egmont soil and (b) Taupo soil for the preliminary experiments. PV is the number of water filled pore volumes leached. Vertical bold dashed lines represent the change from pre-leaching to leaching stages..... 197

Figure B.1. Flowchart with the basic algorithm for the evaluation of the adsorption model with IPA. 206

Figure B.2. User interface of the VisualBasic program built for the evaluation of the adsorption model with IPA. 207

Figure B.3. Flowchart of the general routine to solve the adsorption model. 209

Figure B.4. Flowchart of the routine NR01 for solving the adsorption model without IPA..... 211

Figure B.5. Flowchart of the routine NR02 for solving the adsorption model with IPA 213

Figure B.6. Flowchart of the simplified routine for obtaining the value of the objective function (Φ). 216

Figure B.7. Flowchart of the replication loop routine, showing the hierarchy of the parameter variation..... 218

Figure B.8. Flowchart of the optimisation loop routine. 220

Figure B.9. Variation of the objective function (Equation [B.28], with S) for a range of values of the two Freundlich equation parameters. 221

Figure B.10. Schematic of the step-by-step optimisation process. Sulphate adsorption data are used. Initial guess is k_F = 5 L kg^{-1} and N = 0.5. Optimum values are k_F = 5.35 L kg^{-1} and N = 0.354..... 223

Figure B.11. Flowchart of the sub-routine for finding the confidence interval of the adsorption model parameters. 225

Figure C.1. Flowchart with the basic algorithm for the evaluation of BTCs using the adsorption model with IPA. 228

Figure C.2. User interface of the VisualBasic program built for the evaluation of BTCs using the adsorption model with IPA. 229

Figure C.3. Flowchart with the basic algorithm for the evaluation of the agreement between predicted and observed BTCs by means of the objective function (Φ). 231

Figure C.4. Schematic of the discretisation of the soil column for the numerical calculations. 232

Figure C.5. Flowchart of the Simula_BTC routine, used for solving the solute movement in a soil column using CDE approach coupled with the adsorption model with IPA. 233

Figure D.1. Graph showing two iterations for finding the root of the function $F(x)$ using the Newton-Raphson method. The approximations start at x_1. 236

List of Symbols and Abbreviations

Roman letters

Symbol	Description	Unit
a	Constant used for computing the value of D	-
b	The slope of the linear relationship between S_1 and S_2	-
C	Concentration of a solute dissolved in the soil solution	[mol m^{-3}]
$\hat{C}$	The value of C predicted by the model	[mol m^{-3}]
D	Hydrodynamic dispersion coefficient for solute movement	[m^2 s^{-1}]
D_o	Diffusion coefficient of a solute in water	[m^2 s^{-1}]
D_w	Water diffusivity	[m^2 s^{-1}]
h	Hydraulic head	[m]
i	An integer used as index to indicate the ion species	-
j	An integer used as a counter	-
K_w	Soil hydraulic conductivity	[m s^{-1}]
K_s	Saturated soil hydraulic conductivity	[m s^{-1}]
k_{cb}	Crop coefficient for evapotranspiration	-
k_b	Constant for ion-pair equilibrium in saline solutions	[mol]
k_d	The distribution factor	[L kg^{-1}]
k_F	Parameter of the Freundlich isotherm equation	[L kg^{-1}]
k_s	IPA equilibrium factor for PGA approach	[mol kg^{-1}]
k_c	IPA equilibrium factor for SGA1 approach	[mol L^{-1}]
k_r	IPA equilibrium factor for SGA2 approach	[L kg^{-1}]

M_L	Maximum adsorption capacity, from Langmuir equation	[mol kg^{-1}]
m_{soil}	Dry mass of soil	[kg]
N	Exponent of the Freundlich isotherm equation	-
n_D	The total number of elements in a data set	-
n_P	The number of parameters	-
O	A value from an observed data set	-
P	A value from an predicted data set	-
p	Representation of a generic model's parameter	-
Q	The solute concentration in the soil (volume basis)	[mol m^{-3}]
Q_S	The solute concentration in the soil (mass basis)	[mol kg^{-1}]
Q_A	Amount of solute added to the soil in the MD experiments	[mol]
Q_F	Solute amount in the soil after the MD experiments	[mol]
Q_I	Solute amount in the soil before the MD experiments	[mol]
Q_L	Amount of solute leached during the MD experiment	[mol]
Q_{Sol}	A given amount of solute	[mol]
q_s	Solute flux density in the soil	[mol m^{-2} s^{-1}]
q_w	Water flux density in the soil	[m s^{-1}]
R	Retardation factor for the solute movement in the soil	-
R^2	Pearson correlation coefficient	-
S	Concentration of a solute adsorbed onto the soil particles	[mol kg^{-1}]
$\hat{S}$	The value of S predicted by the model	[mol kg^{-1}]
S_{IP}	Concentration of a solute adsorbed due to IPA	[mol kg^{-1}]
S_s	Single species adsorption concentration	[mol kg^{-1}]

S_{s0}	The intercept of the linear relationship between S_1 and S_2, representing the adsorption of an ion without the presence of its counter ion.	[mol kg^{-1}]
t	Temporal ordinate	[s]
v	Water velocity in the soil	[m s^{-1}]
V_w	Volume of water or solution	[L]
y	The calibration function or a value of that function	[mol L^{-1}]
$\overline{y}$	The average of several realisations of y	[mol L^{-1}]
z	Spatial ordinate, commonly vertical (depth)	[m]

Greek letters

Symbol	Description	Unit
β	Mass balance estimator	[%]
δ	A sink-source term	[mm s^{-1}]
ϕ	Parameter of the Langmuir equation	-
Φ	The objective function	-
Φ_C	The objective function comparing values of C	-
Φ_S	The objective function comparing values of S	-
ϑ	Specific water volume or water-to-soil ratio	[L kg^{-1}]
φ	The weighting factor in the objective function	-
λ	Soil dispersivity	[m]
μ	A generic measurement of a measuring device or procedure	-
θ	Volumetric soil water content	[m^3 m^{-3}]
ρ	Soil bulk density	[kg m^{-3}]

σ_m^2	Variance of the measuring procedure	-
σ_μ^2	Variance of the measurements of a measuring device	-
σ_o^2	The variance of the observed data	-
σ_p^2	The variance of a parameter estimate	-
σ_r^2	Variance of the experimental replications	-
τ	Tortuosity coefficient	-
ψ	Soil water potential	[Pa]

Additional symbols

Symbol	Description	Unit
$\mathcal{D}$	The χ^2 probability density function.	-
$\mathcal{P}_{Adeq}$	The probability of the model adequacy	-
$\mathcal{P}_{Conf}$	The probability for the confidence interval of a parameter estimate	-

Abbreviations:

AEC	Anion exchange capacity
BTC	Breakthrough curve
CDE	Convection-dispersion equation
CEC	Cation exchange capacity
CH	Treatment using $CaSO_4$ and high irrigation rate
CL	Treatment using $CaSO_4$ and low irrigation rate
FDM	Finite-difference model
IPA	Ion-pair adsorption

KH	Treatment using K_2SO_4 and high irrigation rate
KL	Treatment using K_2SO_4 and low irrigation rate
MD	Miscible displacement
NH	Treatment using no fertiliser and high irrigation rate
NL	Treatment using no fertiliser and low irrigation rate
OM	Organic matter
PV	Pore volume = number of WFPV leached through a soil column
PGA	Particle governed approach for describing IPA
SGA1	Linear solution governed approach for describing IPA
SGA2	Radical solution governed approach for describing IPA
RMSE	Root mean squared error
WFPV	Water filled pore volume

CHAPTER 1

1. General introduction

1.1. Introduction

The assessment of the sulphur status of agricultural soils is crucial for a good fertiliser management. Plant-available sulphur in soils can be highly variable in both time and space. Insufficient supply of sulphur causes significant yield losses and a reduction of the crop quality. It also increases plant susceptibility to diseases (Zhao *et al.*, 1999a; Scherer, 2001; Bloem *et al.*, 2005b). To avoid such deleterious effects, the timing of fertiliser application is very important (Schnug and Haneklaus, 1998; Eriksen and Mortensen, 2002; Ahmad *et al.*, 2005). A large proportion, up to 95%, of the total sulphur in agricultural soils is present in organic forms which are unavailable to plants (Edwards, 1998; Scherer, 2001). Sulphate is the main form of inorganic sulphur in most agricultural soils and the only one taken up by plant roots (Scherer, 2001; de Kok *et al.*, 2005). Sulphate dynamics in soils, with respect to its mobility and availability to plants, is related to several phenomena. Sulphate is constantly cycling with the organic forms and therefore is related to microbial activity and its inherent complexity (Watkinson and Kear, 1996a; Scherer, 2001). Sulphate is also adsorbed, via various mechanisms, onto the soil particles. This process not only reduces sulphate leaching, but also its immediate availability to plants (Bolan *et al.*, 1986a; Edwards, 1998; Scherer, 2001).

The sulphate balance is one of the main components of a fertilisation management model. Sulphate movement is linked to water movement, as most solutes in the soil are, although adsorption to the soil particles' surface may also be important. In soils where sulphate is highly mobile, any

improvement in the description of the water movement should result in more reliable estimates of the sulphate balance (Bloem *et al.*, 2005a). In soils with significant sorption capacity, a sound description of this process is also needed to assure the model's reliability (Scheidegger and Sparks, 1996). The knowledge of the processes governing sulphate movement can also lead to the development of improved management practices, with the potential to avoid the deleterious effects of sulphur starvation, and to reduce costs.

The adsorption of sulphate is highly dependent on soil pH. In most soils in temperate climates, sulphate adsorption is negligible at optimal agricultural pH levels (Edwards, 1998; Scherer, 2001). In more acidic soils, sulphate can be retained in the surface of the soil particles by the action of electrostatic forces or more strongly by specific adsorption. Sulphate can interact with cations, such as calcium, in the adsorption process. Specific adsorption of sulphate may lead to an increase in negative charge and consequently enhance cation adsorption (Agbenin, 1997). On the other hand, specific adsorption of calcium has also been shown to increase the retention of sulphate (Bolan *et al.*, 1993). In some soils, particularly those with variable-charge characteristics such as most weathered tropical and volcanic soils, cooperative sorption of sulphate and calcium by means of ion-pair adsorption (IPA) has also been observed (Marcano-Martinez and McBride, 1989; Ajwa and Tabatabai, 1995a; Pearce and Sumner, 1997). The identification of the type of ion adsorption, and subsequently the respective quantities of the adsorbed ions, is a difficult challenge. The large number of processes and factors involved make it almost impossible to describe each one, especially because several may occur simultaneously (Curtin and Syers, 1990; Scheidegger and Sparks, 1996).

IPA is reported to enhance the retention of sulphate in soils in the presence of calcium, as compared to other cations, such as potassium. The process occurring at particle surface level that is responsible for IPA is not yet fully understood, and its modelling is still incipient. Although some chemical

representations have been presented, a mathematical description for use in computer models, for example, is still required. IPA can occur in significant extent in some soils, and therefore influencing the movement of both sulphate and calcium (Bolan *et al.*, 1993; Davis and Burgoa, 1995). IPA has been identified in weathered volcanic soils but despite such soils been present in New Zealand, it seems there have been no studies describing this process. Developments in the description of IPA could help to improve the management of these soils, and potentially also in other soils in which such phenomenon occurs.

Models for estimating the sulphur availability and monitoring its status in the field have been proposed and some are already in use in many parts of the world (Watkinson and Kear, 1996a; Bloem, 1998). Their estimates, however, are too coarse in many cases, thereby compromising their reliability. Better descriptions are needed, both to prevent yield losses and to avoid excess of fertiliser application, with great importance in the increasingly competitive farming business. Since the timing for fertilisation can be decisive for avoiding yield and quality losses, a good description of the sulphur balance is potentially a valuable management tool. Thus an improvement in models reliability would be very useful, since models are, in general, cost effective and can handle diverse temporal and spatial scales.

1.2. Outline of the thesis

This thesis deals with the transport and fate of sulphate in the soil, with special focus on the modelling of sulphate movement in soils with significant presence of ion-pair adsorption.

Some relevant aspects of the quantitative description of sulphate movement in soils and its importance to plants are presented in the initial chapters. A review of the main processes involved in the solute adsorption and movement in soils, as well as the methods for their description are given

in Chapter 2. A more specific review of the literature on the importance of sulphate in plant production and the modelling of sulphate balance in the soil is presented in Chapter 3.

To contribute towards a better understanding and, in particular, a better description of the IPA phenomenon involving sulphate in New Zealand soils, a series of experiments in the laboratory and glasshouse had been carried out using two soils of volcanic origin: the Egmont and Taupo soils. By analysing the results of these experiments, the occurrence of IPA in the Egmont soil was identified and the quantification of its extent was attempted. A mathematical model using three different approaches is proposed and used for describing the adsorption observations, as well as the results from miscible displacement experiments. The relevance of IPA in longer-term experiments was also investigated. For this a pot experiment, using intermittent irrigation and in the presence of active plant growth, was carried out.

We have chosen Egmont and Taupo soils because of their contrasting characteristics with respect to ion retention. Taupo soil is a younger pumice soil with low ion-retention capacity, while Egmont is a variable-charge weathered soil with considerable ion-retention capacity (Molloy, 1988). Both soils are of volcanic origin from the North Island of New Zealand, and have allophane as the main clay constituent. The Taupo soil, however, has a much smaller allophane content. The allophane content affects the anion sorption processes in these soils, including IPA, and thus influences sulphate mobility and its availability to plants. Miscible displacement experiments using sulphate solutions, accompanied by either calcium or potassium, clearly showed evidence of IPA in the Egmont soil, while for the Taupo soil only a sample with high allophane content exhibited similar behaviour. The miscible displacement experiments procedure and the main results are presented in detail in Chapter 4. The summary of all results from this work is shown in the Appendix A.

Following the finding of IPA in the Egmont soil, a series of adsorption data was obtained by means of batch experiments. Using these results and after reviewing other published studies, three approaches were taken for devising a simple mathematical description of IPA. In these approaches the total amount of solute adsorbed is divided into single and ion-pair adsorption. An adsorption model was proposed using these approaches and the Freundlich equation, and it was used for fitting adsorption isotherms to the batch experiment data. The batch data and the procedures for the parameterisation of the adsorption model are given in Chapter 5. Implications of the model set-up are illustrated and the parameter estimates are contrasted with data from the literature.

In Chapter 6, the movement of calcium and sulphate through the soil columns studied in the miscible displacement experiments is described using the proposed IPA approaches coupled with the CDE model. The results of these analyses are discussed and the parameter estimates are compared to those obtained from the batch experiments.

As the laboratory experiments revealed that the Egmont soil exhibits IPA to a considerable extent, and that the leaching of both sulphate and calcium are significantly altered by this phenomenon, a pot experiment was set up in the glasshouse to investigate the possible relevance of IPA on the sulphate balance over a longer term and with plants growing. In this experiment rapeseed (*Brassica napus*) was sown in pots with repacked soil fertilised with either $CaSO_4$ for inducing IPA, or K_2SO_4. Several plant and soil characteristics were monitored. This experiment and the analyses of its results are presented in Chapter 7.

In Chapter 8 a synopsis of the experiments that were carried out and of the analyses of their results is presented. The conclusions from each chapter are linked and the general outcomes listed. Some recommendations for further work are then presented.

1.3. Objectives of the study

The main objective of this thesis is to make a contribution towards a more comprehensive description of the sulphur dynamics in the soil. The research was particularly focused on studying the sulphate adsorption with respect to the presence of different cations. A mathematical description of the ion-pair adsorption was sought, and a computer model was built to simulate the movement of ions which present such interaction.

More specific objectives set for this work were to:

- Investigate the occurrence of IPA in some volcanic soils of New Zealand;
- Investigate the extent of IPA and its effect on ion transport through the soil;
- Introduce a model framework for describing ion adsorption in soils taking the occurrence of IPA into consideration;
- Evaluate the performance of the adsorption model to describe he observed data sets from batch and miscible displacement experiments;
- Investigate some parameterisation procedures and their implication on the validation of the adsorption model;
- Investigate possible effects of IPA on plant uptake;

CHAPTER 2

2. Modelling the movement of solutes in the soil

2.1. Introduction

Natural systems are inherently complex, prone to be unstable, and often in dynamic non-equilibrium. To represent such systems, or the processes that are part of it, humankind has been making use of models. Despite the fact that models are always simplifications, they can be used to predict with reasonable accuracy the behaviour of real systems. Models might describe quite well a particular process under restricted conditions, but attempts to widen the environmental conditions, or to integrate this process with others, can be very challenging. When defining how complex a model should be, one should take into account the natural complexity of the system being modelled, but also, and in many cases more importantly, the purpose of use and the confidence level for the model's representation. A model's complexity also depends on the scale being represented and on the variety of conditions the model should deal with (Aikman and Scaife, 1993; Western and Bloschl, 1999; Wauchope *et al.*, 2002). In general, the simpler the model the bigger the uncertainties. By a simpler model, it is meant here one with a small number of processes considered. Although model complexity also depends on the way the processes are described. The addition of less important side-processes acts as a means of fine tuning the model performance, but this increase in complexity has its costs. The mathematical-computational framework can become overwhelmingly complicated. Also, as the number of parameters required for the representation increases, the work involved in obtaining them can become prohibitive. Furthermore, the possibilities for fitting errors increase proportionally with the addition of extra parameters (Simunek *et al.*, 2003;

Friedel, 2005; McCray *et al.*, 2005). As a result, the reliability of the description may be compromised. This problem is more likely in "general" models, where processes that are important under some conditions may be irrelevant in others, or where the variability of the parameters is high (Probert and Keating, 2000; van den Berg and Driessen, 2002). The study and selection of the relevant processes, and the best way for representing them, is therefore a crucial matter for increasing the reliability of the modelling of natural systems (van den Berg and Driessen, 2002; Wauchope *et al.*, 2002; Simunek *et al.*, 2003).

Numerous computational models for describing and predicting the dynamics of natural systems have been developed over the last three decades, or so. This development has been based on the increasing computational capacity, as well as improved scientific knowledge. The focus of these models has been for both scientific and practical purposes. The modelling of agricultural systems has brought significant improvements to farm productivity and also has raised awareness to environmental concerns (Goudriaan and van Laar, 1994; van den Berg and Driessen, 2002; McCray *et al.*, 2005). The use of models to predict yield, and for the management of nutrients and irrigation is common nowadays, and their use for monitoring the environmental implications of the farming procedures has increased recently (Ledgard *et al.*, 2001; Dragten and Thorrold, 2005). In this area, a reliable description of water flow and solute transport in the unsaturated zone of the soil is often required for predicting the impact of human activities on the environment (Feyen *et al.*, 1998; Kyriakidis and Journel, 1999).

Water is the key substance of central importance in the transport of solutes, whether in the soil or plants (Tinker and Nye, 2000). It is in the water that solute dilution and reactions take place. Water is the main carrier of solutes through the soil, therefore any good description of solute movement depends on a reasonably good description of water flow. Existing descriptions of water-solute movement differ in terms of their underlying assumptions and complexity. They range from relatively simplistic models to more complex

physically based dual-porosity, dual-permeability, and multi-region type models (Simunek *et al.*, 2003). Despite the tendency for using increasingly complex models, simpler solutions can still deliver a good description of the solute dynamics, especially if complemented with some handling of the minor processes which can be relevant under certain conditions (Vogeler, 1997). Certainly adsorption/desorption is a process relevant for the description of reactive solute movement. Adsorption/desorption processes control the amount of solute available to plants and microorganisms, and also for leaching (Edwards, 1998). The adsorption process can be subdivided according to the different bonding reactions, such as electrostatic attraction or various chemical reactions, which may be important in some soils or with some solutes, but not in other situations. These reactions may happen simultaneously and are often very difficult to distinguish (Scheidegger and Sparks, 1996). Some generalisations, however, do result in a good representation of experimental data. Soils with similar physico-chemical properties may respond similarly to certain solute combinations. In this case, the description of the relevant adsorption reactions is a useful tool for improving the general performance of solute movement models.

In this review, an overview of water movement through the soil is first presented. Then the convection-dispersion approach for modelling solute movement is revisited and the implications of solute adsorption on this modelling approach are discussed. Some pertinent aspects of solute adsorption in soils and its modelling that are related with sulphate movement are also discussed. This overview concludes with some comments on model parameterisation and the adjusting models to fit experimental data.

2.2. Water movement

The general balance of water in the soil-plant-atmosphere system can be summarised as shown in Figure 2.1. In this simplified model, the inputs and outputs considered are mainly vertical fluxes, which are of interest for this review. The description of horizontal fluxes, whether on the surface (runoff) or within the soil profile (lateral flow), is in general more complex. The water inputs accounted for are commonly limited to rainfall and irrigation, although upward movement from deeper layers sometimes occurs. Drainage and plant transpiration are the main water outputs, with evaporation from the soil being important only if the plant coverage is absent or partial. Evapotranspiration, which comprises evaporation from the soil and transpiration from plants, is a complex function of soil, plant and atmosphere variables, and it has been the focus of extensive studies due to its importance for irrigation management. Although in simple situations, such as with an extensive area of homogenous plant cover and a non limiting water supply, evapotranspiration can be satisfactorily modelled, it still is a challenge to account for the diversity of plants responses to varying environments conditions.

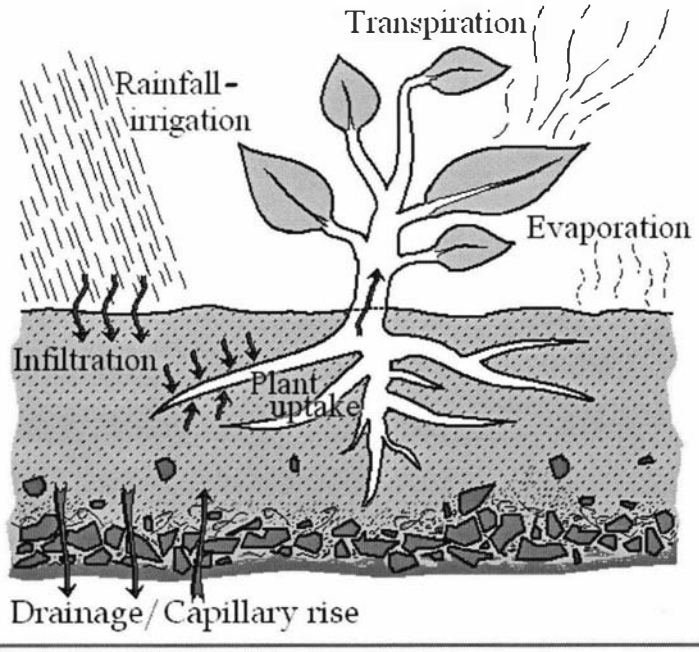


Figure 2.1. Simplified schematic of the water balance components.

Modelling the drainage process, which also may account for the capillary rise and the uptake by plant roots, depending on the approach used, is commonly based on the description of the water flow in terms of energy gradients and the hydraulic conductivity of the soil.

Water in the soil is held by electrostatic and capillary forces, which define its energy status (Kutilek and Nielsen, 1994; Libardi, 2000). To describe the water energy status in the soil the most commonly used measure is the water potential (ψ - kPa). The soil water potential is generally expressed in pressure units (kPa, psi, etc), which are equivalent to energy per volume (kPa = kJ m^{-3}), or, for convenience, by water head units (m). The water potential in the soil can be divided into several components, but the two most important in unsaturated soils are the matric potential, resulting from the electrostatic bonding and capillary forces, and the gravitational potential, which accounts for the differences in level within the earth's gravitational field.

Water in the soil moves spontaneously when there is a difference in the potentials between two regions. Water flows from the highest to the lowest potential, and the speed of movement is dependent on the potential gradient. The classic Darcy's equation represents this relationship:

$$q_w = -K_w \frac{\Delta\psi}{\Delta z} \qquad [2.1]$$

where $\Delta\psi$ (kPa) is the difference in the total soil water potential between two locations apart from each other by Δz (m), and K_w (m s^{-1}) is the soil's hydraulic conductivity. The conductivity describes the ease with which water can move through the soil. It is a function of soil type and structure, and also highly dependent on the water content of the soil. Darcy's equation is often used with the soil water potential expressed in pressure head units (m). Consequently, considering only the matric and gravitational components of the water potential, Equation [2.1] can be expressed, using partial derivative notation, as:

$$q_w = K_w\left(\frac{\partial h}{\partial z} - 1\right) \qquad [2.2]$$

where h (m) is the matric potential head.

For a more general expression of the water dynamics in the soil, the water content in the soil can be described by combining the flux equation and the mass conservation principle, leading to the Richards' equation:

$$\frac{\partial \theta}{\partial t} = \frac{\partial}{\partial z}\left(K_w \frac{\partial h}{\partial z} - K_w\right) + \delta \qquad [2.3]$$

where δ (mm s^{-1}) is a source/sink term. This term accounts for inputs, such as rain or irrigation, and outputs, particularly the plant uptake, or more generally, the evapotranspiration.

To avoid dealing with two variables (θ and h) a common simplification is to introduce the water diffusivity (D_w – m^2 s^{-1}), defined as:

$$D_w = \frac{\partial h}{\partial z}\frac{\partial \theta}{\partial h} \qquad [2.4]$$

The Richards' equation can then be re-written as:

$$\frac{\partial \theta}{\partial t} = \frac{\partial}{\partial z}\left(D_w \frac{\partial \theta}{\partial z}\right) - \frac{\partial K_w}{\partial z} + \delta \qquad [2.5]$$

Both K and D_w are highly dependent on the water content, therefore to solve Equation [2.5] mathematical representations of them as functions of the water content, or the water potential, are needed. The most common set of equations for describing the soil hydraulic characteristics is the Mualen-van Genuchten approach (Mualem, 1976; van Genuchten, 1980).

Preferential flow is not described satisfactorily by these equations *per se*. For this description, different equation sets, or variations of some of these equations, have been proposed. Nonetheless, the most common approach is to divide the soil into two or more fractions with different hydraulic characteristics, and employ the equation set to each fraction. This expedient is

used especially when describing water movement plus the solute or gas transport simultaneously (Feyen *et al.*, 1998; Simunek *et al.*, 2003; Moldrup *et al.*, 2004; Kohne *et al.*, 2006). Although this approach seems to describe better the results of several studies, it is often criticised because the partition of the soil is arbitrary and cannot be directly measured, nor can the many parameters for each fraction. The better fitting obtained is probably just due to the increase in the number of optimised parameters and not due to a better description of the system. This discussion could go further, but is beyond the scope of this review.

The uptake of water by plants is one of the main components of the water balance and greatly influences the distribution of water in the soil profile. Because of this, roots are responsible to a great extent for the movement of solutes in the soil (Clothier and Green, 1997). Therefore, evapotranspiration cannot be ignored when describing solute movement if plants are present. Because the modelling of plant uptake is not going to be attempted in this thesis, further description of these processes is out of the scope of this review. Further informations can be found elsewhere (Clothier and Green, 1997; Allen *et al.*, 1998; Tinker and Nye, 2000; Green *et al.*, 2003).

2.3. Solute movement – the convective-dispersive approach

The description of solute movement in the soil involves dealing with a very complex system governed by many interconnected and dynamic processes. In order to represent this system, simplifications must be made. If required, additional processes may be added to this initial model in order to increase its reliability, but always at the cost of escalating complexity, and the burgeoning need for parameterisation.

A very simple representation of the soil system considers it to consist of tubes of varying sizes (the pores) embedded in a soil matrix (Figure 2.2a). Depending on the degree of saturation, individual pores can contain either

water or air. In this representation, solutes are carried by the water moving through the pores. This process is called convection, or mass flow, and depends on the water flux density and it is unrelated to the solutes' nature. The mathematical representation is given by equation [2.6]:

$$q_s = q_w C \qquad [2.6]$$

where q_s (mol m^{-2} s^{-1}) is the solute flux density, q_w (mm s^{-1} = L m^{-2} s^{-1}) is the water flux density, and C (mol L^{-1}) is the solute's concentration in the soil solution. Solute movement can be retarded if adsorption onto the soil matrix is significant. For reactive solutes, this process needs to be considered for improving the model's performance.

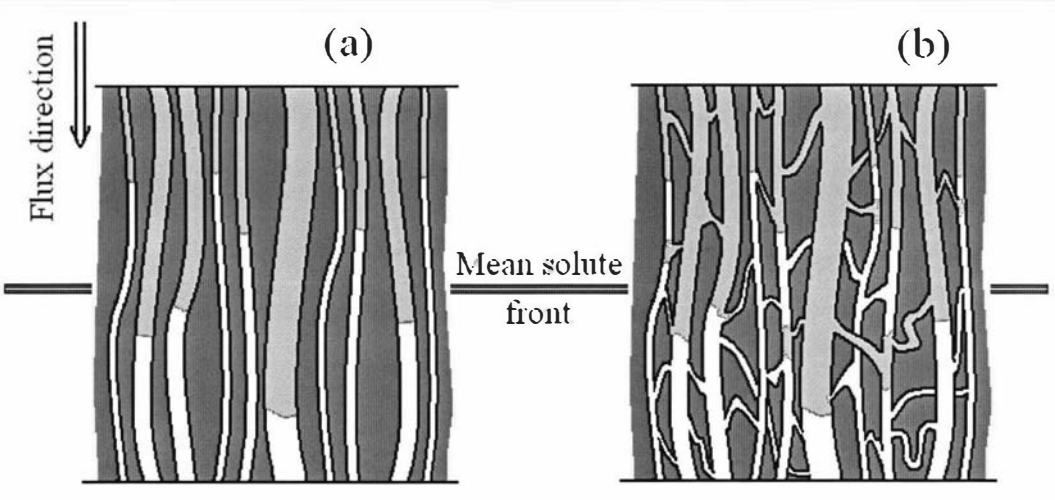


Figure 2.2. Schematic of simplified models for describing the movement of water and solutes in the soil. The dark-grey colour represents the soil matrix, the white and light-grey represent the pores with different solution concentrations. In (a) pores are unconnected and the dispersion is scaled with depth, while in (b) the pore connections produce dispersion independent of depth.

Soil pores have a range of different diameters, so the speed of water moving through the soil is highly variable. Consequently the solute concentration around the invading front spreads out in apparent dispersion

(Figure 2.2a). Modelling the frequency distribution of the movement speed in soil pores, assumed to be isolated, is one way of describing the movement of solutes. Such approach, known as stochastic-convective approach, has been used by several researchers (Jury and Roth, 1990; Tillman, 1991; Heng and White, 1996; Magesan *et al.*, 1999), and it has motivated debate because it involves a non-deterministic modelling.

Clearly the pores in the soil are not all isolated, so a further step towards a more deterministic description is to consider the connection between pores (Figure 2.2b). These interconnections in the soil's porous network lead to a more complex flow pattern induced by mixing, which in turn causes a smoothing in the solute's invasion front and is independent on the front's depth (Figure 2.2b). This depiction is usually modelled using the convective-dispersive approach, with dispersion treated mathematically as a modified (apparent) molecular diffusion.

To demonstrate the effect of dispersion on solute movement, consider a situation where a solute is continuously and evenly applied on the surface of a soil column, and the leachate is collected in the bottom (Figure 2.3). By monitoring the concentration of the outflow solution, a solute's breakthrough curve (BTC) is obtained. If the solute did not interact with the soil matrix, and all pores had the same size, one could expect the theoretical BTC represented by curve A (Figure 2.3). This is termed the piston flow BTC. However, because the water flows at different velocities in pores of different sizes, the flow in the soil is not uniform. So at the bottom of the soil column a small fraction of the solute should arrive quite fast by moving through the larger pores, while another fraction would have much longer travel times. Eventually, the concentration at the bottom of the column reaches the same value as the input solution, but only after a long time. This more realistic BTC would look similar to curve B (Figure 2.3). In the same figure, the effect of solute adsorption on the BTC is represented by curve C, where the appearance of the solute in the outflow is delayed. The slope of the BTC could be altered

by the pore size distribution, and its connectivity. If the soil's physical properties are not homogeneous, or the solute reaction with the soil matrix is more complex, say time dependent, then more complex BTC shapes would be obtained.

The usefulness of BTCs as a tool for studying the movement of water and solutes through the soil has long been recognised, and it still is one of the best means for comparing results from models with measurements. On the other hand, problems with the parameterisation of solute transport models may arise, since different processes can produce similar response (shapes) in the BTC.

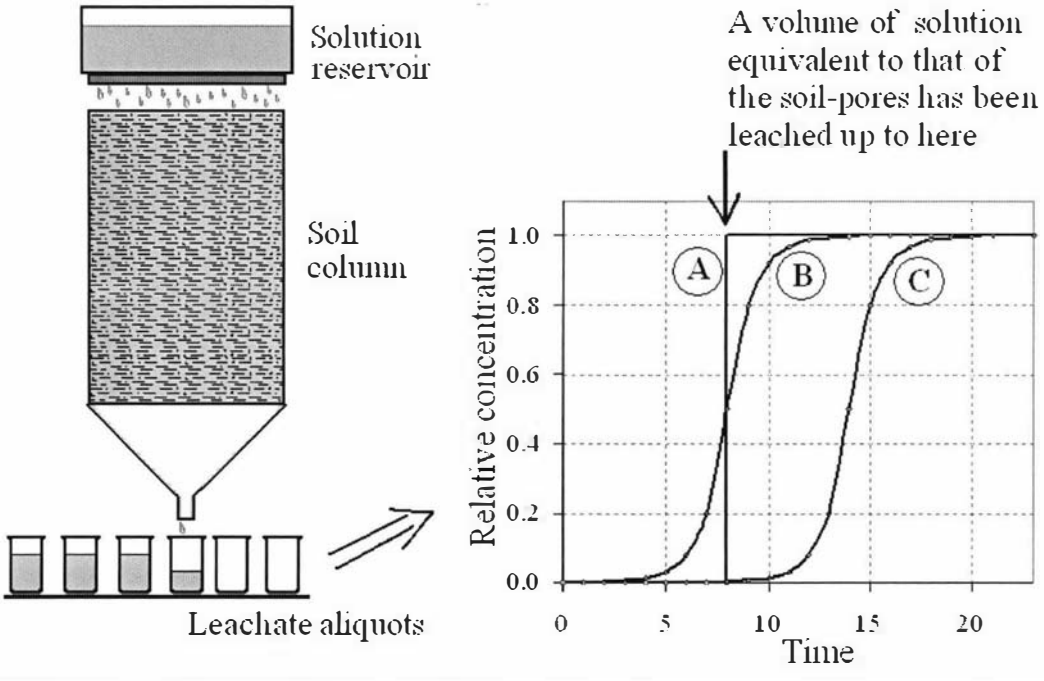


Figure 2.3. Schematic of a miscible displacement experiment in a soil column and three hypothetical shapes for the BTC obtained by monitoring the concentration in the outflow solution over time. A is the piston flow BTC, B is a common BTC for a non-reactive solute, and C is a BTC delayed due to the effect of adsorption. The ordinate axis is the concentration relative to the input solution, and the initial concentration in the soil is assumed to be zero.

Solutes can, however, move through the soil solution even without water movement. This is due to molecular diffusion. Solute diffusion occurs within the pore water whenever there is a concentration gradient. It can be mathematically expressed by:

$$q_s = D_o \frac{\partial C}{\partial z} \qquad [2.7]$$

where D_o ($m^2 s^{-1}$) is the diffusion coefficient in water, or diffusivity, characteristic of each solute and solvent, and z (m) is a spatial ordinate. This process is very slow, typically taking days for moving over millimetres, therefore it may be considered negligible in many practical situations compared to the mass transfer caused by the water flow. However, when water is flowing, the dilution due to the interconnections in the soil pores and the uneven distribution of velocities causes an effect that can be described in an analogous way to diffusion. Indeed, often the two processes are treated together, describing what is termed hydrodynamic dispersion.

With the two processes described above combined, the convection-dispersion approach for describing solute flux density can be written as:

$$q_s = D\theta \frac{\partial C}{\partial z} - q_w C \qquad [2.8]$$

where D ($m^2 s^{-1}$) is the hydrodynamic dispersion coefficient for the solute movement in the soil. The hydrodynamic dispersion coefficient is a parameter used to describe the combined effects of dispersion, diffusion and convective mixing (Kutilek and Nielsen, 1994), and is dependent on the soil structure, solute type, and the water flow velocity. It is commonly described by:

$$D = \lambda v^a + \tau D_o \qquad [2.9]$$

where λ (m) is the dispersivity, v ($m s^{-1}$) is the water velocity given by the ratio of the flux density and the volumetric soil water content, τ is the soil tortuosity, and a is a constant, generally assumed to be one. Unless the water

flux is very slow, the second term in Equation [2.9] is considerably small, and can be disregarded.

Combining the mass-conservation principle with the convective-dispersive approach for solute flux, the convection-dispersion equation (CDE) can then be defined as a partial differential equation:

$$\frac{\partial Q}{\partial t} = \frac{\partial}{\partial z}\left(\theta D \frac{\partial C}{\partial z}\right) - \frac{\partial}{\partial z}(q_w C) + \delta \qquad [2.10]$$

where Q (mmol L) is the total solute concentration per unit of soil volume, and δ (mmol L^{-1}) is a source-sink term to account for reactions, plant uptake, or solute sources. Under non-steady conditions this equation has to be solved simultaneously with the water flow description. A description of the solute adsorption or plant uptake should also be included if pertinent.

The CDE model assumes that the flow through the soil occurs relatively uniformly throughout the soil volume. This is not always a valid assumption. Approaches such as the partition of the soil into so-called "mobile" and "immobile" fractions have been proposed to deal with such situations. However in many cases, the increase in complexity and number of parameters do not lead to a proportional improvement in the model's performance. Also with some assumptions about some additional processes, the CDE can often be used with satisfactory results (Vogeler, 1997). The mathematical treatment of the CDE is less complicated, and analytical solutions have even been developed for simple boundary and initial conditions.

A simpler formulation of the CDE is obtained assuming steady-state conditions for the water flow and for non-reactive solutes:

$$\frac{\partial Q}{\partial t} = \theta D \frac{\partial^2 C}{\partial z^2} - q_w \frac{\partial C}{\partial z} \qquad [2.11]$$

In the simpler case where the adsorption can be disregarded, the term Q is replaced by C and the solution is rather easy. Otherwise if solute adsorption

can be described satisfactorily by a linear relationship, the movement can be described by:

$$R\frac{\partial C}{\partial t} = D\frac{\partial^2 C}{\partial z^2} - v\frac{\partial C}{\partial z} \qquad [2.12]$$

where R is the retardation factor, defined by:

$$R = 1 + \frac{\rho}{\theta}k_d \qquad [2.13]$$

where ρ is the soil bulk density, θ is the volumetric soil water content and k_d is the adsorption partition factor, to be defined in Section 2.5.

The value of R indicates if there is adsorption (R>1), or exclusion (R<1). Because adsorption retards the movement of solutes the value of R also gives an indication of this delay, and therefore the strength of the adsorption. For example, a value of two for R indicates that the solute will take twice as long to move as compared to the movement of inert tracers. Due to the complex interactions among soil-water movement, diffusion, and adsorption processes, several measured BTCs can be reasonably well described by equation [2.12]. This then exposes a weakness of the use of BTCs for solute movement analysis, it is equivalent to the so-called equifinality problem described in hydrology (Beven and Binley, 1992; Beven and Freer, 2001). Many processes cannot be distinguished by solely analysing BTCs. In cases where the simpler approach is not satisfactory, or there is the necessity for further discrimination of the processes involved, more general CDE formulations as well as solute adsorption, solute reactions, and the water flow, should be studied and modelled concomitantly. For solving this, numerical procedures are often used.

2.4. Ion adsorption

An amount of a solute present at a solid-solution interface can be partially dissolved in the solution and partially retained into the solid phase. In the solid phase, the solute can be present as a precipitated mineral, adsorbed onto the particles' surface, or being part of the organic matter pool (Figure 2.4). Several processes can act for exchanging ions from or to the solid phase and the solution. The partition between the two fractions, dissolved and sorbed, is of prime importance for defining the behaviour and environmental fate of the solute (Burau and Zasoski, 2002). While the soil solution is the reactive phase and provides ions to be taken up by plants and microorganisms, as well as to be leached, the sorption into the solid phase nonetheless acts as the main control of the solution composition.

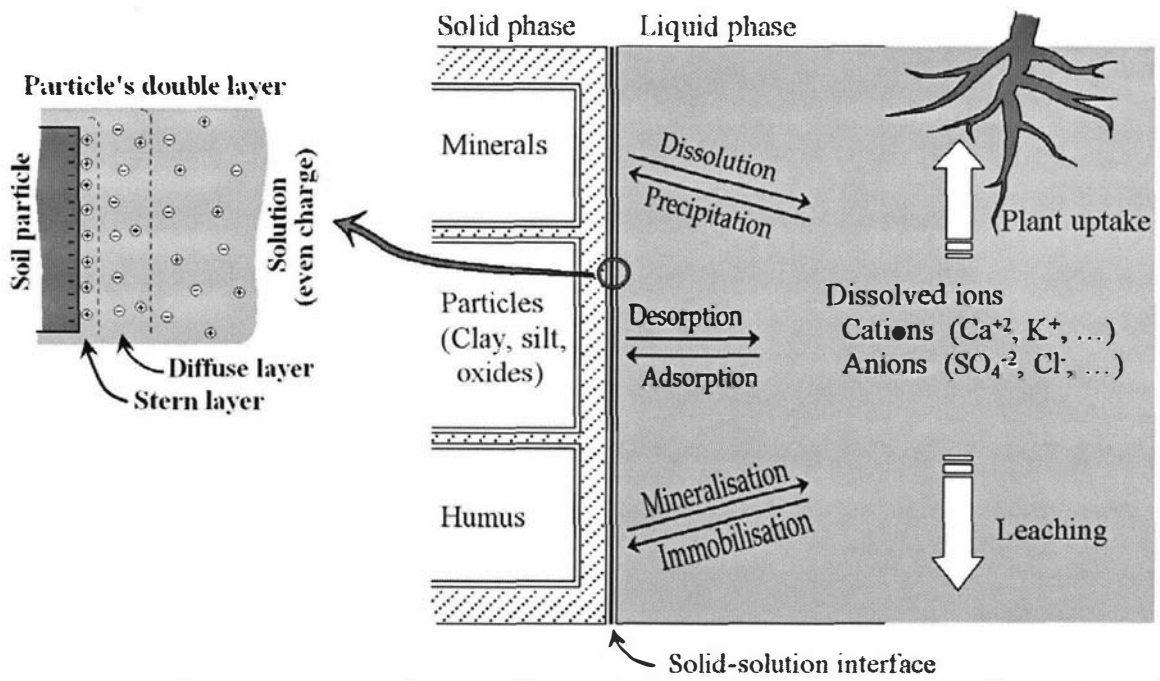


Figure 2.4. Schematic of the solid-solution interface and the main processes involving the ions present in this system. Also, in the detachment, it is a representation of the solid-solution interface in more detail, regarding the adsorption/desorption processes, with cations (⊕) and anions (⊖) retained in the particle's doubles layer.

Adsorption is one of the most important chemical processes in soils, and has been one of the most studied aspects of soil chemistry (Scheidegger and Sparks, 1996). Adsorption affects the transport of nutrients and contaminants in soils, and defines the amount of nutrients available to plants and microorganisms (Sposito, 1984; Burau and Zasoski, 2002). Adsorption is a term that is generally used to refer to the disappearance of solutes from solution with the presumption of them being bonded to a solid phase (Burau and Zasoski, 2002). However for this usage, the term sorption seems to be more appropriate (Scheidegger and Sparks, 1996). Adsorption can be more suitably defined as the accumulation of a substance at an interface of a solid surface and a bathing solution (Scheidegger and Sparks, 1996). Absorption may be used to identify the process in which the substance is taken up through the surface into the solid phase. Sorption therefore would include both, adsorption and absorption, plus precipitation (if mediated by the solid surface). Sorption is determined in practice by the extent of solute removal from the solution after equilibration in batch or leaching experiments (Scheidegger and Sparks, 1996; Burau and Zasoski, 2002). To quantify the true adsorption, the absorption and precipitation fractions should be separated. However, these fractions are often difficult to distinguish, and the use of the term adsorption to cover such general cases is widely spread (Scheidegger and Sparks, 1996).

The forces involved in the adsorption process can be either physical or chemical. Physical interactions comprise from weak van der Waals' forces to electrostatic outer-sphere complexes. The chemical interactions include several inner-sphere processes, such as covalent bonding, hydrogen bridges, etc. (Sparks, 1989; Scheidegger and Sparks, 1996; Bolan *et al.*, 1999b). The mechanism involved in the adsorption process depends on the type of surfaces available and the nature of the solute. Inorganic surfaces are in general highly polar, and contain both positive and negative charge sites. Organic surfaces are more complex and may have polar and nonpolar regions. Electrostatic

bonding of ions can happen at charged polar surfaces, while chemical interactions can occur in both polar and non-polar surfaces, but these are only significant with certain solutes (Sposito, 1984; Scheidegger and Sparks, 1996).

The release of adsorbed ions is often referred to as desorption. Although most studies in soil chemistry have focused on the adsorption of solutes in soils, the desorption process is also very important (Scheidegger and Sparks, 1996; Edwards, 1998; Zhang and Selim, 2005). The release of ions can increase the amount of nutrients available to plants but it also allows them to be leached. The desorption process is often more difficult to describe than adsorption (Selim and Zhu, 2005; Alves and Lavorenti, 2006). The reaction may be slower and not all the adsorbed solute may be released. Consequently corresponding equilibrations, forward and backwards, would not coincide (Verburg and Baveye, 1994; Undabeytia *et al.*, 1998; Zhang and Selim, 2005; Wadaskar *et al.*, 2006). This is normally called hysteresis or non-singularity, and may be caused by operational problems, such as a failure to attain equilibrium (Sparks, 1989; Zhang and Selim, 2005). Nevertheless, real hysteresis can occur and seems to depend especially on the type of adsorbent (Scheidegger and Sparks, 1996).

Many studies on the various aspects of adsorption-desorption processes have been published, however no real mechanistic information has yet been recorded (Scheidegger and Sparks, 1996; Burau and Zasoski, 2002). Adsorption isotherms are purely mathematical representations of macroscopic data and they do not directly imply a reaction mechanism. Also, it is not possible to separate adsorption from other sorption processes. Surface complexation models are often more complex and can describe adsorption over a wider range of experimental conditions. But they also do not provide a mechanistic description. In addition, different models can fit a given data set equally well, due to the large number of fitting parameters (Scheidegger and Sparks, 1996). Simpler models, especially adsorption isotherms, assume that the reactions in the adsorption-desorption process happen fast enough to be

considered instantaneous. Consequently the ions in the solution and the solid phase are assumed to be in equilibrium. This is seldom, if ever, true (Barrow, 1992b; Scheidegger and Sparks, 1996). Most reactions in soil are time dependent, and are influenced by fast-changing environmental variables, such as temperature and pH (Barrow, 1992a; Barrow and Cox, 1992). The rate of many reactions is also dependent on the type of soil components involved, for instance adsorption is much faster onto kaolinite than it is onto vermiculite (Scheidegger and Sparks, 1996). The reaction speed also depends on the type of surface complex, for example outer-sphere complexation is fast and reversible while inner-sphere complexation is slower and is, or may appear to be, irreversible (Sparks, 1989). Different ions may have a preference for different complexation processes. For example, ions that are adsorbed in inner-sphere, such as phosphate, are more strongly bonded. The term specific adsorption has been used to differentiate this from the weaker, fast reaction, outer-sphere adsorption (Sposito, 1984; Burau and Zasoski, 2002). Sorption reactions in the soil can be generally described by a fast stage followed by a slower one (Scheidegger and Sparks, 1996). Fast reactions can occur in milliseconds to some hours, depending on the criterion used to separate fast from slow reactions (Figure 2.5). Slow sorption can take place over several days or longer. Diffusion into soil micropores has been suggested as one reason for slow reaction times (Sparks, 1996), so soil structure may influence the speed of adsorption. Reactions with microbial biomass also happen at a slower rate than electrostatic adsorption, and may also deplete ions, such as sulphate, from the soil solution (Randlett et al., 1992; Watkinson and Kear, 1996a). Thus such reactions may also be unwittingly included in the general sorption process as part of slow adsorption.

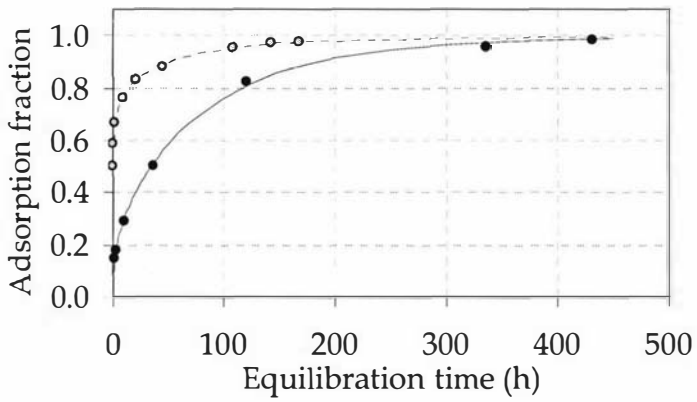


Figure 2.5. Examples of the dynamics of phosphate adsorption: Relations between the fraction of solute adsorbed and equilibration time for two different soils. Adapted from Aharoni *et al.* (1991).

2.5. Adsorption isotherms

At the solid-solution interface (Figure 2.4) the amount of solute bonded onto the solid surface (S - mol kg^{-1}) and dissolved in the solution (C - mol L^{-1}) are exchanged until a thermodynamic equilibrium is reached (Sposito, 1984; Burau and Zasoski, 2002). This equilibrium, represented in Equation [2.14], is the balance between the solute's activities in the two phases. Activity is a useful notion in electrochemistry and describes the "restlessness" of a chemical species in its environment (Oldham and Myland, 1994). A system is at equilibrium if the activity of all its components is the same. In the case of ions in an aqueous solution, the activity is a complex function of the concentration (plus temperature and pressure). Dissolved ions tend to move to different areas (diffusion), or to a different state (precipitation or adsorption), with lower activity in order to reach equilibrium (Oldham and Myland, 1994).

$$S \underset{k_{adsorption}}{\overset{k_{desorption}}{\rightleftharpoons}} C \qquad [2.14]$$

The question of whether the ions are bonded to the solids, or dissolved in the solution, is crucial for determining the fate of these ions in the environment (Burau and Zasoski, 2002). Therefore the description of this partition is of prime importance for a wide variety of agricultural and environmental studies. This description can become very complex, if one wants to account for most of the factors that affect this adsorption-desorption reaction.

Simpler models are also commonly used, as they are easier to handle and can lead to reasonable descriptions of real data, although they can be employed only under more restricted situations. Here a review of some simpler models is presented. This will provide the basis for further discussion later in the thesis.

Considering the simple representation of the solute equilibrium of Equation [2.14], the total content of an ion in the soil (Q, mmol L^{-1} soil) is obtained by:

$$Q = \theta C + \rho S \qquad [2.15]$$

where θ (L L^{-1}) is the soil water content and ρ (kg L^{-1}) is the soil bulk density.

The ratio between the amount of solute dissolved in the solution and the amount adsorbed in the soil at equilibrium is called the distribution factor or partition coefficient, k_d (L kg^{-1}):

$$k_d = \frac{S}{C} \qquad [2.16]$$

This factor may represent the equilibrium constant of Equation [2.14] ($k_{adsorption\text{-}desorption}$) in the simplest situation where the environmental conditions are steady, and the reaction rates are equivalent in both directions. The distribution factor is a function of temperature, and often also dependent on the concentration of solute and the pH. The relation of several sets of

dissolved-adsorbed data points collected at the same temperature is termed an adsorption isotherm. Such isotherms have been extensively used to summarise adsorption data in the soil. A linear adsorption isotherm can be represented by Equation [2.16] with k_d constant, and is often used in simple models, or when the variation range of the solute concentration is small. In most cases, however, adsorption isotherms are non-linear. To describe this relationship several equations have been proposed (Kinniburgh, 1986; Altin *et al.*, 1998; Hinz, 2001; Burau and Zasoski, 2002). Two simple and most common equations are the Freundlich (Equation [2.17]) and Langmuir (Equation [2.18]). Examples of their shapes are shown in Figure 2.6.

The Freundlich equation is given by:

$$S = k_F C^N \qquad [2.17]$$

where k_F (L kg^{-1}) and N are fitting parameters. It can be seen that as N approaches one, the isotherm becomes linear and k_F becomes the distribution factor. At low concentrations the Freundlich equation tends towards a linear relationship, which agrees with some theoretical assumptions derived from Henry's law (Kinniburgh, 1986). This equation has been found to better suit most adsorption data sets, in spite of having no limit for maximum adsorption (Elzinga *et al.*, 1999; Wu *et al.*, 2002; Alves and Lavorenti, 2004).

The Langmuir equation is given by:

$$S = M_L \frac{\phi C}{1 + \phi C} \qquad [2.18]$$

where M_L (mmol kg^{-1}) and ϕ (L mmol^{-1}) are fitting parameters. This equation is asymptotic to a maximum value defined by M_L. This agrees with the intuitive notion that there are a maximum number of adsorption sites. This is consistent with, for example, most phosphate adsorption data (Cajuste *et al.*, 1998; Casagrande *et al.*, 2003; Magesan *et al.*, 2003a). This equation does not approach a linear shape at low concentrations. The parameter ϕ is often

referred to as being related to the binding energy (He *et al.*, 1994; Dubus and Becquer, 2001; Sullivan *et al.*, 2003).

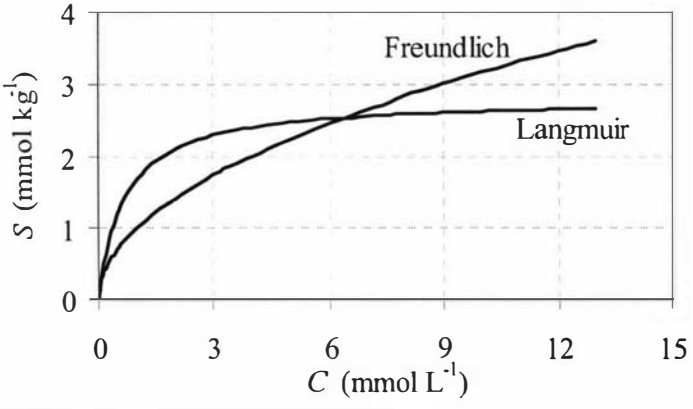


Figure 2.6. Examples of adsorption isotherm equations. For Freundlich equation, k_F = 1 L kg^{-1} and N = 0.5; for Langmuir equation, M_L = 2.8 mmol kg^{-1} and ϕ = 1.5 L mmol^{-1}.

These equations were proposed some 90 years ago and they are still being commonly used, probably due to their simplicity and their ability to fit a wide range of adsorption data (Kinniburgh, 1986; Hinz, 2001). Nonetheless, to account for experimental deviations or more complex theoretical assumptions, some variations for these equations have been suggested (Altin *et al.*, 1998; Ludwig *et al.*, 1999; Hinz, 2001; Burau and Zasoski, 2002; Wu *et al.*, 2002; Bodmann *et al.*, 2004; Barrow *et al.*, 2005). Although some physical meaning for the isotherms parameters have been tentatively proposed, these equations are probably best viewed as just being mathematical representations of macroscopic adsorption data. These adsorption isotherms, can still be successfully used for problems at a macroscopic level, although they are not mechanistic models of the solid-solution interface reactions (Scheidegger and Sparks, 1996; Burau and Zasoski, 2002).

Three major problems arise when using adsorption isotherms for modelling the fate of ions in the soil. Firstly, these equations imply that the

reactions in the soil are instantaneous, so that the soil-solution system remains always in equilibrium. This is, however, rarely true. Many researchers state that the dynamics of adsorption-desorption processes should not be ignored for an accurate prediction of the fate and movement of solutes in the soil (Verburg and Baveye, 1994; Scheidegger and Sparks, 1996; Undabeytia *et al.*, 1998; Zhang and Selim, 2005; Wadaskar *et al.*, 2006). Of course this depends on the level of detail and degree of confidence desired, as well as the characteristics of the system being described (Ludwig *et al.*, 1999; Sarkar *et al.*, 2006). A division of the process into instantaneous and time dependent reactions may also be employed (Selim *et al.*, 2004). The second problem involved in the use of simple adsorption isotherms is that variations in soil temperature and pH can be significant, and this can amplify the uncertainties to levels beyond acceptability. To avoid discrepancies, it is always recommended using the isotherms under similar conditions to those in which they have been determined. Sub-functions of the isotherms parameters dependent on pH or temperature have also been employed to overcome such problems (Curtin *et al.*, 1993; Sullivan *et al.*, 2003). The third issue to be considered when using simple adsorption isotherms is whether the adsorption and desorption processes follow the same relationship. Different interactions with the environment, and especially different dynamics, can alter the equilibrium between adsorbed and solution phases, resulting in hysteresis. This has been observed in many studies (Undabeytia *et al.*, 1998; Korom, 2000; Selim and Zhu, 2005; Zhang and Selim, 2005; Wadaskar *et al.*, 2006), although the effects were small or non-existent in other studies (Aylmore *et al.*, 1967; Gustafsson, 1995).

Despite these problems, it seems that the Freundlich and Langmuir equations still have a valuable role in the modelling of solute movement. Due to their simplicity and small number of parameters, the data set needed for a reasonable description using these equations can be relatively small (Kinniburgh, 1986; Schulthess and Dey, 1996; Elzinga *et al.*, 1999). As a

consequence their parameters are easy to obtain and there are plenty of values in the scientific literature for comparisons and reference (Shaffer and Stevens, 1991; Elzinga *et al.*, 1999; Korom, 2000; Imtiaz *et al.*, 2006). Also in many cases, the predictions using such simple models can be comparable in accuracy with predictions from more complex models (Wu *et al.*, 2002; Dubus *et al.*, 2004). Being simple, they are easy to handle and can be incorporated into larger environmental models. Small adaptations, such as non constant parameters that vary in relation to the environmental conditions, can widen the range of applicability of these equations with little increase in complexity (Curtin *et al.*, 1993; Wu *et al.*, 2002; Sullivan *et al.*, 2003).

2.6. Model fitting and parameterisation

For a reliable modelling of natural systems, two basic issues should be addressed. Firstly an appropriate model should be chosen and secondly its parameters have to be correctly estimated (Sen and Srivastava, 1990). To select a model, one has to consider first the purpose of the modelling, define the accuracy required and the scale at which to work. Defining the degree of generalisation is also important because uncertainties and complexity tend to increase as the description becomes more general. Also it is important to take into account the availability of the required parameters, or otherwise the procedure for obtaining them.

The estimation of a model's parameters, also referred to as parameterisation, is a crucial part of the modelling process (Sen and Srivastava, 1990; Vrugt *et al.*, 2002). Having a good model with the wrong parameters is worthless. For the parameterisation of a model it is important to have some information on the variability of the parameters and correlations between the processes involved, since this can restrict the use of a particular parameter set.

The evaluation of parameters can involve direct measurement, such as plant size or the amount of rain over a certain period. Literature specific or generalised data, such as for the particle size distribution and the bulk density of a soil, might be used as well. Finally, parameters may have to be estimated by means of specific experimentation and model fitting. The parameters needed and the procedures used to obtain them should be taken into account, as far as possible, when planning experiments or the data collection required to implement the model. The degree of uncertainty on the estimates, especially if they are obtained in indirect measurements, is also relevant when considering the amount of data necessary and procedures used to analyze the data (Sen and Srivastava, 1990; Vrugt *et al.*, 2002; Friedel, 2005).

Non-equilibrium and spatial variability are the rule for natural processes and therefore their parameterisation necessarily involves stochastic relations (Kyriakidis and Journel, 1999; Simunek *et al.*, 2003). The spatio-temporal variability is usually not fully described when using simplified models, what may amplify the uncertainties. Commonly, the uncertainty of a model is the sum of several components involving the model design, the parameter estimation, and the errors in obtaining the data against which to compare the model. The definition of the scale at which the model should be used, and the processes relevant at that scale, are the main factors to consider when defining the model complexity, because this has implications on the degree of uncertainty (Western and Bloschl, 1999; Friedel, 2005). Several other aspects can also affect the model's uncertainty, such as the natural variability and the level of knowledge of the processes involved. However, the uncertainties in obtaining data are inherent to any measurement procedure, and can only be minimised rather than eliminated (Pugh and Winslow, 1966). This can be done by selecting the appropriate procedure, followed by a good execution and the use of the best available equipment.

It is in the link between the data and the model where most of the possible refinement is possible and the model's reliability is defined. This link

encompasses the parameterisation and the checking of model components, or the model in general, contrasted with the observed data. Parameterisation often involves the comparison of two measures in order to verify their relationship. Whether comparing two measured data sets or a measured and a predicted data set, several statistical tools are available. Minimisation of the least squared errors and maximum likelihood are common procedures employed for fitting mathematical models to data (Sen and Srivastava, 1990; Jacques *et al.*, 2002; Vrugt *et al.*, 2002; Dubus *et al.*, 2004; Mertens *et al.*, 2006). The goodness of fit and model performance can be assessed by analysis of variance, error tracking, correlation indexes (Pearson or Spearman), and other procedures (Pugh and Winslow, 1966; Conover, 1980; Willmott *et al.*, 1985; Vrugt *et al.*, 2005). More recently the use of Monte Carlo recursive procedures for bootstrapping and inverse modelling have been successfully used for identifying uncertainties in models, and the relevance of the various model components (Huang *et al.*, 2003; Hupet *et al.*, 2003; Hupet *et al.*, 2005; Mertens *et al.*, 2006). The analysis of spatial and temporal variability, and the procedures to model it have also improved significantly in the last two decades (Kyriakidis and Journel, 1999; De Cesare *et al.*, 2001; Heuvelink and Webster, 2001; Oliver, 2004). The inclusion of these techniques on water and solute movement models show promising results (Snepvangers *et al.*, 2003; Wilson *et al.*, 2004; De Iaco *et al.*, 2005; Hupet and Vanclooster, 2005).

The estimation of parameters can be compromised by not considering the probability distribution function presented by the data set and the occurrence of correlation between parameters (Sen and Srivastava, 1990; Beulke and Brown, 2006). Furthermore, for a reliable parameterisation, the behaviour of errors and their propagation into different components of the model should be considered (Pugh and Winslow, 1966; Sen and Srivastava, 1990; Bruzzone and Moreno, 1998). Analysis of the error distribution may also lead to advances in understanding the processes being modelled (Friedel, 2005; Hupet *et al.*, 2005; Vrugt *et al.*, 2005).

CHAPTER 3

3. Sulphur in crop production

3.1. Introduction

Although sulphur is essential for plant growth, and is present in plants at amounts similar to those of phosphorus, it has not received much attention for years (Scherer, 2001). Sulphur's importance to plants and bacteria is closely linked to nitrogen, as both are directly involved in the photosynthesis process. The more evident nutritional concerns on nitrogen have, perhaps, overshadowed sulphur studies. The major processes involving sulphur in plant metabolism are the synthesis of cysteine and methionine, two amino-acids essential to build proteins and a series of other secondary products. These processes have long been described, but the side effects on plant health, the pathways for sulphur uptake and the plants' response to sulphur starvation have only more recently been the focus of scientific studies (Droux, 2004; Bloem *et al.*, 2005b; Nikiforova *et al.*, 2005; Hawkesford and De Kok, 2006).

The reasons for this lack of interest can be credited to the fact that sulphur nutrition used to be an almost irrelevant issue (Edwards, 1998; Scherer, 2001). The use of highly purified fertilisers, lower return of farmyard manure, the use of high yielding and sulphur-demanding crop varieties, plus the reduction in atmospheric deposition, especially in the northern hemisphere, due to a decrease in air pollution, are the most cited causes for the increasing number of reports on nutritional problems involving sulphur (Haneklaus *et al.*, 1999; Blake-Kalff *et al.*, 2001; Scherer, 2001; Zhao *et al.*, 2001; Malhi and Gill, 2006). The advance of agriculture into areas with nutritionally poor soils, such as many tropical areas, and the intensification of farming, with

a larger removal of nutrients from the field can be included in the reasons for the increasing interest in sulphur dynamics in agricultural environments (Eriksen *et al.*, 1998; Alves and Lavorenti, 2004). Supplying sulphur, whether by composed fertilisers or specifically by sulphur amendment, has become a common recommendation in many parts of the world. There is a need to establish standard procedures to assess sulphur nutritional status, as well as the deficiency thresholds (Pinkerton, 1998; Schnug and Haneklaus, 1998; Blake-Kalff *et al.*, 2000). Studies of the dynamics of sulphur in the soil also require more attention (Bloem *et al.*, 2005a; Edmeades *et al.*, 2005).

In the soil, sulphate is the most important form of inorganic sulphur. It is the mobile form which can be taken up by plants and microorganisms, and also it is the form that reacts with soil particles and it is prone to be leached (Edwards, 1998; Scherer, 2001). Losses of sulphate via leaching can be considerable in low retentive soils and/or after liming or fertilisation (Bolan *et al.*, 1988; Santoso *et al.*, 1995; Bloem, 1998). Adsorption onto the soil particles is the main process that mitigates or retards losses of sulphate by leaching. On the other hand adsorption also diminishes the amount readily available to plants. The adsorption of sulphate is highly dependent on the soil pH, and also can be easily displaced by phosphate and organic anions (Bolan *et al.*, 1986b; Edwards, 1998; Jara *et al.*, 2006). On the other hand the presence of cations, in particular calcium, can enhance the retention of sulphate (Marcano-Martinez and McBride, 1989; Bolan et al., 1993; Ajwa and Tabatabai, 1995a; Mora et al., 2005). Sulphate can be adsorbed both in the electrostatic outer-sphere and in the inner-sphere of the soil particles. Interactions of sulphate with cations in the adsorption process is quite complex. Specific adsorption of sulphate and the subsequent increase in cation adsorption have been reported (Agbenin, 1997); cation-induced sulphate retention by a similar process has also been identified (Bolan *et al.*, 1993). In some soils, especially variable-charge tropical and volcanic soils, the increase in sulphate and cation retention, particularly calcium, seems to occur cooperatively. In this process,

retention increases in equivalent amounts for both ions (Marcano-Martinez and McBride, 1989; Ajwa and Tabatabai, 1995a; Pearce and Sumner, 1997). This has been termed salt adsorption or ion-pair adsorption (IPA) (Marcano-Martinez and McBride, 1989; Qafoku and Sumner, 2002).

The occurrence of IPA increases the retention of sulphate, and therefore can retard the leaching process. On the other hand, retention by IPA seems to be reversible (Qafoku and Sumner, 2002), so it would not reduce significantly the availability of sulphate to plants. The study of IPA is still incipient and a better description of it is needed. There is no mathematical relationship proposed to evaluate the amount of sulphate adsorbed due to IPA that could be used for modelling. Also the relevance of IPA in the presence of growing plants has not yet been investigated.

Meanwhile, the use of models to describe agricultural systems, as well as for use in decision support tools, has been increasing. The identification of relevant processes is essential for improving the models' reliability and to widen the usefulness of such tools. Sulphur balance models have been proposed, and a few are being used to predict or to monitor the field sulphur nutritional status. However improvements are still required (Bloem, 1998; Bloem *et al.*, 2005a; Edmeades *et al.*, 2005). Due to the ever increasing competition faced by farming businesses, improvements, even small ones, for preventing losses, or increase yield or quality, can make a difference for sustainable practices.

3.2. Importance of sulphur for plants

Recently there have been a number of publications reviewing the role of sulphur in plant metabolism, the deleterious effects of its deficiency, and in the responses to it by plants (Droux, 2004; Hawkesford *et al.*, 2005; Nikiforova *et al.*, 2005; Hawkesford and De Kok, 2006). Also there are reviews on the broader role of sulphur in crop production (Edwards, 1998; Scherer, 2001). A

number of books covering the effect of sulphur and its deficiency in plants, as well as the modelling of its balance in soils, have also been published (Marschner, 1995; Schnug, 1998; Abrol and Ahmad, 2006). In this section, a brief overview of the relevance of sulphur for plants and the basic processes involving sulphur nutrition is presented.

Sulphur is an essential nutrient for the growth and physiology of plants (Scherer, 2001). Its content, however, varies significantly among different plant species, with reported values ranging from 0.1% up to 6% of dry mass (de Kok *et al.*, 2005). Sulphur requirements for good plant growth are distinct among plant families, with smaller variations among species within each family. These differences are reflected in the sulphur content of their seeds (percentage of dry weight): 0.18-0.19% for graminae, 0.25-0.3% for leguminosae and 1.1-1.7% for cruciferae (Marschner, 1995). The distribution of sulphur in the plant is relatively homogeneous, with little variation between shoot and roots, or between young and old leaves (Marschner, 1995). However, the chemical form in which most sulphur is present may vary with tissue age (Blake-Kalff *et al.*, 1998). Especially in oil-producing plants, seeds may accumulate a substantially high portion of plant sulphur at the end of the crop season (Matula and Zukalova, 2001; Naeve and Shibles, 2005).

The uptake of sulphur by plants takes place mainly in the roots, and sulphate is the ion taken up in the normal physiological pH range (Marschner, 1995). Uptake occurs at relatively low rates, varying between 2 to 10 mmol kg^{-1} day^{-1} (fresh weight) (de Kok *et al.*, 2005). The maximum uptake rate occurs at soil concentrations above around 0.1 mmol kg^{-1} (Hawkesford, 2000). Sulphate is transported through plants in the xylem. The uptake of sulphate by plants is active (energy dependent), and strictly controlled (de Kok *et al.*, 2005). It has been shown that plants, especially when in deficiency, can also directly absorb atmospheric gaseous sulphur compounds, such as H_2S and SO_2 (Durenkamp and De Kok, 2005; Yang *et al.*, 2006). The assimilation of sulphur is in many cases similar to that of nitrogen. However, sulphur can

also be assimilated without reduction, and can be re-oxidised to sulphate (Marschner, 1995).

Sulphur is a constituent of the amino-acids cysteine and methionine, and consequently of many proteins. These amino-acids are also the precursors of many coenzymes and other secondary plant metabolites (Marschner, 1995; Scherer, 2001). Because of its role in protein synthesis, sulphur is strongly linked to the nitrogen metabolism in plants. The nitrogen to sulphur ratio (N:S) of plants reflect that of the plant protein composition. The N:S ratio varies among different families, being around 40 for leguminosae, 30 for cereals (Marschner, 1995), and it may be less than 10 for brassicas (Blake-Kalff *et al.*, 2000). These ratios may vary in different growth stages and in case of nutrient deprivation (Marschner, 1995; Blake-Kalff *et al.*, 2000). Selenate can compete with sulphate in the uptake process, while phosphate, nitrate, or chloride seem to have no effect (Scherer, 2001). Selenium may be assimilated in the plants in a way analogous to sulphur, due to their atomic similarities. Competition with sulphur seems to be a major cause of selenium toxicity (Shrift, 1969; White *et al.*, 2004).

Deficiency of either sulphur or nitrogen can result in similar symptoms, making visual assessment difficult. Sulphur deficiency inhibits general protein synthesis, although the production of low sulphur-containing protein may be stimulated (Marschner, 1995). Accumulation of starch is also enhanced. Because proteins in leaves are mainly located in the chloroplasts, sulphur deficiency causes a direct reduction in the chlorophyll content and can consequently jeopardise the photosynthesis process (Ahmad and Abdin, 2000). The result of this is chlorosis, which is similar to nitrogen deficiency. However, because sulphur is distributed more homogeneously in plants than nitrogen, its deficiency symptoms can be found in both young and old leaves (Freney *et al.*, 1978; Schnug and Haneklaus, 2005). In legumes, the nitrogenase activity in the root nodules is affected by sulphur deficiency earlier than the photosynthesis. This causes a shortage in nitrogen supply, and therefore the

symptoms of sulphur and nitrogen deficiency cannot be distinguished (Marschner, 1995; Scherer, 2001). Morphologically the effect of sulphur deficiency is also similar to nitrogen deficiency, with shoot growth being suppressed more severely than root growth. Sulphur deficiency also may reduce transpiration not only by a decrease in leaf area, but also by reducing the hydraulic conductivity of the roots (Karmoker *et al.*, 1991). Sulphur deficiency decreases the efficiency of nitrogen assimilation (Schnug *et al.*, 1993; Fismes *et al.*, 2000; Jackson, 2000), and can consequently decrease the plant's response to nitrogen fertilisation. As a side effect, this may increase nitrogen leaching through the rizosphere into the groundwater (Haneklaus *et al.*, 1999).

The main effect of sulphur shortage is a reduction of crop yield. Reported losses can reach up to 70% for rapeseed and 50% for cereals (Zhao *et al.*, 2001). Beside that, sulphur deficiency, even at low intensity, may alter the quality of crops. For example, sulphur deficiency can reduce the baking quality of wheat flour (Kettlewell *et al.*, 1998; Zhao *et al.*, 1999b; Hagel, 2005), and change the oil content and taste of brassicas (Haneklaus *et al.*, 1999; Zhao *et al.*, 1999a; Bloem *et al.*, 2004; Malhi and Gill, 2006). Susceptibility to plant diseases is also enhanced by sulphur deprivation (Bloem *et al.*, 2005b; Dubuis *et al.*, 2005; Klikocka *et al.*, 2005), and flowers may even become less attractive to bees (Schnug and Haneklaus, 2005). The shortage of sulphur during the development period of plants causes irreversible losses in yield and/or crop quality, even without visible symptoms of deficiency (Zhao *et al.*, 1999a; Scherer, 2001; Schnug and Haneklaus, 2005). Therefore the timing of fertilisation to ensure an adequate sulphate supply is important (Haneklaus *et al.*, 1995; Eriksen and Mortensen, 2002; Ahmad *et al.*, 2005).

3.3. Diagnosis of sulphur status

Several procedures have been proposed to estimate the crop needs and the amount of plant available sulphur in the field. This allows intervention to

avoid crops suffering from sulphur deficiency (Nguyen and Goh, 1994; Pinkerton, 1998; Schnug and Haneklaus, 1998; Blake-Kalff *et al.*, 2000; Bloem *et al.*, 2005a; Edmeades *et al.*, 2005). Fertiliser needs may be estimated before sowing by assessing the crop demands and the available amount in the soil. Other factors such as mineralisation, or mid-season fertilisation may also be considered. In places where deficiency is likely to occur, monitoring the sulphur status over the season may be a better option, especially if the available sulphur can vary significantly, say for example, by leaching due to lack of adsorption.

It is difficult to define *a priori* the amount of sulphur in the soil available to plants for a growing season. The balance of sulphur (sulphate) available in the soil is a result of inputs (atmospheric depositions, fertilisation, etc.) and outputs (leaching, plant uptake) and the cycling between organic and inorganic forms (Edwards, 1998; Scherer, 2001). This cycling is dependent on microbial activity, which is seasonal and itself dependent on several environmental factors. As a consequence, the available sulphur content in the soil can be highly variable, especially in soils with high organic content. Soil analysis is useful then only for the time around when it has been taken (Schnug and Haneklaus, 1998).

A high degree of uncertainty can be expected estimating the sulphur needs based in an early soil analysis and the estimated sulphur balance. Therefore, it should be employed only if the risks or costs of wrong fertilisation are low. Under-fertilisation can result in sulphur starvation, while excess of fertilisation implies extra costs. Besides, sulphur may then be leached to the ground water and water bodies. Although there is no significant environmental issues related to the presence of sulphate in water, there are regulatory standards for its content in the water (Bast, 1991; Stewart et al., 2006). Taste change is the main effect caused by the presence of sulphate in the water. As a consequence, monitoring the sulphur status throughout the

growth season, and proper intervention, is the recommended procedure (Scherer, 2001; Bloem *et al.*, 2005a).

Monitoring the plants seems to be the best way to obtain reliable sulphur nutritional status data (Stuiver *et al.*, 1997; Zhao *et al.*, 1997; Schnug and Haneklaus, 1998; Blake-Kalff *et al.*, 2000). Several plant parameters may be employed for determining the nutritional status, and research is still being carried out to assess their advantages and disadvantages, as well as their thresholds (Blake-Kalff *et al.*, 2000; Scherer, 2001). Amongst the objective parameters, the total sulphur content in leaves is the most commonly used (Schnug and Haneklaus, 1998; Blake-Kalff *et al.*, 2000; Scherer, 2001). Thresholds vary with plant species, and even varieties. For wheat, for example, deficiency occurs if the concentration is below 2 mg g^{-1} (Withers et al., 1995). For rapeseed this value range from 3 to 3.5 mg g^{-1} for "single-" or "double-low" varieties, respectively (Scherer, 2001). The threshold for rapeseed was found to be 2.5 mg g^{-1} in Australia (Pinkerton, 1998), while Schnug and Haneklaus (1994) suggest two threshold levels; 6.5 mg g^{-1} where yield and quality losses occur without visible symptoms and a value around 3 mg g^{-1}, where symptoms become visible. These variations may partly reflect the different stages that samples were collected, as well as differences in the environment that influence the potential crop yield (Blake-Kalff *et al.*, 2000; Scherer, 2001). The fact that sulphur is mobile within the plant adds to the problem, and this makes total sulphur concentration a parameter of low sensitivity. The sulphate content was found to be more sensitive (Scaife and Burns, 1986), but also more dependent on the growth stage (Blake-Kalff *et al.*, 2000). Besides sulphate measurement is prone to higher uncertainties, as compared to those of total sulphur, which *per se* was found to be very high (Crosland *et al.*, 2001). The N:S ratio has also been suggested as a useful parameter to assess plant nutritional status (Rasmussen *et al.*, 1977). However, it is influenced by both nitrogen and sulphur supply, and may reflect surplus as well as deficiency of either one, making interpretation difficult (Scherer,

2001). Furthermore two analyses are needed, increasing the possibility of errors (Jones, 1986; Blake-Kalff *et al.*, 2000). Plant metabolites related to sulphur have also been tentatively used for estimating sulphur nutritional status (Scherer, 2001). The more common are; glutathione content (Zhao *et al.*, 1996), amides content in roots (Bell *et al.*, 1995) and malate to sulphate ratio (Blake-Kalff *et al.*, 2000). Although some are more sensitive (glutathione) or more accurate (malate), their analyses require specialised equipment. More studies to define better their threshold values are also needed.

The deficiency of sulphur may also be detected by visual inspection, although the symptoms may be confused with those of nitrogen. Even in plants where the visible symptoms are singular of sulphur deficiency, as for brassicas (Schnug and Haneklaus, 2005), damage to plant growth, and consequently yield and quality, are already significant by the time the symptoms become noticeable (Schnug and Haneklaus, 1998; Scherer, 2001). As a matter of fact, the problem with timing for detecting sulphur deficiency is also true for the tissue analysis (Pinkerton, 1998; Blake-Kalff *et al.*, 2000). Most analyses are recommended to be done at the beginning of the flowering stage, however, by the time the results are ready it is often too late for remediation in the same growing season.

An indirect way of "monitoring" sulphur nutritional status over the growing season is by using models (Scherer, 2001; Bloem *et al.*, 2005a). In soils with low sulphate retention, the water balance coupled with a plant stage chart for sulphur requirements may be used for estimating the sulphur status. Some versions of this, such as Schwefel-Schätzrahmen (BASF) or MOPS (Bloem, 1998), are already being used in northern Europe. Because of their simplicity, the estimates of these models are often too coarse for efficient fertilisation management, and over-fertilisation has been reported (Bloem, 1998). Improvements in such models, especially on sulphur movement/ storage, would refine their estimates and thus make them more useful for avoiding sulphur losses (Bloem, 1998; Bloem *et al.*, 2005a). In New Zealand, a

model for the sulphur requirement in pastures was developed in early 80's (Sinclair and Saunders, 1984). This model considers that the accumulation of sulphur in the soil has reached steady-state. Although subsequent tests showed reasonable agreement with long-term field data (Goh and Nguyen, 1997), a need for a dynamic model had been suggested (Saggar *et al.*, 1981; Nguyen and Goh, 1994). This has lead to the development of a quasi-equilibrium model (Watkinson and Perrot, 1990). These developments, and an extensive database have been incorporated in the Overseer® model (of New Zealand Pastoral Research Institute Ltd - AgResearch) to assist consultants on fertiliser management (Wheeler and Thorold, 1997; Edmeades *et al.*, 2005). However, this is not a deterministic model and still requires validation in a wider variety of environments (Edmeades *et al.*, 2005).

3.4. Sulphur in the soil

Sulphur in the soil may be divided into two major pools, the organic and the inorganic sulphur fractions, and it is continuously cycling between these fractions (Edwards, 1998; Scherer, 2001). Generally more than 90% of the total sulphur is present in organic forms, although it can be up to 98% (Bloem, 1998). In the soil profile, the organic sulphur distribution follows that of the organic matter (Scherer, 2001). The amount of sulphur and distribution over time in the organic pool depends on environmental conditions, such as soil moisture and temperature, as well as land management practices (Watkinson and Kear, 1996a; Scherer, 2001). The organic pool is highly variable in composition. It includes plant and animal residues, microorganisms, and humus (Freney, 1986). Soil microbial biomass can contain from 1.5% to 5% of the organic sulphur (Banerjee *et al.*, 1993; Wu *et al.*, 1993), with an ideal N:S ratio of about 10, although this value can become as high as 100 under sulphur deficiency (Banerjee *et al.*, 1993). Organic forms of sulphur are unavailable to plants, and thus must be mineralised to sulphate in order to be taken up

(Castellano and Dick, 1991; Banerjee and Chapman, 1996). The C:S ratio can be used to estimate the release of sulphur from the organic pool (Barrow, 1961). At C:S values smaller than 200, mineralisation occurs. With C:S above 400, immobilisation takes place. Between these values neither of the processes dominates. Interactions with nitrogen are more variable and seem to be dependent on various environmental and biochemical factors (Scherer, 2001). The addition of carbon sources, such as straw, tends to increase the amount of sulphur immobilisation into the soil organic pool (Saggar *et al.*, 1981; Eriksen *et al.*, 1998). Conversely the addition of organic matter with high sulphur content, such as young rapeseed leaves, increases the release of sulphate (Wu *et al.*, 1993; Mengel, 1996).

Although the microbial biomass represents a small fraction of the soil's organic sulphur, it is considered the most active pool for sulphur mineralisation (Banerjee and Chapman, 1996; He *et al.*, 1997). And it can cycle very fast. Therefore this fraction is of great importance in the sulphur cycle (Randlett *et al.*, 1992), and may act as a link between the other organic forms, and the inorganic fraction (Tan et al., 1994; Watkinson and Kear, 1996a). A quasi-equilibrium model (Watkinson and Perrot, 1990) uses a mineralisable organic sulphur (MOS) pool (Figure 3.1) to account for the fast exchange between organic and inorganic forms of sulphur. This MOS pool is not necessarily the same as the microbial biomass, although it should include it (Watkinson and Perrot, 1990). Exchange between the pools should be highly correlated with the microbial activity. This model accounts reasonably well for the seasonal variations in available sulphur in the soil (Watkinson and Kear, 1996b; Edmeades et al., 2005).

The inorganic sulphur form in the soil is generally mostly sulphate (Edwards, 1998; Scherer, 2001). Sulphate can be dissolved in the soil solution, adsorbed onto the soil particles, or precipitated as a salt (Edwards, 1998). In calcareous soils, sulphate impurities in $CaCO_3$ precipitates can account for a significant fraction of the total soil sulphur. Also, tidal marsh soils contain

large amounts of sulphur as sulphide metal, such as pyrite, that can be readily oxidised to sulphate (Scherer, 2001). These acid-sulphate soils pose an environmental issue as coastal lands are being reclaimed drained. Nevertheless, in terms of the sulphur balance in most agricultural soils, sulphate is the form of interest.

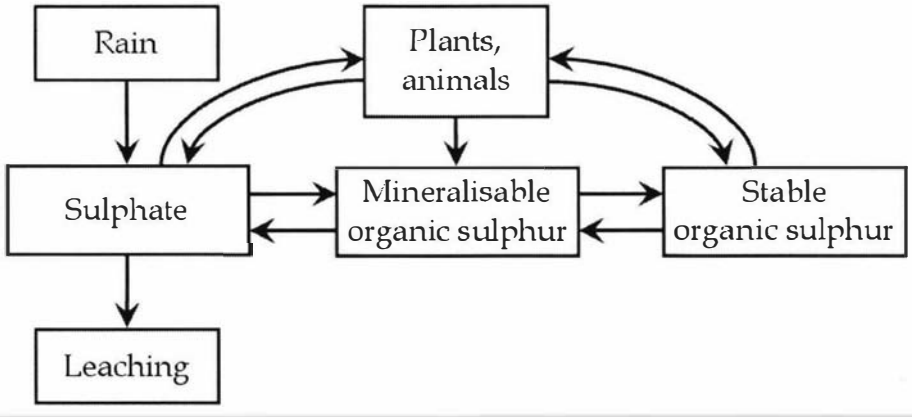


Figure 3.1. Schematic of the quasi-equilibrium model for sulphur exchange between the organic and inorganic pools. Redrawn from Watkinson and Kear (1996a).

The mobility of sulphate, or how easy it moves through the soil, is directly, and inversely, related to its adsorption onto soil particles. Soils with low adsorption capacity, such as sandy soils, retain small quantities of sulphate and therefore are prone to be leached. On the other hand, in clayey soils leaching can be negligible (Scherer, 2001). Sulphate retention, however, is not a direct function of particle size, as the particles must first contain a significant number of positive sites on their surfaces. The pH, therefore, has great influence in sulphate adsorption, since it may influence the charge status of the soil particles (Bolan *et al.*, 1988; Ludwig *et al.*, 1999; Rietra *et al.*, 1999; Alves and Lavorenti, 2004; Ishiguro *et al.*, 2006). Sulphate adsorption is practically nil at pH above 6.5 (Scherer, 2001), because too few positive sites are available for holding sulphate at high pH (Bolan *et al.*, 1986a). Sulphate is also easily released by phosphate ions (Geelhoed *et al.*, 1997; Cajuste *et al.*,

1998; Casagrande *et al.*, 2003; Pigna and Violante, 2003; Jara *et al.*, 2006). Adsorption can also be reduced by organic anions, such as oxalate and citrate (Casagrande *et al.*, 2003; Mora *et al.*, 2005; Jara *et al.*, 2006). Consequently, soils with higher amounts of organic matter tend to have a low sulphate retention capacity. Specific adsorption of sulphate has also been reported, and this is a reason why increasing pH does not significantly release sulphate in some tropical soils (Agbenin, 1997; Foloni and Rosolem, 2006).

Cations may help to increase sulphate retention in soils. Positive charges created due to specific adsorption of calcium have been reported to result in enhancement of sulphate adsorption (Bolan *et al.*, 1993). Retention of sulphate in the presence of cations due to ion-pair adsorption (IPA) has been described, especially with calcium as the counter ion (Marcano-Martinez and McBride, 1989; Alva, 1993; Ajwa and Tabatabai, 1995a). The IPA results in an increase of the total amount of sulphate retained in the soil when compared to the situation without the counter ion (Qafoku and Sumner, 2002). It seems to be common to many soils, but has been identified specially in variable-charge soils, such as many tropical and volcanic soils.

The greater the amount of sulphate adsorbed, the smaller the amount leached. On the other hand, the fraction of sulphate that is adsorbed may not be readily available to be taken up by plants. In situations where sulphate is strongly adsorbed by the soil, any intervention that reduces its retention should increase its availability to plants. These treatments include using lime for increasing soil pH, and the addition of competitive ions, such as phosphate (Bolan *et al.*, 1986a; Santoso *et al.*, 1995; Fahrenhorst *et al.*, 1999; Serrano *et al.*, 1999; Scherer, 2001). These practices and the higher amounts of organic matter in the uppermost soil layer are responsible for the higher proportion of available sulphate in this layer (Eriksen, 1996; Scherer, 2001). The distribution of sulphate in the soil profile is highly variable, and depends on the soil type, environmental conditions and land use (Edwards, 1998; Scherer, 2001).

Although gaseous losses to the atmosphere by volatilisation may occur (Edwards, 1998; Eriksen *et al.*, 1998), the main potential factor responsible for sulphur depletion in soils, other than plant uptake, is leaching (Edwards, 1998; Scherer, 2001). The amount leached depends on the mobility of sulphate, and the amount of water being leached. Increasing the amount of sulphate in the soil, due to fertilisation for example, should increase the potential for leaching (Santoso *et al.*, 1995; Scherer, 2001). Bare soils also present high potential to be leached (Kirchmann *et al.*, 1996). Soils prone to preferential water flow may show less sulphate depletion by leaching if the sulphate is present inside the aggregates (Bloem *et al.*, 2005a). Also leaching is expected to be minimal during the plants active growth period (Scherer, 2001). It has been estimated that up to 60 kg ha^{-1} $year^{-1}$ of sulphate losses due to leaching occur in low retentive German soils (Bloem, 1998). In New Zealand, losses of up to 89 kg ha^{-1} $year^{-1}$ have been reported (Nguyen and Goh, 1993; Edmeades *et al.*, 2005).

CHAPTER 4

4. Interactions between sulphate and cations in allophanic soils during miscible displacement experiments

4.1. Introduction

The management of the nutritional status of agricultural fields is one of the hallmarks of the green revolution. The addition of fertilisers has become a common practice, and this has resulted in a significant increase in food production. In many areas fertilisation can be an important fraction of the costs related to crop production. On the other hand, yield losses caused by nutrient deficiency can shrink the already narrow profit margin of most of the farms. Because this margin is narrowing, and also due to increasing concerns about the environmental effects of fertilisers, a more precise description of the field nutritional status and potential losses through leaching and gaseous emissions is needed. For many years sulphur has received little attention from researchers, although more recently studies of the management of sulphur status in soils and the processes involved in its mobility have increased (Scherer, 2001; Hawkesford and De Kok, 2006). Describing the balance of sulphur in the soil is a basic tool for assisting fertiliser management. One of the most important components of this balance is the description of sulphate movement. Sulphate is the mobile form of sulphur in soils and also the form taken up by plant roots (Edwards, 1998; Scherer, 2001). There have been many studies examining the processes involved in the movement of sulphur in soils, and models describing these processes have been presented. Some of the models describing the sulphur balance are being used by consultants for

fertiliser management. However, it has been argued that more studies are required to improve the reliability of these models (Bloem, 1998; Edmeades *et al.*, 2005). Sulphate retention onto soil particles can have an important effect on its movement and availability to plants. Phenomena such as specific adsorption or ion-pair adsorption (IPA) involving sulphate have been identified in many soils and can significantly affect its movement (Marcano-Martinez and McBride, 1989; Bolan *et al.*, 1993; Mora *et al.*, 2005). Variable-charge soils, such as many volcanic and tropical soils, are often associated with these adsorption phenomena. Although these soils have become important for world agriculture, few studies have been performed to examine the effects of adsorption phenomena on sulphate movement in these soils. New Zealand, which has soils with such characteristics, similarly needs more research on sulphate movement.

This chapter describes a series of miscible displacement (MD) experiments performed in the laboratory using two volcanic soils from New Zealand's North Island. These soils were chosen because of their contrasting ion adsorption capacities. Preliminary experiments were set up to identify the sulphate-movement characteristics in these soils, and to examine possible interactions with the accompanying cations. The results of these experiments indicated a strong relationship between sulphate and calcium adsorption in one of the soils. Further MD experiments were conducted in order to identify the possible phenomena involved. Results from experiments applying sulphate solutions with calcium or potassium as the accompanying cation indicated ion-pair adsorption as the most likely phenomenon. Further experiment with calcium solutions without sulphate confirmed this hypothesis. Comparisons between results for both soils also support this conclusion.

These experiments and the relevant results have been written up in a scientific article and this published paper forms the main part of this chapter. As not all of the experiments results were presented in this article, the

unpublished results are then shown in Appendix A, where the results of all the columns are summarised in a series of graphs for comparison. The experimental procedures used in all the experiments are the same as those described in this chapter. The results of these experiments instigated further studies, and a solute movement model which includes a mathematical description of the IPA phenomenon has been developed. This model was tested against the data sets obtained from these studies. This work is described in the subsequent chapters.

4.2. Cation influence on sulphate leaching in allophanic soils

by: Rogerio Cichota, Iris Vogeler, Nanthi S. Bolan and Brent E. Clothier
from: Australian Journal of Soil Research 45(1):49-54, 2007.

4.2.1. Abstract

We have examined the influence of the ionic composition of soil solution on the movement of sulphate and calcium in two New Zealand soils with differing allophane content. For this study, we have carried out a series of miscible displacement experiments using repacked and intact soil columns, in which sulphate was applied in the presence of either calcium or potassium as the accompanying cation. Our results showed that sulphate leaching was significantly retarded in the soil with higher allophane content when applied with calcium. On the other hand, no effects were observed for all studied soils when potassium was used as the accompanying cation. In addition, in soils with high allophane content, calcium also had its retention increased when sulphate was present. The increase in sulphate adsorption was accompanied by corresponding increase in calcium adsorption. These findings evidenced the presence of co-adsorption, or ion-pair adsorption (IPA), in allophane-containing soils. The extent of this adsorption is dependent on the soil pH, the accompanying cation and the allophane content of the soil.

Additional keywords: Breakthrough curve; Calcium, Ion-pair adsorption; Miscible-displacement experiment; Potassium.

4.2.2. Introduction

Sulphur deficiencies in soils have been increasingly reported in many countries worldwide including New Zealand (Nguyen and Goh, 1994; Schnug *et al.*, 1995; Scherer, 2001; Edmeades *et al.*, 2005), especially since the reduction of air pollution enforced by 'clean air' legislation (Henderson, 1996; Greenstone, 2004). The use of non sulphur-containing nitrogen (N) or phosphorus (P) fertilisers, such as urea and di-ammonium phosphate, and the introduction of new high yielding and sulphur-demanding crop cultivars tend to intensify this problem. Sulphur deficiency in soils leads to yield losses and can influence crop quality, as well as increase plant susceptibility to some diseases (Zhao *et al.*, 1999a; Bloem *et al.*, 2005b; Klikocka *et al.*, 2005; Rausch and Wachter, 2005). In many cases, specific sulphur amendment to these soils is required.

Sulphate (SO_4^{2-}) is the most important inorganic form of sulphur in soils and is readily available to plants. It is applied to the soil through different available sulphur fertilisers, with different accompanying cations. Ammonium sulphate, potassium sulphate and gypsum (dihydrated calcium sulphate), alone or as part of single superphosphate, are some of the important sulphur sources used in agriculture. Gypsum is used as a source of calcium and sulphate, and also as an amendment to improve soil structure (Bolan *et al.*, 1993). Substantial sulphate losses via leaching can occur in soils with low retention capacity, and this has been observed in New Zealand (Edmeades *et al.*, 2005). Pumice soils are an example for these low retentive soils, and they present the highest yield responses for sulphur fertilisation in New Zealand, in

contrast, for example, with the variable-charge Egmont soils, which are more effective in the retention of sulphate (Edmeades *et al.*, 2005).

The sulphate content in soils is in a dynamic equilibrium with other forms of sulphur, especially organic forms. This equilibrium may vary over the year (Tan *et al.*, 1994). Nevertheless, because sulphate is the mobile form of sulphur, leaching is, in general, related to fertiliser input. It has been shown that sulphate adsorption can be influenced by the presence of other ions in the soil solution. The influence may be competitive for ions with the same charge, such as phosphate, or it can be cooperative for ions with opposite charge, such as calcium. The interaction also depends on the properties of the soil. Specific adsorption of anions may increase the soil net negative charge and thus allow further cation adsorption. This has been reported in many studies, especially involving phosphate (Ryden and Syers, 1976; Bolan *et al.*, 1988; Agbenin, 1996; Bolan *et al.*, 1999a; Bolan *et al.*, 1999b), or sulphate (Alva *et al.*, 1990; Curtin and Syers, 1990). Cations can also be specifically adsorbed and induce the retention of anions in soils (Bolan *et al.*, 1993; Cajuste *et al.*, 1998). Cooperative adsorption that occurs without changing the soil net charge has also been observed, especially in variable-charge soils (Marcano-Martinez and McBride, 1989; Alva et al., 1990; Ajwa and Tabatabai, 1995a; Qafoku et al., 2000; Qafoku and Sumner, 2002). In these cases, cation adsorption increases due to the presence of an anion, and vice versa. Because the amount of additional adsorption resulting from the co-adsorption process is equivalent to the ratio of the molar masses of the anion and cation, this process has also been called salt adsorption, or ion-pair adsorption (IPA) (Marcano-Martinez and McBride, 1989; Qafoku and Sumner, 2002).

IPA seems to be a phenomenon related to variable-charge soils, although not all studies with variable-charge soils indicate IPA. Even though it can occur with various ion combinations, IPA is more likely to happen with multivalent ions (Ajwa and Tabatabai, 1995a; Pearce and Sumner, 1997). IPA has been identified, in particular, for calcium and sulphate (Marcano-Martinez

and McBride, 1989; Alva *et al.*, 1990; Bolan *et al.*, 1993; Davis and Burgoa, 1995; Mora *et al.*, 2005). Despite many studies describing the IPA phenomenon in soils, its influence on sulphate leaching has not been well explored yet. If the adsorption of both calcium and sulphate is influenced by each other, then their movement through the soil is also likely to be affected by these interactions.

To determine these interactions, we conducted a series of experiments in order to unravel the influence of cations on the movement of sulphate in two contrasting New Zealand soils. These soils are contrasting in relation to their variable-charge components and ion adsorption capacity. In this paper, we describe experimental observations from several miscible displacement experiments. Evidences of IPA in the variable-charge soil are shown, and its effect on sulphate leaching is determined and contrasted with the results from the low-adsorptive soil.

4.2.3. Material and methods

4.2.3.1. Soil

Two New Zealand soil types were used. One soil was Egmont loam (Typic Dystrandept), an Allophanic Soil from South Taranaki (Hurleyville, Patea) which is dominated by variable-charge components; and the other was Taupo soil (Typic Vitrandept) a low allophane-containing Pumice Soil from the Taupo region (Hurakia airstrip, Mangakino). The Egmont soil is a weathered soil of volcanic origin, containing allophane as the main clay component (Molloy, 1988). It has a well developed structure and the bulk density is usually below 900 kg m^{-3}. The weakly weathered and well-drained Taupo soil has almost no structure, and a bulk density ranging from 600 to 800 kg m^{-3}. Soil samples were collected in pastoral fields between the depths of 0.05 m to 0.20 m. Some basic properties of the soils are presented in Table 4.1. To illustrate the influence of soil mineralogy on the IPA process, one

additional experimental run was carried out with a Taupo soil with higher allophane content than the soil previously described.

Table 4.1. Selected properties of the experimental soils.

Soil	pH	Sand [1]	Silt	Clay	Allophane [2]	OM [3]	CEC [4]	Calcium	Sulphate [5]
	(H_2O)	———		($g\ kg^{-1}$)	———		($mmol_c\ kg^{-1}$)	($mmol\ kg^{-1}$)	
Egmont	4.6	390	460	150	92	110	343	36.8	1.75
Taupo	6.3	820	110	70	24	1	17	2.4	0.21
Taupo (T_a)	5.6	700	150	150	54	16	59	5.4	1.80

[1] Particle size measured by the pipette method; [2] Allophane determined by Al:Si ratio (Parfitt and Wilson, 1985); [3] organic matter (OM) by loss on ignition method; [4] CEC and calcium using NH_4OAc (1.0 M) extraction method (pH 7); [5] sulphate by KH_2PO_4 extraction (0.01 M).

4.2.3.2. Miscible displacement experiments

Breakthrough curves (BTCs) for calcium, potassium, chloride, and sulphate were measured in the leachate of four columns each soil, Egmont (identified by letter E) and Taupo (identified by letter T). The additional allophanic Taupo soil column was identified by T_a. Each experiment was divided into two phases: a pre-leaching event, which aimed to minimise indigenous ions and attain a known soil solution composition; and a main leaching event for applying the appropriate sulphate solutions. Details of the solutions used in the experiment and characteristics of the soils columns are presented in Table 4.2. For Taupo soil, and two columns of Egmont soil, two different concentrations for the leaching solution were used, in order to investigate any influence of concentration on sulphate movement. For each concentration an intact soil and a repacked soil column were used with Taupo soil. T_a was an intact sample. In the case of the Egmont soil, only repacked samples were available.

As single adsorption, and possibly IPA were expected to occur in the Egmont soil, in addition to the leaching with $CaSO_4$ solutions, we used two

other columns set up to determine the BTCs of sulphate and calcium when leached without (or minimizing) the influence of each other. In these columns, K_2SO_4 and $CaCl_2$ were used in the leaching solutions.

Table 4.2. Concentration of the leaching solutes and some physical characteristics of the Egmont (E) and Taupo (T) soil columns used in the miscible displacement experiments (columns T_a, T_1 and T_3 were intact samples).

Column	Solution concentration (mol L^{-1})		ρ [1]	θ [2]	$WFPV$ [3]	q_w [4]
	Pre-leaching	Leaching	(kg m^{-3})	(m^3 m^{-3})	(cm^3)	(mm h^{-1})
E_1	0.0067 - $CaCl_2$	0.005 - $CaSO_4$	754.8	0.643	819.2	44.11
E_2	0.0133 - $CaCl_2$	0.01 - $CaSO_4$	754.5	0.607	763.2	29.86
E_3	0.03 - KCl	0.01 - K_2SO_4	769.7	0.627	789.1	20.48
E_4	0.0133 - $CaCl_2$	0.01 - $CaCl_2$	752.4	0.638	807.9	34.30
T_a	0.0133 - $CaCl_2$	0.010 - $CaSO_4$	892.8	0.550	700.5	9.25
T_1	0.0133 - $CaCl_2$	0.010 - $CaSO_4$	859.6	0.465	580.9	41.87
T_2	0.0133 - $CaCl_2$	0.010 - $CaSO_4$	884.6	0.468	580.7	46.64
T_3	0.0067 - $CaCl_2$	0.005 - $CaSO_4$	839.8	0.454	578.6	33.23
T_4	0.0067 - $CaCl_2$	0.005 - $CaSO_4$	683.0	0.409	511.1	72.91

[1] ρ is the soil bulk density; [2] θ is the soil water content; [3] $WFPV$ is the water filled pore volume; [4] q_w is the water flux density in the leaching stage.

All leaching experiments were conducted under unsaturated conditions, at a pressure potential of -0.10 kPa, except for the allophanic Taupo soil (T_a), which was at -0.05 kPa. The columns were 0.15 m high and had diameter of 0.10 m. The experiments were carried out following a procedure similar to that described by Magesan *et al.* (2003b). The solution was applied using a disk permeameter placed in the top of the soil column (Figure 4.1). The leachate solution was collected in small aliquots varying from 50 mL to

100 mL, the collecting containers were in a pressure controlled chamber. The pre-leaching solution (Table 4.2) was applied until at least 5 pore volumes (PV) of leachate was collected; after this the input solution was immediately replaced by the main leaching solution, and applied until another 5 PV of leachate was collected.

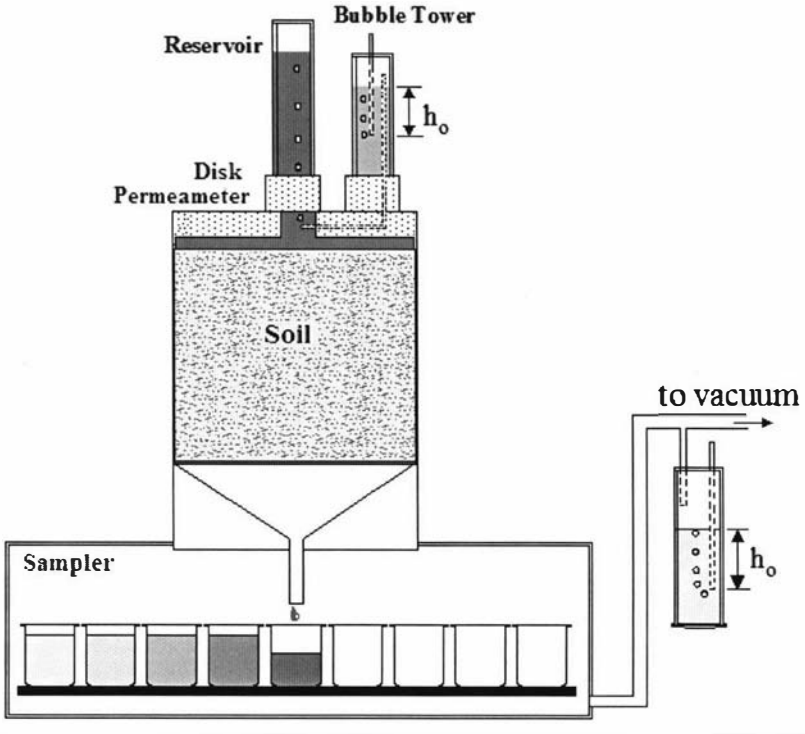


Figure 4.1. Schematic of the leaching apparatus used in the miscible displacement experiments.

4.2.3.3. Soil and leachate analyses

The leachate aliquots were analysed for pH and the concentrations of sulphate, chloride, calcium, potassium and magnesium. Similar analyses were carried for the soils before and after leaching. Sulphate was extracted using KH_2PO_4 (0.01 M), and NH_4OAc (1.0 M) was used to extract cations. Soil pH was measured in water. Calcium, potassium, and magnesium were determined using atomic absorption spectroscopy, sulphate was measured by

the methylene blue method (Johnson and Nishita, 1952), and chloride by the mercury thiocyanate-iron method (Florence and Farrar, 1971).

To assess the performance of the analyses, since we used only one replication, the ion mass balance (β, %) was evaluated. β was defined as the ratio between the sum of the final ion amount in the soil (Q_F) plus the amount collected in the leachate (Q_L), and the sum of the initial amount of ion in the soil (Q_I) plus the amount added via leaching solution (Q_A):

$$\beta = 100\frac{Q_F + Q_L}{Q_I + Q_A} \qquad [4.1]$$

4.2.4. Results and discussion

The mass balance for chloride, calcium, and sulphate for each leaching column is presented in Table 4.3. The recovery for all solutes was close to 100%, indicating good performance of the experimental procedure.

The BTCs for sulphate highlight the differences between the soils with respect to cation-induced sulphate leaching (Figure 4.2). The BTCs for Taupo soil indicate negligible sulphate sorption for this soil, even though it was applied simultaneously with calcium. There was no effect of the concentration of $CaSO_4$ leaching solution on the shape of BTC. However the spread of the solution, or its dispersivity, was slightly greater for intact soil columns than for repacked ones. For the columns with Egmont soil where sulphate was applied with calcium (e.g. E_2), the BTCs were noticeably delayed, indicating that sulphate adsorption has occurred (Figure 4.2b). On the other hand, when using potassium as the accompanying cation (E_3), sulphate was only slightly retarded (adsorbed) in the Egmont soil, and the BTC was almost identical to those obtained with the non-allophanic Taupo soil. Sulphate retention was also high in the allophanic Taupo soil (column T_a), being even larger than in the Egmont soil (Figure 4.2a). Differences in soil pH might also have influenced these variations in sulphate adsorption. It is known that adsorption

capacity of variable charge components such as allophane is dependent on soil pH. However retention of sulphate in column E_3, leached with K_2SO_4, presents only slightly higher retention compared with the Taupo columns, despite the differences in pH which would favour greater sulphate adsorption in Egmont soil. Therefore, the presence of calcium was the main contributing factor for the increase in sulphate retention.

Table 4.3. Mass balance (%) for chloride (Cl^-), Calcium (Ca^{2+}) and sulphate (SO_4^{2-}) for all soil columns of the miscible displacement experiments on Egmont (E) and Taupo (T) soils.

	E_1	E_2	E_3	E_4	T_a	T_1	T_2	T_3	T_4
Cl^-	101.6	103.4	106.7	n.a.	102.6	102.1	104.5	95.7	104.8
Ca^{2+}	94.3	92.4	107.9	98.5	92.8	100.8	100.5	102.4	98.5
SO_4^{2-}	97.6	102.4	93.5	102.4	95.4	91.7	92.9	94.0	90.6

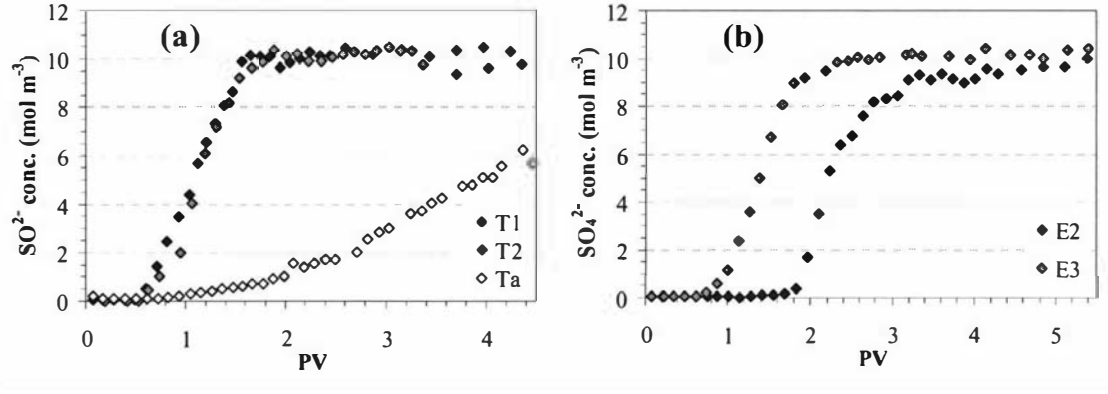


Figure 4.2. Measured sulphate breakthrough curves (BTCs) for some columns with Taupo soil (a) and Egmont soil (b). Columns T_1, T_2, T_a, and E_2 were leached with 0.01 M $CaSO_4$, and E_3 with 0.01 M K_2SO_4. PV is the equivalent pore volumes of the columns.

Similarly, calcium behaviour differed between the two contrasting soils. No significant calcium adsorption occurred in the non-allophanic Taupo soil, and its BTCs followed a predictable pattern, with the concentration dropping from the pre-leaching value to the final leaching level (Figure 4.3a). Again column T_a (allophanic Taupo soil) exhibited a different BTC, closer to those of Egmont soil. For the Egmont soil, only column E_4, which was leached without sulphate, exhibited a calcium BTC with similar shape to those of Taupo soil, although presenting a delay caused by the higher calcium adsorption in this soil (Figure 4.3b). Those columns leached with $CaSO_4$ solution (e.g. E_2) showed an additional calcium adsorption which caused a significant drop in the concentration of the leachate solution. This drop coincided with the decrease of chloride, and subsequent rise of sulphate concentrations. Measurements of magnesium and potassium confirmed that, at this stage, calcium was the only major cation present. Although column E_3 was pre-leached with more than six PV of potassium solution, a small concentration of calcium could still be measured in the output solution when the leaching (with sulphate) started. This concentration also dropped to almost zero before sulphate could reach the end of the column, indicating again interaction between calcium and sulphate.

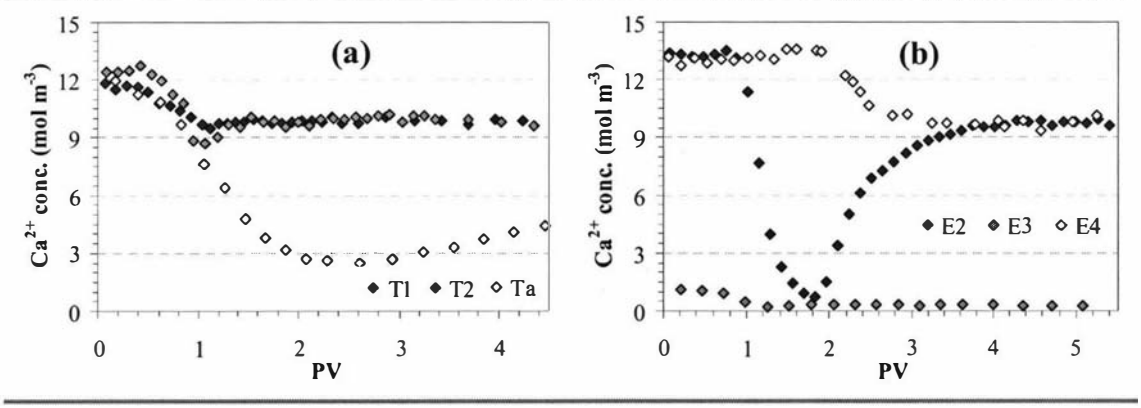


Figure 4.3. Measured calcium breakthrough curves (BTCs) for some columns with Taupo soil (a) and Egmont soil (b). Columns T_1, T_2, T_a, and E_2 were leached with 0.01 M $CaSO_4$, and E_3 with 0.01 M K_2SO_4, and E_4 with 0.01 M $CaCL_2$. PV is the equivalent pore volumes of the columns.

These results suggest that there are cooperative interactions between sulphate and calcium in the Egmont soil that enhance their adsorption. Some authors (Bolan *et al.*, 1993; Cajuste *et al.*, 1998), suggested that specific adsorption of calcium could lead to an increase in positive charge, and therefore promote additional amount of anions, such as sulphate and chloride, to be adsorbed. However the chloride BTC obtained from the column leached without calcium (E_3), was nearly identical to that with calcium (E_2) (Figure 4.4). This indicates that there was no response by chloride to this possible charge enhancement, as would be expected in this case. Furthermore, the shapes of the calcium BTCs (Figure 4.3) show that the adsorption of calcium was also noticeably influenced by the presence of sulphate.

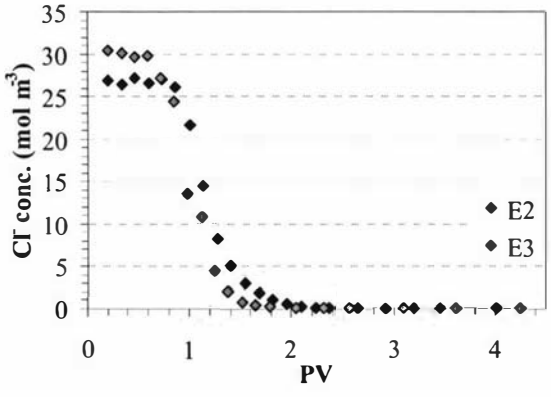


Figure 4.4. Measure chloride breakthrough curves (BTCs) for some columns of Egmont soil. Column E_2 was leached with 0.013 $CaCl_2$, followed by 0.01 M $CaSO_4$, and E_3 with 0.03M KCl followed by 0.01 M K_2SO_4. PV is the equivalent pore volumes of the columns.

In a similar way, sulphate-specific adsorption can be ruled out as the sole explanation for the observed increase in the adsorption of calcium. Specific adsorption of anions has been reported to occur in variable-charge soils, especially with phosphate (Ryden and Syers, 1976; Bolan *et al.*, 1988; Agbenin, 1996; Bolan *et al.*, 1999b; Mora *et al.*, 2005), but also occur with sulphate (Alva *et al.*, 1990; Curtin and Syers, 1990). However for column E_3,

where the leaching solution was K_2SO_4, the adsorption of sulphate was very small (Figure 4.2a), and similar to those from Taupo soil (Figure 4.2b).

Some specific adsorption of sulphate might also have occurred, however. The amount of adsorbed sulphate in column E_3, although very small, was enough to alter the pH of the soil solution (Figure 4.5). A pH increase, probably caused by the release of OH^- due to ligand-exchange sulphate adsorption, was observed when the chloride concentration was dropping and sulphate was being adsorbed. This would have caused an increase in negative charges, and subsequent adsorption of potassium, and its BTC showed a drop at the same time (Figure 4.6). Columns E_1 (not shown) and E_2 also exhibited a peak in the pH measurements (Figure 4.5), which coincided with the drop in the calcium concentration in the leachate (Figure 4.3). Column E_4 did not exhibit any significant alteration in the pH. This increase in negative charge does not seem to have been enough to explain the shape of the calcium BTCs, although it probably accentuated their shape.

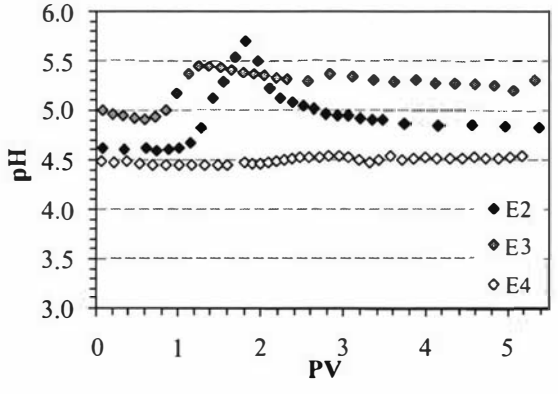


Figure 4.5. Measured pH of the leachate from three columns with Egmont soil. Column E_2 was leached with 0.01 M $CaSO_4$, and E_3 with 0.01 M K_2SO_4, and E_4 with 0.01 M $CaCL_2$. PV is the equivalent pore volumes of the columns.

The mutual adsorption of sulphate and calcium is clearly not negligible, and needs to be considered when modelling sulphur movement in allophanic soils. Assuming a linear Freundlich adsorption isotherm, the BTCs of sulphate reveal a distribution coefficient, k_d, of 0.35 L kg $^{-1}$ for column E_3 and about 1.20 L kg $^{-1}$ for columns E_1 and E_2. The leaching of sulphate could thus be largely over, or underestimated, if co-adsorption, or IPA, with the accompanying cation is not considered. Similarly, the leaching of calcium would also be poorly predicted.

The likelihood of IPA is also strongly supported by comparing the amounts of additional adsorption of calcium and sulphate in the columns. The difference between the final sulphate concentration of columns E_2 and E_3 represented an additional retention of 8.96 mmol kg^{-1} in column E_2, which had calcium as the accompanying cation (the same sulphate concentration applied to both columns). This value is approximately the same as the difference of calcium concentrations between columns E_2 and E_4, namely 8.44 mmol kg^{-1}. Additional adsorption of equivalent amounts of an anion and a cation is one basic tenet of IPA theory (Marcano-Martinez and McBride, 1989; Qafoku and Sumner, 2002).

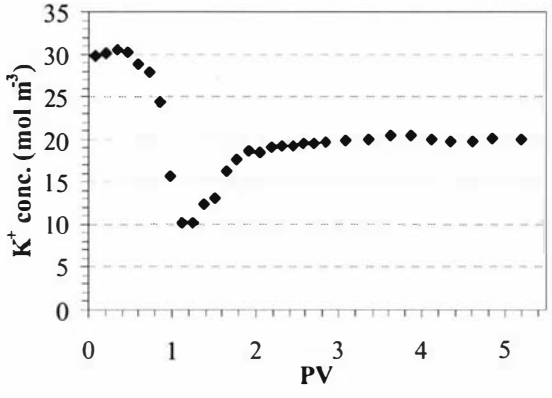


Figure 4.6. Measured potassium breakthrough curve (BTC) of Egmont soil, column E_3 leached with 0.01 M K_2SO_4. PV is the equivalent pore volumes of the column.

The fact that the pH of leachate presented almost no differences before and after simultaneously applying calcium and sulphate, and the equivalent amounts of additional retention of both ions provide strong evidence for IPA in the Egmont soil. The presence of allophane gives this soil its variable-charge characteristic, and this has been commonly related to IPA (Qafoku and Sumner, 2002; Mora *et al.*, 2005). In Taupo soil, almost without allophane, no additional adsorption was observed, whereas column T_a, containing this soil with significant allophane content exhibited quite similar behaviour to the Egmont soil columns.

Studies of ionic interactions which result in IPA are still incipient and the mechanisms involved have yet to be clarified. Soil mineralogy, pH and soil ionic composition are the main factors with influence on sulphate adsorption and movement in allophanic and other variable charge soils. The role of these factors on IPA needs to be addressed. The influence of IPA on ion movement especially in variable charge soils can be large enough not to be ignored, and certainly still demands further studies.

4.2.5. Conclusions

Results from several miscible displacement experiments with two New Zealand soils, Egmont and Taupo, have revealed differences in the adsorption processes. In the case of the low allophane-containing Taupo soil, the adsorption process and the movement of sulphate were not affected by the solution composition. For this soil, the use of intact or repacked columns only changed slightly the dispersive spread of the solute.

In the Egmont soil, with higher allophane content, evidence of ion-pair adsorption (IPA) was found. Both sulphate and calcium adsorption increased significantly when applied simultaneously. Also the molar mass of the extra adsorption due to IPA was similar for both ions. For the Taupo soil, only the column with a significant allophane content showed similar behaviour.

Therefore allophane seems to be a crucial component determining the ion retention capacity of these New Zealand soils. Our results also show that the IPA is likely to occur in allophane-containing soils. The extent of IPA can be large and should not be ignored when describing sulphur or calcium movement in such soils.

CHAPTER 5

5. An adsorption model with IPA – Description and parameterisation

5.1. Introduction

An adsorption model can be defined as a representation of the relevant processes that define the thermodynamic status of a given solute (or solutes) in a soil-solution system. This broad meaning is restricted here as a set of mathematical expressions that can be used for describing the adsorption status of the soil-solution system. That is, the relative amounts of solute dissolved in the solution and that adsorbed onto the soil particles. The description of the equation set used in the adsorption model, and the different procedures used for estimating their parameters are the main subjects of this chapter. A general framework for presenting adsorption data and the description of the relationships between its components is briefly introduced and discussed. Then three mathematical approaches are proposed for describing IPA. These approaches, as well as different ways for their parameterisation, are described.

The term parameterisation is used here to denote the process for estimating values for the parameters of a model. The estimation procedure may or may not provide information on the variability, or degree of uncertainty, of the resolved values. Three different parameterisation procedures, covering a broad range of methodologies for exploring data sets, are employed. These procedures are hereafter referred to as the data analysis, least squares, and inverse modelling methods. Their characteristics are discussed and the resulting parameter sets are compared.

An adsorption data set, obtained in batch experiments using sulphate and calcium solutions in a wide range of concentrations, is presented. This data set is used for estimating the parameters of the adsorption model with IPA by employing the three parameterisation procedures. With the data analyses procedure it was possible to make comparisons of IPA-related relationships using data from different soils presented in published articles and our data from the batch experiments presented in this chapter. The use of these three parameterisation procedures also allowed to compare techniques and to find the best set of parameters and the confidence measures of them.

5.2. Describing solute equilibrium in the soil

Basically the soil-solution system can be considered as a volume of water solution (V_w - L), a mass of soil solids (m_{soil} - kg) with a certain adsorption capacity, and a quantity of solute or ions (Q_{Sol} - mol). A more common characterisation uses the relative ratios, water content (θ - $m^3\ m^{-3}$), soil bulk density (ρ - $kg\ m^{-3}$), and total solute concentration (Q - $mol\ m^{-3}$). The solute equilibrium in this system is represented by the exchanges between the adsorbed (S - $mol\ kg^{-1}$) and dissolved (C - $mol\ m^{-3}$) phases:

$$S \underset{k_{adsorption}}{\overset{k_{desorption}}{\rightleftharpoons}} C \qquad [5.1]$$

A simple adsorption model which describes the partition of Q between these two fractions is commonly expressed by:

$$Q = \theta C + \rho S \qquad [5.2]$$

To be able to compare data obtained under various conditions or with different water-to-soil ratios, as well as to have the three components (Q, C, and S) at the same order of magnitude, the total solute concentration on a soil mass basis (Q_S - $mmol\ kg^{-1}$) can be defined as:

$$Q_S = \vartheta C + S \qquad [5.3]$$

Now the same units are used for both Q_S and S, and C is given in mmol L^{-1} (= mol m^{-3}), and the specific water volume, or water-to-soil ratio, ϑ (L kg^{-1}) is defined as:

$$\vartheta = \frac{\theta}{\rho} = \frac{V_w}{m_{soil}} \qquad [5.4]$$

with ρ expressed in kg L^{-1}.

Note that Equation [5.3] is equal to Equation [5.2] divided by ρ. This form has some advantages for the mathematics, which will become evident later in this chapter. It can be seen that the use of ϑ in Equation [5.3] facilitates its use with data from batch experiments, where commonly V_w and m_{soil} are given, as well as from miscible displacement experiments, or field experiments, where θ and ρ are known.

Adsorption data sets, such as those obtained in batch experiments, are commonly represented graphically as a relationship between S and C (Figure 5.1). However, the quantities actually measured are Q and C; with the values of S subsequently obtained from Equation [5.3]. For simplicity, it is assumed here that the adsorption data are obtained at equilibrium. Therefore each pair (C,S) is referred to as equilibrium data points. Furthermore, the relationship between S and C is expressed mathematically by an adsorption isotherm, such as the Freundlich equation:

$$S = k_F C^N \qquad [5.5]$$

Using this equation in the adsorption model implies that C is the independent variable and S the dependent variable. The underlying objective of the adsorption model, however, is delivering the values of C and S, for a given Q_S.

These relationships for a soil-solution system (Equation [5.3] and Equation [5.5]) can be seen in the adsorption graph (Figure 5.1). The diagonals, representing Equation [5.3] at different values of Q_S, seem to be

generally ignored. These diagonals represent constraints on the values of the equilibrium data points. Consider, for example, the point ① in Figure 5.1. If, for any reason, such as changes in temperature, pH, etc. (apart from changes in the amount of the solute), the adsorption conditions change then exchange between C and S will occur in order to reach a new equilibrium. In this process the equilibrium point will move to another place (point ②), to a different isotherm for example, but it will be along the same diagonal. The point would only move off the diagonal if the amount of solute is changed.

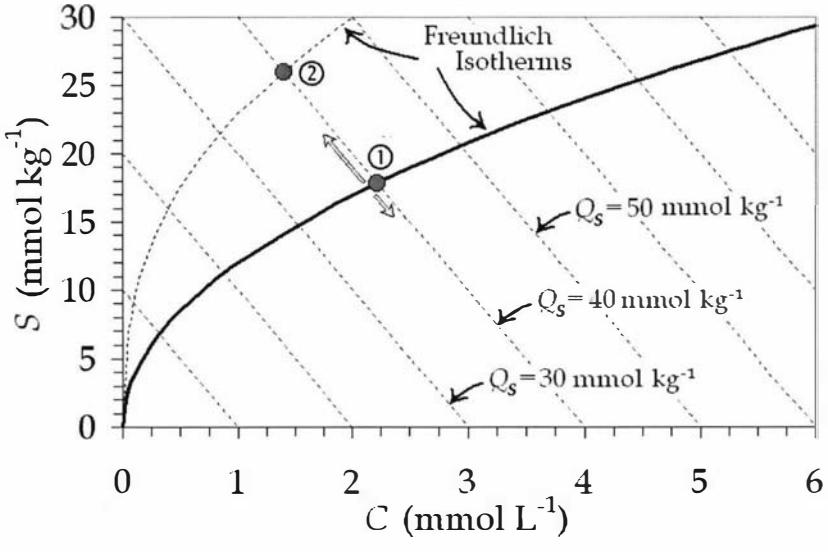


Figure 5.1. Adsorption graph showing the diagonals corresponding to constant solute amounts and two different equilibrium conditions, represented by Freundlich isotherms (k_F = 12 L kg^{-1}, N = 0.5 for continuous line and k_F = 22 L kg^{-1}, N = 0.5 for dashed line). The data point moves from ① to ② due to changes in the equilibrium conditions following the path constrained by Equation [5.3] (Q_S = 40 mmol kg^{-1}). All diagonals assume ϑ = 10 L kg^{-1} (from a batch experiment for example).

Consider now that the addition of another solute causes the equilibrium conditions to change due to induced IPA. This results in an increase in S. The first assumption for the adsorption model with IPA presented here, is that the value of S can be divided into two fractions:

$$S = S_s + S_{IP} \quad [5.6]$$

where S_s (mmol kg^{-1}) is the single solute adsorption described by a classical equation, such as the Freundlich isotherm (Equation [5.5]), and S_{IP} (mmol kg^{-1}) is the additional retention due to IPA. This partitioning of S can be seen in Figure 5.2. Changing the equilibrium point from ① to ② due to IPA results in a decrease in C, and as a consequence of S_s (point ③). This shows that the value of S_{IP} cannot be quantified by analysing the values of C and S in these two points without previously knowing the single species adsorption isotherm. This is a major problem for analysing the extent of IPA, since single-ion isotherms are, in general, difficult to obtain. To account for the values of S_s and S_{IP} mathematical models need to be employed. This demands, due to the high number of parameters, an extensive data set for parameterisation.

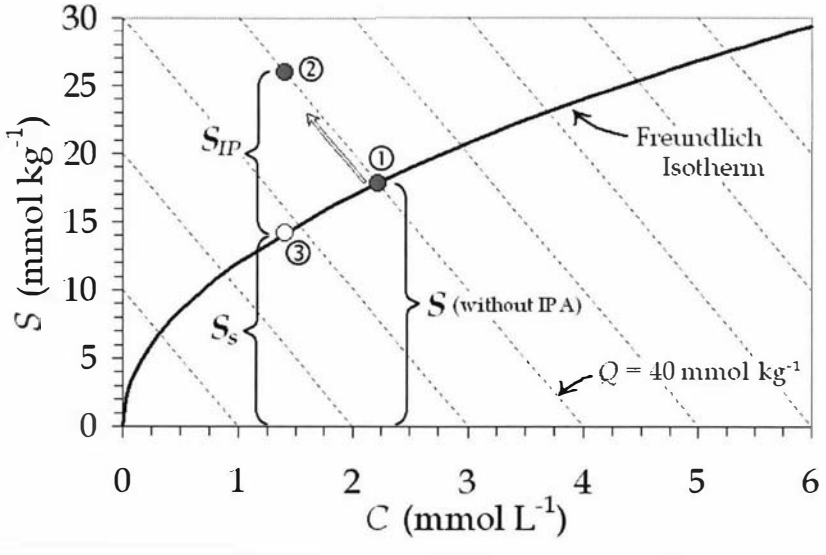


Figure 5.2. Adsorption graph showing the partition of S into S_s and S_{IP}. Point ① represents the initial condition, without IPA, and ② is the final equilibrium with IPA, after the addition of a counter ion. This results in a move from ① to ② following the diagonal described by Equation [5.3] (Q_S = 40 mmol kg^{-1}, ϑ = 10 L kg^{-1}). Point ③ represents the S_s value under IPA equilibrium. The Freundlich isotherm describes S_s (k_F = 12 L kg^{-1}, N = 0.5).

The Freundlich equation has also been used for describing adsorption data sets obtained in the presence of IPA (Marcano-Martinez and McBride, 1989; Bolan *et al.*, 1993; Mora *et al.*, 2005). In these studies IPA and single adsorption were not separated. Therefore, the isotherms can only be used for soil-solution systems with the same ionic combination. The shape of the isotherms in these representations can become quite unusual depending on the combination and concentrations of the solutes. For example, Marcano-Martinez and McBride (1989) found values above unity for N when fitting a Freundlich equation to adsorption data points obtained with equivalent amounts of sulphate and calcium. From these equations, unfortunately, one cannot directly obtain values for S_{IP}.

For the purpose of this thesis, focusing on sulphate and calcium adsorption and their interactions, an adsorption model is based on Equation [5.3] combined with Equation [5.6], and S_{IP} is set to be identical for both ions:

$$Q_{S,i} = \vartheta C_i + S_{s,i} + S_{IP} \qquad [5.7]$$

where the index i represents the solute species and is going to be used hereafter for generalizing the equations.

Because S_{IP} is equivalent and dependent on both solutes, the adsorption model has to consider them simultaneously. The general equilibrium thus can be represented by:

$$\begin{array}{l} S_{s,1} \xleftrightarrow{k_{F,1}} C_1 \\ \qquad\qquad\quad S_{IP} \\ S_{s,2} \xleftrightarrow{k_{F,2}} C_2 \end{array} \qquad [5.8]$$

A generic equilibrium factor is introduced to relate S_{IP} with the other concentrations. For describing this relation, three different approaches are proposed. One relates S_{IP} to S_s and in the other two S_{IP} is related to C. The term IPA equilibrium factor, or simply IPA factor, is used in a general way, independently of the approach considered. As for single adsorption, it is

assumed here that the IPA equilibrium factor is independent of the direction of the reaction (sorption or desorption) and of the solute concentration.

For the description of the different IPA approaches the notation "$2/i$" is introduced as an index for identifying the counter solute. This notation is useful to indicate the counter ion, since i can be either one or two; and helps to simplify the mathematical representation.

5.2.1. Approach 1: Particle governed approach (PGA):

Single species adsorption is considered to be driven by interactions of the solute with the surface of the soil particles. For simplicity it can, therefore, be seen as particle-surface governed adsorption. To describe S_{IP} in a similar way, it is assumed that the additional adsorption is also driven by surface interactions. Consequently, it is assumed that the bigger S_s is the bigger S_{IP} can be. As S_{IP} is assumed to be zero if S_s of any of the two interacting solutes is zero. This condition is met if:

$$S_{IP} \propto S_{s,i} S_{s,2/i} \qquad [5.9]$$

Using a simple equilibrium factor, k_s (kg mmol^{-1}), the equation for this approach becomes:

$$S_{IP} = k_s S_{s,i} S_{s,2/i} \qquad [5.10]$$

This approach renders a linear relationship between S_1 and S_2 when $Q_{S,1}$ is kept constant, as has been shown in some studies (Bolan *et al.*, 1993).

5.2.2. Approach 2: "Linear" solution governed approach (SGA1):

In this approach S_{IP} is related solely to the concentration of the solutes dissolved in the soil solution. This second approach, as well as the third, is a simplified mathematical version inspired by the model presented by Qafoku

and Sumner (2002), and using the ion-pair equilibrium of dissolved salts. The equation for the description of IPA becomes:

$$S_{IP} = \vartheta k_c C_i C_{2/i} \qquad [5.11]$$

where ϑ, the specific water volume, is used to ensure dimensional homogeneity, and k_c (L mmol^{-1}) is the equilibrium factor.

In their article, Qafoku and Sumner (2002) point out that IPA is normally observed in highly leached soils which are composed of particles with opposite net charge (for example, kaolinite (-) and iron or aluminium oxides (+)). According to their approach, the double layer of these two particles can expand to the extent that they overlap each other. This would contribute for mutual neutralisation, but also for creating areas where ions could be trapped without the need for surface-charge balancing. That could also allow salt adsorption or IPA to occur (Figure 5.3). This overlap, and therefore the amount of IPA, may be a function of the ionic strength of the soil solution (Qafoku and Sumner, 2002).

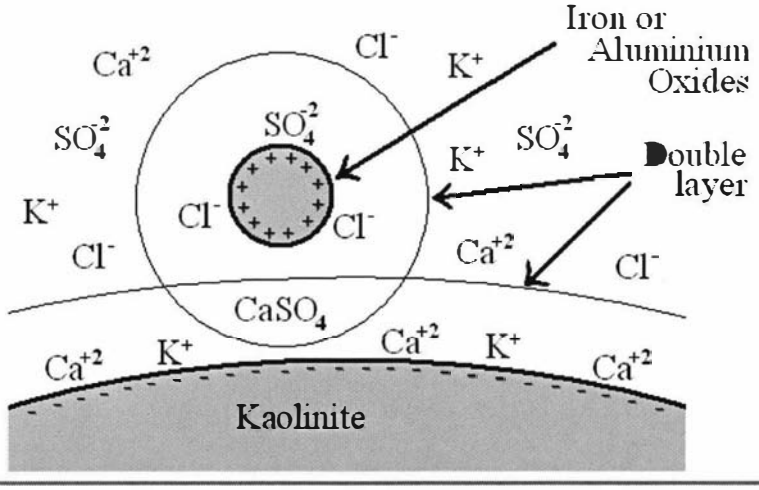


Figure 5.3. Schematic of the IPA model from Qafoku and Sumner (2002). The overlap of the double layer of two soil particles with opposite charge can trap ions as ion-pairs.

When a salt is dissolved in water its molecules usually dissociate into individual ions. However, this dissociation is not complete, even below the concentration where precipitation would occur, and ion-pairs are formed (Oldham and Myland, 1994). The equilibrium between the ion-pairs and the dissociated ions of salt solutions is described by an equilibrium constant, k_b (L mmol^{-1}):

$$k_b = \frac{C_{anion} C_{cation}}{C_{Salt}} \qquad [5.12]$$

where C (mmol L^{-1}) is the concentration of the subscripted species in the solution.

Note the similarity of this description with Equation [5.11]. It seems reasonable to imagine that the bigger the likelihood of having ion-pairs in the soil solution, the more likely it is that these pairs would be retained in the soil, trapped in the overlaps of the soil particles double layers. Multivalent ions have smaller k_b than monovalent ions, and therefore more ion-pairs (Oldham and Myland, 1994). They are also more likely to exhibit IPA in soils (Ajwa and Tabatabai, 1995a). This was not considered by Qafoku and Sumner (2002), and it is not known of any attempt to make such a link. Further studies should be carried to test this idea.

5.2.3. Approach 3: "Radical" solution governed approach (SGA2):

This approach is similar to the second one, with the concentrations of the solutes dissolved in the soil solution used for estimating S_{IP}. But now the square root of their product is used, and k_r (L kg^{-1}) is the IPA equilibrium factor:

$$S_{IP} = k_r \sqrt{C_i C_{2/i}} \qquad [5.13]$$

This approach has been derived from the analyses of the literature data when estimates of S_{IP} were plotted against $C_i C_{2/i}$. The data presented by

Marcano-Martinez and McBride (1989) had this relationship with a non-linear shape. A generalisation using an exponential equation merging SGA1 and SGA2 could be envisaged. However the square-root seemed to be appropriate for that particular data set as well as for the adsorption data of this thesis. These relations are presented below in the data analysis procedure for estimating the IPA factor. As this third approach was only considered after a paper with the results of the adsorption model fitting had been accepted for publication (presented in Chapter 6), and to avoid the introduction of another parameter, the exponent is set constant to 0.5 and Equation [5.13] is considered an alternative approach.

5.3. Adsorption data set

5.3.1. Methods

Experiments using the batch method were carried out for obtaining a data set describing the adsorption of calcium and sulphate at various concentrations in a New Zealand Allophanic Soil. This soil, Egmont loam soil (a Typic Dystrandept), showed significant evidence of IPA in miscible displacement experiments (as discussed in Chapter 4). Soil samples were collected from between 0.05 and 0.20 m depth, air dried, sieved (2 mm), and stored in plastic bags. Some chemical characteristics of the original soil are shown in Table 5.1.

This soil contained significant amounts of indigenous sulphate and especially calcium (Table 5.1). Thus it would not have been possible to obtain equilibrium solutions at low concentrations from the batch experiments, consequently making it impossible to find values close to S_s. To diminish the influence of the indigenous ions, around 1 kg of soil was packed into a PVC column and leached with different solutions using the same apparatus as in the miscible displacement experiments shown in Chapter 4. This soil column was leached with 4 PV of $MgCl_2$ solution (10 mmol L^{-1}), followed by 4 PV of

KCl (10 mmol L^{-1}), and finally around 3 PV of distilled water. The final ion concentrations in the soil are also shown in Table 5.1. After leaching, the soil was taken out of the column, air dried, and sieved again. This soil was used for most of the batch-experiment equilibrations, only the two basic series, as described below, were performed using the original soil along with the leached one.

Table 5.1. Selected chemical characteristics of Egmont soil, original soil and after leaching with magnesium and potassium solutions:

	Original soil	Leached soil
pH (H_2O)	4.6	4.7
Calcium [1] (mmol kg^{-1})	44.6	7.1
Magnesium (mmol kg^{-1})	8.3	23.6
Potassium (mmol kg^{-1})	4.7	32.3
Sodium (mmol kg^{-1})	7.3	0.9
CEC (mmol kg^{-1})	343	363
Sulphate [2] (mmol kg^{-1})	1.75	0.81

[1] Cations and CEC were determined using NH_4OAc extraction method (pH 7);
[2] KH_2PO_4 extractable.

The batch experiments can basically be divided into five series of adsorption equilibrations. The sulphate adsorption isotherms were determined at two different levels of calcium (0 and 4 mmol L^{-1}), and the calcium isotherms with two different levels of sulphate (0 and 4 mmol L^{-1}). Also the isotherms of both solutes were determined simultaneously at equimolar concentrations.

Nine solution concentrations between 0 and 15 mmol L^{-1} were used in these series. Additional combinations were also used to widen the coverage of possible combinations. A schematic of the (nominal) combinations between solutions with sulphate and calcium used in the equilibrations is shown in

Figure 5.4. A few combinations, due to errors in the preparation of the solutions, did not realise the nominal concentrations, in particular those with equimolar solution, where the actual concentration was around 85% of the nominal value. The results of these equilibrations were still used with the appropriate corrections. All equilibrations were done with duplicate samples. Sulphate solutions were prepared with K_2SO_4 and calcium solutions with $CaCl_2$. The equimolar solutions were prepared using $CaSO_4$, and KCl was used to maintain constant the ionic strength.

Sulphate concentration (mmol L^{-1})	Calcium concentration (mmol L^{-1})								
	0	1	2	4	6	8	10	12	15
0	**xxx**	x	x	xx	x	x	x	x	x
1	x	**x**		x		o		o	
2	x		**x**	x	**o**	o			
4	xx	x	x	**xx**x	x	x	x	x	**x**
6	x		o	x	**x**	o	**o**		
8	x	**o**	**o**	x	**o**	**x**o	o	o	
10	x			x	o	o	**x**o		
12	x	o		x		o		**x**	
15	x			x					**x**

Figure 5.4. Schematic of the combinations of solutions of sulphate and calcium used in the batch experiments. Cells marked with x represent the basic series of isotherms, and o denotes the additional combinations. Two or more symbols in a cell indicate multiple replicates and the symbols in bold specify combinations that did not exactly match the nominal value for at least one of the solutes.

The equilibrations were performed in centrifuge tubes where four grams of air-dried soil was mixed with 25 mL of solution. The soil was dried

only for some ours to facilitate handling, but avoiding over-drying what might have resulted in changing the allophane properties (Shoji et al., 1993). A drop of chloroform was used to inhibit microbial activity. After shaking for 24 hours in an end-over-end shaker at room temperature, the samples were centrifuged for 5 min at 8000 rpm, and filtered (Whatman 42) to separate the solution from the soil. The solution was then stored in a cold room prior to further analysis. Sulphate was determined by the methylene blue method (Johnson and Nishita, 1952), and calcium using atomic absorbance spectroscopy. The adsorbed amount was computed as the difference between the amount in the equilibrium solution before and after equilibration.

5.3.2. Results

The results showed that the adsorption of both calcium and sulphate was influenced by the presence of the respective counter ion. The adsorption of sulphate almost doubled when calcium was present at large concentrations. Calcium showed higher overall adsorption as compared to sulphate. The addition of sulphate in the solution also caused a marked increase in the sorption of calcium. The data set is summarised in Figure 5.5, and the individual series are shown in more detail later in this chapter. The diagonals with equi-amounts of solute are clearly visible in Figure 5.5. Using a simple linear relation along these diagonals the adsorption values at zero content of the counter ions were inferred. These estimates, also shown in Figure 5.5, are very similar to the data obtained at minimum concentration of the counter ion. This was somehow not expected, especially for sulphate, since the amount of calcium in the soil, even after leaching, was still considerable (Table 5.1). This might also indicate that 7.1 mmol kg^{-1} of calcium have little influence on sulphate adsorption. On the other hand, the data set showed significant variability and the statistical uncertainties for these estimates were found to be quite high (up to 13%).

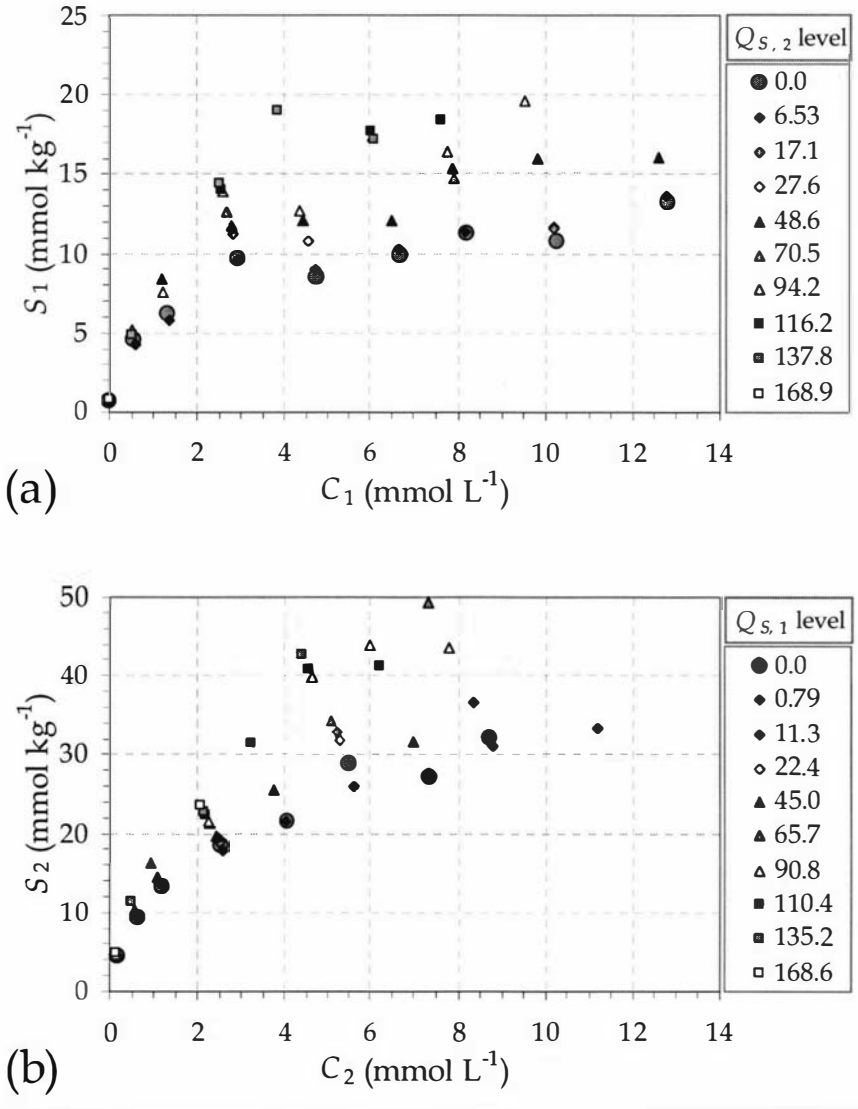


Figure 5.5. Measured adsorption data for sulphate (a) at different levels of calcium (Q_2, mmol kg^{-1}), and for calcium (b) at different levels of sulphate (Q_1, mmol kg^{-1}). The series labelled as zero level represents estimates of the adsorption values at the absence of the counter-ion. The procedure to estimate them is explained in the text.

The influence of the indigenous counter ion on the results of the experiment can be seen by comparing the adsorption isotherms obtained in the original soil with those of the leached soil (Figure 5.6). For sulphate the adsorption was greater in the original soil as compared to the leached one,

while no visible differences could be observed for calcium. The influence on the sulphate adsorption was expected because of the significantly higher amount of indigenous calcium (Table 5.1). This supports the decision to use the leached soil for most of the equilibrations.

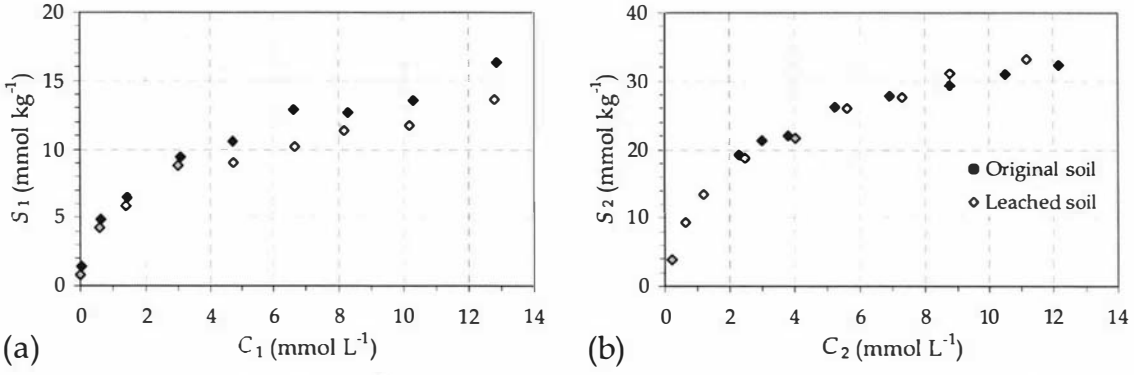


Figure 5.6. Measured adsorption data for sulphate (a) and calcium (b) determined with solutions of K_2SO_4 or $CaCl_2$ respectively, using either the original or the leached soil.

No significant changes in pH were found at the various solution concentrations for most of the equilibrations (Figure 5.7). Only those series of equilibrations using K_2SO_4 solutions exhibited a slight increase in pH at higher concentrations (with both the original and the leached soil). This might indicate some specific adsorption for sulphate. The presence of calcium somehow inhibits this pH increase, since equilibration with $CaSO_4$ or with a K_2SO_4 plus $CaCl_2$ did not exhibit any significant pH alterations.

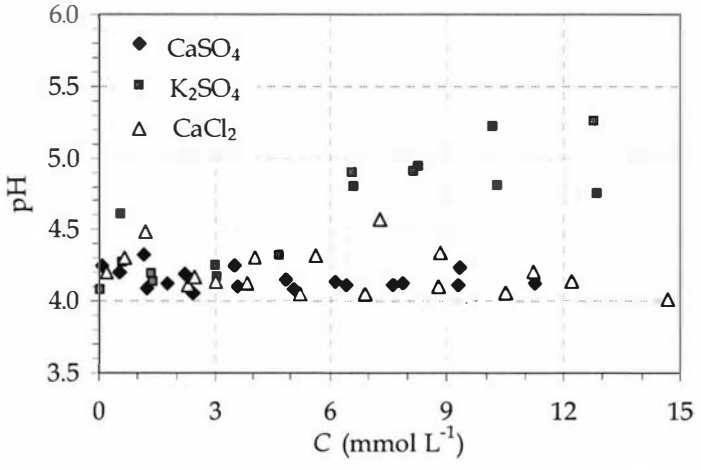


Figure 5.7. Variations in the pH of the solution after equilibration in the batch experiments plotted against the solutes' concentration.

5.4. Parameterisation of the adsorption model

5.4.1. Procedure 1 – Data Analysis

This procedure is referred to as "data analysis" because the parameters of the adsorption model are estimated by exploratory analysis of experimental data sets. Data sets from two published articles (Marcano-Martinez and McBride, 1989; Bolan *et al.*, 1993) are initially used and later the adsorption data set presented above is also explored. Because there are insufficient data in the published articles, no actual model fitting is performed in this analysis, and therefore the parameter uncertainties are not considered. Estimates of the values for the IPA factor are pursued in this analysis in order to compare the different soils in relation to IPA. Also the different approaches could be compared in different soils.

This procedure was primarily used to identify the possible approaches for describing IPA. Therefore the following discussion also supports the presentation of the three approaches. The relationships established in this procedure, and the parameter values found, are also used for comparisons

between the adsorption data of this thesis and those with different soils from the literature.

5.4.1.1. Summary of the published data sets

Bolan *et al.* (1993) presented results from batch experiments with four different soils, two variable-charge soils from the pacific islands (Seqaqa and Fagaga) and two constant-charge soils from England (Davistow and Healaugh). Sets of adsorption equilibrium data for sulphate were obtained with and without a background concentration of calcium (15 mmol L^{-1}). K_2SO_4, $CaSO_4$, and $CaCl_2$ solutions at concentrations between 0 - 15 mmol L^{-1} were used. Freundlich isotherms were fitted to the adsorption data (Figure 5.8a). Additionally, linear relationships were presented to describe the increase in sulphate adsorption at increasing calcium concentration (Figure 5.8b).

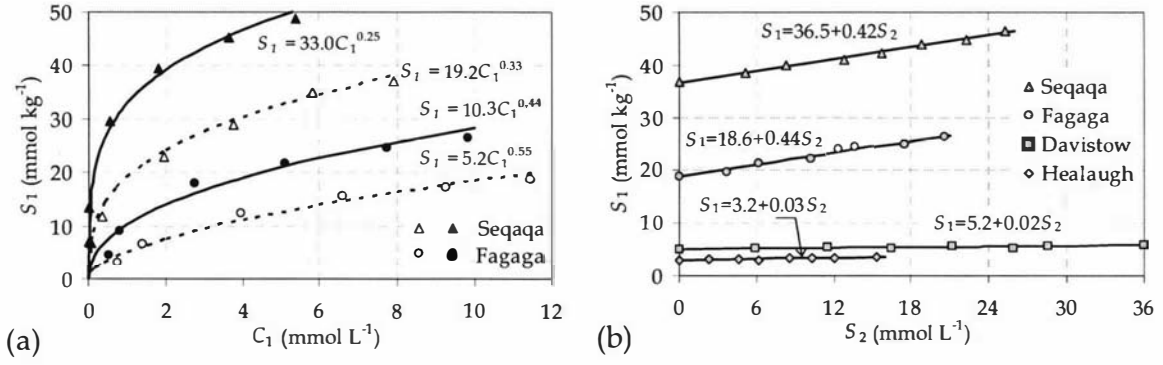


Figure 5.8. (a) Adsorption isotherms for sulphate with (black symbols) and without (white symbols) calcium in two tropical soils. In (b) the enhanced sulphate adsorption (S_1) at increasing amounts of calcium (S_2) in four soils presented by Bolan *et al.* (1993).

The data presented by Marcano-Martinez and McBride (1989) that are of interest here, comprise the Freundlich isotherms for sulphate and calcium in two tropical variable-charge soils from Brazil. The soils are both oxisols from the A horizon, and are described as dark-red (DRA) and red-yellow (RYA). The isotherms were determined for both ions alone, using K_2SO_4 or $CaCl_2$

respectively, and combined, using $CaSO_4$. Similar to the previous study, the Freundlich isotherm was fitted to the data sets with and without the counter ion without separating S_s and S_{IP} (Figure 5.9).

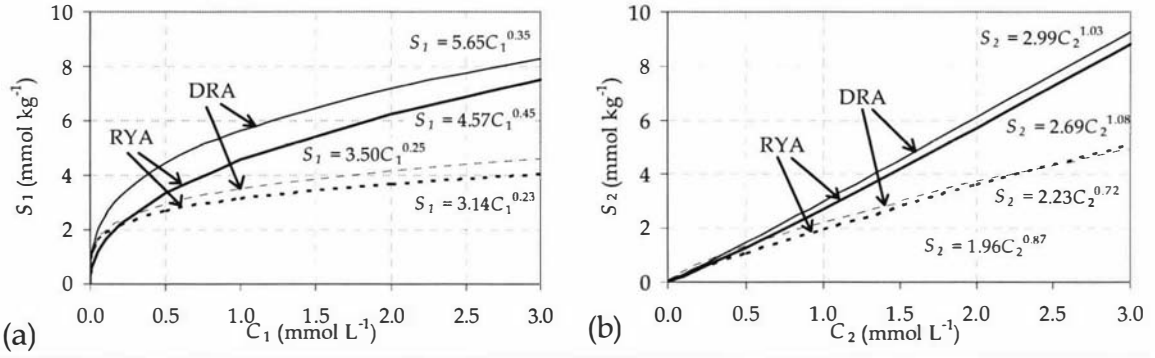


Figure 5.9. Freundlich adsorption isotherms for sulphate (a) and calcium (b) for two tropical soils. Data were obtained with the counter ion (continuous line) or without (dashed line) (adapted from Marcano-Martinez and McBride (1989)).

5.4.1.2. Estimating the IPA factor – Literature data

To estimate values of k_s in Equation [5.10], using the linear relationship presented by Bolan *et al.* (1993) shown in Figure 5.8b, consider the general form:

$$S_1 = S_{s0,1} + bS_2 \qquad [5.14]$$

where $S_{s0,1}$ (mmol kg^{-1}) is the amount adsorbed of solute 1 (sulphate) without calcium, and b is the fitting slope.

For finding k_s values using these data, Equation [5.14] can be re-written as:

$$S_{s,1} + S_{IP} = S_{s0,1} + b\left(S_{s,2} + S_{IP}\right) \qquad [5.15]$$

And rearranging:

$$S_{IP} = \frac{1}{(1-b)}\left(S_{s0,1} - S_{s,1} + bS_{s,2}\right) \qquad [5.16]$$

And equating with Equation [5.10]:

$$k_s S_{s,1} S_{s,2} = \frac{1}{(1-b)}\left(S_{s0,1} - S_{s,1} + bS_{s,2}\right) \quad [5.17]$$

Finally, isolating k_s:

$$k_s = \frac{1}{S_{s,1}(1-b)}\left(\frac{S_{s0,1} - S_{s,1}}{S_{s,2}} + b\right) \quad [5.18]$$

This expression enables the estimation of the value of k_s using the parameters provided by Bolan *et al.* (1993). To evaluate the value of $S_{s,1}$, the isotherm determined without calcium can be used. The k_s values for the four soils used by Bolan *et al.* (1993) are presented in Table 1. The first two soils exhibited the higher response for sulphate adsorption when calcium was added, that is higher S_{IP}, and this can be seen in their respective values for b and k_s. This procedure cannot be used to estimate k_s values from the Marcano-Martinez and McBride (1989) data, since the relationship expressed by Equation [5.14] is not available.

Table 1. Parameter k_s estimated using Equation [5.18] and its parameters as given by Bolan *et al.* (1993):

Soil	$S_{s0,1}$	b	k_s
	(mmol kg^{-1})	-	(kg mmol^{-1})
Seqaqa	36.5	0.42	0.0190
Fagaga	18.6	0.44	0.0311
Davidson	3.2	0.03	0.0041
Healaugh	5.2	0.02	0.0135

Another way to evaluate the values of the IPA factors is by trying to estimate the values of S_{IP}, and then applying the equations of the respective IPA approaches. The adsorption isotherms provided in both articles allow, with some mathematics, the estimation of the values of S and S_s, and consequently S_{IP}. However, because the functions presented did not consider

the assumptions used here to define the IPA approaches, the relationship between the estimated values of S, S_s, and S_{IP} might not be consistent. For example, it is assumed here that the effect of IPA is additive over S_s. However, the use of some of the isotherms presented in the two articles resulted in negative estimates of S_{IP}, at lower concentrations. This is the case of the calcium isotherms provided by Marcano-Martinez and McBride (1989). Statistical, or mathematical, features may be responsible for such discrepancies, such as the value of the parameter N being greater than one. Nonetheless, these estimates of S_{IP} can still provide valuable information about the adsorption with IPA, especially when very low concentrations are avoided.

For the data of Bolan *et al.* (1993), the values of S were obtained at several concentrations of calcium (S_2), using the linear equation provided (Equation [5.14]). Then, using the Freundlich isotherms determined in the presence of calcium, C_1 was obtained. This value was applied to the Freundlich equation determined without calcium, and that results in $S_{s,1}$. Consequently, S_{IP} could be determined. Assuming this value to be the same for calcium, $S_{s,2}$ was found by subtracting S_{IP} from S_2. C_2 could be found using the given isotherm. However only one value for total sulphate ($Q_{S,1}$) could be used, which is the one used in that study.

A similar procedure was employed using the relationships provided by Marcano-Martinez and McBride (1989). Here, S_i and C_i (for both solutes) were estimated giving values for $Q_{S,i}$ and then using the isotherms determined with $CaSO_4$. $S_{s,i}$ was calculated with the isotherms of K_2SO_4 or $CaCl_2$, and then the values of S_{IP} were obtained. Note that $Q_{S,i}$ was equivalent for both solutes. Using these procedures with several values of $Q_{S,i}$, data sets with estimates of S_{IP} were obtained and then employed for assessing values of the IPA factor.

Using the estimated values of S_{IP} and $S_{s,i}$ or C_i, in the respective equations for IPA (Equations [5.10], [5.11], and [5.13]), several values of the IPA factor were found. As expected, large variability was found.

Nevertheless, the average of the values estimated using calcium and sulphate were remarkably consistent for some approaches. That is, the estimates tended to a constant value, if those determined at small concentrations are rejected (Figure 5.10). For the data of Bolan *et al.* (1993) the SGA1 approach rendered more stable results with k_c values of 0.04 and 0.015 L mmol for the two soils. For the other approaches, single values for k_s and k_r are much harder to identify (Figure 5.10a).

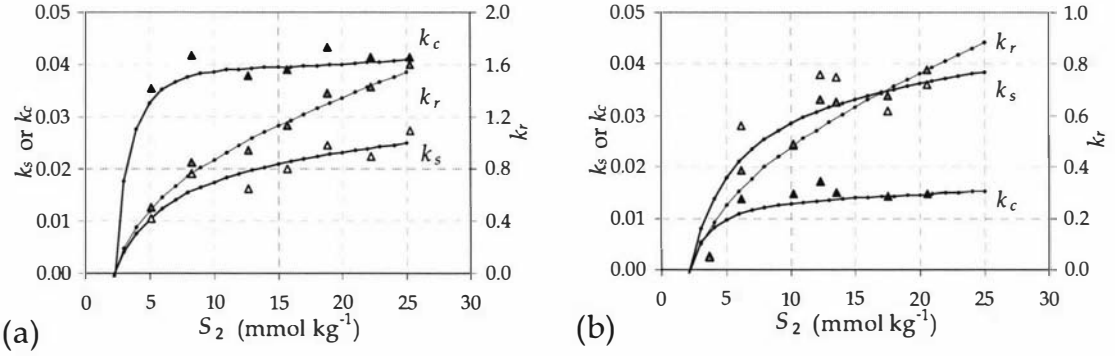


Figure 5.10. IPA factors estimated at various concentrations of calcium (S_2) for Seqaqa (a) and Fagaga (b) soils (adapted from Bolan *et al.* (1993)). Isolated dots are estimates for data values and lines are estimates using the given Freundlich equations.

Conversely the PGA and SGA2 approaches have resulted in more stable estimates of the IPA factor for the Marcano-Martinez and McBride (1989) data, with estimates from both sulphate and calcium isotherms possible. Although large variability was found between estimates at small concentrations, the values did tend to converge (Figure 5.11). Furthermore, the tendencies of the estimated values are very similar for both soils, with k_s at about 0.15 kg mmol^{-1} and k_r around 1.2 L mmol^{-1}. Unlike the other approaches, or to the data of Bolan *et al.* (1993), the results using SGA1 exhibited higher estimated values of the IPA factor at lower concentrations (Figure 5.11b and e).

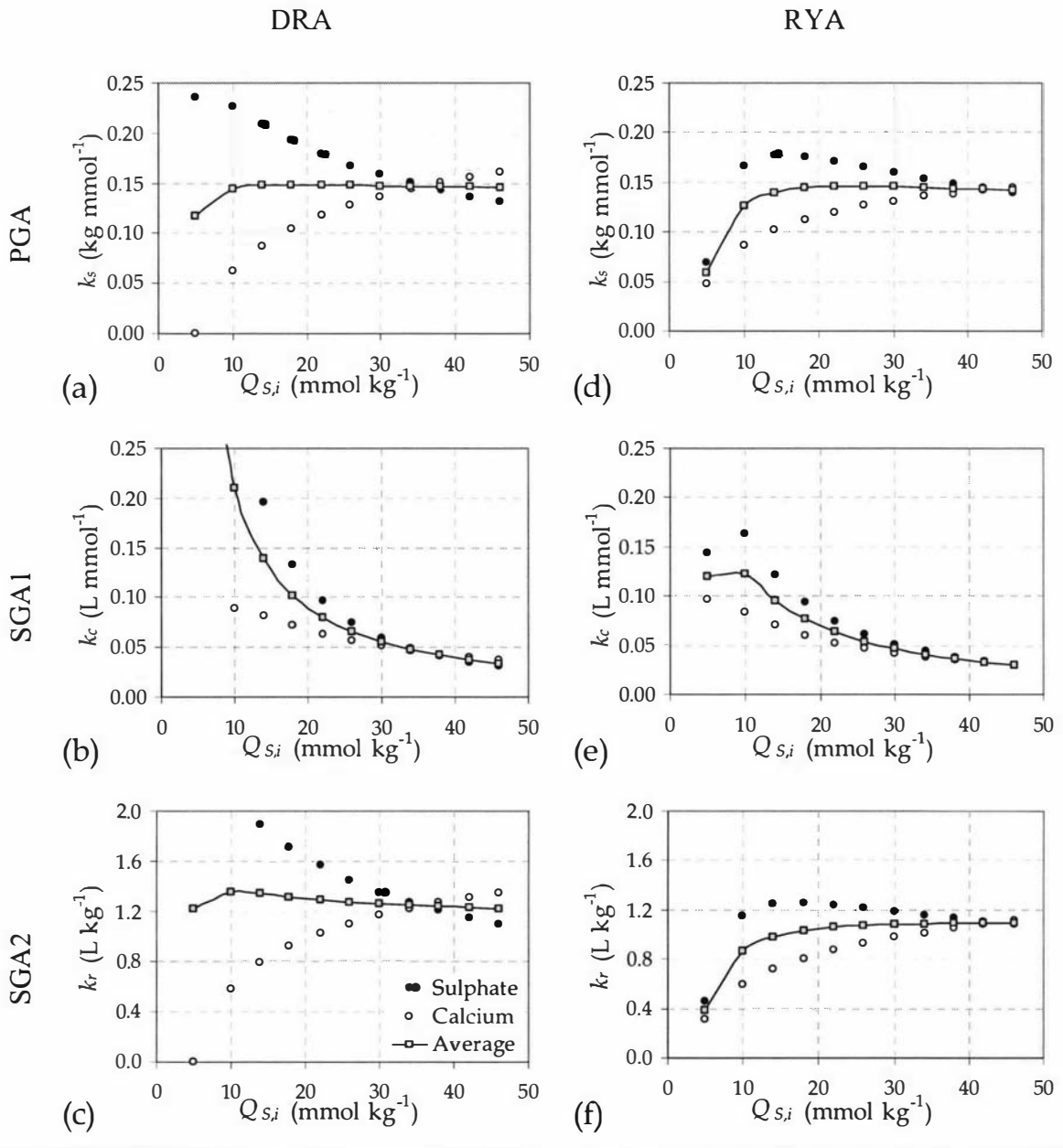


Figure 5.11. IPA factor estimated at various concentrations of sulphate and calcium, at equivalent amounts for two soils presented by Marcano-Martinez and McBride (1989). Dots represent estimates using sulphate (●) or calcium (○) values and their average (■).

To avoid dealing with several values of the IPA factor, a different analysis can be performed using the linearised forms of the IPA approaches. The linearised forms were obtained by plotting the several estimated values of

S_{IP} against the product in the right-hand side of the equations for IPA (Equations [5.10], [5.11], and [5.13]). A unique value for the IPA factor is then obtained by simply estimating the slope of this relation.

The results of these analyses are presented in Figure 5.12 and 5.13, for the data of Bolan *et al.* (1993) and Marcano-Martinez and McBride (1989), respectively. For both soils, SGA1 seems to describe best the adsorption data presented by Bolan *et al.* (1993). This agrees with the previous analyses (Figure 5.10), where the IPA factor was most stable with this approach. Also, the values of k_c were very close to those already estimated. The values for k_s and k_r are also of similar magnitude to those previously calculated. Similarly, the results for the data of Marcano-Martinez and McBride (1989) corresponded with the previous analyses. Both PGA and SGA2 seem to better describe the data of both soils, and the values of the IPA factors are also very close to those already estimated.

In addition, it can be pointed out that the variation between the four soils of the IPA factors is reasonably similar for each of the approaches used. The IPA factor for PGA varies roughly one order of magnitude between the soils in the two articles, while it is in the same order for SGA1 and SGA2. Although some of the approaches seem better for one, or other, of the data sets, it is still not possible to favour anyone of them for the general modelling of IPA.

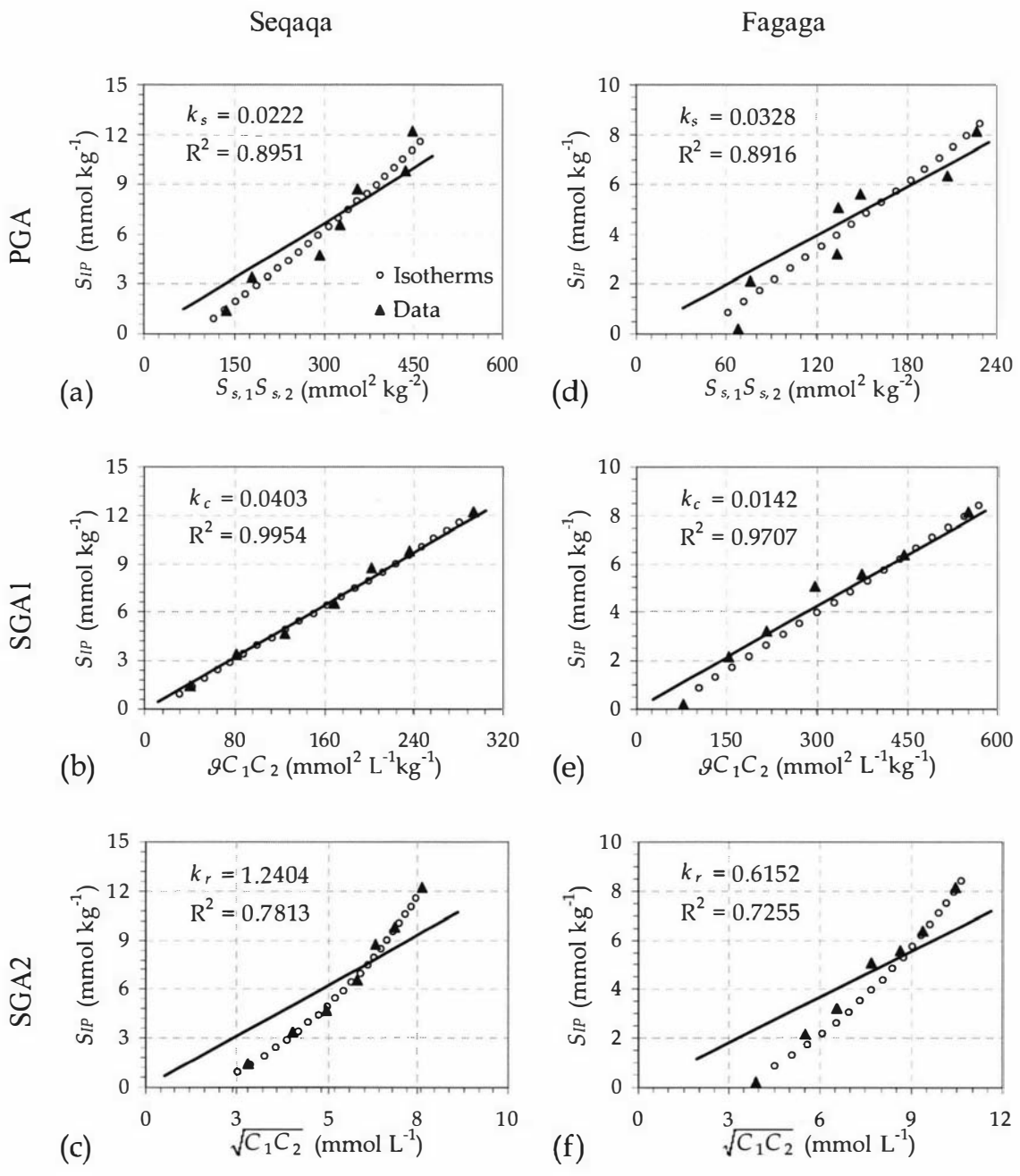


Figure 5.12. Estimates of IPA factor for the three proposed approaches of IPA. Relationship estimated using data or isotherms for two soils presented by Bolan *et al.* (1993). Dots represent S_{IP} estimates from data (▲) and from isotherms (o), and the line is from the linear regression.

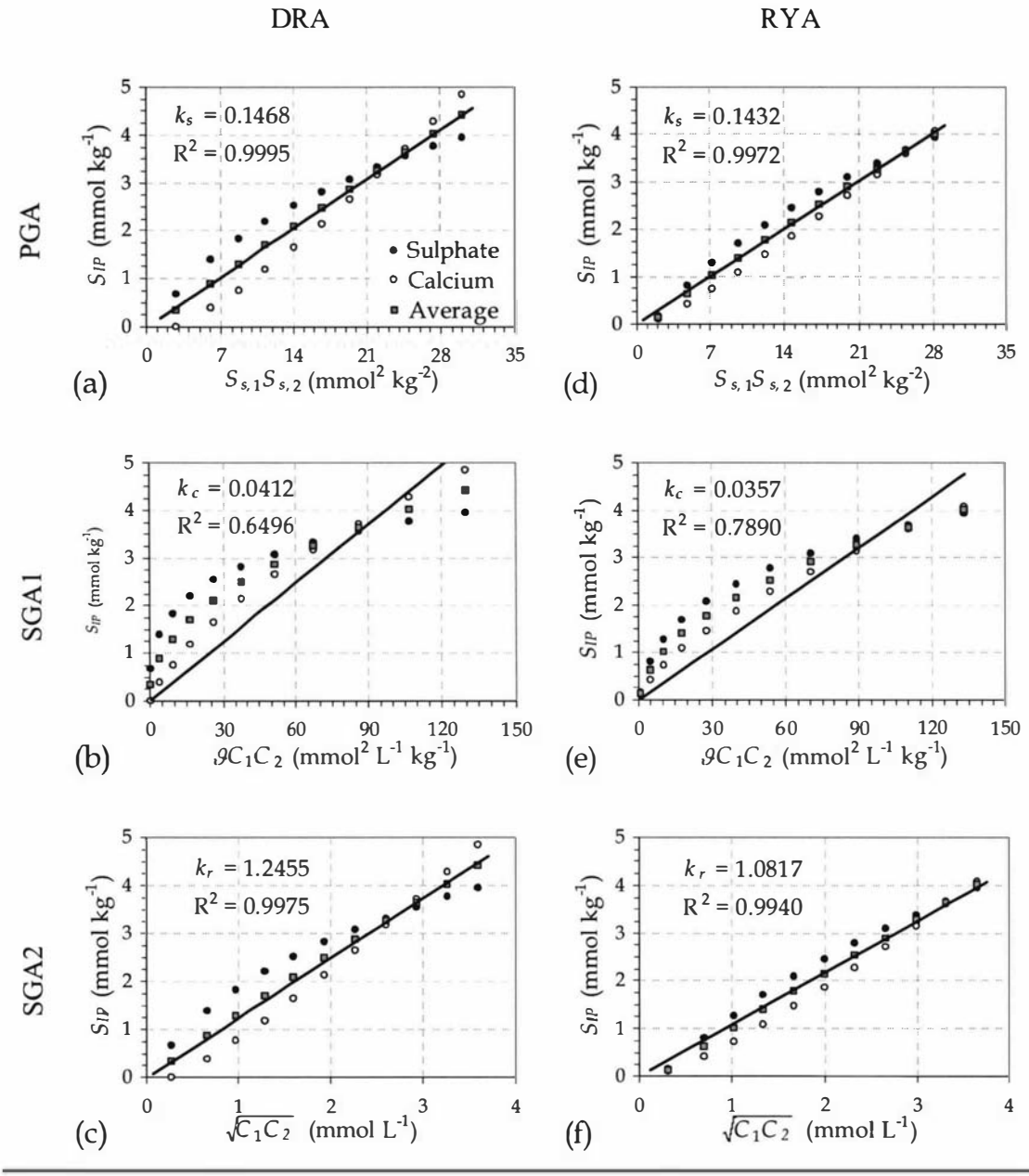


Figure 5.13. Estimates of IPA factor for the three proposed approaches of IPA. Relationships estimated using isotherms from two soils presented by Marcano-Martinez and McBride (1989). Dots represent estimates using sulphate (●) or calcium (○) values and their average (▣), and the line is the linear regression.

5.4.1.3. Estimating the IPA factor – Present data set

To allow comparisons with the results of the two articles previously presented, the adsorption data obtained in the batch experiments with Egmont soil, described in section 5.3, were analysed in a similar way. The Freundlich equation was fitted to selected data sets for estimating values of S_{IP}. Linear relationships for describing the increase of adsorption due to IPA were also used.

The enhancement of adsorption of sulphate in the Egmont soil, with increasing amounts of calcium was described reasonably well by a linear function in similar way as described by Bolan *et al.* (1993). Here, various lines could be obtained, since different amounts of sulphate could be considered. Three examples are shown in Figure 5.14a. Corresponding relationships for describing the increase of calcium adsorption with increasing amounts of sulphate were also obtained. Again the fitting results were reasonably good (Figure 5.14b).

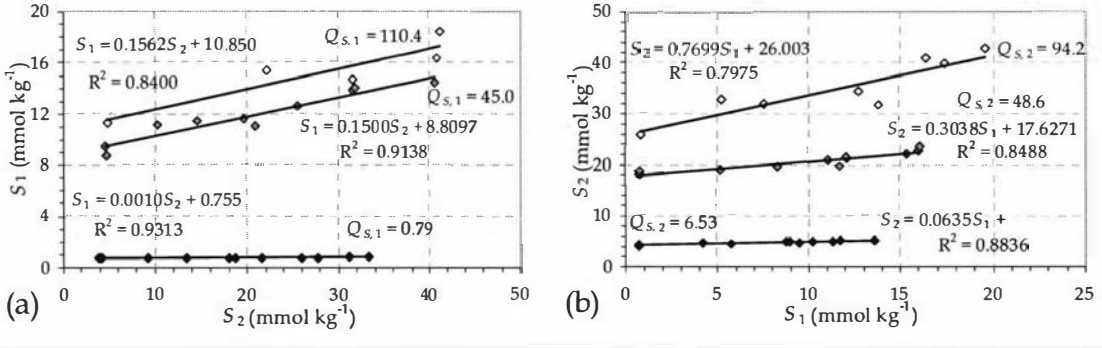


Figure 5.14. Linear relationships for the enhanced adsorption of sulphate (a) and calcium (b), with increasing amounts of the counter ion.

Nonetheless, the estimated values of k_s, using Equation [5.18], showed great variability, especially for those estimates based on calcium (Figure 5.15). These variations are due to differences in the slope of the lines describing

calcium adsorption (Figure 5.14b), however the reasons for this are not known. For sulphate this variability also existed, but to a lesser extent. Despite this problem, a mean value for k_s of around 0.02 kg mmol^{-1}, can be devised in Figure 5.15, disregarding the high values from calcium.

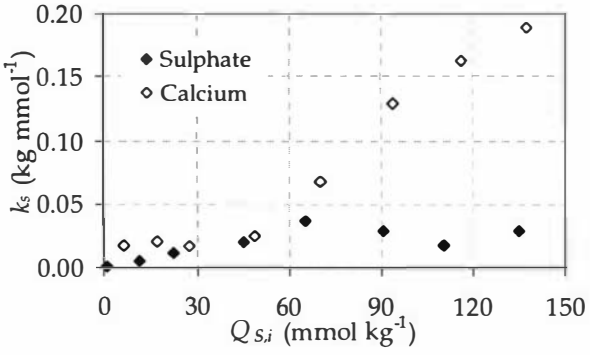


Figure 5.15. Estimated values of k_s using Equation [5.18] with parameters of the linear relationships for sulphate (◆) and calcium (◇).

Freundlich equations were also fitted to the adsorption data from the Egmont soil derived from the equilibration with $CaSO_4$ in a similar way to that described for the Marcano-Martinez and McBride (1989) data. For determining the isotherms without the counter ion, the estimated values presented in section 5.3 were used (see Figure 5.5). The results of these fittings are shown in Figure 5.16. These Freundlich equations were then used to estimate values of S_{IP} and then the values of the IPA factor in the same way as presented earlier for the literature data.

The estimated values for the IPA factor for this soil exhibited similar variation at different concentrations to those form the data of Marcano-Martinez and McBride (1989) and Bolan *et al.* (1993), with great variability at smaller concentrations, and the average tending to a constant value (Figure 5.17a to c). Here the data dispersion is even higher than for those of the literature data. Both PGA and SGA2 approaches provided more consistent estimates, with the IPA factor stabilising at values just above 0.03 kg mmol^{-1}

and 1.2 L mmol^{-1}, respectively. These estimates are very close to the values of the IPA factor determined by the linearisation of Equations [5.10], [5.11], and [5.13] (Figure 5.17d to f). SGA2 seems to be best suited for describing this data set, as its relationship presented the best fit (Figure 5.17f), although PGA had a very similar level of agreement.

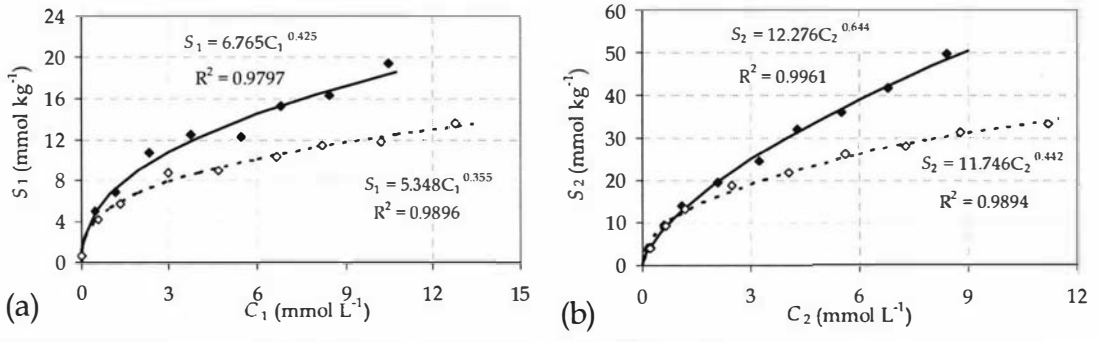


Figure 5.16. Freundlich equations fitted to adsorption data of sulphate (a) and calcium (b). (◆) are results from equilibrations of $CaSO_4$ solutions, and (◇) are estimates of the adsorption without the counter ion.

Similar to the results found for the literature data, all the estimated values for the IPA factor for Egmont soil showed consistency within each approach. Their magnitude is also close to the values from the literature data. For Egmont soil, the approach SGA1 seems to be least suited for describing IPA, similar to the soils studied by Marcano-Martinez and McBride (1989), but contrary to the soils studied by Bolan *et al.* (1993). While PGA and SGA2 showed equivalent goodness of fit for their linearised relationships for the Marcano-Martinez and McBride (1989) data, PGA seems not to be as good as SGA2 for Egmont soil. It is not possible to rule out any of the approaches; however SGA2 seems to be the best approach for describing the adsorption data for Egmont soil.

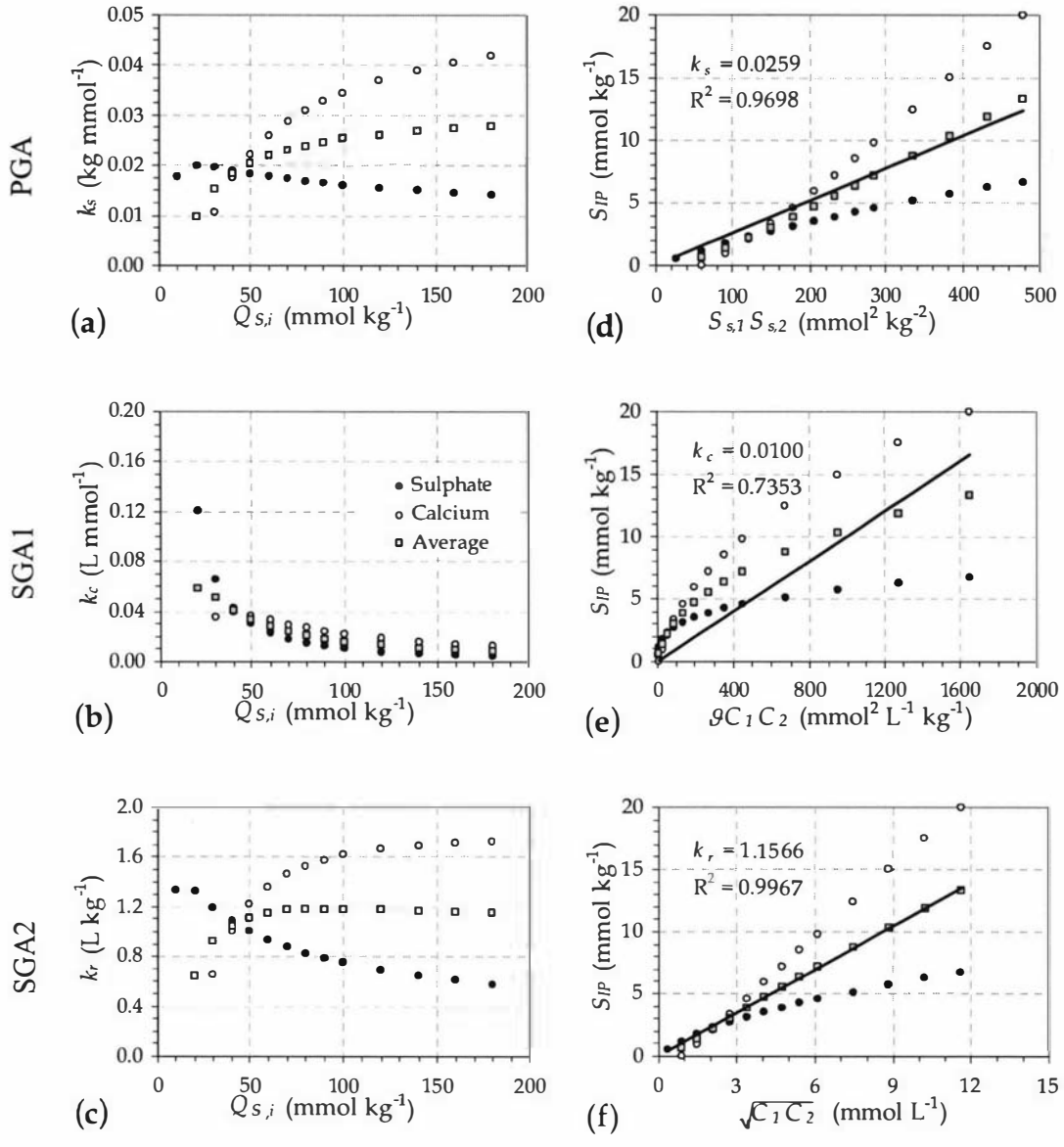


Figure 5.17. Estimates of the IPA factor for the three proposed IPA approaches determined at different concentrations (a, b, c). Linearised relationships of Equations [5.10], [5.11], and [5.13] for estimating a general IPA factor for each of the three IPA approaches (d, e, f). Dots represent estimates using sulphate (●) or calcium (○) values and their average (▣), and the line is the linear regression.

5.4.2. Procedure 2 – Least Squares

The least squares method is probably the most common procedure used for estimating parameter values of a function or model. For this method, it is assumed that the best set of parameters is the one that produces the smallest deviations, or errors, between the observed data (O) and those predicted (P) by the model. Therefore in this procedure the parameter values are varied in the search of a set that minimises an estimator of the deviations. Mathematically the estimator, or objective function (Φ), commonly used is the sum of the squared errors:

$$\Phi = \sum_{j=1}^{n_D} \left(O_j - P_j \right)^2 \qquad [5.19]$$

where j is an integer varying between 1 and n_D, the number of elements in the data set.

Fitting a simple model to a data set using this method is a procedure that has been extensively documented and various statistical packages contain this as a standard feature. Although several independent variables can be used, only one dependent variable is commonly allowed. For a simple adsorption model the value of Q_S is given and the values of C or S are obtained in response. Only C, or S, is needed because they are related. In the case of adsorption with IPA, the model has to be solved for two solutes simultaneously, because S_{IP} is equivalent for both solutes and dependent on their relative concentrations. This means having two independent and two dependent variables. Such a set up is not common in statistical packages. A way used here to overcome this limitation is to sum the two dependent variables, which results in a 3D problem for parameter estimation.

For processing the adsorption data of this thesis, C was chosen as the independent variable, because it facilitates better the mathematical representation. To define the independent variable two possibilities were

considered: the sum of Q_S or the sum of S. The equations of the adsorption model using PGA could therefore be written as:

$$Q_{S,2} + Q_{S,1} = \vartheta(C_1 + C_2) + k_{F,1}C_1^{N_1} + k_{F,2}C_2^{N_2} + k_s\left(k_{F,1}C_1^{N_1}\right)\left(k_{F,2}C_2^{N_2}\right) \quad [5.20]$$

$$S_2 + S_1 = k_{F,1}C_1^{N_1} + k_{F,2}C_2^{N_2} + k_s\left(k_{F,1}C_1^{N_1}\right)\left(k_{F,2}C_2^{N_2}\right) \quad [5.21]$$

Using SGA1:

$$Q_{S,2} + Q_{S,1} = \vartheta(C_1 + C_2) + k_{F,1}C_1^{N_1} + k_{F,2}C_2^{N_2} + \vartheta k_c C_1 C_2 \quad [5.22]$$

$$S_2 + S_1 = k_{F,1}C_1^{N_1} + k_{F,2}C_2^{N_2} + \vartheta k_c C_1 C_2 \quad [5.23]$$

And for SGA2:

$$Q_{S,2} + Q_{S,1} = \vartheta(C_1 + C_2) + k_{F,1}C_1^{N_1} + k_{F,2}C_2^{N_2} + k_r\sqrt{C_1 C_2} \quad [5.24]$$

$$S_2 + S_1 = k_{F,1}C_1^{N_1} + k_{F,2}C_2^{N_2} + k_r\sqrt{C_1 C_2} \quad [5.25]$$

These 3D transformed equations were then entered in the TableCurve™ package (Jandel Scientific) for parameterisation by the least squares method. The parameters found are presented in Table 5.2, and examples of the 3D graphs showing the performance of the fitting procedure are shown in Figure 5.18.

The use of a sum of two variables as the dependent variable is a problem for this procedure, since it may cause bias in the estimation process. Variations in the concentration of one of the solutes may be compensated by variations on the other. This is especially critical if the magnitude of one solute is much bigger than the other. As a consequence, the model's goodness of fit and the values for the estimate errors have to be treated with caution. These values should, however, be useful for a preliminary evaluation, especially for comparisons between the IPA approaches.

The use of Q_S also smoothes the variations in the independent variable, as compared to the use of S (Figure 5.18). This is reflected in the differences of

the values of R^2 (Table 5.2). Nonetheless the obtained parameter estimates were quite similar using either Q_S or S.

Table 5.2. Parameters of the adsorption model obtained by least squares fitting using the three proposed IPA approaches and two different response variables (as explained in the text).

	PGA		SGA1		SGA2	
	$Q_{S,1} + Q_{S,2}$	$S_1 + S_2$	$Q_{S,1} + Q_{S,2}$	$S_1 + S_2$	$Q_{S,1} + Q_{S,2}$	$S_1 + S_2$
$k_{F,1}$	3.425 (1.32)	3.425 (1.32)	8.670 (2.44)	8.702 (2.46)	5.528 (2.26)	5.601 (2.26)
N_1	0.3596 (0.04)	0.3596 (0.04)	0.2624 (0.10)	0.2604 (0.10)	0.1989 (0.12)	0.1947 (0.12)
$k_{F,2}$	10.802 (1.07)	10.802 (1.07)	11.058 (2.22)	11.043 (2.23)	10.319 (2.18)	10.248 (2.20)
N_2	0.4806 (0.04)	0.4806 (0.04)	0.5307 (0.08)	0.5310 (0.08)	0.5119 (0.08)	0.5143 (0.08)
k_s, k_c or k_r	0.0716 (0.03)	0.0716 (0.03)	0.0138 (0.002)	0.0138 (0.002)	1.8477 (0.18)	1.8503 (0.18)
R^2	0.9981	0.9697	0.9968	0.9483	0.9980	0.9683
St. Err.	3.1612	3.1612	4.1276	4.1276	3.2301	3.2301

Notes: The subscript index represents the solute, 1 for sulphate and 2 for calcium. Values in brackets represent the error associated with the parameter estimate. St. Err. is the model's standard error.

Units: $k_{F,1}$: L kg^{-1}; k_s: kg $mmol^{-1}$; k_c :L $mmol^{-1}$; k_r: L kg^{-1}; St. Err.: mmol kg^{-1}.

Remarkably, all the three approaches resulted in similar values for the parameters of the Freundlich isotherm for calcium. Also the errors are relatively small compared to the other parameters. For sulphate the errors are bigger and the estimates are notably different when using different IPA approaches. This may be a result of a higher variability in the sulphate data. The IPA factor presented more variable responses for both the estimate, and its error. The overall results indicate PGA as the most suitable approach, with smaller estimated errors and higher R^2 value.

Visual inspection of the 3D graphs shows very little differences between the approaches if using the sum of Q_S (Figure 5.18). On the other hand, using the sum of S reveals a distinct pattern for SGA1 as compared to PGA and SGA2. This is notable along the C_1 axis, where a better description of sulphate

adsorption is apparent for SGA1 (Figure 5.18e). However, as shown in Table 5.2, this is not evident in the overall result, where SGA1 showed the highest standard error. This feature illustrates the problem with evaluating the model when using the sum of the two solutes as the dependent variable.

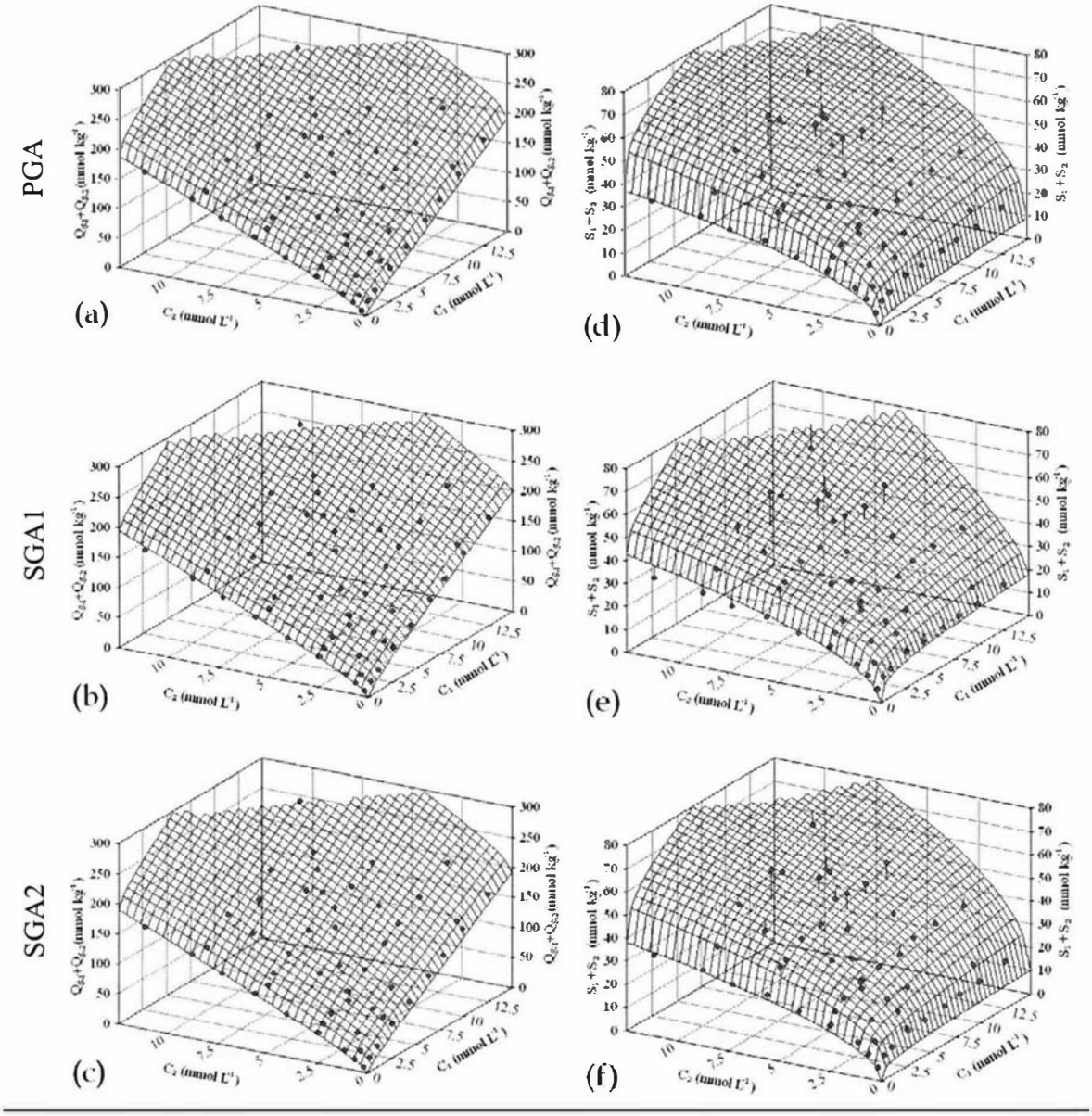


Figure 5.18. 3D representations of the fitting of the adsorption model with IPA using the least squares method. Results for the two response variables and the three proposed IPA approaches are shown.

5.4.3. Procedure 3 – Inverse Modelling

5.4.3.1. Introduction

Inverse modelling is a broad term used in general for referring to an iterative method for analysing the sensitivity of a previously defined model to variations in its parameters. Commonly this procedure is used to search for an optimum set of parameters that makes the specified model to provide the best description of a given observed data set. An objective function is defined, and then used for assessing the agreement between the model and the observed data. The values that minimise the objective function are selected as the optimum parameter set. Different objective functions, as well as procedures for their minimisation, can be used. Here, the maximum-likelihood approach is used, with the assumptions of data independence, and normal (Gaussian) error distribution, that is, first and second-order stabilities (Sen and Srivastava, 1990; Hollenbeck and Jensen, 1998).

This method is valuable for use with models involving complex mathematics, or indirect relations. It also allows the simultaneous evaluation of more than one relation (model) (Hollenbeck and Jensen, 1998; Friedel, 2005; Mertens *et al.*, 2006). This means, theoretically, that this procedure allows the study of models with a broader range of designs and complexity(Sonnleitner *et al.*, 2003; Friedel, 2005). However, the number of simulations needed for a reliable model evaluation can be prohibitively high, especially for complex models with large number of parameters. Also in such cases problems for finding a unique representation (equifinality) of the parameters may arise (Beven and Freer, 2001; Hupet *et al.*, 2003). The analysis of model uncertainties and the evaluation of the confidence intervals for the estimated parameters can also be carried out using this method. However, this is difficult in more complex cases, especially if correlation exists between the parameters, and as visual inspection is not possible for models with more than three parameters (Hollenbeck and Jensen, 1998; Hupet *et al.*, 2005). Nonetheless the flexibility of

this method makes it highly attractive, and its use in water and solute movement studies has been increasing rapidly in recent years.

5.4.3.2. Maximum-likelihood method for inverse modelling

As already mentioned, in this method an objective function is used for assessing the agreement between a given model and an observed data set. A general form of the objective function, for a given parameter (p) of the model, can be written as (Hollenbeck and Jensen, 1998):

$$\Phi(p) = \sum_{j=1}^{n_D} \varphi_j \left[O_j - P_j(p) \right]^2 \qquad [5.26]$$

where O_j represent the observed data values and $P_j(p)$ are the corresponding values predicted using the model with the parameter p, φ_j are weights for the residual values, and j is an integer varying for 1 to n_D, the number of elements in the data set.

Equation [5.26] is the generalised weighted least-squares estimator. With φ_i set to one, it represents the ordinary least squares estimator, while maximum-likelihood estimator is obtained by setting φ_i based on the information of the measurement errors (Hollenbeck and Jensen, 1998).

Searching for the minimal discrepancies between an observed data set and a model's predictions is also the *modus operandi* of the maximum-likelihood estimator. However the discrepancies are now quantified taking into account the uncertainty of the observations. This gives meaning to the variations in the objective function. Here the inverse variance (σ_o^2) in the observations is used:

$$\varphi_j = \frac{1}{\sigma_{o,j}^2} \qquad [5.27]$$

Setting the weighting factor equal to the reciprocal of the data variances formalises the principle that the precision of the parameter estimate should be related to the precision of the data. Using Equation [5.27] as weighting factor

also normalises the squared differences in the objective function to the unit variance. This means that their sum will present a χ^2 probability distribution (Hollenbeck and Jensen, 1998). This property is stronger the larger the data set is, as compared to the number of parameters.

The characteristics of the variations in $\Phi(p)$ represent the information about the parameter p. This can be visualised as in Figure 5.19. The shape of the objective function provides information about the degree of certainty in the parameter estimate. The bigger the curvature of $\Phi(p)$, the smaller the certainty. That is, a deep incised valley-form for $\Phi(p)$ is better than that of a shallow valley-form. Also the objective function provides information on the adequacy of the model. The value of $\Phi(p)$ should be "small" when minimised, which means that only random variations, such as measurement imprecision or natural variability, are responsible for the non-perfect match between the model and the data (a perfect match would have $\Phi(p) = 0$). The rate at which the value of $\Phi(p)$ changes when p varies indicates the sensitivity of the model to that parameter, and provides information about the confidence intervals for the optimum value of p.

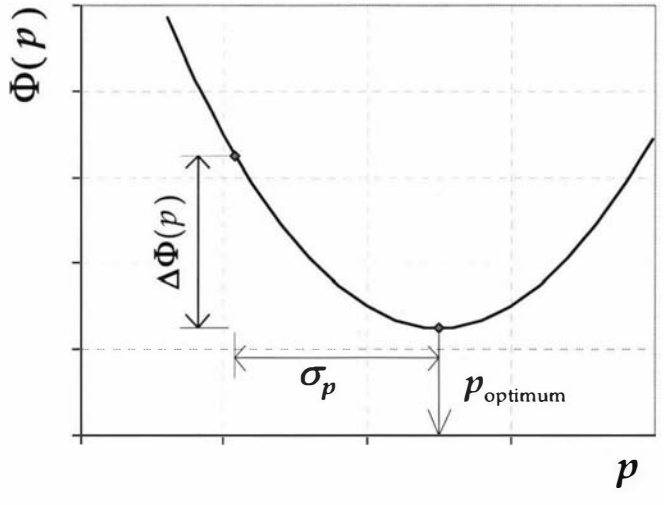


Figure 5.19. Representation of the information about the parameter estimate (p) contained in the objective function ($\Phi(p)$).

Equation [5.27] is the representation for one parameter, but $\Phi(p)$ can be extended to any number of unknown parameters. In this case the graphical representation is no longer a single curve, $\Phi(p)$ is a surface with as many dimensions as the number of parameters. The minimisation of the objective function with a large number of parameters requires an optimisation algorithm and a good set of first "guesses" to initiate the procedure, because the presence of local minima is likely for complex models. Commonly a visual inspection *a priori* is employed for narrowing down the range of the parameter's value and to investigate the relation between the different parameters. These procedures are often time consuming and can become quite chaotic with a large number of parameters, especially if they are correlated.

Once the global minimum value of $\Phi(p)$ is found, the adequacy of the model and the confidence intervals for the parameters can be evaluated. As the maximum-likelihood estimator follows a χ^2 probability distribution (Press *et al.*, 2002), the probability of model adequacy ($\mathcal{P}_{Adeq}$) can be found by:

$$\mathcal{P}_{Adeq} = 1 - \mathcal{D}(\Phi(p), n_D - n_P) \qquad [5.28]$$

where $\mathcal{D}$ is the χ^2 cumulative density function for $\Phi(p)$ minimum and $n_D - n_P$ degrees of freedom, and n_P represents the number of parameters.

The confidence intervals of the estimate of p can also be found using the relationship of the objective function with the χ^2 distribution. Defining the probability level ($\mathcal{P}_{Conf}$), the variation of the objective function is given by:

$$\Delta\Phi(p) = \mathcal{D}^{-1}(\mathcal{P}_{Conf}, n_P) \qquad [5.29]$$

where $\mathcal{D}^{-1}$ is the inverse cumulative χ^2 distribution. The variation in $\Phi(p)$ represents a variation in p (see Figure 5.19). The standard deviations of the estimate of p (σ_p) can be found by defining $\mathcal{P}_{Conf}$ as 68.3% (assuming a normal probability distribution).

However, the description of the confidence intervals of a parameter estimate in models with more than one parameter is more complex. In such

cases the confidence intervals of the parameters are interrelated and a multivariate confidence region should be considered. This confidence region is determined by Equation [5.29] for all possible parameter combinations, therefore it has n_P dimensions. The graphical representation is impossible for more than three parameters and its visualisation is already difficult for more than two (Hollenbeck and Jensen, 1998; Friedel, 2005; Hupet *et al.*, 2005). Common alternatives include calculating σ_p for each parameter using Equation [5.29] with optimum values for the other parameters, or showing the confidence ellipsoids for various pairs of parameters.

5.4.3.3. Objective function for the adsorption model

The choice of the variable to be used for assessing the agreement of the adsorption model with the observed data should again be considered before setting the objective function. Now the limitation for the number of dependent variables, stated in the least squares procedure, no longer holds. The adsorption model can now deal with the question posed at the beginning of this chapter: What are the values of the solute equilibrium components (C, S_s, and S_{IP}) for a given solute amount (Q_S)?

The dependent variable can be any one of the equilibrium components, since the components are related. However, because the observed data set contains C and S, without values for S_s and S_{IP}, only two possible basic objective functions can be devised:

$$\Phi(p) = \sum_{i=1}^{2}\sum_{j=1}^{n_D} \frac{1}{\sigma_{C_{i,j}}}\left[C_{i,j} - \hat{C}_{i,j}\right]^2 \qquad [5.30]$$

$$\Phi(p) = \sum_{i=1}^{2}\sum_{j=1}^{n_D} \frac{1}{\sigma_{S_{i,j}}}\left[S_{i,j} - \hat{S}_{i,j}\right]^2 \qquad [5.31]$$

where $\hat{C}_{i,j}$ and $\hat{S}_{i,j}$ are the j replicate values of solute i estimated by the model using the parameter p.

An exploratory analysis of Equation [5.30] revealed it to be less sensitive (with a higher curvature) to changes in the parameter values as compared to Equation [5.31]. This feature is possibly due to the exponential nature of the relation between *C* and *S*, which means that a small variation in the ion-partition produce larger effect in *S* than in *C*. The minimum value for Equation [5.31] is several times bigger than is for Equation [5.30]. Also these two functions "point" to slightly different values, that is, the estimate of a given parameter is slightly different if using one or another equation. To use the information contained in the variation of both components, a third objective function, coupling C and S, was introduced:

$$\Phi(p) = \sum_{i=1}^{2} \left\{ \sum_{j=1}^{n_D} \frac{1}{\sigma_{S_{i,j}}} \left[S_{i,j} - \hat{S}_{i,j} \right]^2 + \vartheta^2 \sum_{j=1}^{n_D} \frac{1}{\sigma_{C_{i,j}}} \left[C_{i,j} - \hat{C}_{i,j} \right]^2 \right\} \qquad [5.32]$$

where ϑ^2 scales the second term to the same order of magnitude as the first.

This third function has variation pattern somewhat in between of those of Equations [5.30] and [5.31]. However its variation is more difficult to interpret since it is composed by two different variables, *C* and *S*. An example comparing these functions is presented in Figure 5.20. The objective functions were normalised to their minimum value to have them at the same scale. The differences between Equations [5.30] and [5.31] were similar using either SGA1 or SGA2, and considerably smaller using PGA.

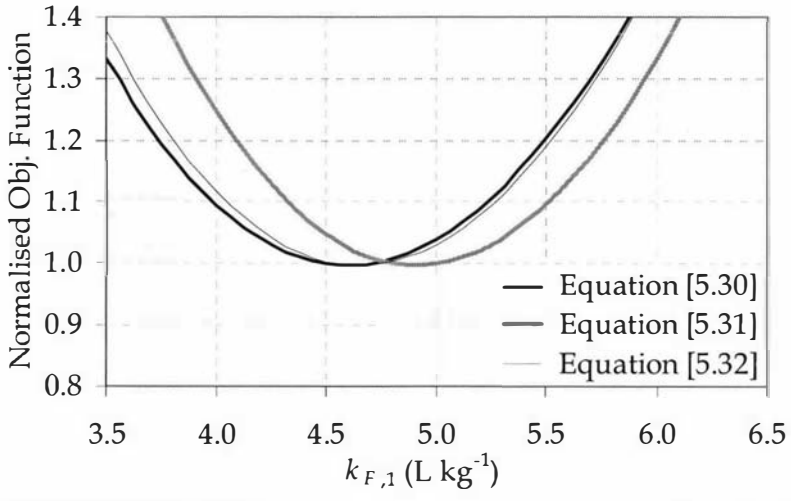


Figure 5.20. Example of a comparison between the variation of the three objective functions normalised to their minima with varying the parameter $k_{F,1}$, using the SGA2 approach.

5.4.3.4. Estimation of the data variance

When using the maximum-likelihood procedure, the variances of the observations (σ_o^2) should be known, or some justifiable estimation of them should be made (Hollenbeck and Jensen, 1998). This is a problem for the adsorption data of Egmont soil, because the variance is not known. Since the batch experiment comprised only two replicates for each equilibration, the values for the variance cannot be directly estimated. To overcome this problem, an exploratory analysis of the measurements was performed, and some functions were devised to relate the variation and the magnitude of the measurements.

To describe the uncertainty of the adsorption data, the variance of each data point was estimated as being composed of two fractions, one due to the measuring procedure (σ_m), and another due to variations in the experiment replications (σ_r), that is, the uncertainties in the preparation and execution of the batch procedure. The variations in the measuring procedure were considered to result from the sensitivity of the measuring device (σ_{m1}) and the

uncertainties in the conversion of the initial measures into concentration (σ_{m2}), using a calibration curve.

The variability of the measuring procedure is easier to estimate compared to the uncertainties in the batch experiment because it does not depend on the number of replicates in the experiment. However, the errors on the measuring device are not expressed in concentration units, so demand conversion. Also, the dilution rate must be taken into account.

To evaluate the sensitivity and repeatability of the measuring "device", data from some samples that were measured several times were used. The variation in these measurements was found to be correlated to the magnitude of the measures for both sulphate and calcium: correlations were found of 0.98 for calcium and 0.85 for sulphate. Linear equations were fitted for their description (Figure 5.21). These variations need to be converted into concentration. For each sample j, this was done using:

$$\sigma_{m1,j} = \sqrt{\left(\frac{\partial y_j}{\partial \mu}\right)^2 \sigma^2_{\mu,j}} \qquad [5.33]$$

where μ is the measure, y_j is the calibration function, and $\sigma_{\mu j}$ is the standard deviation of the measurements of sample j.

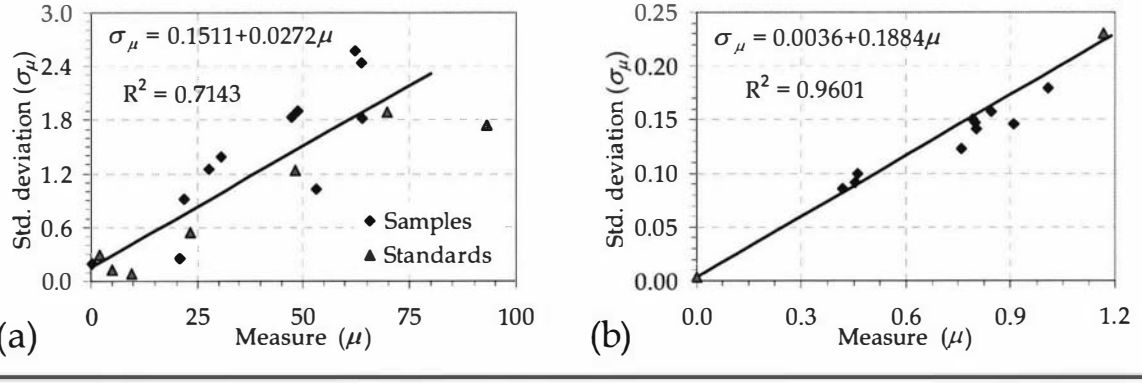


Figure 5.21. Relationships for the standard deviation of the measurements for sulphate (a) and calcium (b). Data comprises some samples of the batch experiment, and some solutions with a standard (known) concentration.

The standard errors of the fittings for the calibration curve were used to evaluate the variations on the measurement procedure due to the conversion of the measurements into concentration. The errors in converting the measurements were found not to be related to the magnitude of the measurements, with correlations index of 0.05 for sulphate and -0.03 for calcium. Therefore, the averages of the standard deviations of the calibration curves were used: with σ_{m2} = 0.51 mmol L^{-1}, from 4 values for calcium, and for sulphate σ_{m2} = 0.29 mmol L^{-1}, from 10 values. The standard deviation for the measuring procedure was then computed by:

$$\sigma_{m,j}^2 = \sigma_{m1,j}^2 + \sigma_{m2}^2 \qquad [5.34]$$

The value of $\sigma_{m,j}$ was further corrected according to the dilution of the respective sample. That is, measurements of samples diluted by a factor of three (2:1), for example, had its deviation ($\sigma_{m,j}$) also corrected by that factor.

The variations between the replicates of the equilibrations in the batch experiments also could be related to the magnitude of the concentration measured (0.62 for calcium and 0.63 for sulphate). Although the correlation is not as large as for the measurement errors, this relation is the better tool available for estimating the uncertainties of the batch procedure. A linear function with intercept at the origin was then assumed (Figure 5.22). The average of the normalised deviations had to be used to estimate the variability of each equilibration:

$$\sigma_{r,j} = \overline{y}_j \frac{1}{n_D} \sum_{j=1}^{n_D} \frac{y_j - \overline{y}_j}{\overline{y}_j} \qquad [5.35]$$

where y_j represents the concentration measured for any of the two replicates of the equilibration j, and $\overline{y}_j$ is the average at each equilibration.

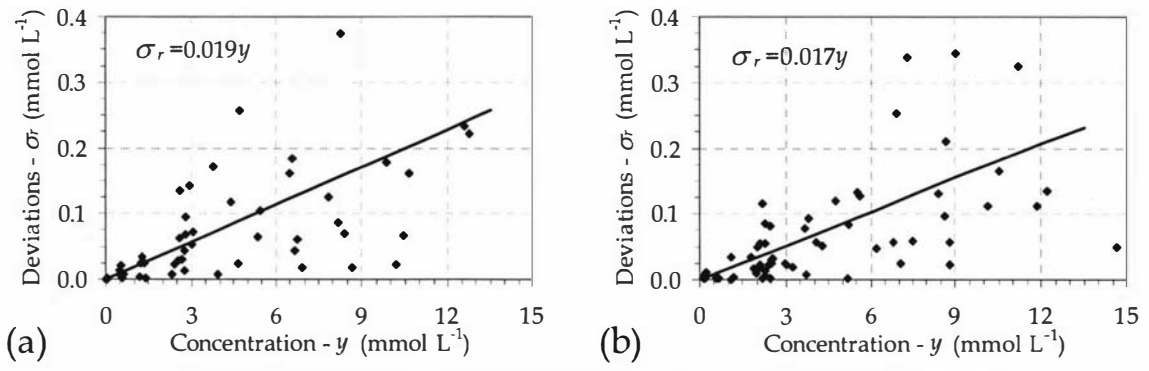


Figure 5.22. Relationships between variation and the magnitude of the concentration in the batch experiment equilibration for sulphate (a) and calcium (b). Dots represent calculated values and the lines are the estimation using Equation [5.35].

The variance of the observations in the adsorption data set was finally estimated by the composition of the two variation fractions:

$$\sigma_{o,j}^2 = \sigma_{m,j}^2 + \sigma_{r,j}^2 \qquad [5.36]$$

5.4.3.5. Fitting the adsorption model

Comparisons between the adsorption data set for Egmont soil and the results of the adsorption model with each of the three proposed IPA approaches were used to explore the model's sensitivity, and to search for the best set of parameters to describe the data set. These comparisons were based on the values of the objective function and the deviations between the estimated values and the observed data. A computer program using VisualBasic language was written for this purpose. A description of this program is given in Appendix B.

The optimised values found using the inverse modelling procedure are similar to those obtained by the least squares procedure, and the relative variations between the approaches also follow comparable patterns. The parameter sets for the adsorption model estimated by inverse modelling are

shown in Table 5.3. In this procedure Equations [5.30] or [5.31] were used as the objective function. Results using Equation [5.31], which contrasts the values of S, are potentially better for comparisons with those from the least squares procedure (those which used $S_1 + S_2$ as the response variable), as both use similar independent variables.

Table 5.3. Parameters of the adsorption model obtained by inverse modelling procedure for the three proposed IPA approaches. Two objective function, Φ_C (Equation [5.30]) and Φ_S (Equation [5.31]), were used. The standard error and R^2 are calculated accordingly for $C_1 + C_2$ and $S_1 + S_2$.

	PGA		SGA1		SGA2	
	Φ_C	Φ_S	Φ_C	Φ_S	Φ_C	Φ_S
$k_{F,1}$	4.241 (1.351)	4.216 (0.146)	6.132 (2.797)	6.540 (0.316)	4.598 (2.628)	4.915 (0.306)
N_1	0.368 (0.185)	0.3479 (0.021)	0.266 (0.235)	0.229 (0.032)	0.295 (0.272)	0.240 (0.041)
$k_{F,2}$	10.921 (1.891)	11.085 (0.230)	12.315 (2.456)	12.774 (0.308)	10.728 (2.312)	10.950 (0.286)
N_2	0.546 (0.112)	0.532 (0.013)	0.510 (0.130)	0.492 (0.015)	0.557 (0.139)	0.543 (0.016)
k_s, k_c or k_r	0.0401 (0.023)	0.0430 (0.003)	0.0188 (0.016)	0.0176 (0.002)	1.6403 (0.933)	1.6430 (0.104)
R^2	0.9752	0.9761	0.9679	0.9695	0.9766	0.9775
St. Err.	2.744	2.690	3.160	3.048	2.673	2.611

Notes: The subscript index represents the solute, 1 for sulphate and 2 for calcium. Values in brackets represent the error associated with the parameter estimate. St. Err. is the model's standard error.

Units: $k_{F,1}$: L kg^{-1}; k_s: kg mmol^{-1}; k_c: L mmol^{-1}; and k_r: L kg^{-1}; St. Err.: mmol kg^{-1}.

Again the PGA and SGA2 approaches rendered better fitting than SGA1. In general, the former two approaches presented estimates of the Freundlich equation parameters more similar to each other than to the SGA1 approach. The similarities exhibited for the calcium Freundlich parameters here are not as strong as those found in the least squares procedure. On the other hand, the Freundlich parameters for sulphate are now much closer to each other than those found in the least squares. The deviations of the estimates by inverse modelling are also more similar for the different approaches. The similarities between the Freundlich parameters amongst the

three IPA approaches are desirable, since this would suggest independence of the IPA description. However, the adsorption model presented here is not deterministic and thus it does not allow reaching such conclusion.

The inverse modelling procedure is better suited for finding the adsorption model parameters than is the least squares method. This is evidenced by the fitting standard errors, which are much smaller here. The improvement was especially significant for the SGA1 approach, with the standard error reduced by some 25%. Unlike in the former parameterisation procedure, here the best overall fitting was reached by using the SGA2 approach for describing IPA, although it is not significantly different from PGA.

Another noticeable difference between the parameterisation results of either the inverse modelling, or the least squares procedures, is the standard errors of the estimated parameters (Table 5.3). Here the deviations are in general much smaller than those estimated in the least squares procedure. This differences may be attributed to the use of different response variables, the different number of degrees of freedom (here double), and the estimation procedure *per se.* The estimated errors of Table 5.3 represent the expected variation of each parameter without variation of the others, that is, without correlation, and with a linear variation. This is an over-simplification, useful for a first evaluation. However, since there are interactions between the parameters, the real confidence intervals should consider theses correlations. This poses a problem, because even graphical representations can only deal with no more than three parameters at once.

To give a better idea of the relationships between the various parameters, graphs comparing the effect of pairs of parameters are presented here (Figure 5.23 to Figure 5.25). These graphs are organised in a matrix fashion contrasting all possible pairs of the five parameters, in each graph the

ellipsoids representing the variation of the objective function (Equation [5.31]) are shown as a function of the two parameters.

Strong non-linearity can be seen in the comparisons between the two parameter of the Freundlich Equation (k_F and N) for each solute, being more pronounced for calcium. This non-linearity makes the values presented in Table 5.3 to be less representative of the real deviations. Comparisons between the parameters tend more strongly to be non-linear when using PGA (Figure 5.23) compared to the other two approaches. Also the PGA approach exhibited greater sensitivity, that is, variations in the objective function are more pronounced when varying the parameters values. As a consequence the estimated errors for the parameter are smaller (Table 5.3). The minimum of the adsorption model is also easier to find, and thus the computer routine is much faster using PGA.

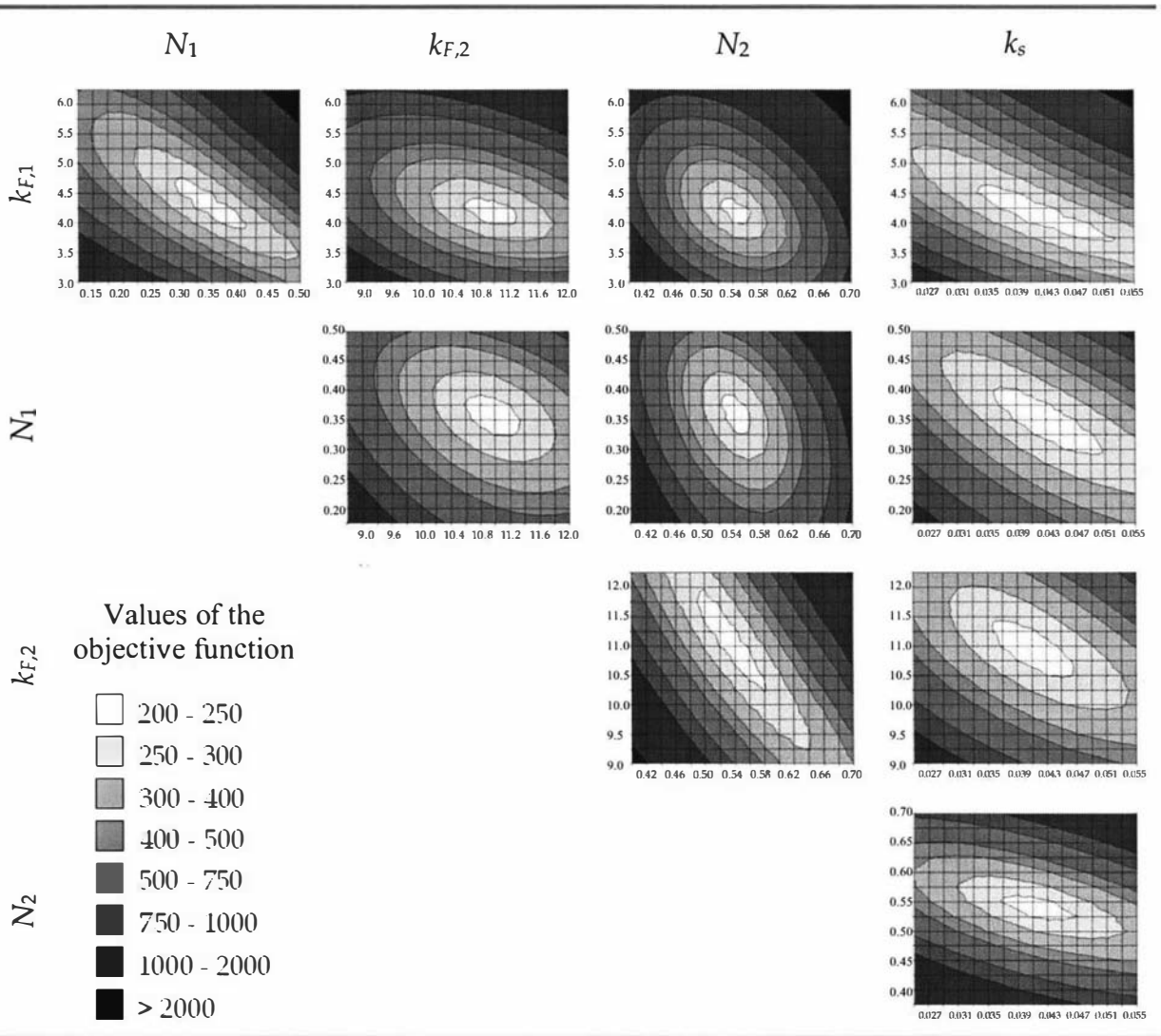


Figure 5.23. Relationships between pairs of parameters of the adsorption model, using the PGA approach. The other parameters were set at optimum values.

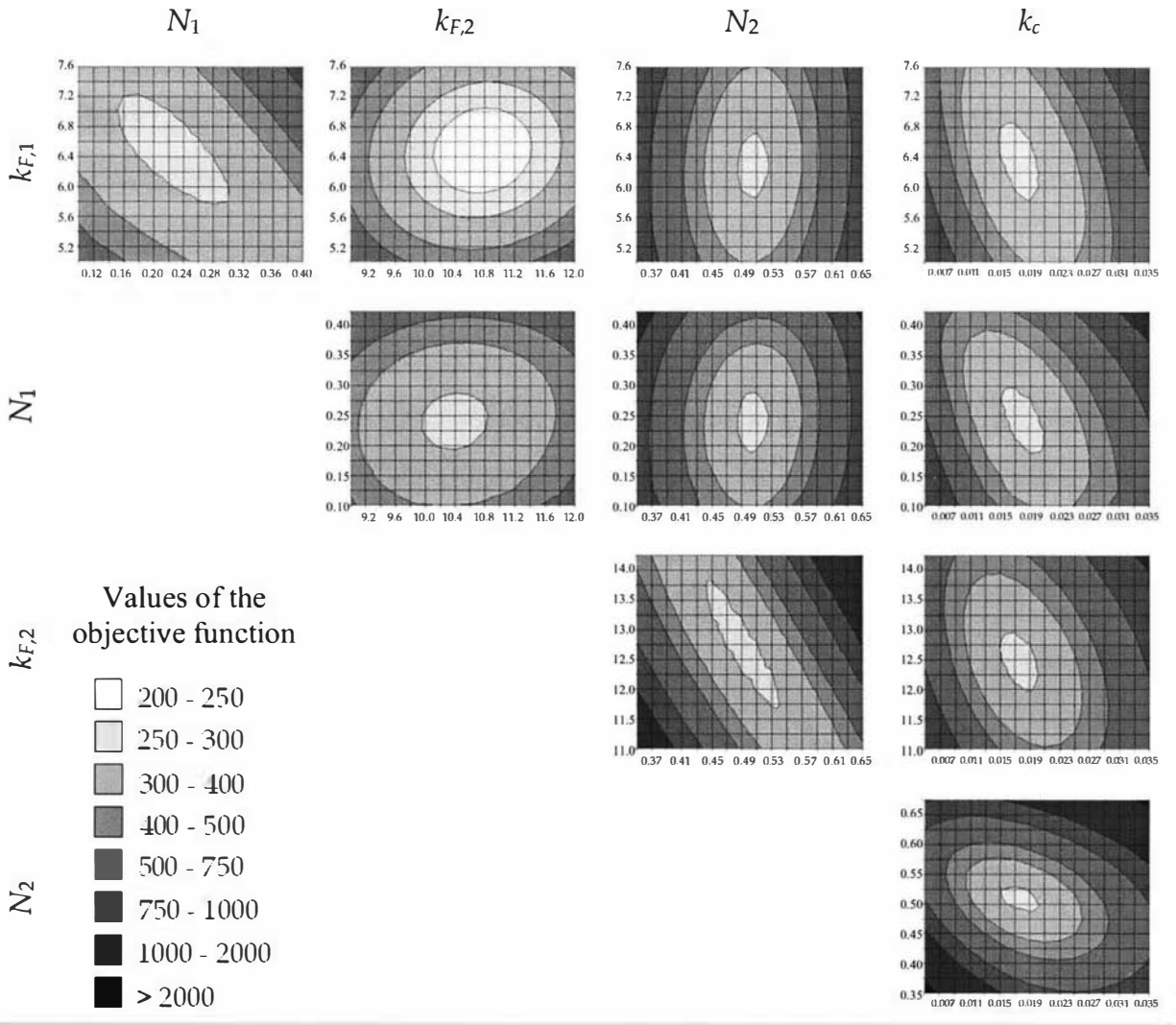


Figure 5.24. Relationships between pairs of parameters of the adsorption model, using the SGA1 approach. The other parameters were set at optimum values.

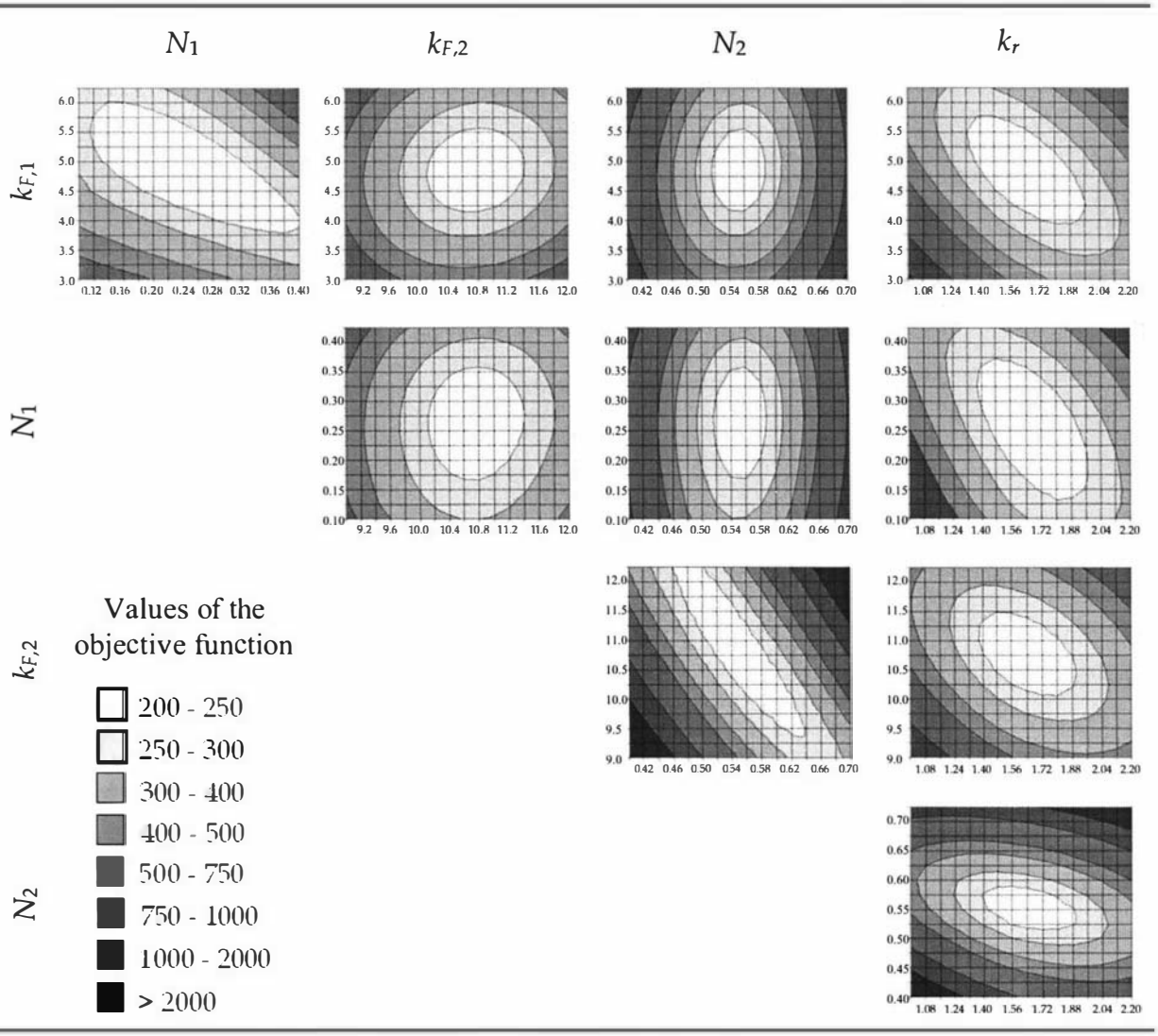


Figure 5.25. Relationships between pairs of parameters of the adsorption model, using the SGA2 approach. The other parameters were set at optimum values.

5.5. Summary and conclusions

The general framework of an adsorption model which takes into account the presence of IPA has been presented. Three mathematical approaches for describing the amount of solute retained in the soil due to IPA were introduced and their relationships were briefly discussed. An adsorption data set for Egmont soil obtained in a series of batch experiments using solutions with calcium and/or sulphate was also presented. In order to estimate values of the parameters for the adsorption model to describe the adsorption data set, three procedures for parameterisation have been described. A computer program to solve the adsorption model has been written and it was successfully used for the exploratory analysis and the parameterisation of the model.

In the first parameterisation procedure, named data analysis, the Egmont soil data set was compared with data presented in two published articles with different soils. Estimates of the IPA factor from the literature data revealed consistency in their magnitude, and agreed with estimates using the Egmont soil data. However, the best approach for describing the data differed between the two published articles. The other two parameterisation procedures, least squares and inverse modelling, rendered values of the IPA factor for Egmont soil of similar magnitude, and also consistent with those found in the data analysis. The Freundlich equation parameters for sulphate found in the least squares procedure differed significantly when using different IPA approaches, on the other hand they were very similar for calcium. For the inverse modelling procedure the values of the Freundlich equation were consistent for both ions, what may suggest independence from the IPA approach used. The inverse modelling procedure seems to be best suited for the parameterisation process, since it resulted in better overall agreement between the model and the observed data set. The deviations in the

parameters estimates were also smaller for the inverse modelling compared to the least squares procedure.

Both PGA and SGA2 showed the best overall agreement for describing the adsorption data set, with SGA2 being slightly better. SGA1 was found to be the least suitable description of IPA for the Egmont soil in all the three parameterisation procedures. However it was the best for one of the literature data sets, while PGA was best for the other. As a consequence of this, and because the description of the data set of Egmont soil was still reasonably good using any of the three approaches, it is not yet possible to favour or disregard any of the approaches.

The procedures for describing the adsorption data and the proposed routine with inverse modelling have performed well, allowing useful data exploratory analyses, and the optimisation of the parameters for the adsorption model. The suitability of this modelling procedure is further investigated in an attempt to predict the movement of sulphate and calcium through the soil (Chapter 6). For this, a convective-dispersive description of solute movement, coupled with the adsorption model presented in this chapter, is used for simulating the simultaneous leaching of those ions from the soil. These simulations are contrasted to the results of the miscible displacement experiments presented in Chapter 4.

CHAPTER 6

6. Ion-pair adsorption and its effect on the movement of sulphate and calcium in an allophanic soil

6.1. Introduction

Volcanic soils with variable-charge characteristics are likely to adsorb sulphate in significant amounts (Pigna and Violante, 2003; Mora *et al.*, 2005). Different binding phenomena have been identified in such soils, and ion-pair adsorption (IPA) seems to be a relevant one. The previous chapters showed that Egmont soil, an allophanic soil from the North Island of New Zealand, exhibits IPA involving sulphate and calcium to a considerable extent. Both batch and miscible displacement experiments have shown evidence of it, and the latter indicate that the movement of both solutes are affected by each other when present simultaneously in the soil.

In chapter 5 three approaches to describe IPA were presented. These mathematical functions were used in an adsorption model which had been fitted to represent a data set obtained in batch experiments. Features of this model were presented in Chapter 5, along with an exploratory analysis, using inverse modelling techniques. The adsorption data set from the batch experiment could be reasonably well described by any of the three approaches, although slight differences were found between them. In this chapter some of those results are reviewed and the adsorption model is applied, coupled with the convection-dispersion equation (CDE), to describe the movement of sulphate and calcium in the soil. Data obtained in the miscible displacement experiments presented in chapter 4 are used in this modelling. The main part

of this chapter consists of an article published in the Soil Science Society of America Journal. In this article only two of the proposed IPA approaches were used. The third was proposed after the paper's acceptance. The same applies to the work for estimating the measurements variances, presented in Chapter 5, thus the parameters for the batch data presented here were obtained by inverse modelling without using the variance as a weighting factor (this is also true for the BTC data, where the variances could not be estimated). Therefore the parameters deviations are not expressed (since they cannot be considered reliable). Also, because of this, the values of the parameters differ slightly from those shown in Chapter 5. The results of the model fitting using the third approach are presented at the end of the chapter. The schematic of the computer program used in the simulations is shown in the Appendix C.

6.2. Simultaneous adsorption of calcium and sulphate and its effect on their movement

by: Rogerio Cichota, Iris Vogeler, Nanthi S. Bolan and Brent E. Clothier
from: Soil Science Society of America Journal, 71(3): 703-710, 2007

6.2.1. Abstract

Ion retention in variable charge soils can be enhanced by the presence of certain ions with opposite charge, thereby influencing the movement of these ions through the soil profile. However studies examining these interactions are still incipient, especially regarding its modelling. We present results from batch and miscible displacement experiments describing calcium (Ca^{2+}) and sulphate (SO_4^{2-}) movement in a variable-charge soil from New Zealand. Evidence was found for ion-pair adsorption (IPA) of both calcium and sulphate. The results were modelled using the convection-dispersion equation (CDE), coupled with two different mathematical approaches proposed to account for IPA. The first approach related IPA to the single soil adsorption

capacity, which is governed by particle-surface phenomena. For the second approach, IPA was related solely to the soil solution concentration. Both these approaches described reasonably well the adsorption data, from the batch experiment, as well as the breakthrough curves from the miscible displacement experiments. The first approach showed better overall agreement. However, significant differences were found when the adsorption parameters were identified fitting models to data from either batch or miscible displacement experiments. Although more studies are needed to better understand IPA, our results showed that the extent of IPA can be large and it should not be ignored when predicting sulphate and calcium movement in variable-charge soils.

6.2.2. Introduction

Ion adsorption onto soil particles can be influenced by the presence of other ions in the soil solution. Same-charge ions compete for adsorption sites, whereas opposite charged ions may cooperate to increase adsorption. Specific adsorption of ions, which leads to an increase of the net soil charge, has been used to explain results of several studies (Curtin and Syers, 1990; Alva, 1993; Cajuste *et al.*, 1998; Bolan *et al.*, 1999a). Either anions or cations can drive this process, and subsequently increase the adsorption of opposite charged ions. Also interactions other than, or additionally to specific adsorption have been suggested (Ajwa and Tabatabai, 1995a; Pearce and Sumner, 1997; Ishiguro et al., 2006). It has also been observed, especially in variable-charge soils, that cooperative adsorption can occur without changing the net soil charge (Marcano-Martinez and McBride, 1989; Fahrenhorst *et al.*, 1999; Qafoku and Sumner, 2002). In this case, cation adsorption increases because of the presence of an anion, as well as vice versa. Because the amount of additional adsorption resulting from this co-adsorption process is equivalent to the ratio of the molar mass of the anion and cation, this process has also been called salt

adsorption or ion-pair adsorption (IPA) (Marcano-Martinez and McBride, 1989; Qafoku and Sumner, 2002).

IPA seems to be a common phenomenon in variable-charge soils (Pearce and Sumner, 1997; Qafoku and Sumner, 2001). Although it can occur with various ion combinations, it is more likely to happen with multivalent ions (Ajwa and Tabatabai, 1995a; Pearce and Sumner, 1997). IPA has been identified in particular for the adsorption of calcium and sulphate in variable charge-soils (Marcano-Martinez and McBride, 1989; Bolan *et al.*, 1993; Davis and Burgoa, 1995; Mora *et al.*, 2005).

Various reasons have been suggested for the occurrence of IPA involving sulphate and calcium, and some physico-chemical models attempting to describe IPA have been presented. Marcano-Martinez and McBride (1989) and Bolan et al. (1993) invoked charge-balance models to describe the mechanisms of specific adsorption of sulphate, or calcium, which is favoured by the presence of the counter ion. The release of potential determining ions such as H^+ or OH^- is balanced by the subsequent adsorption of the counter ion. Although they present differences, both models use surface-charge reactions to explain IPA, and therefore will be regarded here as one common model. In contrast, Qafoku and Sumner (2002) presented an ingenious physical model to explain IPA. According to their model, in highly weathered soils composed of mainly two different soil components with opposite net charge (kaolinite and iron or aluminium oxides, for example), the double layer of each particle type can expand and overlap the zone of influence of the other. In these intersections the electric field of one particle balances the other. According to the authors, ions can be trapped as ion-pairs in these intersections, because there is no need for electrical charge balancing. This model is in agreement with several observations when IPA occurs, such as no changes in the net soil charge and pH; the additional adsorption is in equivalent amounts of counter ions; and the fact that IPA is observed when the soil contains opposite charged particles (Wada, 1984; Qafoku and Sumner,

2002). None of these approaches, however, provide a means to describe the amount of solute adsorbed as ion-pair and its subsequent equilibrium with the soil solution concentration.

It has been shown that the sulphate adsorption isotherms are significantly distorted when calcium is present in variable-charge soils (Marcano-Martinez and McBride, 1989; Bolan *et al.*, 1993; Mora *et al.*, 2005). Higher adsorption in the presence of the counter ion leads to biased estimation of the adsorption parameters. The use of these parameters could result in large errors for predictions made under different conditions, such as with different concentrations of the counter ion. Some studies have already shown that IPA can significantly influence the leaching of ions from the soil (Bolan *et al.*, 1993; Davis and Burgoa, 1995; Qafoku and Sumner, 2001). In miscible displacement experiments, the classical breakthrough curve (BTC) is delayed when IPA is present, because the retardation factor is increased. The normal sigmoidal-shape of the BTC can also be distorted depending on the extent of IPA. Coupled sulphate and calcium transport in the soil with IPA has not been well explored yet, and the modelling of the leaching of these ions under such conditions is still incipient, especially when attempting to quantify the extent of IPA.

Contrasting batch data with miscible displacement experiments may provide insights for further understanding of this phenomenon. It has already been shown that adsorption parameters estimated by batch experiments can differ significantly from those found by methods with smaller water-to-soil ratios, as in the unsaturated transient-flow method (Katou *et al.*, 2001) or miscible displacement experiments (Altfelder *et al.*, 2001; Maraqa, 2001). Such divergences seem not to have been investigated when IPA is present.

Allophane is one of the most important constituents with variable-charge in volcanic soils, thus being related to its pH-dependent net charge and adsorption of ion-pairs (Pigna and Violante, 2003; Mora *et al.*, 2005; Ishiguro *et*

al., 2006). Gypsum application is often recommended in these soils for supplying both calcium and sulphate resulting from reduced leaching due to the enhanced adsorption (Mora *et al.*, 2005). Using an allophanic variable-charge soil from New Zealand, a series of batch and miscible displacement experiments was conducted in order to investigate the effect of cations on sulphate leaching. Evidences of IPA for calcium and sulphate in this soil are illustrated. We also present two approaches for modelling the partition of the solutes between the adsorbed and solution phases in order to achieve thermodynamic equilibrium. Thus, we expect to contribute towards a better understanding of this phenomenon and its relevance for solute leaching and retention in the soil.

6.2.3. Material and methods

6.2.3.1. Soil

The soil used for this study was the Egmont loam, an Allophanic Soil (Typic Dystrandept) from South Taranaki, New Zealand. It is a weathered soil of volcanic origin, containing allophane as the main clay mineral, but also considerable amounts of iron (Fe) and aluminium (Al) oxides. It has a well developed structure and the bulk density is usually below 900 kg m^{-3} (Molloy, 1988). Soil samples were collected from the top 0.20 m depth. Some characteristics are presented in Table 1.

6.2.3.2. Batch experiments

Three series of solute adsorption isotherms were determined: sulphate adsorption isotherms at different levels of calcium; calcium isotherms with different amounts of sulphate; and the simultaneous adsorption isotherms for calcium and sulphate added at equimolar concentrations. Several adsorption values of calcium and sulphate were measured at various concentrations of these solutes (0; 1; 2; 4; 6; 8; 10; 12; and 15 mmol L^{-1}), with duplicate samples

for each equilibration. Sulphate solutions were prepared with K_2SO_4 and calcium solutions with $CaCl_2$. Equimolar solutions were prepared using $CaSO_4$, and KCl was used to maintain the ionic strength constant.

Because this soil already had considerable indigenous amounts of sulphate and calcium, the soil was first leached with a solution of $MgCl_2$ (10 mmol L^{-1}), followed by a solution of KCl (10 mmol L^{-1}), and finally distilled water in order to reduce the influence of the counter ions. This procedure lowered the indigenous (Table 6.1) calcium and sulphate levels to 6.5 and 0.8 mmol kg^{-1}, respectively. Adsorption isotherms were determined using the leached soil, and checked against samples of the original soil.

Table 6.1. Selected properties of the Egmont soil used in the experiments.

$pH_{(H_2O)}$	Sand	Silt [1]	Clay	Allophane [2]	OM [3]	CEC [4]	AEC [5]	Calcium [6]	Sulphate [7]
	%					— $mmol_c\ kg^{-1}$ —		— mmol kg^{-1} —	
4.6	39	46	15	9.2	11	343	6.7	36.8	1.75

[1] Particle size measured by the pipette method; [2] By Al:Si ratio (Parfitt and Wilson, 1985); [3] Organic matter, measured by the loss on ignition method; [4 and 6] NH_4Ac extraction method (pH 7); [5] Ion substitution using Cl; [7] KH_2PO_4 extractable.

Four grams of air-dried soil were equilibrated with 25 mL of solution in centrifuge tubes by shaking for 24 hours in an end-over-end shaker at room temperature. After this equilibration period, the samples were centrifuged for 5 min at 8000 rpm, and filtered (Whatman 42) to separate the solution from the soil. The solution was then analyzed; the adsorbed amount was computed as the difference between the amount in the equilibrium solution before and after equilibration. Sulphate was determined by the methylene blue method (Johnson and Nishita, 1952), and calcium using atomic absorbance spectroscopy. The detection limits were approximate 0.005 mmol L^{-1} for sulphur and 0.025 mmol L^{-1} for calcium.

6.2.3.3. Miscible displacement experiments

Four miscible displacement experiments with repacked columns using Egmont soil were performed. Details of the experiments are presented in Table 6.2. Two columns (E_1 and E_2) were leached with different concentrations of $CaSO_4$ following a pre-leaching with $CaCl_2$, thus allowing to examine the influence of IPA on the BTCs at different solute concentrations. Another column (E_3) was leached with K_2SO_4 in a Ca-impoverished soil due to pre-leaching with KCl. This produced a BTC for sulphate with minimum influence of calcium. Finally another column was leached with solutions containing calcium only, using $CaCl_2$, but with the same step change in calcium concentration as column E_2. The columns E_3, and E_4 therefore present the situation where sulphate and calcium, respectively, are leached with the same concentrations as in columns E_2, but with minimum IPA.

Table 6.2. Concentration of the leaching solutions and some physical characteristics of the soil columns used in the miscible displacement experiments on Egmont soil.

Column	Solution concentration (M)		ρ[1]	θ[2]	$WFPV$[3]	q_w[4]
	Pre-leaching	Leaching	(kg m^{-3})	(m^3 m^{-3})	(cm^3)	(mm h^{-1})
E_1	0.0067 - $CaCl_2$	0.005 - $CaSO_4$	755	0.64	819	44.1
E_2	0.0133 - $CaCl_2$	0.01 - $CaSO_4$	755	0.61	763	29.9
E_3	0.03 - KCl	0.01 – K_2SO_4	770	0.63	789	20.5
E_4	0.0133 - $CaCl_2$	0.01 - $CaCl_2$	752	0.64	808	34.3

[1] ρ is the soil bulk density; [2] θ is the volumetric soil water content; [3] $WFPV$ is the water filled pore volume; [4] q_w is the water flux density in the leaching stage.

All leaching experiments were conducted under unsaturated conditions, at a constant pressure potential of -0.1 kPa (at both column ends). The columns were 0.15 m high and had diameter of 0.10 m. The experiments were carried out following a procedure similar to that described by Magesan

et al. (2003b). The solution was applied using a disk permeameter placed in the top of the column. The leachate solution was collected in small aliquots of between 50 mL to 100 mL, the collecting containers were in a pressure controlled chamber (Figure 4.1). These aliquots were analyzed for sulphate and calcium concentrations as described for the batch experiment. Chloride concentration was also analyzed using the mercury thiocyanate-iron method, with a detection limit of 0.085 (Florence and Farrar, 1971). Similar analyses were carried out for the soils before and after leaching, with sulphate being extracted with a KH_2PO_4 solution, and calcium using NH_4Ac.

6.2.3.4. Partition of the soil solute concentrations considering IPA

We used the simple approach where the total solute in the soil (Q, mol m^{-3}) can be divided into adsorbed (S, mol kg^{-1}) and solution (C, mol m^{-3}) phases. The mass balance for a given ion in the soil can therefore be described by:

$$Q = \theta C + \rho S \qquad [1]$$

where θ is the soil water content ($m^3\ m^{-3}$) and ρ is the soil bulk density ($kg\ m^{-3}$). The quantities S and C should be in a thermodynamic equilibrium:

$$S \underset{k_{d,a}}{\overset{k_{d,d}}{\rightleftharpoons}} C \qquad [2]$$

Considering that the distribution coefficient, k_d ($m^3\ kg^{-1}$), is invariant for both adsorption and desorption processes, different functions have been presented to relate the concentration in the soil solution and the amount of solute adsorbed onto the soil particles. This adsorption component we call "single adsorption" (S_S, mol kg^{-1}), and it is described by the non-linear Freundlich isotherm:

$$S_S = k_F C^N \qquad [3]$$

where k_F is a variable equivalent to k_d and N is an empirical fitting parameter.

As shown in batch experiments described elsewhere (Marcano-Martinez and McBride, 1989; Bolan et al., 1993; Ajwa and Tabatabai, 1995b), if IPA is present, the amount of adsorbed ion increases in the presence of its counter ion. Therefore, IPA is regarded as an additional adsorption over the single one (S_{IP}, mol kg^{-1}). The total amount of adsorption will then be the sum of these two quantities:

$$S = S_S + S_{IP} \qquad [4]$$

The partition between the different solute components in the soil (C, S_S, and S_{IP}) that leads to thermodynamic equilibrium has not yet been explored. In an attempt to identify this partition and to describe the results of the column experiments, two approaches are presented here. The first one is designated a particle governed approach (PGA). Here it is assumed that IPA is driven by particle surface interactions similar to those of the single adsorption. It is therefore implicit that the higher the single adsorption (S_S) the higher the additional one (S_{IP}) should be. For this we follow observations that the amount of additional adsorption of sulphate in the presence of calcium can be reasonably well described using a linear regression relationship between sulphate and calcium adsorbed concentrations (Bolan *et al.*, 1993). Thus, assuming that such relationship is also linear for calcium additional adsorption, the following equation can be derived:

$$S_{IP} = k_s S_{S,SO_4} S_{S,Ca} \qquad [5]$$

where k_s (kg mol^{-1}) is the IPA factor, and considered to be independent of the solute concentration.

Alternatively, the value of S_{IP} can be determined by assuming an equilibrium between the additional amount adsorbed and the soil solution concentration, similar to that of equation [2]. An equilibrium coefficient, or ion-pair factor (k_c, L mol^{-1}), is used to relate these amounts. Here also, it is predicted that k_c does not depend on the concentration. This approach does

not imply any direct interaction with the soil particle surfaces. Therefore this is designated a solution governed approach (SGA1), and can be written as:

$$S_{IP} = \frac{\theta}{\rho} k_c C_{SO_4} C_{Ca} \qquad [6]$$

where the ratio between soil water content and soil density is used to adjust the units. This is the water-to-soil ratio.

Equation [6] is similar to the stability equation of ion-pairs dissolved in an aqueous solution, where the amount of the ion-pairs ($CaSO_4^0$) is proportional to the product of the concentration of the dissociated ions (Ca^{2+} and SO_4^{2-}). It seems reasonable to assume that the higher the concentration of $CaSO_4^0$, the greater the likelihood of this ion-pair to be adsorbed. For example, these ion-pairs could be trapped in the neutral overlaps of the particles' double layer following the model presented by Qafoku and Sumner (2002). On the other hand, there has been no detailed investigation of this.

Prediction of the partitioning of the total concentration of each solute into C, S_S, and S_{IP}, was carried out using a Newton-Raphson procedure to solve the equation:

$$\left[\rho\left(S_{S,Ca^{2+}} + S_{IP}\right) + \theta C_{Ca^{2+}} - Q_{Ca^{2+}}\right]^2 + \left[\rho\left(S_{S,SO_4^{2-}} + S_{IP}\right) + \theta C_{SO_4^{2-}} - Q_{SO_4^{2-}}\right]^2 = 0 \qquad [7]$$

where S_{IP} is equivalent for both solutes. The equilibrium was assumed instantaneous, following equation [3] for S_S, and equations [5] or [6] for S_{IP}. Because the values of S were found to be more sensitive to the changes in the adsorption parameters, they were used to evaluate the model fittings by contrasting predicted to observed values.

6.2.3.5. Solute movement in the soil:

The concentration of each solute in the soil solution, at time t (s) and depth z (m), was predicted using the Convection-Dispersion Equation (CDE) (equation [8]), assuming the water flux density (q_w, m s^{-1}) to be steady. The

dispersion coefficient (D, $m^2\ s^{-1}$) was estimated using data from both solutes and also the chloride BTCs.

$$\frac{\partial Q}{\partial t} = \theta D \frac{\partial^2 C}{\partial z^2} - q_w \frac{\partial C}{\partial z} \quad [8]$$

To solve equation [8], a finite difference model (FDM) with central differences was written based on equation [9]. The soil column was divided into layers of thickness Δz (m), where the solute concentration was considered homogeneous and in equilibrium with the soil matrix during each time-step Δt (s). After computing the movement at each Δt, variations in Q were partitioned into C, S_S, and S_{IP} following the partitioning procedures described above. Both, solute movement and adsorption were simulated using a computer procedure written in Visual Basic language.

$$Q_{z,t} = Q_{z,t-1} + \Delta t \left(\theta D \frac{C^2_{z+1,t-1} - 2C_{z,t-1} + C^2_{z-1,t-1}}{4\Delta z^2} - q_w \frac{C_{z+1,t-1} - C_{z-1,t-1}}{2\Delta z} \right) \quad [9]$$

6.2.4. Results and discussion

6.2.4.1. Batch experiment

The adsorption of both calcium and sulphate was clearly affected by the presence of the respective counter ion. Figure 6.1 show examples of sulphate and calcium isotherms for the leached soil, at three different levels of the counter ion. Also shown, for comparisons between these sets and with those from other studies, are the adjusted Freundlich isotherms (without considering IPA). The parameters are in the range reported elsewhere (Marcano-Martinez and McBride, 1989; Bolan *et al.*, 1993; Mora *et al.*, 2005), although comparisons are difficult because of differences in soil mineralogy and specially due to the strong dependency on pH of the surface charge of the allophanic soils (Bolan *et al.*, 1999a; Mora *et al.*, 2005). In our case, no significant changes in pH were found when varying the concentration of the equilibrium solution, except for those with higher concentration of K_2SO_4 where a slight increase in pH

occurred, indicating some specific adsorption of sulphate. Nonetheless strong evidence for IPA is provided by the enhanced adsorption of both ions when its counter ion is present in increasing amounts.

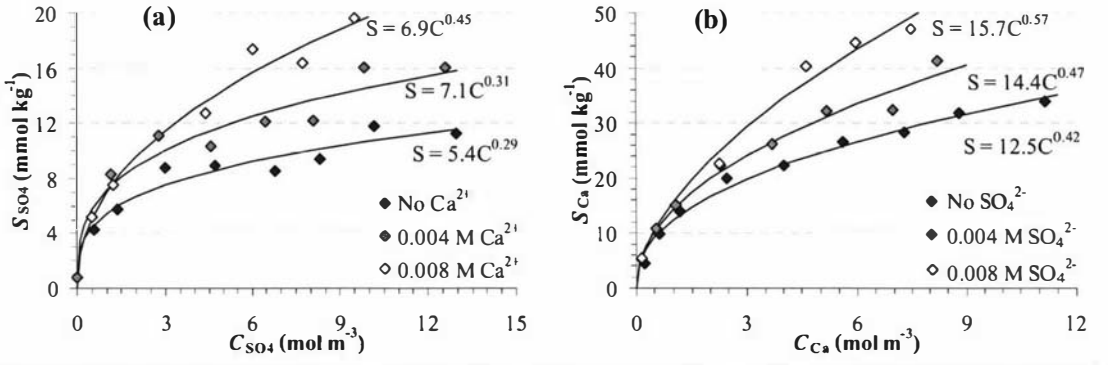


Figure 6.1. Observed adsorption isotherms for sulphate (a) and calcium (b) using three different amounts of the counter ion in the added solution. Lines show adjusted Freundlich isotherms without considering ion-pair adsorption (IPA).

Table 6.3 shows the adjusted parameter values for the isotherms using the two approaches for describing IPA. Both approaches, PGA or SGA1, allow solving the equations for the equilibrium between solution and sorbed concentrations quite easily, although the solution must be done simultaneously for both ions. Good agreement between predicted and measured values was found with both approaches. However, there are considerable differences in the shape of the isotherms evaluated by the two approaches. In particular, the values for S_{IP} were estimated to be much higher using PGA compared with SGA1, especially at lower concentrations. This causes the shape of the single adsorption isotherm to be significantly different between the two approaches. In Figure 6.2 isotherms for both sulphate and calcium obtained equilibrating different amounts of $CaSO_4$ are presented (therefore in approximate equimolar amounts), and modelled using both IPA approaches. This example shows how the estimates of S_{IP} differ when

increasing the solute concentration. Because both approaches use a product formula (of either S_S or C), there is a tendency to exponentially increase the estimates of S_{IP} when the amount of solute increases. As C is favoured at higher concentrations (due to N<1), SGA1 estimates increasingly higher values for S_{IP}. This produces a rather unusual shape for the total adsorption (Figure 6.2c). This feature is not as pronounced in the other sets, where the amount of the counter ion was fixed. Nevertheless it indicates that this approach is not complete in the simple way presented here, demanding further investigation. Marcano-Martinez and McBride (1989) have also found the isotherm (for calcium) with N above 1 when equimolar amounts of calcium and sulphate were added to the soil.

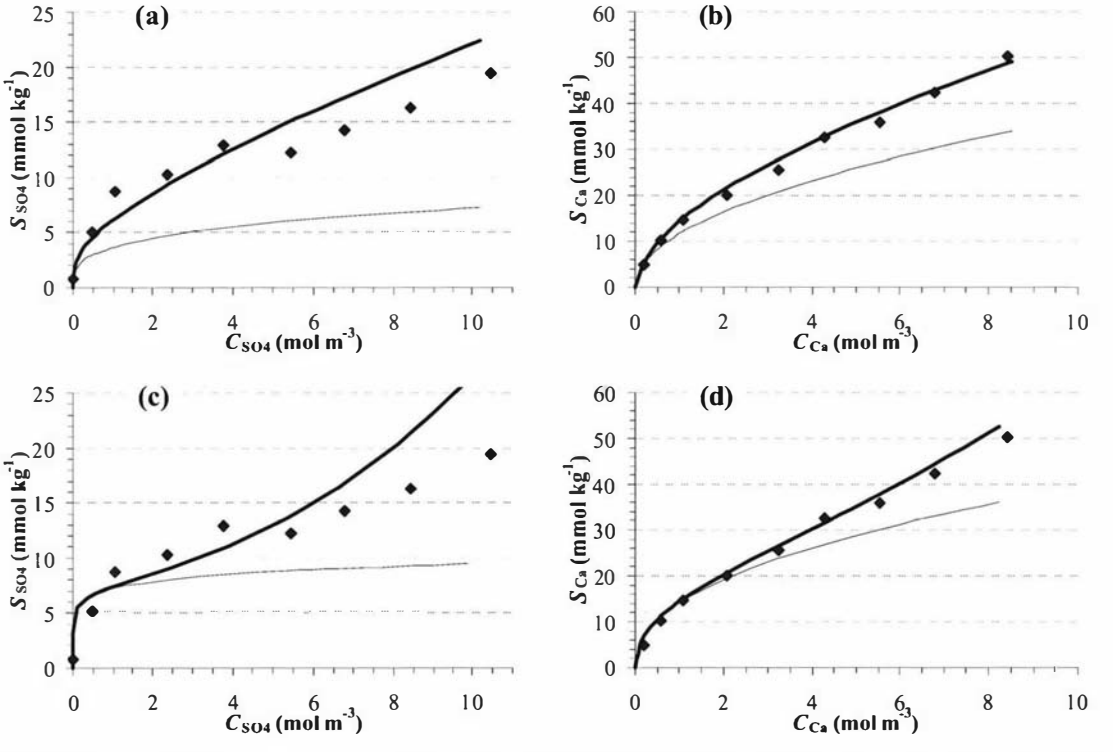


Figure 6.2. Adsorption isotherms for sulphate and calcium, added in equimolar amounts. Dots show observed data, bold lines represent modelled S, and thin lines show S_S as estimated using the particle governed approach, PGA (a and b) or solution governed approach, SGA1 (c and d).

Table 6.3. Adjusted parameters of Freundlich isotherms and the IPA (ion-pair adsorption) factor for sulphate and calcium. The adjustment was made using batch experiment data. Also presented are the agreement measures (contrasting measured against estimated values of $S_{SO4} + S_{Ca}$).

	k_{F,SO_4}	N_{SO_4}	$k_{F,Ca}$	N_{Ca}	k_s or k_c	R^2	RMSE [1]
PGA	3.64	0.30	11.61	0.50	0.061	0.9735	2.858
SGA1	7.21	0.12	14.15	0.44	0.017	0.9628	3.153

[1] Root mean squared error (mol kg^{-1})

It was not possible to determine the Freundlich parameters for the single adsorption simply by regression analysis of the data set in which no counter ion was added, because the soil still had some residual amount of calcium and sulphate. The best fit using the three-phase equilibrium model (Equation [7]) gave quite unusual values for the Freundlich isotherm parameters, especially when SGA1 was used to describe IPA. In particular, the value of the exponent *N* was relatively small compared with those reported in the literature (Marcano-Martinez and McBride, 1989; Bolan *et al.*, 1993; Bolan *et al.*, 1999a; Mora *et al.*, 2005). In fact, the shape of the sulphate isotherms suggests that the maximum limit for the single adsorption of this ion had been reached.

It is also important to stress that large uncertainties and/or correlation between parameters may be expected because of the high number of parameters (five) which need to be adjusted simultaneously. For example the value of *N* will be clearly restricted when the IPA factor is increased. The problem of adjusting models with high number of parameters has been the focus of several studies (for example, (Abbaspour et al., 2004; Vrugt et al., 2005; Beulke and Brown, 2006; Mertens et al., 2006), and frequently involve extensive computer work. Although care must be taken when using such multi-parameter models, the problem of parameterisation does not invalidate their use. A better understanding of the sensitivity and correlation of the

model parameters is important but beyond the scope of this paper. Further investigations examining the sensitivity analysis of various parameters will be discussed in a subsequent paper.

6.2.4.2. Miscible displacement experiments

Clear evidence for IPA was also found in the miscible displacement experiments. The adsorption of both calcium and sulphate increased in the presence of the other. The breakthrough of the sulphate solution of columns E_1 and E_2 occurred at a different time to that of column E_3 (Figure 6.3a). This indicates that the presence of calcium in the former has retarded the movement of sulphate in the soil due to increased adsorption. Furthermore, for columns E_1 and E_2 the calcium concentration in the leachate dropped to almost zero when the accompanying anion changed from chloride in the pre-leaching to sulphate in the main leaching phase. This contrasts significantly with column E_4, which was leached without replacing chloride by sulphate (Figure 6.3b). Retardation of BTC and changes in their shape have been reported (Bolan *et al.*, 1993; Qafoku and Sumner, 2001; Nakajima *et al.*, 2002) and IPA was used to explain those results. In addition to this, the final solute concentration in columns E_2, E_3, and E_4 can be compared, as they can be regarded as replications which contained either both calcium and sulphate, only sulphate, or only calcium, respectively. The difference in sulphate between columns E_2 and E_3 represented an additional retention of 18.4 mmol kg^{-1}. This is about the same amount as the difference for calcium between columns E_2 and E_4, which was 19.2 mmol kg^{-1}.

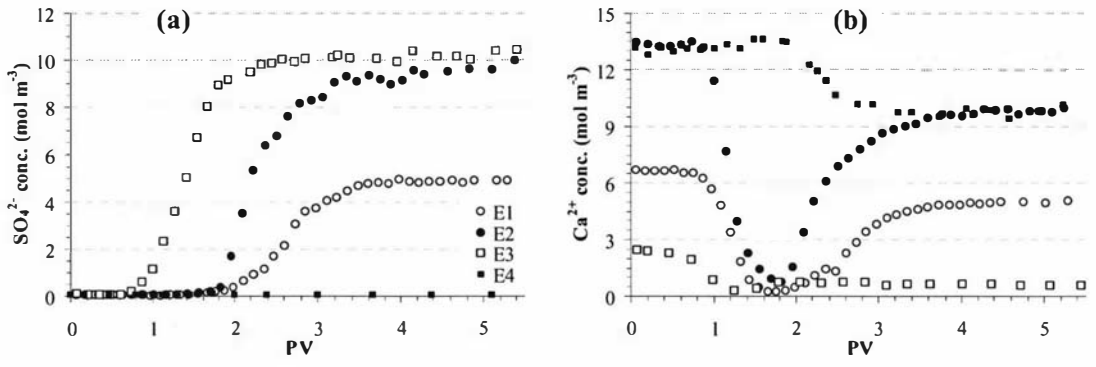


Figure 6.3. Measured breakthrough curves (BTCs) for sulphate (a) and calcium (b), for the four experimental columns. Columns E_1 and E_2 leached with $CaSO_4$, E_3 leached with K_2SO_4, and E_4 with $CaCl_2$ (see Table 6.2).

Although we had no replications, these comparisons are relevant considering the good mass balance attained, with recoveries deviations within 7% limit. Similar to the batch experiment, the pH increased when K_2SO_4 was added to the soil (column E_3), and the change was equivalent to that experiment (from 4.7 to 5.2). For columns E_1 and E_2, the pH before and after the introduction of sulphate solution was the same, although a peak occurred during the displacement. No changes in pH occurred in column E_4.

Problems of non-uniqueness can be found when evaluating parameters by fitting models to miscible displacement data, because of the number of the unknown parameters and their related effects on BTCs shape (Friedel, 2005; Kohne *et al.*, 2006). Obtaining larger amounts of data and independent estimation of some parameters are used to reduce this problem. In our case, the value of the dispersion coefficient (*D* from equation [8]) was obtained using the chloride data, which had shown negligible adsorption, and the adsorption parameters found with the batch experiment data were used as starting estimates. Frequently, however, adsorption parameters found in batch experiments cannot be used for describing miscible displacement results (Heng *et al.*, 1999; Katou *et al.*, 2001; Maraqa, 2001). The different hydraulic

regime, especially the water-to-soil ratio and the time for equilibrium, is generally suggested as the reason for this disagreement.

Table 6.4. Adjusted parameters of Freundlich isotherms and the IPA (ion-pair adsorption) factor for sulphate and calcium. The adjustment was made using data from columns E_1 and E_2 of the miscible displacement (using $CaSO_4$ solution). Also presented are the agreement measures (measured vs. estimated values of the leachate concentration).

		k_{F,SO_4}	N_{SO_4}	$k_{F,Ca}$	N_{Ca}	k_s or k_c	R^2	RMSE [1]
E_1	PGA	0.45	0.60	0.38	0.60	4.75	0.9928	0.199
	SGA1	2.00	0.20	0.20	0.80	0.22	0.9300	0.604
E_2	PGA	0.45	0.55	0.35	0.63	3.75	0.9923	0.397
	SGA1	2.3	0.12	0.25	0.75	0.10	0.9785	0.671

[1] Root mean squared error (mol m^{-3})

The chloride data showed no significant adsorption in this soil (Figure 6.4). Fitting a CDE model to the chloride data revealed consistent values for *D*. As this parameter has only a small effect, the average value of 2.0 $m^2\ s^{-1}$ was assumed for all columns. Table 6.4 shows the adsorption parameters found by inverse modelling using equation [9], and the two IPA approaches to describe the data of columns E_1 and E_2. Interestingly, while the values of the distribution factor were much smaller than those of the batch experiment, as expected, the IPA factor was found to be much larger, especially for PGA. This suggests that IPA is more likely to occur at smaller water-to-soil ratios, contrary to the single adsorption. Frequently the restricted access to adsorption sites is used to explain the decrease in the single adsorption found in miscible displacement experiments. This would also apply for IPA, unless the phenomenon responsible for IPA is different from that of the single adsorption.

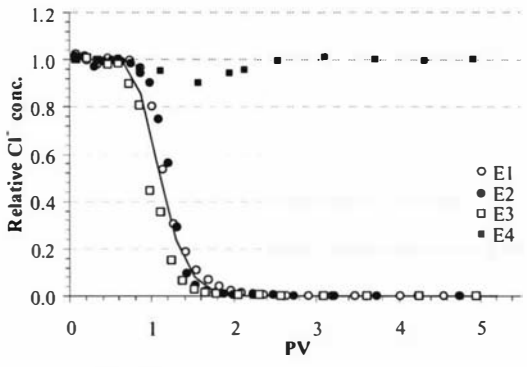


Figure 6.4. Measured chloride breakthrough curves (BTCs) for the four experimental columns, also is shown the adjusted model. Concentration is relative to the input solution. Columns E_1 and E_2 leached with $CaSO_4$, E_3 leached with K_2SO_4, and E_4 with $CaCl_2$ (see Table 6.2).

The BTCs modelled with IPA predicted the results from the column experiments reasonably well (Figure 6.5). However, the description using the PGA resulted in better agreement, as we were able to better simulate the drop of calcium in the presence of sulphate. This difference between the two approaches is a result of the fact that at low concentrations PGA estimates higher amounts of IPA (see isotherms on Figure 6.2). Equilibrium may, therefore, occur with a very low value of C and a larger value of S (S_S + S_{IP}). For SGA1 only a small fraction of the solute is adsorbed by IPA in relation to the single adsorption, and thus equilibrium occurs with smaller values of S at low solution concentrations. We speculate that the discrepancies between the measured and the simulated BTC using SGA1 are due to the adsorption/desorption processes of the solutes not being fast enough to be considered instantaneous. If the desorption of calcium was not as fast as adsorption, as has been shown elsewhere (Verburg and Baveye, 1994; Undabeytia *et al.*, 1998), it would result in a higher concentration of calcium in the adsorbed phase. This would, therefore, produce a more pronounced reduction in the concentration of this ion in the solution phase.

Clearly, more studies are required to better understand the IPA phenomenon and thus describe with greater precision the movement of solutes in soils displaying it. The extent of IPA can be considerably large, and its influence on the solute leaching is evident. Our approaches for describing IPA do allow predictions of the general patterns of the adsorption isotherms and BTCs, and this provides a starting point for further investigations.

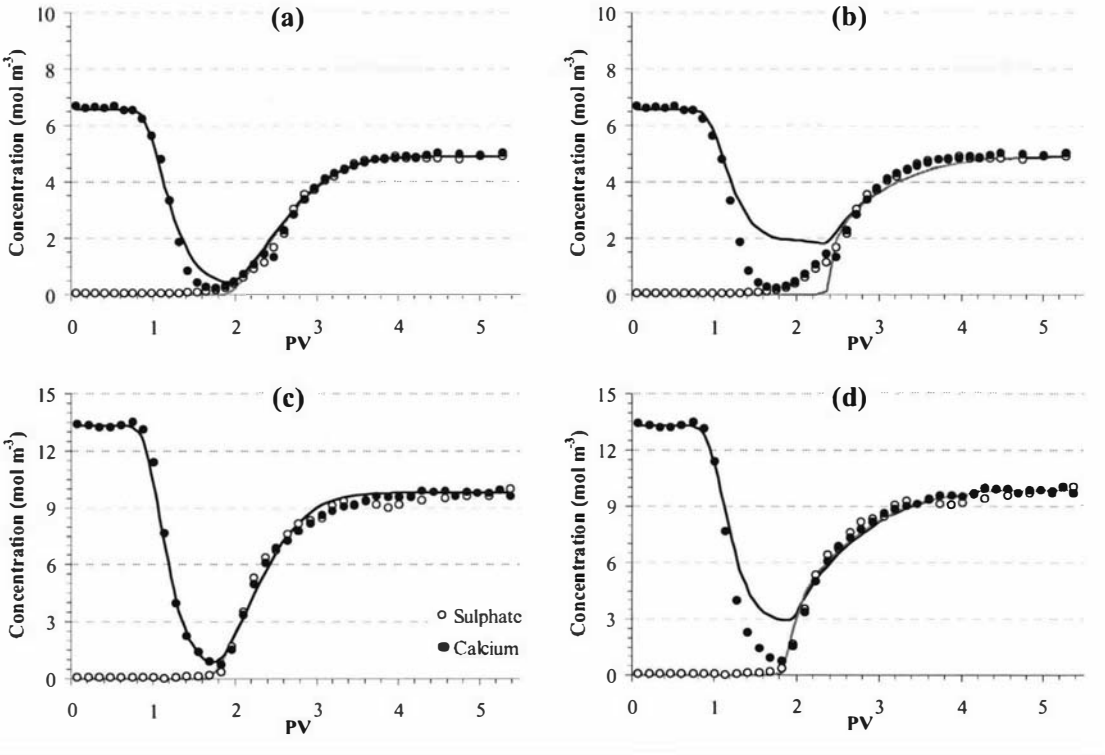


Figure 6.5. Measured (dots) and modelled (lines) breakthrough curves (BTCs) for sulphate and calcium from columns E_1 (a and b) and E_2 (c and d) (leached with $CaSO_4$). Ion-pair adsorption (IPA) was described using the particle governed approach, PGA (a and c) and solution governed approach, SGA1 (b and d).

6.2.5. Conclusions

We present evidence of IPA in the Egmont soil, which is dominated by variable-charge components. Both sulphate and calcium adsorption increased significantly when applied simultaneously. Results from both batch and

miscible displacement experiments showed features that supported the theory of cooperative adsorption for these two solutes as ion-pairs. Two simple approaches were used to describe IPA, in which the adsorbed solute is partitioned into different components. These two approaches were used for modelling our experimental data.

Both the sulphate and calcium adsorption isotherms were well described by a Freundlich model, plus IPA. Using the CDE model coupled with either of the two approaches for describing ion adsorption, we achieved a reasonable description of the shape of the breakthrough curves. However, the PGA model, which relates IPA to the soil's single adsorption capacity, resulted in better overall agreement.

Our approaches for describing IPA can be used to estimate the simultaneous movement of sulphate and calcium in soils. However, more work must be done to obtain a better understanding of the IPA phenomenon and for further model development. The extent of IPA should not be ignored when describing sulphur or calcium dynamics in these variable charge soils.

6.3. BTC description using the SGA2 approach

As already mentioned, this approach was developed after the acceptance of the article just presented. As shown in Chapter 5, this approach and SGA1 can be considered different versions of a general power equation. However, the fitting of the adsorption model to the batch data revealed that the performance of this approach is similar or slightly better than the PGA approach. That third approach was then used to verify if this trend would repeat again for the BTCs from the miscible displacement experiments with Egmont soil leached simultaneously with sulphate and calcium solution.

The measures of agreement between the model and the data set given, by the R^2 and RMSE, did confirm that trend. SGA2 showed good performance

(Table 6.5), which was only marginally better than the PGA approach (Table 6.4). The shape of the modelled BTC is also very similar to that of PGA (Figure 6.6). The parameters found using the miscible displacement data set were also considerably different from those of the batch experiment (Table 6.3). The differences for the IPA factor between estimates from the two data sets followed a dissimilar pattern to that found for PGA and SGA1 approaches. Here the IPA factor is smaller than the one from the batch data, while it was significantly higher for the other two approaches. Unfortunately a possible explanation for this could not be found. The values for the Freundlich equation parameters found for SGA2 were quite similar to those of PGA, but here the differences between estimates for the two columns were larger.

Nevertheless, the model performed well for describing the miscible displacement experiments data using the SGA2 approach for evaluating the IPA adsorption. The general level of agreement for both experimental data sets showed that PGA and SGA2 are equally suitable for modelling the movement of sulphate and calcium. On the other hand, the differences in the parameter values when fitted to data from batch or miscible displacement experiments suggest that further investigation is needed.

Table 6.5. Adjusted parameters of Freundlich isotherms and the IPA (ion-pair adsorption) factor for sulphate and calcium using SGA2 approach. The adjustment was made using data from columns E_1 and E_2 of the miscible displacement (using $CaSO_4$ solution). Also presented are the agreement measures (measured vs. estimated values of the leachate concentration).

	k_{F,SO_4}	N_{SO_4}	$k_{F,Ca}$	N_{Ca}	k_r	R^2	RMSE [1]
E_1	0.14	0.59	0.24	0.56	1.15	0.9963	0.195
E_2	0.29	0.49	0.07	0.97	0.85	0.9951	0.392

[1] Root mean squared error (mol m^{-3})

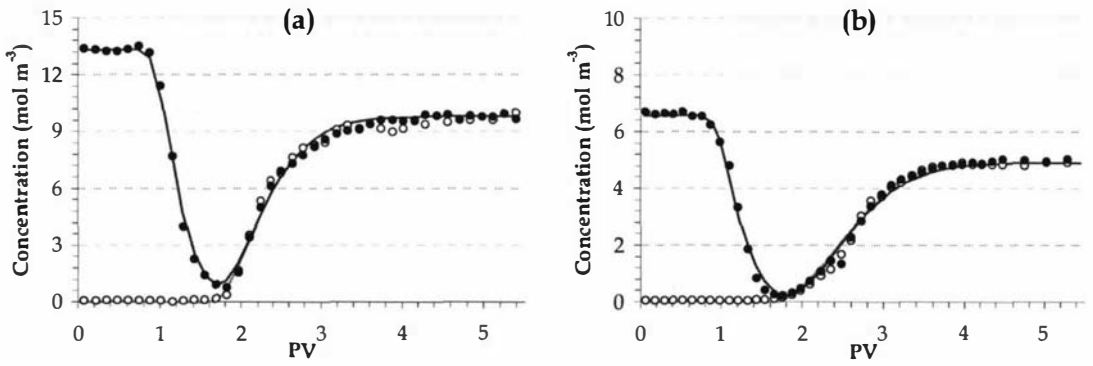


Figure 6.6. Measured (dots) and modelled (lines) breakthrough curves (BTCs) for sulphate and calcium from columns E_1 (a) and E_2 (b) (leached with $CaSO_4$). Ion-pair adsorption (IPA) was described using the SGA2 approach.

CHAPTER 7

7. Sulphate and calcium movement in an allophanic soil – The relevance of ion-pair adsorption in the soil-plant system

7.1. Introduction

As already described, the retention of an ion in the soil may be influenced by the presence of other ions in the soil solution. Cooperative retention of opposite-charged ions, termed here ion-pair adsorption (IPA) has been identified for the ion-pair sulphate-calcium in some soils with variable-charge characteristics (Marcano-Martinez and McBride, 1989; Bolan *et al.*, 1993; Qafoku and Sumner, 2002). In the previous chapters results from several laboratory experiments were used to demonstrate that such phenomenon also occur with these ions in the New Zealand's Egmont soil. This soil has allophane as the main clay mineral, and therefore possesses variable-charge characteristics. In volcanic soils with high content of allophane or imogolite, sulphate can be expected to be adsorbed in additional amounts when calcium content is elevated (Pigna and Violante, 2003; Mora *et al.*, 2005). Gypsum ($CaSO_4.2H_2O$) fertilisation has been recommended for these soils for supplying both calcium and sulphate because of the lower risk of leaching due to the enhanced adsorption (Mora *et al.*, 2005).

Because IPA changes ion retention, it can influence the leaching through the soil of the involved ions. This effect has been observed in sulphate and calcium breakthrough curves from miscible displacement experiments in laboratory, shown in the previous chapters and in the literature (Bolan *et al.*, 1993; Davis and Burgoa, 1995). However, conditions in the field with plants

are quite different to those in the laboratory. Well controlled field experiments are difficult to carry out, and so far no studies of IPA under field conditions have been reported. A plant-and-soil study using lysimeters in a greenhouse seems to be a valuable means for testing laboratory findings under more realistic conditions. Such study has not yet been used for exploring the possible effects of IPA on sulphate leaching, or plant uptake. It is also not known whether or not ions retained due to IPA are available to plants. IPA seems to be readily reversible when the ionic composition of the soil solution is changed (Qafoku and Sumner, 2002). Since plants can alter the balance of ions in the soil, due to selective uptake, it is possible that IPA could be reversed by plants. Longer-term trials, with intermittent irrigation, may also alter the soil ionic composition and consequently might alter the extent of IPA over time. In these cases, the relevance of IPA for the solute movement through the root zone might be quite different from its influence verified in laboratory studies using bare soil.

The influence of the accompanying cation on sulphate leaching in New Zealand's Egmont soil has been demonstrated in the previous chapters comparing the results of various short-term miscible displacement experiments. To further investigate the relevance of IPA under more realistic conditions involving plant growth over a relative long period, a plant experiment was set up in the glasshouse. Since the adsorption of sulphate is enhanced by the presence of calcium, and thus its leaching delayed, it was hypothesised that the use of $CaSO_4$ as an IPA-inducing fertiliser should improve the sulphur supply to plants as compared to the use of K_2SO_4. For assessing the relevance of IPA in this soil-plant system, the plant growth and nutrient uptake was measured, as well as the concentration in the leached solution. It was assumed that sulphate should remain longer in the soil treated with $CaSO_4$, and thus the amount taken up by the plants would increase, and this could possibly affect the plant growth.

7.2. Materials and methods

7.2.1. Soil

For this experiment the Egmont loam soil was used. This soil has already been described in previous chapters, see Table 6.1 for a list of some of its properties.

7.2.2. Plant experiments

The pots used in this experiment had upper diameter of 0.2 m and 0.165 m height. Soil was filled up to a depth of 0.15 m to a bulk density of around 720 kg m^{-3}. Six different treatments comprising of different fertilisers and irrigation rates were used. These treatments are hereafter referred to as NL, NH, CL, CH, KL, and KH, where the first letter stands for the fertiliser used, namely: none (N); $CaSO_4$ (C); and K_2SO_4 (K), and the second letter stands for the irrigation rate: low rate (L), to equate to the daily evapotranspiration; and a high rate (H), approximately double the evapotranspiration. This higher irrigation rate was used to ensure appreciable leaching would occur. The fertilisers, at a rate of 30 kg ha^{-1} (100 mg kg^{-1} of soil) of sulphur, were dissolved in water and thoroughly mixed with the soil before packing the soil into the pots. Three replications were used for each treatment. In addition to this, six extra pots per treatment were used for destructive sampling to monitor plant development at various intervals during the experiment.

About ten seeds of rapeseed (*Brassica napus*) were sown into each pot, and after germination six plants were left per pot. Sulphur-free nutrient solution (Hoagland solution) was supplied to the plants (about 15 mL $week^{-1}$) with the irrigation water to ensure an adequate nutrient supply. Seeds were sown on 15th September, 2004, and plants were harvested on 15th December, 2004, just before flowering. Water was supplied daily, generally in the morning. The irrigation amount to be added was calculated by weighing each of the pots before irrigation. The high irrigation rate was applied from 30th

October onwards (Figure 7.1), consequently leaching started only early in November (5th November for most pots). The leachate was monitored from 3rd to 12th December (Figure 7.2). The leachate was collected in buckets placed underneath the pots. These buckets were emptied before the irrigation on the following day started. At time intervals of about 10 days some of the additional pots were harvested for monitoring plant growth over time. One pot for each treatment was used at each time. Measurements and analyses were performed in a similar way to the main pots, as described below.

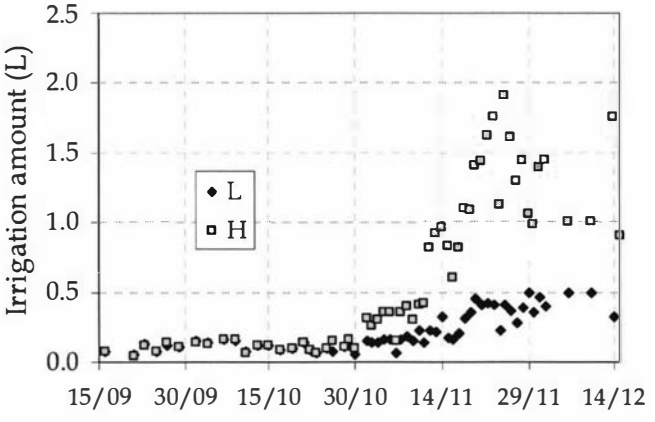


Figure 7.1. Average of the water applied per pot for the two irrigation treatments, low irrigation rate (L) and high irrigation rate (H).

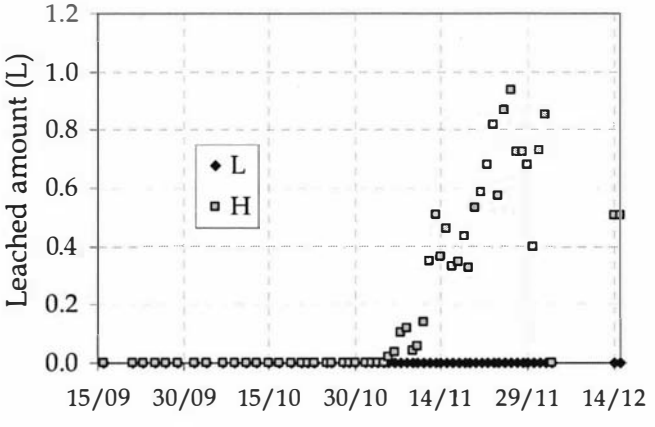


Figure 7.2. Average of the solution amount leached per pot for the two irrigation treatments, low irrigation rate (L) and high irrigation rate (H).

7.2.3. Plant and soil analyses

At the end of the experiment, the plants were cut off at the soil surface. After recording the weight, height, and leaf area, the plant shoots were oven-dried (65°C) and stored for further analyses. The roots were washed off the soil, and after their weight and length were determined, samples were also oven-dried and stored. Both roots and shoots were analyzed for sulphur, calcium and potassium. For the analysis, alkali sodium hypobromide digestion was used for extracting sulphur (Tabatabai and Chae, 1982), and nitric acid digestion for cations (Huang and Schulte, 1985). The determination of their concentrations used the methods described below. Some of the plant samples were also analyzed for sulphur and calcium with the particle-Induced X-ray Emission - PIXE (Kennedy and Markwitz, 2002).

At harvest, the soil was divided into five layers, allowing then the soil analyses separate for different depths. The soil and the collected leachate were also analyzed for total sulphur, sulphate, calcium and potassium. Sulphate was extracted from the soil using KH_2PO_4 (0.01 mol L^{-1}) and cations using NH_4OAc (1 mol L^{-1}). For the determination of total soil sulphur, a sodium bicarbonate fusion was used (Tabatabai and Bremner, 1970). Finally, sulphur was determined by the methylene blue method (Johnson and Nishita, 1952), and cations using atomic absorbance spectroscopy. The data sets were subject to an analysis of variance, with the differences between treatments being assessed using the Tukey test (5% prob.).

7.3. Results and discussion

7.3.1. Plant growth and nutrient uptake

Plant growth was greater when extra irrigation water was supplied, while the addition of fertilisers resulted in a much smaller response. The plants growing in high-rate irrigated pots had mass and leaf area about 45% higher than those of the low-rate pots, for each of the three fertiliser treatments

(Figure 7.3). Supplying fertiliser produced a 15% increase in both the plant mass and the leaf area compared to the non-fertilised pots. However there were no differences between the two fertiliser sources, $CaSO_4$ and K_2SO_4. The differences in plant growth were noticeable only in the last 30 days of the experiment (Figure 7.3). It seems, therefore, that the differences between the two fertilisers, caused by the IPA effect, were not significant when most of the plant growth occurred. In this phase, late in the experiment, the different nutrient supply (especially sulphate) would have become important because of the higher growth rate associated with higher demand. By this later time, the evapotranspiration rate had also increased, due to both higher temperatures and larger leaf areas. Therefore the pots with low irrigation rate probably experienced some water shortage at the end of the day. This would explain the positive effect of the high irrigation treatment.

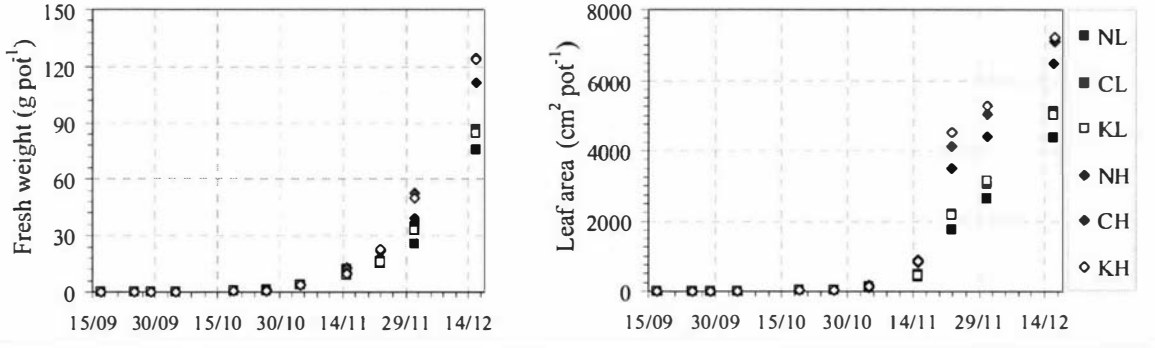


Figure 7.3. Development of the plants fresh weight and leaf area over the experimental time for the six treatments: no fertiliser (N), $CaSO_4$ (C), K_2SO_4 (K), low irrigation rate (L), and high irrigation rate (H).

The root distribution, whether described by mass or length, also only exhibited appreciable differences between the two irrigation rates (Figure 7.4). These differences were actually significant only in the top layer. While the root length distribution was quite homogeneous in the profile for the pots with low-rate irrigation, in the high-rate pots the top layer had a markedly high root content (Figure 7.4).

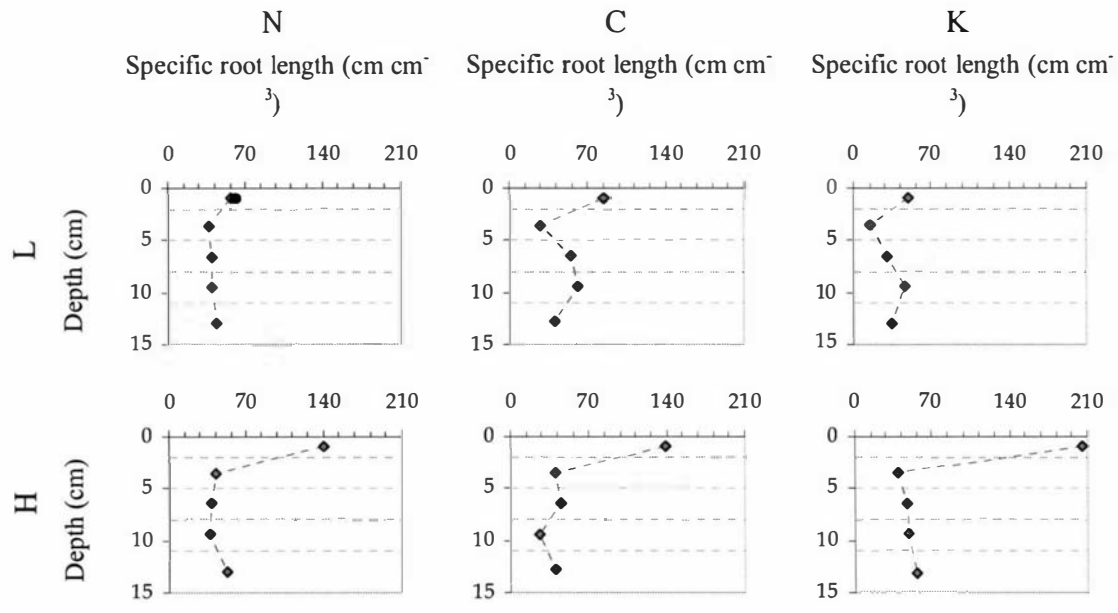


Figure 7.4. Specific root length distribution in the soil profile for the six treatments: no fertiliser (N), $CaSO_4$ (C), K_2SO_4 (K), low irrigation rate (L), and high irrigation rate (H).

The uptake of both sulphate and potassium by plants was higher in those pots where these ions were added, whereas calcium fertilisation did not result in higher uptake of this ion (Figure 7.5). This indicates that the calcium content in the soil was not a limiting factor. The measured sulphur concentration in the plants revealed that all treatments suffered deficiency, since all measurements of the shoot sulphur concentration were below the threshold of 3 mg S g^{-1} (Table 7.1) (Scherer, 2001). Again lower values were found for those pots that were not fertilised. No significant differences were found between the two fertilisers used, although those plants from the treatment with $CaSO_4$, showed higher sulphur content. The sulphur deficiency was more severe for the high-rate irrigated pots where visible symptoms were noticed at the end of the trial. Plants in the pots with the high-rate irrigation had also lower concentrations of calcium and potassium than those with the lower irrigation. This can be considered a dilution effect, since the plants with higher irrigation rate had also higher biomass.

Table 7.1. Sulphur concentration in the plants from the six treatments: no fertiliser (N), $CaSO_4$ (C), K_2SO_4 (K), low irrigation rate (L), and high irrigation rate (H). All values in mg g^{-1} dry mass.

	Root	Shoot	Whole
NL	2.33	1.42	1.70
NH	2.71	1.26	1.54
CL	4.13	2.23	2.67
CH	4.04	1.59	2.00
KL	3.90	2.46	2.70
KH	3.57	1.81	2.16

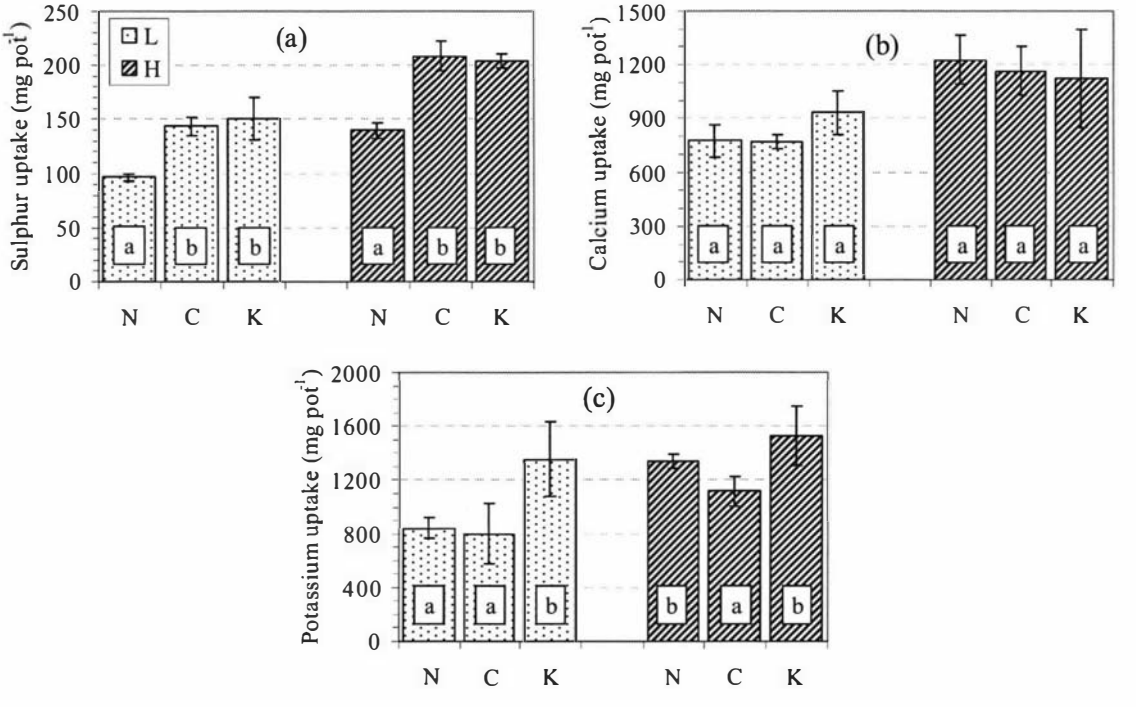


Figure 7.5. Averages of sulphur, calcium, and potassium uptake per pot for the six treatments: no fertiliser (N), $CaSO_4$ (C), K_2SO_4 (K), low irrigation rate (L), and high irrigation rate (H). Vertical lines represent the standard deviation. Columns with the same letter in the boxes, for each irrigation treatment, did not differ significantly (Tukey test at $P<5\%$).

7.3.2. Leachate

Analyses of the collected leachate provided the best data to determine the relevance of IPA in the plant growth experiment. Measurable leaching amounts occurred only in those pots with the high irrigation rate. The quantities of sulphate leached were quite small compared to the amounts in the soil, the amounts increased in the order: no-fertiliser < $CaSO_4$ < K_2SO_4 (Figure 7.6a), although the differences were not statistically significant. The total amount of calcium leached indicated that this ion had its retention enhanced in those pots where sulphate has been added. The highest amount of calcium leached was verified in the non-fertilised pots (Figure 7.6b). No significant differences could be identified between the total amounts of calcium leached from the two treatments with fertiliser. A better insight into the relevance of IPA can be obtained by observing the concentration of the leachate over the time. The sulphate concentration in the leachate was different between the treatments, and it increased in the same order as the total quantities leached (Figure 7.7a). This was found throughout the experiment, although towards the end these differences were much smaller. Similarly, the concentration of calcium in the leachate was about 15% smaller at the beginning of the leaching process for the treatment with $CaSO_4$ as compared to that with K_2SO_4, despite extra calcium being added to this treatment. It is in fact smaller than the non-fertilised pots (Figure 7.7b). After about two weeks, these differences could no longer be distinguished. Although these differences were again not statistically significant, they do suggest that IPA is relevant for the leaching only in the short term, just for a week or so after the application of the fertilisers. Depending on the retention capacity of soils continued leaching reduces the relevance of IPA for the retention of calcium and sulphate.

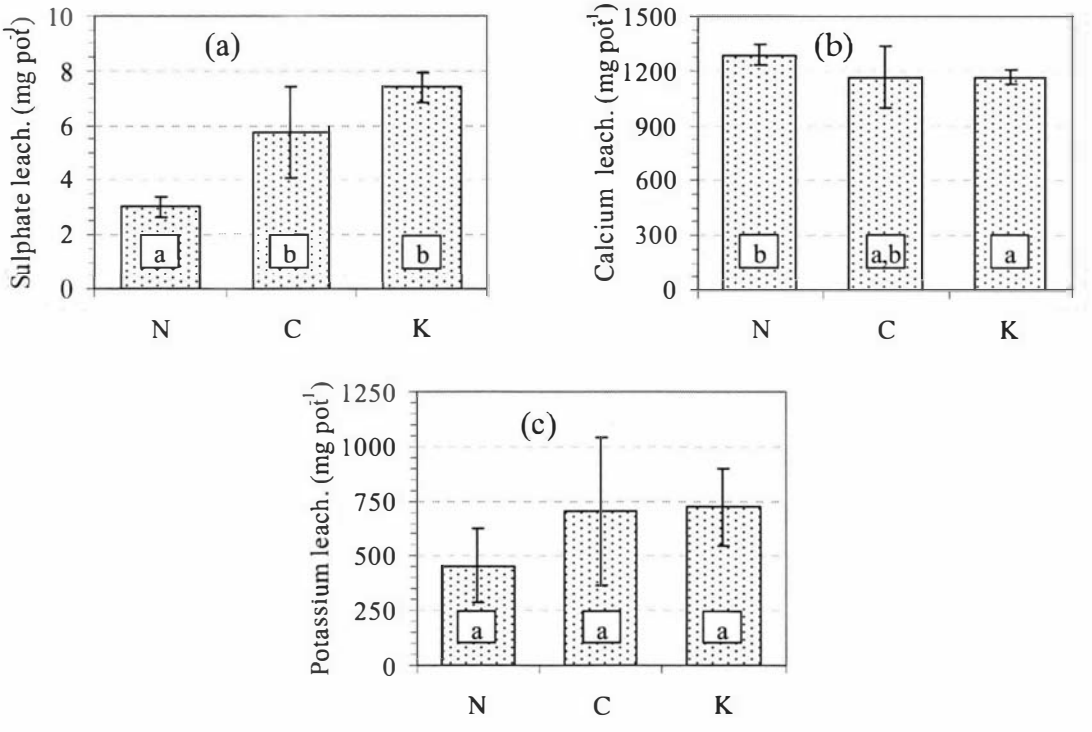


Figure 7.6. Average per pot of the leached amounts of sulphate, calcium, and potassium for the three treatments with high-rate irrigation: no fertiliser (N), $CaSO_4$ (C), K_2SO_4 (K). Vertical lines represent the standard deviation. Columns with the same letter in the boxes did not differ significantly (Tukey test at P<5%).

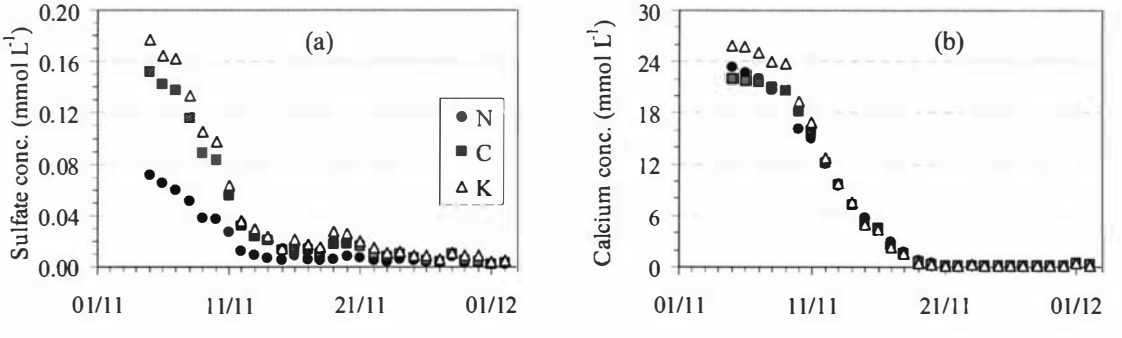


Figure 7.7. Concentration of sulphate and calcium in the leachate during the experimental time, for the three treatments with high-rate irrigation: no fertiliser (N), $CaSO_4$ (C), K_2SO_4 (K).

7.3.3. Soil ion concentration

The final ion concentration in the soil revealed different response patterns for sulphate, calcium and potassium (Figure 7.8). The final sulphate concentrations showed responses to fertilisation and, to a much smaller extent, to irrigation. Calcium concentrations responded to irrigation only, and potassium showed no clear differences. Since potassium was supplied to the soil via the nutrient solution, this lack in differences could be expected. The calcium content in the soil was smaller in the high-rate irrigated pots. These variations were mainly a result of leaching and the higher uptake in those pots. For sulphate, although the final concentration was higher in those pots where fertiliser was applied, no significant effects could be found in relation to the fertiliser used.

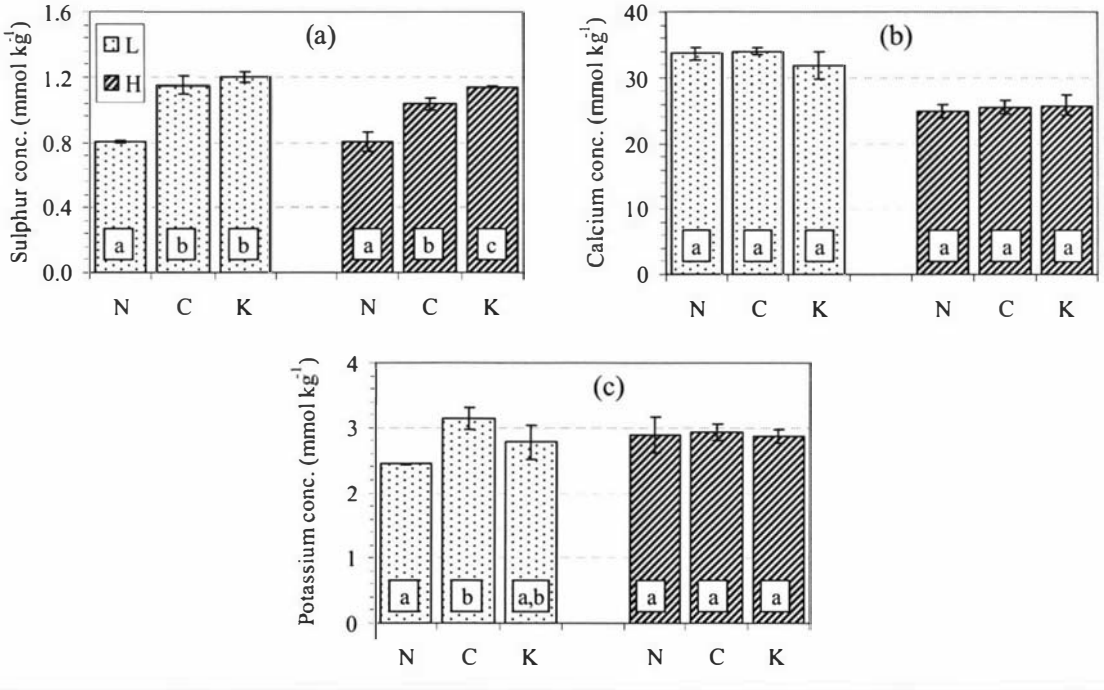


Figure 7.8. Average per pot of the final soil concentration of sulphate, calcium, and potassium for the six treatments: no fertiliser (N), $CaSO_4$ (C), K_2SO_4 (K), low irrigation rate (L), and high irrigation rate (H). Vertical lines represent the standard deviation. Columns with the same letter in the boxes, for each irrigation treatment, did not differ significantly (Tukey test at P<5%).

The distribution in the soil profile of the three measured ions has shown differences only between the two irrigation rates (Figure 7.9). Sulphate distribution in the profile was somehow homogeneous for all treatments, with a higher concentration in the bottom layer for the pots with higher irrigation. Calcium was leached down the profile similarly for all pots, the difference between the irrigation treatments is evidenced by the calcium content in the lower layers. The differences between treatments were much smaller for the potassium concentration, with a noticeable accumulation in the top layer. This potassium accumulated should have come from the nutrient solution.

The measured values of the final concentrations of sulphate and calcium in the five soil layers of each pot showed no correlation to each other (Figure 7.10). It seems that the high initial calcium content in the soil has masked the contrasting effects of the addition of $CaSO_4$ or K_2SO_4 on sulphate retention, as observed in Chapter 5. Concurred for this also, the fact that sulphate concentration in the soil was relatively small. Concomitantly the cycling of sulphur into mineralised and organic forms, would have also been important in this relatively long-term experiment, and also contributed to the lack in correlation between calcium and sulphate concentrations in the soil. Finally, the uptake by the plant roots should have had an effect on the final distribution of these ions, because sulphate is actively taken up by plants (de Kok *et al.*, 2005).

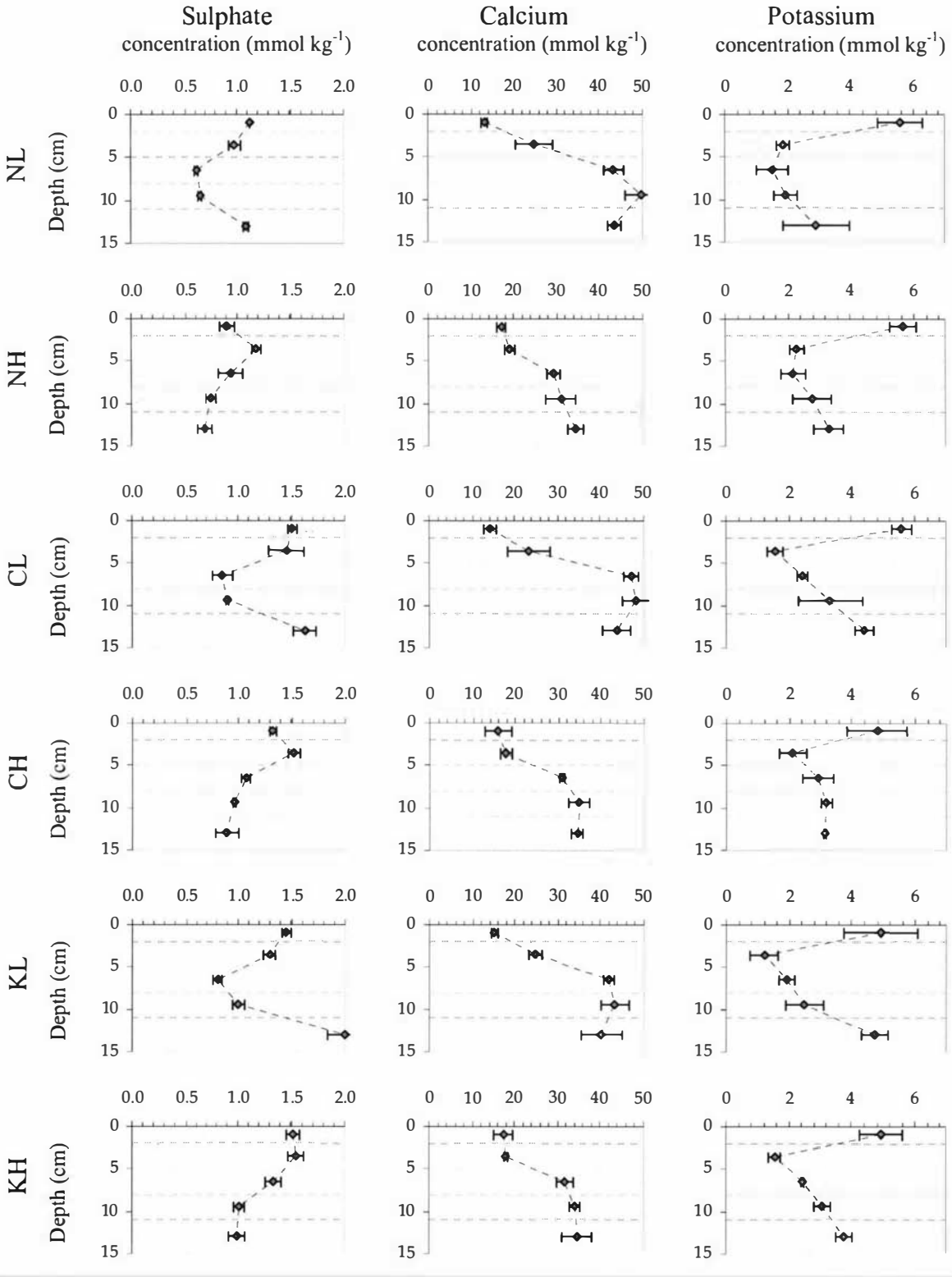


Figure 7.9. Concentration profile of sulphate, calcium, and potassium for the six treatments: no fertiliser (N), $CaSO_4$ (C), K_2SO_4 (K), low irrigation rate (L), and high irrigation rate (H).

Although the results of this study revealed no effects of IPA on plant response to nutrient uptake, they do suggest the need for further research. The use of soil with a smaller indigenous calcium content, for example, might emphasise the relevance of IPA, at least in the short term. The interactions between IPA and plant uptake should be a subject for further studies. Fertilisation in the middle of the growing season could provide an opportunity to investigate the relevance of IPA during a period of high active plant growth, and therefore high ion uptake. Since laboratory studies do show that retention of sulphate and calcium is significantly enhanced by IPA, studies under realistic conditions should continue to improve our understanding of IPA in the presence of growing plants and under non-steady water flow.

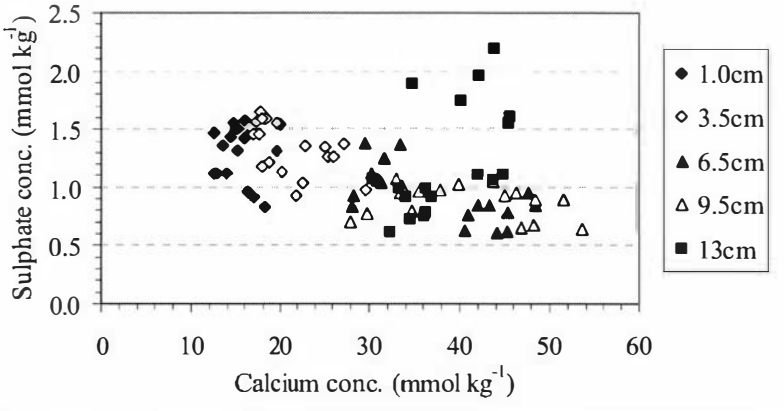


Figure 7.10. Comparison between the final soil concentrations of calcium and sulphate measured in five different depths of each pot of all treatments.

7.4. Summary and conclusions

Following batch and column studies that have identified ion-pair adsorption involving sulphate and calcium in the Egmont soil, a pot experiment conducted in glasshouse has been performed to determine the relevance of IPA in this variable-charge soil under conditions more realistic than those in the laboratory. The effect of IPA on the leaching of sulphate, and

the possible response of plants to this effect, was examined in repacked soil lysimeters. $CaSO_4$ was used to induce IPA in contrast to K_2SO_4, and a control. Also, two irrigation rates were employed. Plant growth, ion uptake, soil and leachate concentrations were analyzed over a period of three months.

Although plant growth and ion uptake exhibited a response to fertilisation, there were no differences between the two fertilisers. Therefore there was no evidence for the effect of IPA on plant growth or ion uptake. Plant growth did respond significantly to extra irrigation. The leachate data from the experiment suggest that IPA is important only in the short-term. After just over a week, the results did not show significant evidence of IPA following $CaSO_4$ fertilisation. As a consequence, it seems that the differences between the treatments were no longer significant when plant growth became appreciable. This explains the lack of response from the plants.

The fact that no correlation was found between the final contents of calcium and sulphate in the soil is probably associated with the active plant uptake of sulphate, which was in deficit, in conjunction with the initial high content of calcium in the soil. The sulphur cycling in the soil may have also influenced this result, as the organic matter content was quite high.

The basic outcome from this experiment is that the expected effect of IPA on plant uptake of sulphate could not be verified. Furthermore, the concentration in the leachate, and the final soil contents, showed also little evidence of IPA. Nonetheless, some evidence for $CaSO_4$ delaying the leaching of both sulphate and calcium in the early stages was found. Further studies are suggested to determine the time span after fertilisation during which IPA is relevant for reducing sulphate and calcium leaching. Also the need for a deeper understanding of the interaction between plant uptake and IPA in the soil requires further investigation.

CHAPTER 8

8. Final summary and conclusions

With an increasing number of reports of sulphur deficiency worldwide, a good fertilisation management has to consider the sulphur nutritional status of crops. Sulphur deficiency can cause plant yield and quality losses, and consequently reduce the already narrow profit margin of agricultural production. For comprehensive management of the field nutritional status a reliable description of sulphur balance in the soil is needed. One of the most important aspects of the sulphur dynamics in the soil is the transport of sulphate. Sulphate is the mobile form of sulphur in soils, which can be taken up by plants or leached down the soil profile. Water movement and adsorption onto the soil particles are the main factors controlling the transport of sulphate in soils, therefore a better understanding of these processes can potentially lead to improvements in the description of the sulphur balance.

The objective of this thesis, taken these considerations into account, is to make a contribution towards a more comprehensive description of the sulphur dynamics in the soil. For this a better understanding of the sulphate movement in soils is sought. More particularly, the influence of the presence of different cations on the adsorption of sulphate, and the consequences on their transport through the soil are examined.

To verify the influence of cations on the movement of sulphate, series of experiments with two soils from the New Zealand's North Island were performed. These soils, Taupo and Egmont soils, were chosen because of their contrasting ion adsorption capacities. Two series of experiments were performed in the laboratory, comprising miscible displacement experiments and batch equilibrations. A pot trial with the Egmont soil was also carried out

for examining the cation-influenced sulphate movement under more realistic conditions, with active plant growth.

Results from the miscible displacement experiments presented in Chapter 4 have shown the occurrence of very little adsorption of both ions in the Taupo soil, which has a low allophane content. Conversely, the results showed that sulphate, and especially calcium, are noticeably adsorbed in the Egmont soil, which contains large amounts of allophane. The amounts of sulphate and calcium adsorbed were strongly correlated in the Egmont soil, and in a different Taupo soil sample, with a higher allophane content. Sulphate adsorption was enhanced when it was applied with calcium, as compared to potassium. Analogously, calcium retention increased in the presence of sulphate in contrast to chloride. This cooperative enhanced retention of sulphate and calcium reveals the occurrence of ion-pair adsorption (IPA) in these soils. Allophane is the main variable-charge clay mineral in both soils, and seems to be responsible for their strong adsorption characteristics, including the occurrence of IPA. The results of the miscible displacement experiments clearly demonstrate that IPA can affect the movement of both ions to a considerable extent, and therefore IPA should not be ignored when studying the transport of sulphate in these soils.

Results from the batch experiments, with various combinations of sulphate and calcium additions, confirmed the synergetic interaction between the adsorption of these ions in the Egmont soil. This relationship was examined in more detail in these experiments, and a comprehensive data set was obtained. Based on the analysis of this data set, plus the review of published data, an adsorption model has been introduced in Chapter 5. For evaluating the amount of solute adsorbed as ion-pair using this model, three different mathematical approaches were proposed. A data analysis procedure based on the literature data was used for a preliminary comparison of these approaches. This procedure also provided a means for comparing the adsorption characteristics of Egmont soil with the soils from the published

data. The IPA factor, used in the description of the simultaneous adsorption of sulphate and calcium due to IPA, showed consistency within each approach for all the data analysed, although the best approach for describing the data could not be established.

Two alternative parameterisation procedures were also presented in Chapter 5. These procedures were employed for finding the best set of parameters to use in the adsorption model for describing the results from the batch experiments. The procedure that used an adapted least squares method resulted in similar values of the IPA factor to those from the initial data analysis. On the other hand, the estimated Freundlich adsorption parameters exhibited large variability. The inverse modelling procedure, using the maximum likelihood method, seemed to be the best for parameterisation. The values of the parameters found were more consistent and the model's agreement to the observed data set was best using this procedure over the former approach. The three approaches have shown good agreement to the observed data. But one, named SGA1, exhibited slightly higher deviations. The computer program, presented in the Appendix B, built to solve the adsorption model performed well to evaluate the agreement between the model's prediction and the observed data set using the maximum likelihood method.

The proposed adsorption model, coupled with the convective-dispersive approach for describing solute transport, was tested against the data obtained in the miscible displacement experiments. Again a computer program, presented in Appendix C, was used for evaluating the agreement between the model and the observed data. These comparisons, shown in Chapter 6, indicate that any of the three approaches for describing IPA can be successfully used to simulate the movement of sulphate and calcium in the soil. The approach SGA1 again showed the largest deviations, while the other two performed similarly. However, the parameter set found using the data from the miscible displacement experiments was significantly different from

those found with the batch experiment data set. These differences were not surprising, since there are several reports in the literature of divergence between parameters obtained from batch and from miscible displacement experiments.

As discussed in Chapter 7, the results of the pot trial were mostly inconclusive to show any effect of IPA in the plant uptake. It was expected that the leachate from the soil would exhibit some differences in the sulphate losses, and these differences would be detected in the plant uptake, and thus in the plant growth. However, plant growth showed stronger response to irrigation than to sulphur fertilisation, and no response to the type of fertiliser applied. Also, the final concentration of sulphate in the soil was not correlated to the content of calcium. The leachate concentration did show some response to IPA, although with low significance. The effect of IPA on solute leaching was negligible after some days of intermittent irrigation. On reflection, this could perhaps have been expected, as the IPA is reported to be reversible. Further studies are, therefore, required to determine the time span that IPA is relevant for reducing sulphate leaching. The contrast between the use of potassium or calcium as the sulphate accompanying ion was probably reduced by the high level of indigenous calcium in the soil.

The effect of IPA in the reduction of sulphate leaching could be more interesting with mid-season fertilisation, when there is more active plant growth, since any delay in the leaching process would provide plants with a longer time to take up the added sulphate. An experiment under such conditions could be used perhaps to better demonstrate the interaction between IPA and plant uptake.

The model introduced here should also be tested in different soils and under a wider range of conditions. More studies are also required to better define IPA, since the mechanism for IPA is not well understood. Various soils of volcanic and tropical origin with variable-charge components are reported

to present behaviour compatible with the occurrence of IPA, in such cases the adsorption model presented here has the potential to assist in for further investigation, and also, in enhancing the reliability of descriptions of the sulphur dynamics in soils.

In summary, it has been demonstrated that IPA occur in the allophanic Egmont soil, and is likely to occur in other soils with a considerable allophane content. An adsorption model, considering three alternative approaches for evaluating the extent of IPA, has been presented. Using a comprehensive adsorption data set, this model was parameterised and tested. The proposed model is not a deterministic one, but it is simple and performed well when describing the adsorption data set, and the literature data. The model was also successfully applied to describe the results from the miscible displacement experiments. However, it was not possible to favour any one of the proposed approaches for the description of IPA. The relevance of IPA for the leaching of sulphate in short-term experiments was clearly demonstrated. However, longer-term experiments should be carried out to better evaluate its relevance over time.

With the narrowing profit margin, and increasing pressure from environmental legislation, farming systems are in need for more reliable tools for fertilisation management. The work presented in this study provides a significant contribution towards a more reliable description of the behaviour of sulphate in the field. This is accomplished by improving the understanding of the adsorption of sulphate in the soil, and its effect on sulphate transport.

REFERENCES

Abbaspour, K.C.; Johnson, C.A.; and van Genuchten, M.T. 2004. Estimating uncertain flow and transport parameters using a sequential uncertainty fitting procedure. *Vadose Zone Journal*, 3:1340-1352.

Abrol, Y.P. and Ahmad, A. 2006. *Sulphur in Plants*. Kluwer Academic Publishers, Dordrecht. 424 p.

Agbenin, J.O. 1996. Phosphorus sorption by three cultivated savanna Alfisols as influenced by pH. *Fertilizer Research*, 44:107-112.

Agbenin, J.O. 1997. Sulfate retention by kaolinitic alfisols from Nigerian savanna. *Soil Science Society of America Journal*, 61:53-57.

Aharoni, C.; Sparks, D.L.; Levinson, S.; and Ravina, I. 1991. Kinetics of soil chemical reactions - relationships between empirical equations and diffusion models. *Soil Science Society of America Journal*, 55:1307-1312.

Ahmad, A. and Abdin, M.Z. 2000. Photosynthesis and its related physiological variables in the leaves of Brassica genotypes as influenced by sulphur fertilization. *Physiologia Plantarum*, 110:144-149.

Ahmad, A.; Khan, I.; Anjum, N.A.; Diva, I.; Abdin, M.Z.; and Iqbal, M. 2005. Effect of timing of sulfur fertilizer application on growth and yield of rapeseed. *Journal of Plant Nutrition*, 28:1049-1059.

Aikman, D.P. and Scaife, A. 1993. Modeling plant-growth under varying environmental-conditions in a uniform canopy. *Annals of Botany*, 72:485-492.

Ajwa, H.A. and Tabatabai, M.A. 1995a. Metal-induced sulfate adsorption by soils. 2. Effects of metal type, valence, and concentration. *Soil Science*, 160:281-290.

Ajwa, H.A. and Tabatabai, M.A. 1995b. Metal-induced sulfate adsorption by soils.1. Effect of pH and ionic-strength. *Soil Science*, 159:32-42.

Allen, R.G.; Pereira, L.S.; Raes, D.; and Smith, M. 1998. Crop evapotranspiration: guidelines for computing crop water requirements. *Irrigation and Drainage Paper No. 56.* FAO, Rome, Italy. 300 p.

Altfelder, S.; Streck, T.; Maraqa, M.A.; and Voice, T.C. 2001. Nonequilibrium sorption of dimethylphthalate--compatibility of batch and column techniques. *Soil Science Society of America Journal*, 65:102-111.

Altin, O.; Ozbelge, H.O.; and Dogu, T. 1998. Use of general purpose adsorption isotherms for heavy metal clay mineral interactions. *Journal of Colloid and Interface Science*, 198:130-140.

Alva, A.K.; Sumner, M.E.; and Miller, W.P. 1990. Reactions of gypsum or phosphogypsum in highly weathered acid subsoils. *Soil Science Society of America Journal*, 54:993-998.

Alva, A.K. 1993. Sorption of calcium and sulfate by sandy soils from flue-gas desulfurization gypsum and phosphogypsum. *Communications in Soil Science and Plant Analysis*, 24:2701-2713.

Alves, M.E. and Lavorenti, A. 2004. Sulfate adsorption and its relationships with properties of representative soils of the Sao Paulo State, Brazil. *Geoderma*, 118:89-99.

Alves, M.E. and Lavorenti, A. 2006. Sulfate desorption from representative soils of the Sao Paulo State, Brazil. *Australian Journal of Soil Research*, 44:291.

Aylmore, L.A.G.; Karim, M.; and Quirk, J.P. 1967. Adsorption and desorption of sulfate ions by soil constituents. *Soil Science*, 103:10-15.

Banerjee, M.R.; Chapman, S.J.; and Killham, K. 1993. Factors Influencing the determination of microbial biomass sulfur in soil. *Communications in Soil Science and Plant Analysis*, 24:939-950.

Banerjee, M.R. and Chapman, S.J. 1996. The significance of microbial biomass sulphur in soil. *Biology and Fertility of Soils*, 22:116-125.

Barrow, N.J. 1961. Studies on mineralization of sulphur from soil organic matter. *Australian Journal of Agricultural Research*, 12:306-&.

Barrow, N.J. 1992a. A brief discussion on the effect of temperature on the reaction of inorganic ions with soil. *Journal of Soil Science*, 43:37-45.

Barrow, N.J. 1992b. The effect of time on the competition between anions for sorption. *Journal of Soil Science*, 43:421-428.

Barrow, N.J. and Cox, V.C. 1992. The effects of pH and chloride concentration on mercury sorption by a soil. *Journal of Soil Science*, 43:305-312.

Barrow, N.J.; Cartes, P.; and Mora, M.L. 2005. Modifications to the Freundlich equation to describe anion sorption over a large range and to describe competition between pairs of ions. *European Journal of Soil Science*, 56:601-606.

Bast, C. 1991. Toxicity summary for sulfate. *Department of Energy - contract no. DE-AC05-84OR21400*. Health and Safety Research Division, Oak Ridge National Laboratory, Oak Ridge, Tennessee, USA. 6 p.

Bell, C.I.; Clarkson, D.T.; and Cram, W.J. 1995. Partitioning and redistribution of sulfur during S-stress in *Macroptilium atropurpureum* cv Siratro. *Journal of Experimental Botany*, 46:73-81.

Beulke, S. and Brown, C.D. 2006. Impact of correlation between pesticide parameters on estimates of environmental exposure. *Pest Management Science*, 62:603-609.

Beven, K. and Binley, A. 1992. The future of distributed models - Model calibration and uncertainty prediction. *Hydrological Processes*, 6:279-298.

Beven, K. and Freer, J. 2001. Equifinality, data assimilation, and uncertainty estimation in mechanistic modelling of complex environmental systems using the GLUE methodology. *Journal of Hydrology*, 249:11-29.

Blake-Kalff, M.M.A.; Harrison, K.R.; Hawkesford, M.J.; Zhao, F.J.; and McGrath, S.P. 1998. Distribution of sulfur within oilseed rape leaves in response to sulfur deficiency during vegetative growth. *Plant Physiology*, 118:1337-1344.

Blake-Kalff, M.M.A.; Hawkesford, M.J.; Zhao, F.J.; and McGrath, S.P. 2000. Diagnosing sulfur deficiency in field-grown oilseed rape (*Brassica napus* L.) and wheat (*Triticum aestivum* L.). *Plant and Soil*, 225:95-107.

Blake-Kalff, M.M.A.; Zhao, F.J.; Hawkesford, M.J.; and McGrath, S.P. 2001. Using plant analysis to predict yield losses caused by sulphur deficiency. *Annals of Applied Biology*, 138:123-127.

Bloem, E. 1998. Sulfur balance of agrarian ecological systems with special consideration of hydrological and soil-physical characteristics "*Schwefel-Bilanz von Agrarökosystemen unter besonderer Berücksichtigung hydrologischer und bodenphysikalischer Standorteigenschaften*". *PhD Thesis*, TU, Braunschweig, Germany.

Bloem, E.; Haneklaus, S.; and Schnug, E. 2004. Influence of nitrogen and sulfur fertilization on the alliin content of onions and garlic. *Journal of Plant Nutrition*, 27:1827-1839.

Bloem, E.; Cichota, R.; Jong van Lier, Q.; Sparovek, G.; and Schnug, E. 2005a. The importance of low mobile soil water for the S supply of plants. *Journal of Plant Nutrition and Soil Science*, 286:1-10.

Bloem, E.; Haneklaus, S.; and Schnug, E. 2005b. Significance of sulfur compounds in the protection of plants against pests and diseases. *Journal of Plant Nutrition*, 28:763-784.

Bodmann, B.E.J.; Dick, D.P.; and Dick, Y.P. 2004. An adsorption isotherm from a micro-state model. *Adsorption-Journal of the International Adsorption Society*, 10:277-286.

Bolan, N.S.; Scotter, D.R.; Syers, J.K.; and Tillman, R.W. 1986a. The effect of adsorption on sulfate leaching. *Soil Science Society of America Journal*, 50:1419-1424.

Bolan, N.S.; Syers, J.K.; and Tillman, R.W. 1986b. Ionic-strength effects on surface-charge and adsorption of phosphate and sulfate by soils. *Journal of Soil Science*, 37:379-388.

Bolan, N.S.; Syers, J.K.; Tillman, R.W.; and Scotter, D.R. 1988. Effect of liming and phosphate additions on sulfate leaching in soils. *Journal of Soil Science*, 39:493-504.

Bolan, N.S.; Syers, J.K.; and Sumner, M.E. 1993. Calcium-induced sulfate adsorption by soils. *Soil Science Society of America Journal*, 57:691-696.

Bolan, N.S.; Naidu, R.; Khan, M.A.R.; Tillman, R.W.; and Syers, J.K. 1999a. The effects of anion sorption on sorption and leaching of cadmium. *Australian Journal of Soil Research*, 37:445-460.

Bolan, N.S.; Naidu, R.; Syers, J.K.; and Tillman, R.W. 1999b. Surface charge and solute interactions in soils. *Advances in Agronomy*, 67:87-140.

Bruzzone, H. and Moreno, C. 1998. When errors in both coordinates make a difference in the fitting of straight lines by least squares. *Measurement Science & Technology*, 9:2007-2011.

Burau, R.G. and Zasoski, R.J. 2002. Soil and water chemistry - Course notes [Online]. Available at *http://lawr.ucdavis.edu/classes/ssc102* (verified in 20-01-2007).

Cajuste, L.J.; Laird, R.J.; Cuevas, B.; and Alvarado, J. 1998. Phosphorus retention by tropical soils as influenced by sulfate application. *Communications in Soil Science and Plant Analysis*, 29:1823-1831.

Casagrande, J.C.; Alleoni, L.R.F.; Camargo, O.A.; and Borges, M. 2003. Phosphate and sulfate adsorption on soils with variable electric charge. *Revista Brasileira de Ciencia do Solo*, 27:51-59.

Castellano, S.D. and Dick, R.P. 1991. Cropping and sulfur fertilization influence on sulfur transformations in soil. *Soil Science Society of America Journal*, 55:114-121.

Clothier, B.E. and Green, S.R. 1997. Roots: The big movers or water and chemical in soil. *Soil Science*, 162:534-543.

Conover, W.J. 1980. *Practical nonparametric statistics*. 2 ed. John Wiley & Sons, New York. 462 p.

Crosland, A.R.; Zhao, F.J.; and McGrath, S.P. 2001. Inter-laboratory comparison of sulphur and nitrogen analysis in plants and soils. *Communications in Soil Science and Plant Analysis*, 32:685-695.

Curtin, D. and Syers, J.K. 1990. Mechanism of sulfate adsorption by 2 tropical soils. *Journal of Soil Science*, 41:295-304.

Curtin, D.; Syers, J.K.; and Bolan, N.S. 1993. Phosphate sorption by soil in relation to exchangeable cation composition and pH. *Australian Journal of Soil Research*, 31:137-149.

Davis, J.G. and Burgoa, B. 1995. Interactive mechanisms of anion adsorption with calcium leaching and exchange. *Soil Science*, 160:256-264.

De Cesare, L.; Myers, D.E.; and Posa, D. 2001. Product-sum covariance for space-time modeling: an environmental application. *Environmetrics*, 12:11-23.

De Iaco, S.; Palma, M.; and Posa, D. 2005. Modeling and prediction of multivariate space-time random fields. *Computational Statistics & Data Analysis*, 48:525-547.

de Kok, L.J.; A., C.; Durenkamp, M.; Koralewska, A.; Posthumus, F.S.; Stuiver, C.E.E.; Yang, L.; and Stulen, I. 2005. Pathways of plant sulfur uptake and metabolism - an overview. *Journal of Plant Nutrition and Soil Science*, 283:5-13.

Dragten, R. and Thorrold, B.S. 2005. Consents for farming: regulating nutrient loss in the lake Taupo catchment. *18 Fertilzer and Lime Research Centre Conference - Developments in fertiliser application technologies and nutrient management*, Palmerston North, NZ. Massey University.

Droux, M. 2004. Sulfur assimilation and the role of sulfur in plant metabolism: a survey. *Photosynthesis Research*, 79:331-348.

Dubuis, P.H.; Marazzi, C.; Stadler, E.; and Mauch, F. 2005. Sulphur deficiency causes a reduction in antimicrobial potential and leads to increased disease susceptibility of oilseed rape. *Journal of Phytopathology*, 153:27-36.

Dubus, I.G. and Becquer, T. 2001. Phosphorus sorption and desorption in oxide-rich Ferralsols of New Caledonia. *Australian Journal of Soil Research*, 39:403-414.

Dubus, I.G.; Beulke, S.; Brown, C.D.; Gottesburen, B.; and Dieses, A. 2004. Inverse modelling for estimating sorption and degradation parameters for pesticides. *Pest Management Science*, 60:859-874.

Durenkamp, M. and De Kok, L.J. 2005. Low levels of H2S may replace sulfate as sulfur source in sulfate-deprived onion. *Phyton-Annales Rei Botanicae*, 45:69-77.

Edmeades, D.C.; Thorrold, B.S.; and Roberts, A.H.C. 2005. The diagnosis and correction of sulfur deficiency and the management of sulfur requirements in New Zealand pastures: a review. *Australian Journal of Experimental Agriculture*, 45:1205-1223.

Edwards, P.J. 1998. Sulfur cycling, retention, and mobility in soils: A review. *General Technical* Report NE-250. USDA Forest Service, Radnon. 18 p.

Elzinga, E.J.; van Grinsven, J.J.M.; and Swartjes, F.A. 1999. General purpose Freundlich isotherms for cadmium, copper and zinc in soils. *European Journal of Soil Science*, 50:139-149.

Eriksen, J. 1996. Incorporation of S into soil organic matter in the field as determined by the natural abundance of stable S isotopes. *Biology and Fertility of Soils*, 22:149-155.

Eriksen, J.; Murphy, M.D.; and Schnug, E. 1998. The soil sulphur cycle, p. 39-74, *In*: Schnug, E. (ed.) *Sulphur in Agroecosystems*, Vol. 2. Kluwer Academic Publishers, Dordrecht. pp. 39-74.

Eriksen, J. and Mortensen, J.V. 2002. Effects of timing of sulphur application on yield, S-uptake and quality of barley. *Plant and Soil*, 242:283-289.

Fahrenhorst, C.; Botschek, J.; Skowronek, A.; and Ferraz, J. 1999. Application of gypsum and lime to increase cation adsorption of a Geric Ferralsol in the Brazilian Amazon region. *Journal of Plant Nutrition and Soil Science*, 162:41-47.

Feyen, J.; Jacques, D.; Timmerman, A.; and Vanderborght, J. 1998. Modelling water flow and solute transport in heterogeneous soils: A review of recent approaches. *Journal of Agricultural Engineering Research*, 70:231-256.

Fismes, J.; Vong, P.C.; Guckert, A.; and Frossard, E. 2000. Influence of sulfur on apparent N-use efficiency, yield and quality of oilseed rape (*Brassica napus* L.) grown on a calcareous soil. *European Journal of Agronomy*, 12:127-141.

Florence, T.M. and Farrar, Y.J. 1971. Spectrophotometric determination of chloride at parts-per-billion level by mercury(II) thiocyanate method. *Analytica Chemica Acta*, 54:373-377.

Foloni, J.S.S. and Rosolem, C.A. 2006. Effect of liming and ammonium sulfate on cotton. I - Cation and anion transport in the soil. *Revista Brasileira de Ciencia do Solo*, 30:425-432.

Freney, J.R.; Spencer, K.; and Jones, M.B. 1978. Diagnosis of sulfur deficiency in wheat. *Australian Journal of Agricultural Research*, 29:727-738.

Freney, J.R. 1986. Forms and reactions of organic S compounds in soils, p. 207-231, *In*: Tabatabai, M. A. (ed.) *Sulfur in agriculture*, Vol. 27. ASA, CSSA and SSSA, Madison. pp. 207-231.

Friedel, M.J. 2005. Coupled inverse modeling of vadose zone water, heat, and solute transport: calibration constraints, parameter nonuniqueness, and predictive uncertainty. *Journal of Hydrology*, 312:148-175.

Geelhoed, J.S.; Hiemstra, T.; and VanRiemsdijk, W.H. 1997. Phosphate and sulfate adsorption on goethite: Single anion and competitive adsorption. *Geochimica et Cosmochimica Acta*, 61:2389-2396.

Goh, K.M. and Nguyen, M.L. 1997. Estimating net annual soil sulfur mineralisation in New Zealand grazed pastures using mass balance models. *Australian Journal of Agricultural Research*, 48:477-484.

Goudriaan, J. and van Laar, H.H. 1994. *Modelling potential crop growth processes*. Kluwer Academics Publishers, Dordrecht. 238 p.

Green, S.R.; Vogeler, I.; Clothier, B.E.; Mills, T.M.; and van den Dijssel, C. 2003. Modelling water uptake by a mature apple tree. *Australian Journal of Soil Research*, 41:365-380.

Greenstone, M. 2004. Did the Clean Air Act cause the remarkable decline in sulfur dioxide concentrations? *Journal of Environmental Economics and Management*, 47:585-611.

Gustafsson, J.P. 1995. Modeling pH-dependent sulfate adsorption in the Bs horizons of podzolized soils. *Journal of Environmental Quality*, 24:882-888.

Hagel, I. 2005. Sulfur and baking-quality of bread making wheat, *In*: de Kok, L. J. and Schnug, E. (eds.). *1st Sino-German Workshop on Aspects of Sulphur Nutrition of Plants*, Shenyang, China. 23 - 27 May 2004. Landbauforschung Völkenrode.

Hamming, R.W. 1973. *Numerical methods for scientists and engineers*. 2nd ed. Dover Publications, New York, US. 721 p.

Haneklaus, S.; Murphy, D.P.L.; Nowak, G.; and Schnug, E. 1995. Effects of the timing of sulfur application on grain-yield and yield components of wheat. *Journal of Plant Nutrition and Soil Science*, 158:83-85.

Haneklaus, S.; Paulsen, H.M.; Gupta, A.K.; Bloem, E.; and Schnug, E. 1999. Influence of sulfur fertilization on yield and quality of oilseed rape and mustard, *In*: Wratten, N. and Salisbury, P. A. (eds.). *Proceedings of the 10th International Rapeseed Congress - New Horizons for an Old Crop*, Canberra, Australia. 26–29 September 1999.

Hawkesford, A.J.; Buchner, P.; Howarth, J.R.; and Lu, C. 2005. Understanding the regulation of sulfur nutrition - from sulfate transporter genes to the field. *Phyton-Annales Rei Botanicae*, 45:57-67.

Hawkesford, M.J. 2000. Plant responses to sulphur deficiency and the genetic manipulation of sulphate transporters to improve S-utilization efficiency. *Journal of Experimental Botany*, 51:131-138.

Hawkesford, M.J. and De Kok, L.J. 2006. Managing sulphur metabolism in plants. *Plant Cell and Environment*, 29:382-395.

He, Z.L.; Yang, X.; Yuan, K.N.; and Zhu, Z.X. 1994. Desorption and plant-availability of phosphate sorbed by some important minerals. *Plant and Soil*, 162:89-97.

He, Z.L.; Wu, J.; Odonnell, A.G.; and Syers, J.K. 1997. Seasonal responses in microbial biomass carbon, phosphorus and sulphur in soils under pasture. *Biology and Fertility of Soils*, 24:421-428.

Henderson, J.V. 1996. Effects of air quality regulation. *American Economic Review*, 86:789-813.

Heng, L.K. and White, R.E. 1996. A simple analytical transfer function approach to modelling the leaching of reactive solutes through field soil. *European Journal Of Soil Science*, 47:33-42.

Heng, L.K.; Tillman, R.W.; and White, R.E. 1999. Anion and cation leaching through large undisturbed soil cores under different flow regimes. 1. Experimental results. *Australian Journal of Soil Research*, 37:711-726.

Heuvelink, G.B.M. and Webster, R. 2001. Modelling soil variation: past, present, and future. *Geoderma*, 100:269-301.

Hinz, C. 2001. Description of sorption data with isotherm equations. *Geoderma*, 99:225-243.

Hollenbeck, K.J. and Jensen, K.H. 1998. Maximum-likelihood estimation of unsaturated hydraulic parameters. *Journal of Hydrology*, 210:192-205.

Huang, C.Y.L. and Schulte, E.E. 1985. Digestion of plant-tissue for analysis by ICP emission-spectroscopy. *Communications in Soil Science and Plant Analysis*, 16:943-958.

Huang, H.; Hassan, A.E.; and Hu, B.X. 2003. Monte Carlo study of conservative transport in heterogeneous dual-porosity media. *Journal of Hydrology*, 275:229-241.

Hupet, F.; Lambot, S.; Feddes, R.A.; van Dam, J.C.; and Vanclooster, M. 2003. Estimation of root water uptake parameters by inverse modeling with soil water content data. *Water Resources Research*, 39:Art. No. 1312.

Hupet, F.; Trought, M.C.T.; Greven, M.; Green, S.R.; and Clothier, B.E. 2005. Data requirements for identifying macroscopic water stress parameters: A study on grapevines. *Water Resources Research*, 41:Art. No. W06008.

Hupet, F. and Vanclooster, A. 2005. Micro-variability of hydrological processes at the maize row scale: implications for soil water content measurements and evapotranspiration estimates. *Journal of Hydrology*, 303:247-270.

Imtiaz, M.; Alloway, B.J.; Aslam, M.; Memon, M.Y.; Khan, P.; Siddiqui, S.U.H.; and Shah, S.K.H. 2006. Zinc sorption in selected soils. *Communications in Soil Science and Plant Analysis*, 37:1675-1688.

Ishiguro, M.; Makino, T.; and Hattori, Y. 2006. Sulfate adsorption and surface precipitation on a volcanic ash soil (allophanic andisol). *Journal of Colloid and Interface Science*, 300:504-510.

Jackson, G.D. 2000. Effects of nitrogen and sulfur on canola yield and nutrient uptake. *Agronomy Journal*, 92:644-649.

Jacques, D.; Simunek, J.; Timmerman, A.; and Feyen, J. 2002. Calibration of Richards' and convection-dispersion equations to field-scale water flow and solute transport under rainfall conditions. *Journal of Hydrology*, 259:15-31.

Jara, A.A.; Violante, A.; Pigna, M.; and Mora, M.D.L. 2006. Mutual interactions of sulfate, oxalate, citrate, and phosphate on synthetic and natural allophanes. *Soil Science Society of America Journal*, 70:337-346.

Johnson, C.M. and Nishita, H. 1952. Microestimation of sulfur in plant materials, soils, and irrigation waters. *Analytical Chemistry*, 24:736-742.

Jones, M.B. 1986. Sulphur availability indexes, p. 549–566, *In*: Tabatabai, M. A. (ed.) *Sulphur in agriculture*. ASA, CSSA and SSSA, Madison,WI. pp. 549–566.

Jury, W.A. and Roth, K. 1990. *Transfer functions and solute movement through soil: Theory and applications*. Birkhauser Verlag, Berlim. 226 p.

Karmoker, J.L.; Clarkson, D.T.; Saker, L.R.; Rooney, J.M.; and Purves, J.V. 1991. Sulfate deprivation depresses the transport of nitrogen to the xylem and the hydraulic conductivity of barley (*Hordeum vulgare* L) roots. *Planta*, 185:269-278.

Katou, H.; Uchimura, K.; and Clothier, B.E. 2001. An Unsaturated Transient Flow Method for Determining Solute Adsorption by Variable-Charge Soils. *Soil Science Society of America Journal*, 65:283-290.

Kennedy, V.J. and Markwitz, A. 2002. heavy metal pollution studies of suspended sediments in Waiwhetu sream water by PIXE. *International Journal of PIXE*, 12:189-197.

Kettlewell, P.S.; Griffiths, M.W.; Hocking, T.J.; and Wallington, D.J. 1998. Dependence of wheat dough extensibility on flour sulphur and nitrogen concentrations and the influence of foliar-applied sulphur and nitrogen fertilisers. *Journal of Cereal Science*, 28:15-23.

Kinniburgh, D.G. 1986. General purpose adsorption isotherms. *Environmental Science Technology*, 20:895-904.

Kirchmann, H.; Pichlmayer, F.; and Gerzabek, M.H. 1996. Sulfur balances and sulfur-34 abundance in a long-term fertilizer experiment. *Soil Science Society of America Journal*, 60:174-178.

Klikocka, H.; Haneklaus, S.; Bloem, E.; and Schnug, E. 2005. Influence of sulfur fertilization on infection of potato tubers with Rhizoctonia solani and Streptomyces scabies. *Journal of Plant Nutrition*, 28:819-833.

Kohne, J.M.; Mohanty, B.P.; and Simunek, J. 2006. Inverse dual-permeability modeling of preferential water flow in a soil column and implications for field-scale solute transport. *Vadose Zone Journal*, 5:59-76.

Korom, S.F. 2000. An adsorption isotherm for bromide. *Water Resources Research*, 36:1969-1974.

Kutilek, M. and Nielsen, D.R. 1994. *Soil Hydrology*. Catena-Verlag, Cremingen-Destedt, Germany. 370 p.

Kyriakidis, P.C. and Journel, A.G. 1999. Geostatistical space-time models: A review. *Mathematical Geology*, 31:651-684.

Ledgard, S.F.; Thorrold, B.S.; Petch, R.A.; and Young, J. 2001. Use of OVERSEER as a tool to identify management strategies for reducing nitrate leaching from farms around Lake Taupo, *In*: Currie, L. D. and Loganathan, P. (eds.). *14th Fertilizer and Lime Research Centre Conference - Precision tools for improving land management*, Palmerston North, NZ. Massey University.

Libardi, P.L. 2000. *Dynamics of the water in the soil "Dinâmica da Água no Solo"*. 2nd ed. EDUSP, Sao Paulo. 344 p.

Ludwig, B.; Khanna, P.; and Prenzel, J. 1999. Some equilibrium approaches to study the retention and release of sulfate in some highly acid german subsoils. *Journal of Environmental Quality*, 28:1327-1335.

Magesan, G.N.; Scotter, D.R.; and White, R.E. 1999. The utility of Burns's equation to describe solute movement through soil under various boundary and initial conditions. *European Journal Of Soil Science*, 50:649-656.

Magesan, G.N.; Bolan, N.S.; and Lee, R. 2003a. Adsorption of atrazine and phosphate as affected by soil depth in allophanic and non-allophanic soils. *New Zealand Journal of Agricultural Research*, 46:155-163.

Magesan, G.N.; Vogeler, I.; Clothier, B.E.; Green, S.R.; and Lee, R. 2003b. Solute movement through an allophanic soil. *Journal of Environmental Quality*, 32:2325-2333.

Malhi, S.S. and Gill, K.S. 2006. Cultivar and fertilizer S rate interaction effects on canola yield, seed quality and S uptake. *Canadian Journal of Plant Science*, 86:91-98.

Maraqa, M.A. 2001. Effects of fundamental differences between batch and miscible displacement techniques on sorption distribution coefficient. *Environmental Geology*, 41:219-228.

Marcano-Martinez, E. and McBride, M.B. 1989. Calcium and sulfate retention by 2 oxisols of the Brazilian cerrado. *Soil Science Society of America Journal*, 53:63-69.

Marschner, H. 1995. *Mineral nutrition of higher plants.* 2nd ed. Academic Press, Amsterdan. 889 p.

Matula, J. and Zukalova, H. 2001. Sulphur concentrations and distribution in three varieties of oilseed rape in relation to sulphur fertilization at a maturity stage. *Rostlinna Vyroba*, 47:14-17.

McCray, J.E.; Kirkland, S.L.; Siegrist, R.L.; and Thyne, G.D. 2005. Model parameters for simulating fate and transport of on-site wastewater nutrients. *Ground Water*, 43:628-639.

Mengel, K. 1996. Turnover of organic nitrogen in soils and its availability to crops. *Plant and Soil*, 181:83-93.

Mertens, J.; Stenger, R.; and Barkle, G.F. 2006. Multiobjective inverse modeling for soil parameter estimation and model verification. *Vadose Zone Journal*, 5:917-933.

Moldrup, P.; Olesen, T.; Yoshikawa, S.; Komatsu, T.; and Rolston, D.E. 2004. Three-porosity model for predicting the gas diffusion coefficient in undisturbed soil. *Soil Science Society of America Journal*, 68:750-759.

Molloy, L. 1988. *Soils in the New Zealand landscape.* NZ Society of Soil Science, Lincoln. 239 p.

Mora, M.D.L.; Shene, C.; Violante, A.; Demanet, R.; and Bolan, N.S. 2005. The effects organic matter and soil chemical properties on sulfate sorption in Chilean volcanic soils, p. 223-244, *In*: Huang, P. M.; Violante, A.; Bollag, J. M.; and Vityakon, P. (eds.). *Soil abiotic and biotic interactions and the impact on the ecosystem and human welfare.* Science Publishers, Enfield, NH. pp. 223-244.

Mualem, Y. 1976. New Model for predicting hydraulic conductivity of unsaturated porous media. *Water Resources Research*, 12:513-522.

Naeve, S.L. and Shibles, R.M. 2005. Distribution and mobilization of sulfur during soybean reproduction. *Crop Science*, 45:2540-2551.

Nakajima, M.; Nishimura, T.; Kato, M.; and Suzuki, S. 2002. Percolation and reactions of Ca solution through acid Kunigami Mahji soil. *Transactions of the 17th World Congress of Soil Science, Symposium 63, Paper Number 790*, Bangkok, Thailand. August 14-21, 2002.

Nguyen, M.L. and Goh, K.M. 1993. An overview of the New Zealand sulfur cycling model for recommending sulfur requirements in grazed pastures. *New Zealand Journal of Agricultural Research*, 36:475-491.

Nguyen, M.L. and Goh, K.M. 1994. Sulphur cycling and its implications on sulphur fertilizer requirements of grazed grassland ecosystems. *Agriculture, Ecosystems & Environment*, 49:173-206.

Nikiforova, V.J.; Kopka, J.; Tolstikov, V.; Fiehn, O.; Hopkins, L.; Hawkesford, M.J.; Hesse, H.; and Hoefgen, R. 2005. Systems rebalancing of metabolism in response to sulfur deprivation, as revealed by metabolome analysis of arabidopsis plants. *Plant Physiology*, 138:304-318.

Oldham, K.B. and Myland, J.C. 1994. *Fundamentals of electrochemical science.* Academic Press, Amsterdam. 496 p.

Oliver, M.A. 2004. Practical geostatistics: Modelling and spatial analysis. *International Journal of Geographical Information Science*, 18:102-U3.

Parfitt, R.L. and Wilson, A.D. 1985. Estimation of allophane and halloysite in three sequences of volcanic soils, New Zealand, p. 1–8, *In*: Caldas, F. and Yaalon, D. H. (eds.). *Volcanic soils. CATENA Suppl. 7.* Catena Verlag, Desdedt, Germany. pp. 1–8.

Pearce, R.C. and Sumner, M.E. 1997. Apparent salt sorption reactions in an unfertilized acid subsoil. *Soil Science Society of America Journal*, 61:765-772.

Pigna, M. and Violante, A. 2003. Adsorption of sulfate and phosphate on andisols. *Communications in Soil Science and Plant Analysis*, 34:2099-2113.

Pinkerton, A. 1998. Critical sulfur concentrations in oilseed rape (*Brassica napus*) in relation to nitrogen supply and to plant age. *Australian Journal of Experimental Agriculture*, 38:511-522.

Press, W.H.; Teukolsky, S.A.; Vetterling, W.T.; and Flannery, B.P. 2002. *Numerical recipies in C++*. 2nd ed. Cambridge University Press, Cambridge. 1032 p.

Probert, M.E. and Keating, B.A. 2000. What soil constraints should be included in crop and forest models? *Agriculture Ecosystems & Environment*, 82:273-281.

Pugh, E.M. and Winslow, G.H. 1966. *The analysis of physical measurements*. Addison-Wesley, Reading. 246 p.

Qafoku, N.P.; Sumner, M.E.; and Radcliffe, D.E. 2000. Anion transport in columns of variable charge subsoils: Nitrate and chloride. *Journal of Environmental Quality*, 29:484-493.

Qafoku, N.P. and Sumner, M.E. 2001. Retention and transport of calcium nitrate in variable charge subsoils. *Soil Science*, 166:297-307.

Qafoku, N.P. and Sumner, M.E. 2002. Adsorption and desorption of indifferent ions in variable charge subsoils: The possible effect of particle interactions on the counter-ion charge density. *Soil Science Society of America Journal*, 66:1231-1239.

Randlett, D.L.; Zak, D.R.; and Macdonald, N.W. 1992. Sulfate adsorption and microbial immobilization in northern hardwood forests along an atmospheric deposition gradient. *Canadian Journal of Forest Research*, 22:1843-1850.

Rasmussen, P.E.; Ramig, R.E.; Ekin, L.G.; and Rohde, C.R. 1977. Tissue analyses guidelines for diagnosing sulfur deficiency in white wheat. *Plant and Soil*, 46:153-163.

Rausch, T. and Wachter, A. 2005. Sulfur metabolism: a versatile platform for launching defence operations. *Trends in Plant Science*, 10:503-509.

Rietra, R.P.J.J.; Hiemstra, T.; and van Riemsdijk, W.H. 1999. Sulfate adsorption on goethite. *Journal of Colloid and Interface Science*, 218:511-521.

Ryden, J.C. and Syers, J.K. 1976. Calcium retention in response to phosphate sorption by soils. *Soil Science Society of America Journal*, 40:845-846.

Saggar, S.; Bettany, J.R.; and Stewart, J.W.B. 1981. Measurement of microbial sulfur in soil. *Soil Biology & Biochemistry*, 13:493-498.

Santoso, D.; Lefroy, R.D.B.; and Blair, G.J. 1995. Sulfur and phosphorus dynamics in an acid soil/crop system. *Australian Journal of Soil Research*, 33:113-124.

Sarkar, M.; Banerjee, A.; and Pramanick, P.P. 2006. Kinetics and mechanism of fluoride removal using laterite. *Industrial & Engineering Chemistry Research*, 45:5920-5927.

Scaife, A. and Burns, I.G. 1986. The sulfate-S total S ratio in plants as an index of their sulfur status. *Plant and Soil*, 91:61-71.

Scheidegger, A.M. and Sparks, D.L. 1996. A critical assessment of sorption-desorption mechanisms at the soil mineral/water interface. *Soil Science*, 161:813-831.

Scherer, H.W. 2001. Sulphur in crop production - invited paper. *European Journal of Agronomy*, 14:81-111.

Schnug, E.; Haneklaus, S.; and Murphy, D.P.L. 1993. Impact of sulfur fertilization on fertilizer nitrogen efficiency. *Sulphur in Agriculture*, 17:8-12.

Schnug, E. and Haneklaus, S. 1994. Sulphur deficiency in Brassica napus: biochemistry, symptomatology, morphogenesis. *Landbauforsch Völkenrode* SH 144. FAL, Braunschweig. 31 p.

Schnug, E.; Haneklaus, S.; Borchers, A.; and Polle, A. 1995. Relations between sulfur supply and glutathione and ascorbate concentrations in *Brassica napus*. *Zeitschrift fur Pflanzenernahrung und Bodenkunde*, 158:67-69.

Schnug, E. 1998. *Sulphur in Agroecosystems*. Kluwer Academic Publishers, Dordrecht. 228 p.

Schnug, E. and Haneklaus, S. 1998. Diagnosis of sulphur nutrition, p. 1-38, *In*: Schnug, E. (ed.) *Sulphur in Agroecosystems*, Vol. 2. Kluwer Academic Publishers, Dordrecht. pp. 1-38.

Schnug, E. and Haneklaus, S. 2005. Sulphur deficiency symptoms in oilseed rape (*Brassica napus* L.) - The aesthetics of starvation. *Phyton-Annales Rei Botanicae*, 45:79-95.

Schulthess, C.P. and Dey, D.K. 1996. Estimation of Langmuir constants using linear and nonlinear least squares regression analyses. *Soil Science Society of America Journal*, 60:433-442.

Selim, H.M.; Gobran, G.R.; Guan, X.; and Clarke, N. 2004. Mobility of sulfate in forest soils: Kinetic modeling. *Journal of Environmental Quality*, 33:488-495.

Selim, H.M. and Zhu, H. 2005. Atrazine sorption-desorption hysteresis by sugarcane mulch residue. *Journal of Environmental Quality*, 34:325-335.

Sen, A. and Srivastava, M. 1990. *Regression analysis - Theory, methods, and applications*. Springer-Verlag, Berlim. 347 p.

Serrano, R.E.; Arias, J.S.; and Fernandez, P.G. 1999. Soil properties that affect sulphate adsorption by palexerults in western and central Spain. *Communications In Soil Science And Plant Analysis*, 30:1521-1530.

Shaffer, P.W. and Stevens, D.L. 1991. Evaluation of Procedures for aggregating nonlinear sulfate adsorption-isotherm data. *Soil Science Society of America Journal*, 55:684-692.

Shrift, A. 1969. Aspects of selenium metabolism in higher plants. *Annual Review of Plant Physiology*, 20:475-494.

Simunek, J.; Jarvis, N.J.; van Genuchten, M.T.; and Gardenas, A. 2003. Review and comparison of models for describing non-equilibrium and preferential flow and transport in the vadose zone. *Journal of Hydrology*, 272:14-35.

Sinclair, A.G. and Saunders, W.M.H. 1984. Sulphur, p. 15-17, *In*: Cornforth, I. S. and Sinclair, A. G. (eds.). *Fertilizer and lime recommendations for pastures and crops in New Zealand*, 2nd ed. Ministry of Agirculture and Fisheries, Wellington. pp. 15-17.

Snepvangers, J.; Heuvelink, G.B.M.; and Huisman, J.A. 2003. Soil water content interpolation using spatio-temporal kriging with external drift. *Geoderma*, 112:253-271.

Sonnleitner, M.A.; Abbaspour, K.C.; and Schulin, R. 2003. Hydraulic and transport properties of the plant-soil system estimated by inverse modelling. *European Journal of Soil Science*, 54:127-138.

Sparks, D.L. 1989. Kinetics of soil chemical processes:210.

Sparks, D.L. 1996. Kinetics of sorption/release processes on natural particles., *In*: Huang, P. M.; Senesi, N.; and Buffle, J. (eds.). *Structure and surface reactions of soil particles*, Vol. 4. John Willey and Sons, New York.

Sposito, G. 1984. *The surface chemistry of soils*. Oxford University Press, New York. 248 p.

Stewart, C.; Johnston, D.M.; Leonard, G.S.; Horwell, C.J.; Thordarson, T.; and Cronin, S.J. 2006. Contamination of water supplies by volcanic ashfall: A

literature review and simple impact modelling. *Journal of Volcanology and Geothermal Research*, 158:296-306.

Stuiver, C.E.E.; DeKok, L.J.; and Westerman, S. 1997. Sulfur deficiency in *Brassica oleracea* L: Development, biochemical characterization, and sulfur/nitrogen interactions. *Russian Journal of Plant Physiology*, 44:505-513.

Sullivan, E.J.; Bowman, R.S.; and Legiec, I.A. 2003. Sorption of arsenic from soil-washing leachate by surfactant-modified zeolite. *Journal of Environmental Quality*, 32:2387-2391.

Tabatabai, M.A. and Bremner, J.M. 1970. An alkaline oxidation method for determination of total sulfur in soils. *Soil Science Society of America Proceedings*, 34:62-65.

Tabatabai, M.A. and Chae, Y.M. 1982. Alkaline oxidation method for determination of total sulfur in plant materials. *Agronomy Journal*, 74:404-406.

Tan, Z.; McLaren, R.G.; and Cameron, K.C. 1994. Seasonal-variations in forms of extractable sulfur in some New Zealand soils. *Australian Journal of Soil Research*, 32:985-993.

Tillman, R.W. 1991. Solute movement associated with intermitent soil water flow. *PhD thesis*, Massey University, Palmerston North.

Tinker, P.B. and Nye, P.H. 2000. *Solute movement in the rizosphere*. Oxford University Press, New York. 444 p.

Undabeytia, T.; Nir, S.; Rytwo, G.; Morillo, E.; and Maqueda, C. 1998. Modeling adsorption-desorption processes of Cd on montmorillonite. *Clays and Clay Minerals*, 46:423-428.

van den Berg, M. and Driessen, P.M. 2002. Water uptake in crop growth models for land use systems analysis I. A review of approaches and their pedigrees. *Agriculture Ecosystems & Environment*, 92:21-36.

van Genuchten, M.T. 1980. A Closed-form equation for predicting the hydraulic conductivity of unsaturated soils. *Soil Science Society of America Journal*, 44:892-898.

Verburg, K. and Baveye, P. 1994. Hysteresis in the binary exchange of cations on 2/1 clay minerals - A critical review. *Clays and Clay Minerals*, 42:207-220.

Vogeler, I. 1997. The convention-dispersion equation – not the question, the answer! *PhD Thesis*, Massey University, Pamerston North.

Vrugt, J.A.; Bouten, W.; Gupta, H.V.; and Sorooshian, S. 2002. Toward improved identifiability of hydrologic model parameters: The information content of experimental data. *Water Resources Research*, 38:Art. No. 1312.

Vrugt, J.A.; Diks, C.G.H.; Gupta, H.V.; Bouten, W.; and Verstraten, J.M. 2005. Improved treatment of uncertainty in hydrologic modeling: Combining the strengths of global optimization and data assimilation. *Water Resources Research*, 41:Art. No. W01017.

Wada, S. 1984. Mechanism of apparent salt absorption in ando soils. *Soil Science and Plant Nutrition*, 30:77-83.

Wadaskar, J.V.; Ekhe, J.D.; and Kale, S.P. 2006. Adsorption-desorption of HCH and endosulfan on a soil. *Environmental Technology*, 27:1011-1017.

Watkinson, J.H. and Perrot, K.W. 1990. A new soil test for sulphate and mineralisable organic sulphur. *New Zealand fertiliser manufacturers research association conference*, Auckland. November, 1990.

Watkinson, J.H. and Kear, M.J. 1996a. Sulfate and mineralisable organic sulfur in pastoral soils of New Zealand.1. A quasi equilibrium between sulfate and mineralisable organic sulfur. *Australian Journal of Soil Research*, 34:385-403.

Watkinson, J.H. and Kear, M.J. 1996b. Sulfate and mineralisable organic sulfur in pastoral soils of New Zealand.2. A soil test for mineralisable organic sulfur. *Australian Journal of Soil Research*, 34:405-412.

Wauchope, R.D.; Yeh, S.; Linders, J.; Kloskowski, R.; Tanaka, K.; Rubin, B.; Katayama, A.; Kordel, W.; Gerstl, Z.; Lane, M.; and Unsworth, J.B. 2002. Pesticide soil sorption parameters: theory, measurement, uses, limitations and reliability. *Pest Management Science*, 58:419-445.

Western, A.W. and Bloschl, G. 1999. On the spatial scaling of soil moisture. *Journal of Hydrology*, 217:203-224.

Wheeler, D.M. and Thorold, B.S. 1997. Pasture response to different sulphur fertiliser strategies and its applications to modelling. *Proceedings of the New Zealand Grasslands Association*, 59:39-43.

White, P.J.; Bowen, H.C.; Parmaguru, P.; Fritz, M.; Spracklen, W.P.; Spiby, R.E.; Meacham, M.C.; Mead, A.; Harriman, M.; Trueman, L.J.; Smith, B.M.; Thomas, B.; and Broadley, M.R. 2004. Interactions between selenium and sulphur nutrition in *Arabidopsis thaliana*. *Journal of Experimental Botany*, 55:1927-1937.

Willmott, C.J.; Ackleson, S.G.; Davis, R.E.; Feddema, J.J.; Klink, K.M.; Legates, D.R.; Odonnell, J.; and Rowe, C.M. 1985. Statistics for the evaluation and comparison of models. *Journal of Geophysical Research*, 90:8995-9005.

Wilson, D.J.; Western, A.W.; and Grayson, R.B. 2004. Identifying and quantifying sources of variability in temporal and spatial soil moisture observations. *Water Resources Research*, 40:Art. No. W02507.

Withers, P.J.A.; Tytherleigh, A.R.J.; and Odonnell, F.M. 1995. Effect of sulphur fertilizers on the grain yield and sulphur content of cereals. *Journal of Agricultural Science*, 125:317-324.

Wu, C.H.; Kuo, C.Y.; Lin, C.F.; and Lo, S.L. 2002. Modeling competitive adsorption of molybdate, sulfate, selenate, and selenite using a Freundlich-type multi-component isotherm. *Chemosphere*, 47:283-292.

Wu, J.; Odonnell, A.G.; and Syers, J.K. 1993. Microbial-growth and sulfur immobilization following the incorporation of plant residues into soil. *Soil Biology & Biochemistry*, 25:1567-1573.

Yang, L.P.; Stulen, I.; and De Kok, L.J. 2006. Sulfur dioxide: Relevance of toxic and nutritional effects for Chinese cabbage. *Environmental and Experimental Botany*, 57:236-245.

Zhang, H. and Selim, H.M. 2005. Kinetics of arsenate adsorption-desorption in soils. *Environmental Science & Technology*, 39:6101-6108.

Zhao, F.J.; Hawkesford, M.J.; Warrilow, A.G.S.; McGrath, S.P.; and Clarkson, D.T. 1996. Responses of two wheat varieties to sulphur addition and diagnosis of sulphur deficiency. *Plant and Soil*, 181:317-327.

Zhao, F.J.; Bilsborrow, P.E.; Evans, E.J.; and McGrath, S.P. 1997. Nitrogen to sulphur ratio in rapeseed and in rapeseed protein and its use in diagnosing sulphur deficiency. *Journal of Plant Nutrition*, 20:549-558.

Zhao, F.J.; Hawkesford, M.J.; and McGrath, S.P. 1999a. Sulphur assimilation and effects on yield and quality of wheat. *Journal of Cereal Science*, 30:1-17.

Zhao, F.J.; Salmon, S.E.; Withers, P.J.A.; Evans, E.J.; Monaghan, J.M.; Shewry, P.R.; and McGrath, S.P. 1999b. Responses of breadmaking quality to sulphur in three wheat varieties. *Journal of the Science of Food and Agriculture*, 79:1865-1874.

Zhao, F.J.; McGrath, S.P.; and Hawkesford, M.J. 2001. Sulphur nutrition and the sulphur cycle Research Report 2000-2001. Institute of Arable Crops - Rothamsted, Harpenden. 36-39 p.

Appendices

List of Symbols and Abbreviations of the Appendices

Roman letters

Symbol	Description	Unit
C	Concentration of a solute dissolved in the soil solution	[mol m^{-3}]
C_0	Initial concentration of a solute in the soil solution	[mol m^{-3}]
C_I	Concentration of a solute in the input solution	[mol m^{-3}]
C_e	Concentration of a solute in the outflow solution	[mol m^{-3}]
$\hat{C}_e$	Concentration of a solute in the outflow solution	[mol m^{-3}]
d	An auxiliary model variable	-
dt	A time-step	[s]
dz	A space-step	[m]
D	Soil hydrodynamic dispersion coefficient	[m^{-2} s^{-1}]
E_{limit}	The limit for the deviation between two estimates	-
F	A generic function	-
G	A generic function	-
i	An integer used as index to indicate the ion species	-
j	An integer used as a counter	-
k_F	Parameter of the Freundlich isotherm equation	[L kg^{-1}]
k_{IP}	A generalised IPA equilibrium factor	-
k_s	IPA equilibrium factor for PGA approach	[mol kg^{-1}]
k_c	IPA equilibrium factor for SGA1 approach	[mol L^{-1}]

k_r	IPA equilibrium factor for SGA2 approach	[L kg^{-1}]
L	The length of the soil column	[m]
L_0	The length of the gradient of a function	-
N	Exponent of the Freundlich isotherm equation	-
n_D	The total number of elements in a data set	-
n_L	The number of layers	-
n_S	The number of simulations	-
O	A value from an observed data set	-
P	A value from an predicted data set	-
P_Q	A value of Q_S predicted by the model	-
p	Representation of a generic model's parameter	-
p_0	The value of a generic parameter in the beginning of a loop	-
p_{ini}	The initial value of a generic parameter	-
P_{end}	The final value of a generic parameter	-
p_{max}	The upper value of a generic parameter	-
p_{min}	The lower value of a generic parameter	-
p_{opt}	The optimum value of a generic parameter	-
p_{step}	The variation step of a generic parameter	-
Q_S	The solute concentration in the soil (mass basis)	[mol kg^{-1}]
q_s	Solute flux density in the soil	[mol m^{-2} s^{-1}]
q_w	Water flux density ion the soil	[m s^{-1}]
S	Concentration of a solute adsorbed onto the soil particles	[mol kg^{-1}]
S_{IP}	Concentration of a solute adsorbed due to IPA	[mol kg^{-1}]
S_s	Single species adsorption concentration	[mol kg^{-1}]

t	Temporal ordinate	[s]
t_{max}	The maximum value for the simulation time	[s]
x	A generic variable	-
y	A generic variable or an integer counter	-
z	Spatial ordinate, commonly vertical (depth)	[m]

Greek letters

Symbol	Description	Unit
Φ	The objective function	-
Φ_C	The objective function comparing values of C	-
Φ_S	The objective function comparing values of S	-
Φ_{opt}	The value of objective function with optimum parameters	-
$\Delta\Phi$	The variation of the objective function	-
ϑ	Specific water volume or water-to-soil ratio	[L kg^{-1}]
θ	Volumetric soil water content	[m^3 m^{-3}]
ρ	Soil bulk density	[kg m^{-3}]
σ^2	Variance of the measurements	-

Additional symbols

Symbol	Description	Unit
$\mathbf{U}$	A unit vector	-
$\mathbf{H}$	The Hessian matrix	-
∇	The gradient of a function	-

Abbreviations:

BTC	Breakthrough curve
CDE	Convention-dispersion equation
E.C.	Electrical conductivity
FDM	Finite difference model
IPA	Ion-pair adsorption
NR01	The routine for solving the adsorption model without IPA
NR02	The routine for solving the adsorption model with IPA
PV	Pore volume = number of WFPV leached through a soil column
PGA	Particle governed approach for describing IPA
SGA1	Linear solution governed approach for describing IPA
SGA2	Radical solution governed approach for describing IPA
Simula_BTC	The routine for the simulation of solute movement in the soil
WFPV	Water filled pore volume

APPENDIX A

A. The miscible displacement experiments

In this appendix a summary of the results from miscible displacement experiments is presented. Initially the data from two preliminary experiments are shown. The results from these experiments showed interesting features that instigated further work, with more detailed experiments and analyses. The second set of experiments, termed main experiments, comprises the theme of Chapter 4, and was also partly used in Chapter 6. Nonetheless, not all the results obtained have been presented in those chapters. These additional results are presented here. For the sake of easing comparisons between different experiments, the results from all columns are summarised here.

A.1. Preliminary experiments

Two preliminary miscible displacement experiments were performed using Egmont and Taupo soils. The equipment and procedure used in these experiments were basically the same as described in Chapter 4. The main characteristics of the two columns, the soils, and the solutions are presented in Table A.1. The pre-leaching phase used solutions of $CaCl_2$, followed by the leaching phase with $CaSO_4$, for both columns. Differently from those of the main experiments, the trials were carried for much longer time, and the flow had been stopped at some times. Also, only part of the leachate was collected in the pre-leaching phase. Because of this, only few chemical analyses were done and these two experiments were not considered for further analyses in this thesis. They are shown here to help understanding the background developments that lead to the main experiments and the proposal of additional batch experiment.

Table A.1. Selected characteristics of the soils columns and solutions used in the preliminary miscible displacement experiments.

	Egmont soil	Taupo soil
ρ [1] (kg m^{-3})	698.0	875.5
WFPV [2] (cm^3)	848.0	654.4
θ_i [3] (m^3 m^{-3})	0.302	0.074
θ_f (m^3 m^{-3})	0.666	0.514
pH (H_2O)	4.92	4.43
q_w [4] (mm h^{-1})	35.4	65.2
Input solutions (mmol L^{-1})		
Pre-Leaching ($CaCl_2$)	10.12	10.60
Leaching ($CaSO_4$)	10.06	8.60
SO_4^{-2} adsorption [5] (mmol kg^{-1})	10.58	1.04
Volume leached (PV)		
Pre-leaching	12.6	5.6
Leaching	14.5	5.2

[1] ρ is the soil bulk density; [2] *WFPV* is the water filled pore volume; [3] θ_i and θ_f are the initial and final soil water content; and [4] q_w is the water flux density in the leaching stage; [5] Adsorption estimated by the difference between the final soil concentration and the concentration in the leaching solution.

The two preliminary experiments were performed for verifying any special feature in the sulphate movement in this two contrasting soils. Also this was a phase for learning how to use the equipment and the procedure for the experiments and the analyses of its results. Only few parameters were measured then, basically the sulphate concentration (Figure A.1) and the pH of the leachate (Figure A.2). These measurements have shown that the movement of sulphate is considerably different between the two soils. With some special feature for the Egmont soil, as evidenced by the pH behaviour

(Figure A.2), at the stage just before the appearance of sulphate in the outflow. This has stimulated the performance of further experiments, and eventually to the identification of ion-pair adsorption in the Egmont soil.

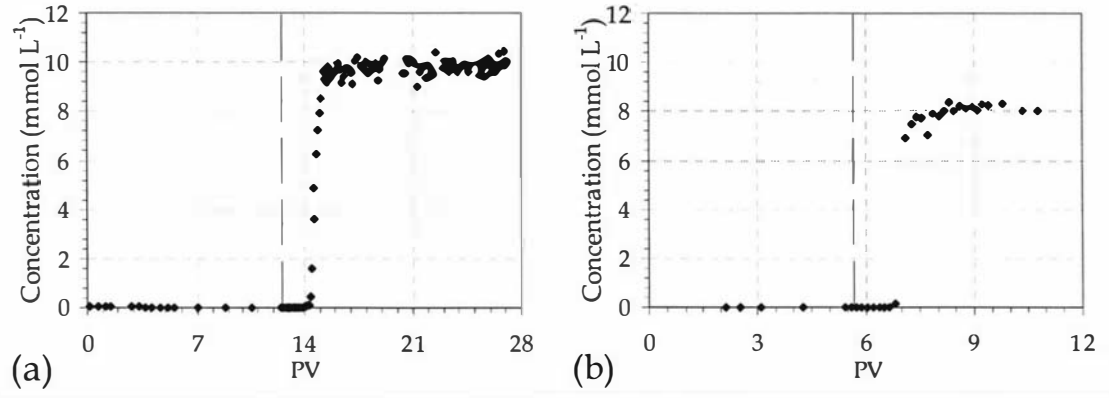


Figure A.1. Measured sulphate breakthrough curves for Egmont soil (a) and Taupo soil (b) for the preliminary experiments. PV is the number of water filled pore volumes leached. Vertical bold dashed lines represent the change from pre-leaching to leaching stages.

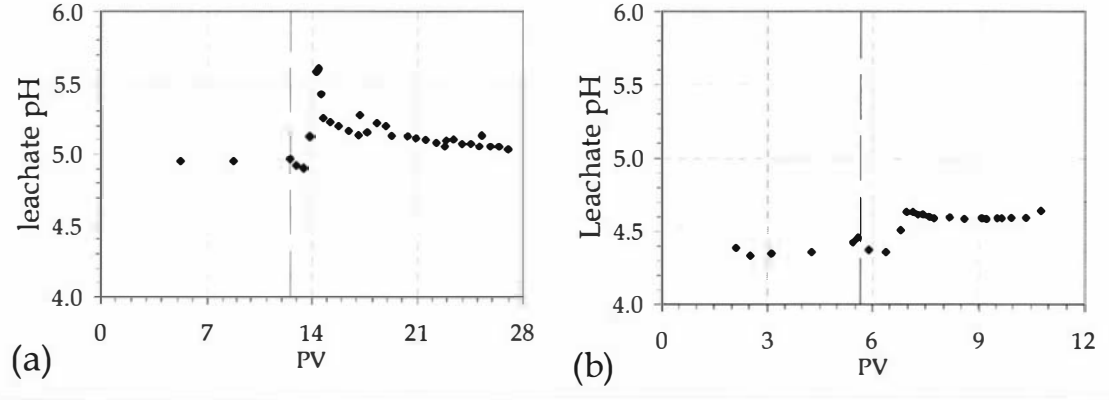


Figure A.2. Leachate pH from the preliminary experiments. (a) Egmont soil and (b) Taupo soil for the preliminary experiments. PV is the number of water filled pore volumes leached. Vertical bold dashed lines represent the change from pre-leaching to leaching stages.

A.2. Main experiments

After the results of the preliminary experiments, a series of more detailed miscible displacement experiments have been performed with both Egmont, and Taupo soils. The experiments comprised 6 columns with Taupo soil (named with letter T), of which 3 were undisturbed and 3 repacked samples. For Egmont soil, 4 columns with repacked soil were used (named by E). An additional column with a Taupo soil (named T_a) from a different location, which had higher allophane content, was also used. A summary with the columns' characteristics, the solutions applied, and some additional results are presented in Table A.2. To allow comparisons between the different columns, the measured properties and ion concentrations in the leachate are shown in the subsequent figures.

The pH and electrical conductivity (E.C.) were measured at room temperature (about 20°C). The concentration of anions was computed as the sum of sulphate and chloride, while cations concentrations were obtained by the sum of the concentrations of calcium, potassium and magnesium. These two concentrations, anions and cations, are presented in charge basis. In general the concentrations of anions and cations are coincident. However, in the early stages of the pre-leaching, especially for the Egmont soil columns (Figure A.3), these concentrations were quite different. The electrical balance should have been equilibrated by the presence of other non-measured ions, such as nitrate.

All columns presented somewhat similar physical characteristics, with the exception of column T_a, with the allophanic Taupo soil (Table A.2). This is also evidenced by similarities in the shape of chloride measurements, since it can be considered an inert tracer (Figure A.4 and Figure A.6). The leaching of the secondary cations was also consistent for each soil, with magnesium exhibiting a more complex shape.

Table A.2. Selected characteristics of the soils columns and solutions of the main miscible displacement experiments.

	E1	E2	E3	E4	Ta	T1	T2	T3	T4	T5	T6
	Repack.	Repack.	Repack.	Repack.	Undist.	Undist.	Repack.	Undist.	Repack.	Undist.	Repack.
ρ [1] (kg m^{-3})	754.5	754.8	769.7	752.4	892.8	859.5	884.6	839.8	683.0	795.3	879.2
WFPV [2]	763.2	819.2	789.1	807.9	700.5	580.8	580.7	578.6	511.1	578.4	607.9
θ_i [3]	0.277	0.273	0.287	0.307	0.333	0.222	0.246	0.247	0.201	0.229	0.251
θ_f	0.607	0.643	0.627	0.638	0.550	0.465	0.468	0.454	0.409	0.448	0.486
Initial soil pH	4.59	4.65	4.44	4.34	5.63	6.28	6.26	6.06	6.06	6.33	6.09
Final soil pH	4.76	4.81	5.26	4.56	5.53	6.05	5.91	6.13	5.85	5.99	5.84
q_w [4] (mm h^{-1})	29.9	44.1	20.5	34.3	9.2	41.9	46.6	33.2	72.9	58.4	46.0
Soil sulphate											
Initial (mmol kg^{-1})	1.75	1.75	1.75	1.75	1.81	0.21	0.21	0.21	0.21	0.21	0.21
Final (mmol kg^{-1})	20.06	13.05	11.09	1.48	11.77	3.93	4.36	2.83	2.25	1.12	1.16
Adsorbed (mmol kg^{-1})	11.96	8.88	8.88	1.48	7.84	-1.50	-0.94	0.08	-0.79	-0.13	-0.24
Soil calcium											
Initial (mmol kg^{-1})	36.85	36.85	36.85	36.85	5.41	2.44	2.44	2.44	2.44	2.44	2.44
Final (mmol kg^{-1})	51.96	46.98	12.04	43.53	19.44	9.41	9.54	6.74	6.37	4.68	4.33
Adsorbed (mmol kg^{-1})	43.87	43.84	12.04	35.38	15.41	3.98	4.24	3.98	3.33	3.44	2.93
Pre-Leaching											
Conc. $CaCl_2$ (mmol L^{-1})	13.5	6.6	21.8	12.7	12.1	12.0	12.0	6.4	5.6	2.8	2.6
pH	5.61	5.54	5.30	5.26	5.41	5.43	5.50	5.40	5.29	5.47	4.45
E.C. (mS cm^{-3})	2.41	1.23	4.02	2.76	2.77	2.40	2.34	1.23	1.15	0.59	0.66
Volume leached (PV)	5.11	4.96	6.36	7.67	6.74	4.55	4.35	6.22	7.63	7.46	6.35
Leaching											
Conc. $CaSO_4$ (mmol L^{-1})	10.2	4.9	15.4	4.8	6.4	10.1	10.0	5.1	5.1	2.2	2.5
pH	5.26	5.41	4.91	5.35	5.20	5.21	5.25	5.34	5.18	5.30	5.22
E.C. (mS cm^{-3})	1.36	0.76	2.56	3.32	1.21	1.37	1.36	0.78	0.76	0.38	0.45
Volume leached (PV)	6.77	6.30	6.73	5.24	7.23	4.55	5.07	7.20	7.71	8.48	8.61
Mass balance											
Cl-	1.02	1.03	1.07	-	1.03	1.02	1.04	0.96	1.05	1.06	0.99
Ca^{2+} [K^+]	0.94	0.92	1.08 [1.07]	0.99 [0.94]	0.93	1.01	1.00	1.02	0.98	0.98	0.97
SO_4^{2-}	0.98	1.02	0.94	1.02	0.95	0.92	0.93	0.94	0.91	0.91	0.92

[1] ρ: soil bulk density; [2] *WFPV*: water filled pore volume; [3] θ_i and θ_f :initial and final soil water content; [4] q_w: water flux density at leaching

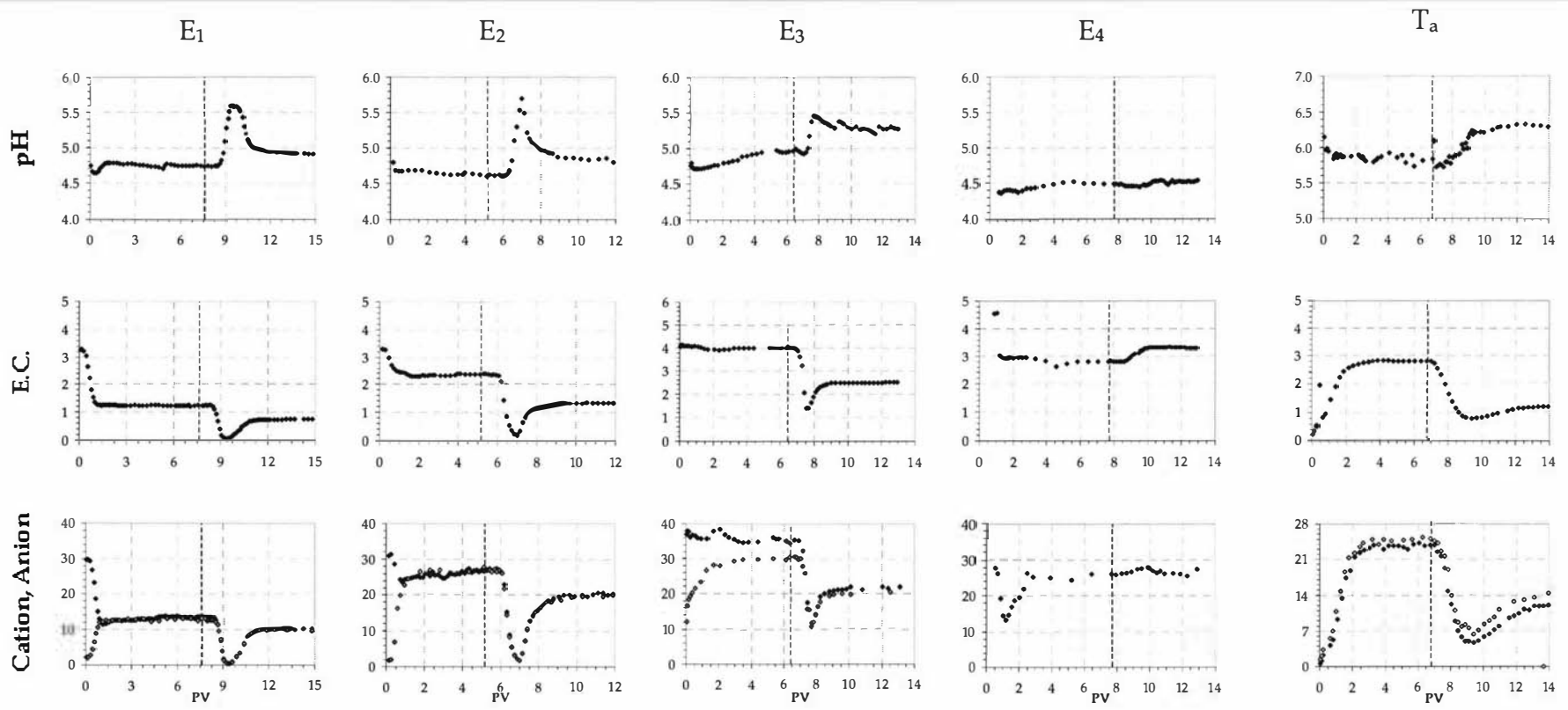


Figure A.3. Measurements of pH, electric conductivity (EC – mS cm^{-3}), and leachate concentrations (mmol L^{-1}) of anions (◇) and cations (◆) from the columns with Egmont soil and the allophanic Taupo soil. PV is the number of water filled pore volumes leached. Vertical bold dashed lines represent the change from pre-leaching to leaching stages.

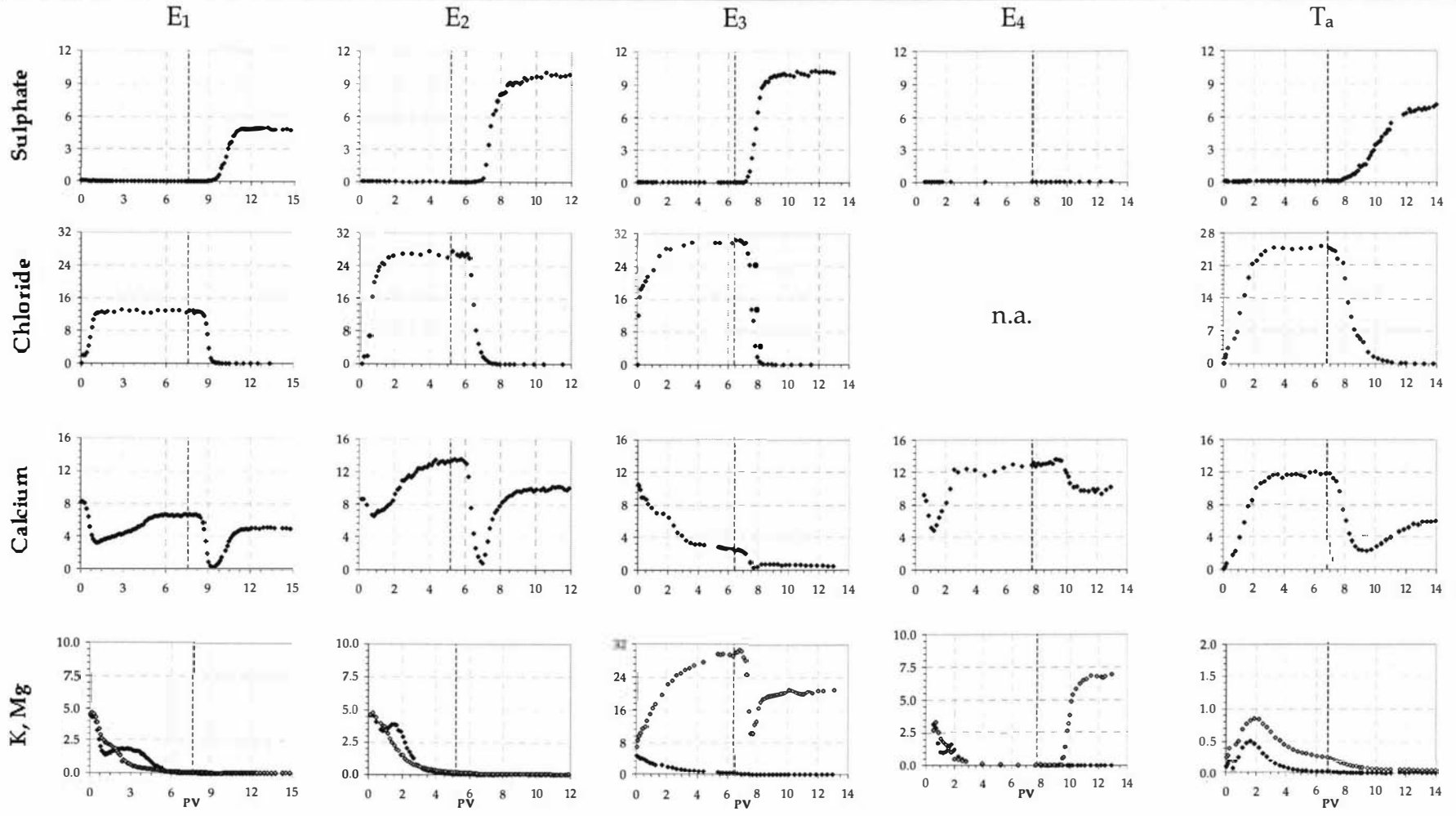


Figure A.4. Measurements of the concentrations of sulphate, chloride, calcium, potassium (◇) and magnesium (◆) of the leachate from the columns with Egmont and the allophanic Taupo soils. All measures are in mmol L^{-1}. PV is the number of

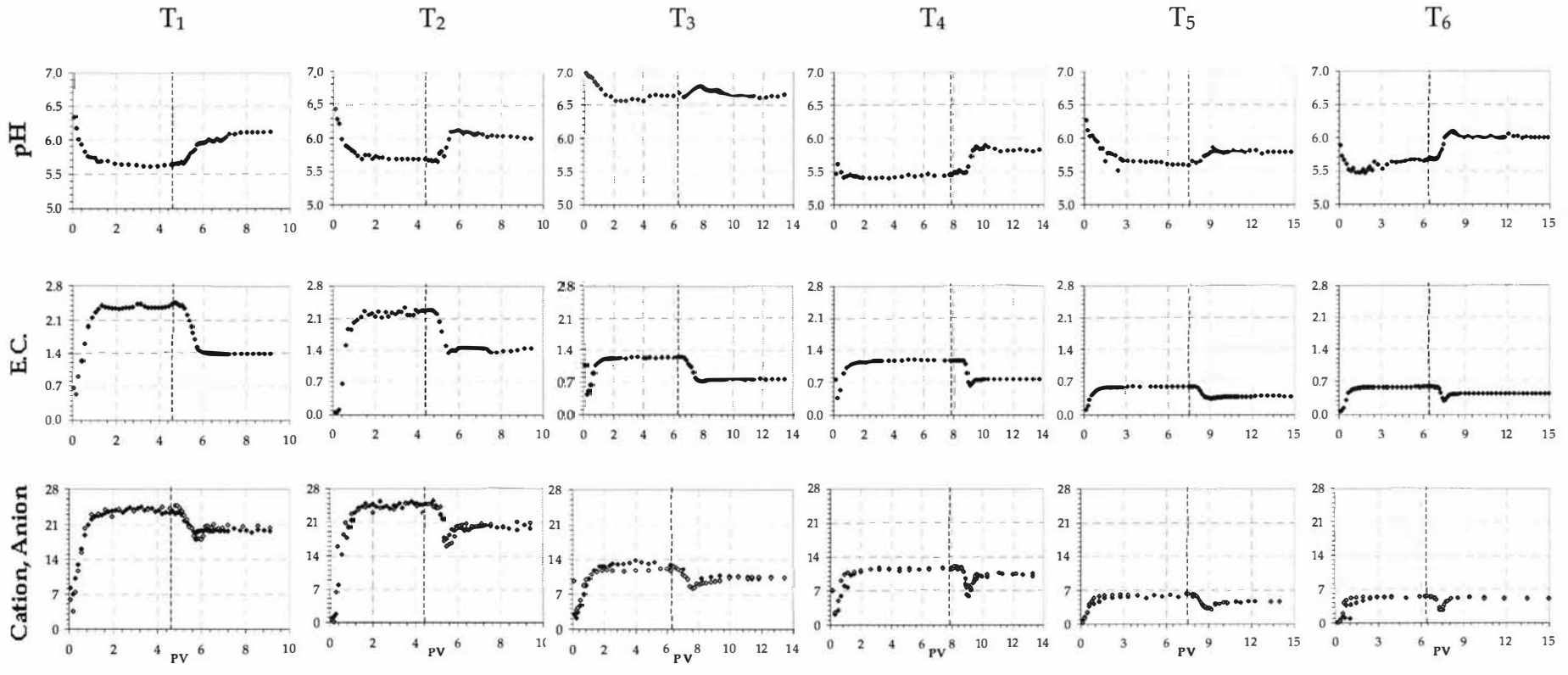


Figure A.5. Measurements of pH, electric conductivity (EC – mS cm^{-3}), and concentrations (mmol L^{-1}) of anions (◇) and cations (◆) of the leachate collected from the columns with Taupo soil. PV is the number of water filled pore volumes leached. Vertical bold dashed lines represent the change from pre-leaching to leaching stages.

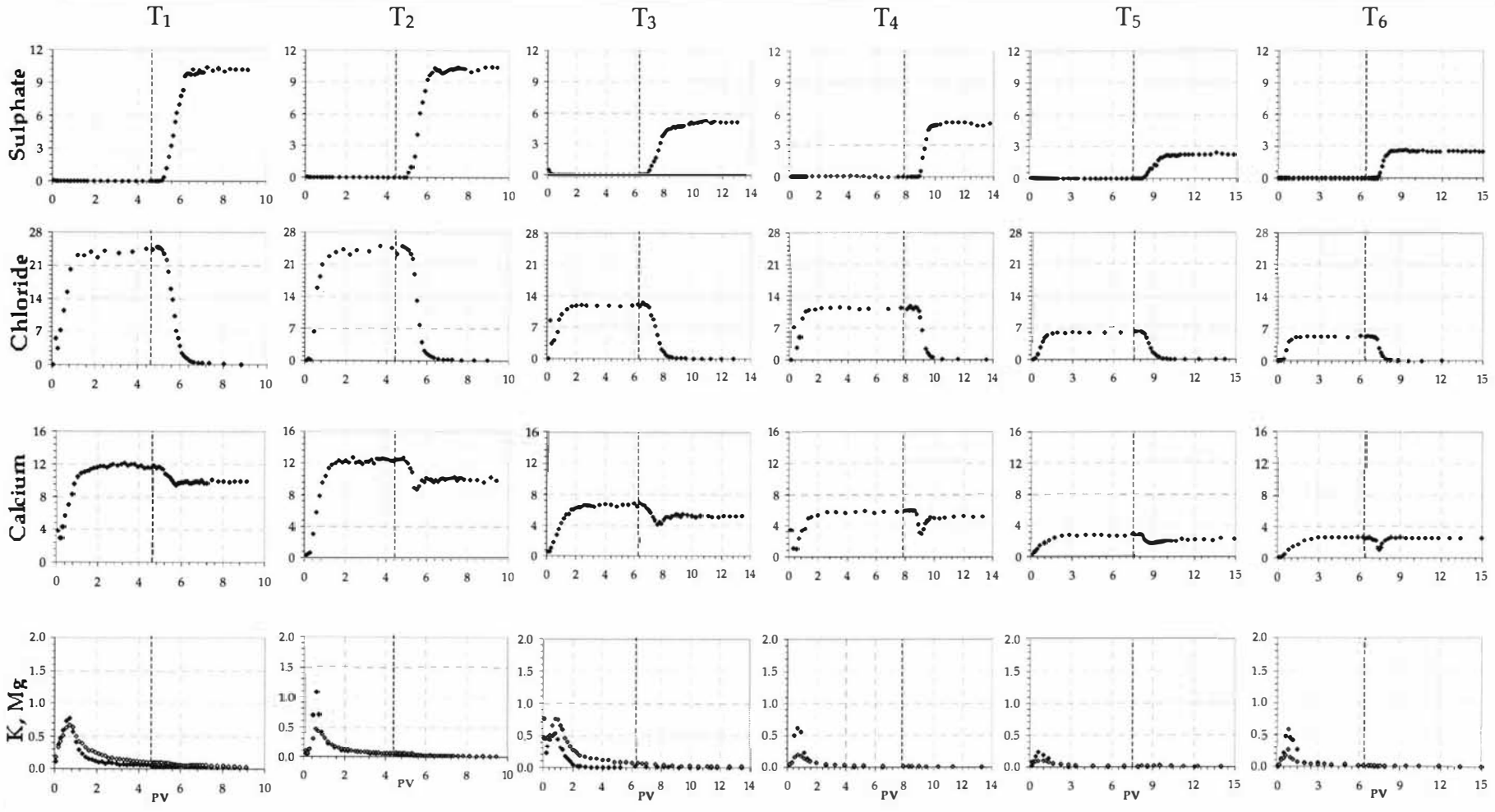


Figure A.6. Measurements of the concentrations of sulphate, chloride, calcium, potassium (◇) and magnesium (◆) of the leachate collected from the columns with Taupo soil. All measures are in mmol L^{-1}. PV is the number of water filled pore volumes leached.

APPENDIX B

B. Solving the adsorption model with IPA

B.1. Presentation of the computer routines

This appendix describes the program built for evaluating the degree of agreement between the proposed adsorption model with IPA and the observed data set presented in Chapter 5. The user interface and a basic description of the routines for solving the adsorption model and for comparing these results to the observed data set are presented here.

The core of the program is the routine for solving the adsorption model, in which the inputs are the total amounts of sulphate and calcium, and the outputs are the adsorption components (C_i, $S_{s,i}$, and S_{IP}). Coupled with this routine is the evaluation of the objective function. These routines can be called by two main loops, which are named here optimisation and replication (see flowchart in Figure B.1). In the optimisation loop the best set of parameters is sought using automatic variation of the parameter values. The output then is the best parameter set, with the confidence intervals, and the values of the predicted adsorption components. For the replication loop, the variation of the parameters is set in advance, thus it is meant for exploratory analyses. The outputs now are the values of the objective function at the various parameter values.

The data set to be read is composed of the observed values from the batch experiments, with the respective estimates of their variance (see Chapter 5). For simplicity only one value for the water-to-soil ratio (ϑ) is used.

In the user interface the program parameters are set. These parameters comprise the IPA approach and the objective function to be used, as well as the

kind of loop to be performed and the initial values of the adsorption model's parameters. The interface, where these parameters are set is shown in Figure B.2.

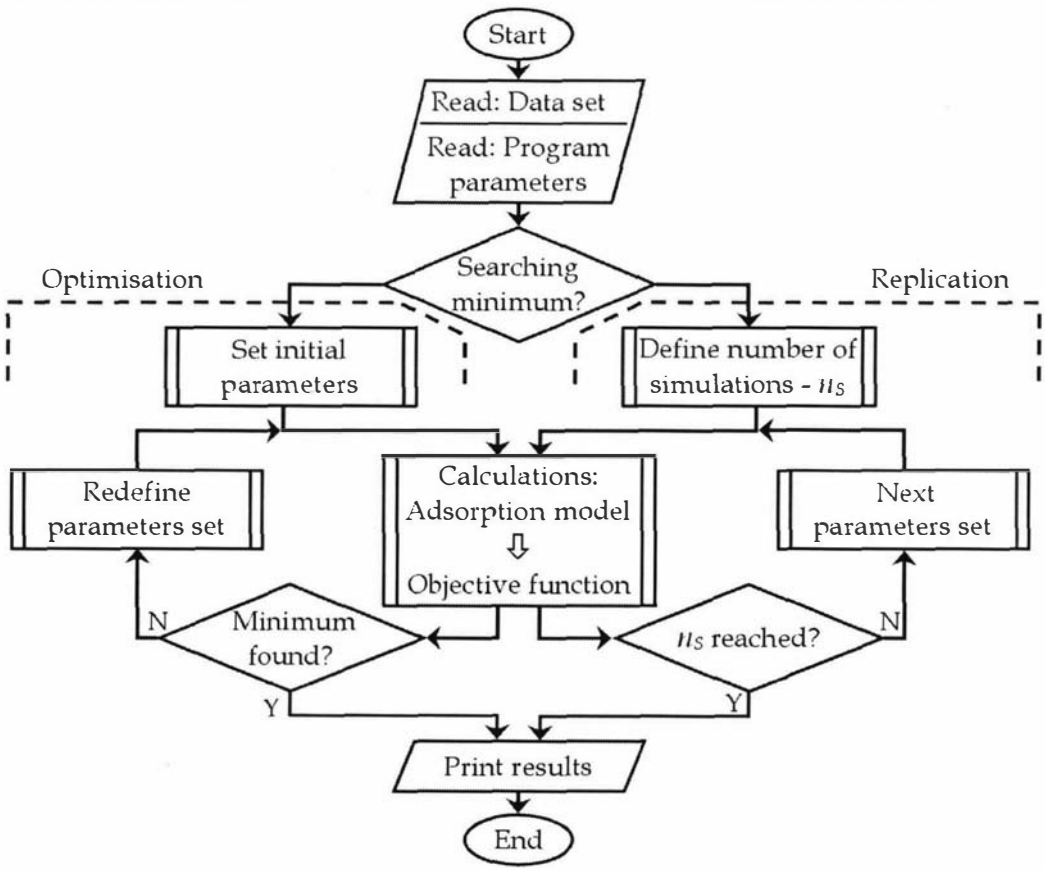


Figure B.1. Flowchart with the basic algorithm for the evaluation of the adsorption model with IPA.

The description of the numbered fields in Figure B.2 follows:

① The file with the observed adsorption data;

② The file where the output is to be saved;

③ Selection of the type of parameter variation: optimisation or replication. The output values are defined accordingly to this choice, as stated before;

④ Selection of the initial values for the adsorption parameters. In the checkbox the parameters which are to be varied can be selected. If optimisation variation was selected before, here the initial value and the initial variation step are entered for the parameters to optimise. Whereas if replication was set, here the initial and final values, as well as the variation step are defined;

⑤ Selection of the proposed IPA approach to be used;

⑥ Selection of the objective function to be used, respectively: Equations [5.30], [5.31] and [5.32].

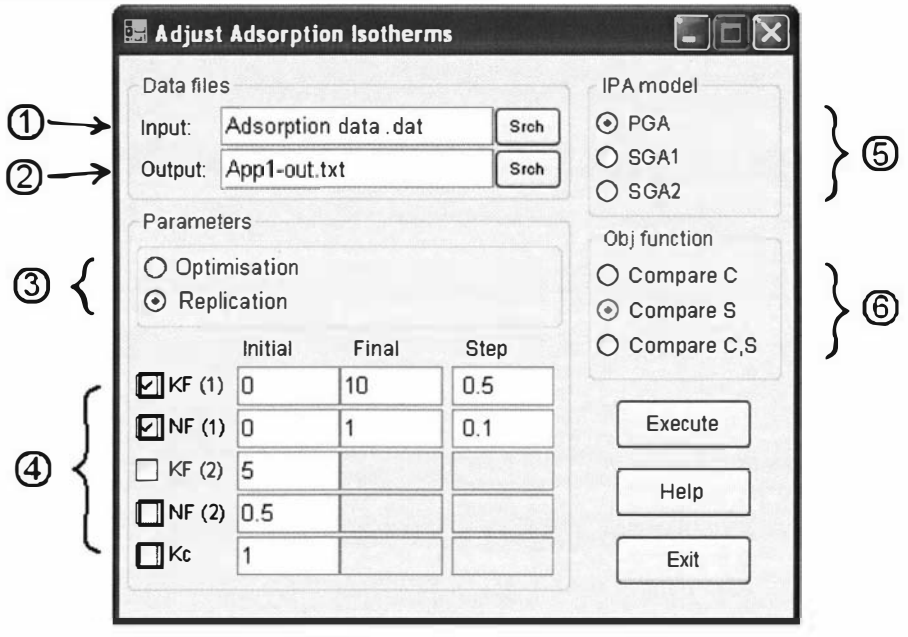


Figure B.2. User interface of the VisualBasic program built for the evaluation of the adsorption model with IPA.

B.2. Routine for solving the adsorption model

In this routine the adsorption components are found for given values of the total amounts (total concentration) of sulphate and calcium. The IPA approach to be used needs to be selected. Here, the mathematical description of the adsorption model is reviewed and its adaptations for computer handling are presented. The Newton-Raphson method is used in several steps for solving the partition of the components in the adsorption model. A description of this method, especially its more uncommon 3D version, is shown in Appendix D.

The adsorption model for a given solute i in the soil is represented by the function:

$$Q_{S,i} = \vartheta C_i + S_{s,i} + S_{IP} \qquad [B.1]$$

where $Q_{S,i}$ (mmol kg^{-1}) is total concentration, ϑ (L kg^{-1}) is the water-to-soil ratio, C_i (mmol L^{-1}) is the dissolved concentration, $S_{s,i}$ (mmol kg^{-1}) is the single adsorption, and S_{IP} (mmol kg^{-1}) is the ion-pair adsorption. The single adsorption is described by the Freundlich equation:

$$S_{s,i} = k_{F,i} C_i^{N_i} \qquad [B.2]$$

with $k_{F,i}$ (L kg^{-1}) and N_i as fitting parameters for each solute.

Although the index i represents a generic solute, here only two solutes are considered, more specifically, sulphate (1) and calcium (2). The notation $2/i$ is used to represent the counter ion. The three approaches for describing IPA presented in Chapter 5 are used here; their mathematical representation will be shown in the respective sub-routine. The general algorithm for the solution of the adsorption model is given in Figure B.3. The subroutines for solving the adsorption model without IPA (NR01) and with IPA (NR02) are described below.

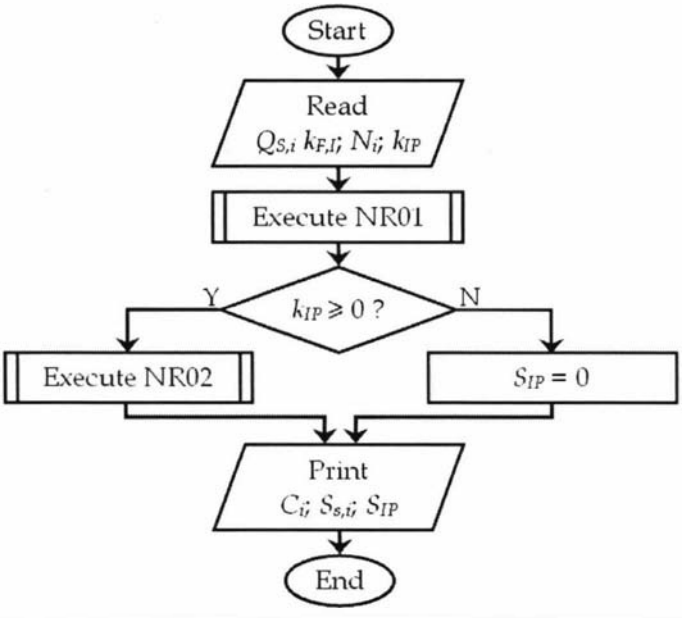


Figure B.3. Flowchart of the general routine to solve the adsorption model.

In each of the sub-routines the solution of the adsorption model is reached if the predicted value ($P_{Q,i}$), resulting from the values of C_i, $S_{s,i}$, and S_{IP}, can be considered equal to the original given value ($Q_{S,i}$).

$$P_{Q,i} \cong Q_{S,i} \qquad [B.3]$$

$P_{Q,i}$ results from applying the chosen values of C_i, $S_{s,i}$, and S_{IP} to the relations described by Equation [B.1] plus Equation [B.2] and that of the IPA approach. Because of their relation to each other, only one of the adsorption components actually needs to be found. The solution is found by varying the chosen component until Equation [B.3] can be assumed to be true, that is, the difference between $P_{Q,i}$ and $Q_{S,i}$ is small enough to be considered nil. The small difference that can be tolerated is the error limit (E_{limit}), set to 10^{-6}. The difference between $P_{Q,i}$ and $Q_{S,i}$ can be appropriately represented by:

$$F_i = P_{Q,i} - Q_{S,i} \qquad [B.4]$$

This general equation is the basis for the solution of the partition of $Q_{S,i}$ into the adsorption components.

B.2.1. Partition of $Q_{S,i}$ without IPA – NR01

For the partition of $Q_{S,i}$ without considering IPA, one has to find the values of C_i. Then, $S_{s,i}$ can be found using equation [B.2]. The value for C_i can be found analytically only if N_i is equal to one, when:

$$C_i = \frac{Q_{S,i}}{\vartheta + k_{F,i}} \qquad [B.5]$$

However, in the case of a non-linear Freundlich equation, the value of C_i must be found numerically. For this, equation [B.4] is developed here as:

$$F_i = \vartheta C_i + k_{F,i} C_i^{N_i} - Q_{S,i} \qquad [B.6]$$

The Newton-Raphson method can then be used to search for the value of C_i that makes F_i to be equal to zero. To ensure that the procedure will converge, let's set the Newton-Raphson equation as:

$$G = F_i^2 \qquad [B.7]$$

With its derivative equal to:

$$\frac{\partial G}{\partial C_i} = 2F_i \frac{\partial F_i}{\partial C_i} \qquad [B.8]$$

where:

$$\frac{\partial F_i}{\partial C_i} = \vartheta + N_i k_{F,i} C_i^{N_i - 1} \qquad [B.9]$$

In the iterative Newton-Raphson method, for each loop j in the procedure, the value of $C_{i,j+1}$ is given by:

$$C_{i,j+1} = C_{i,j} - \frac{G}{\partial G / \partial C_i} \qquad [B.10]$$

With both G and its derivative calculated at $C_{i,j}$. The initial guess is given by Equation [B.5]. Figure B.4 shows the flowchart for this routine.

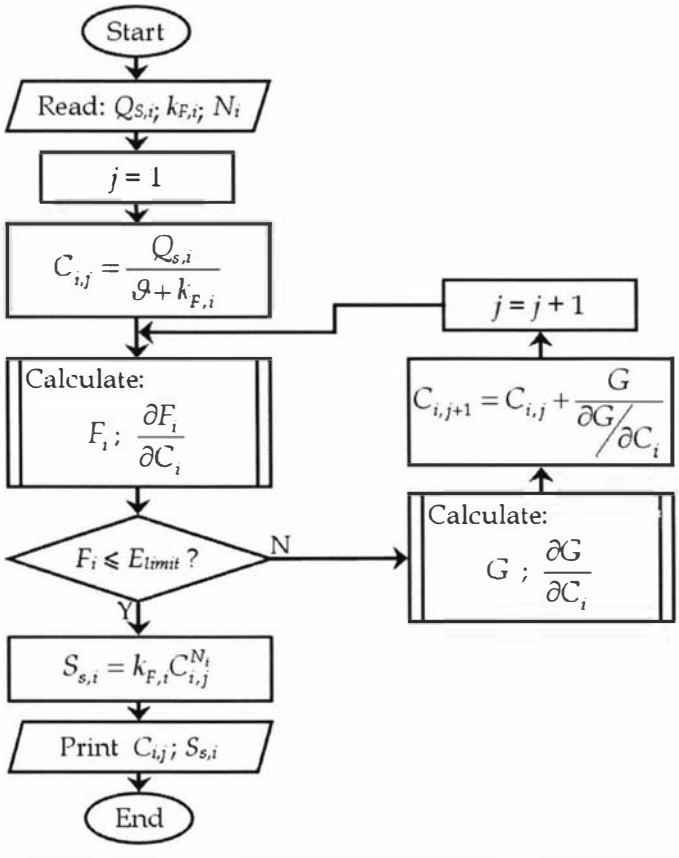


Figure B.4. Flowchart of the routine NR01 for solving the adsorption model without IPA.

B.2.2. Partition of $Q_{S,i}$ with IPA – NR02

With IPA, the partition of the given value of $Q_{S,i}$ needs to include S_{IP}. Therefore the solution for the two solutes has to be found simultaneously, because S_{IP} is common for both. The working function for describing the difference between the modelled and the observed value of $Q_{S,i}$ is set to:

$$F_i = \vartheta C_i + S_{s,i} + S_{IP} - Q_{Si} \qquad [B.11]$$

Again the problem is to find the value of one of the adsorption components that make F_i be equal to zero. $S_{s,i}$ for PGA and C_i for the other approaches are going to be used as the variable for the Newton-Raphson procedure. To solve Equation [B.11] simultaneously for both solutes, the Newton-Raphson equation combining the two solutes is defined as:

$$G = F_i^2 + F_{2/i}{}^2 \qquad [B.12]$$

This is now a 3D equation, with the chosen adsorption component of the two solutes as the independent variables. For applying the Newton-Raphson method, the function to be zeroed and its derivative should be known. Here a general formula of the derivatives can also be devised. Using x_i as a generic variable, which represents any of the adsorption components, the first derivative of G is given by:

$$\frac{\partial G}{\partial x_i} = 2F_i \frac{\partial F_i}{\partial x_i} + 2F_{2/i} \frac{\partial F_{2/i}}{\partial x_i} \qquad [B.13]$$

The initial guess comes from the procedure NR01. Still using the unknown variable x_i, the iterative Newton-Raphson equation becomes:

$$x_{i,j+1} = x_{i,j} - \frac{G\left(\frac{\partial G}{\partial x_i}\right)}{\left(\frac{\partial G}{\partial x_i}\right)^2 + \left(\frac{\partial G}{\partial x_{2/i}}\right)^2} \qquad [B.14]$$

With both G and its derivatives evaluated at $x_{i,j}$. The procedure flowchart is shown in Figure B.5, and the specific solutions for each IPA approach are given afterwards.

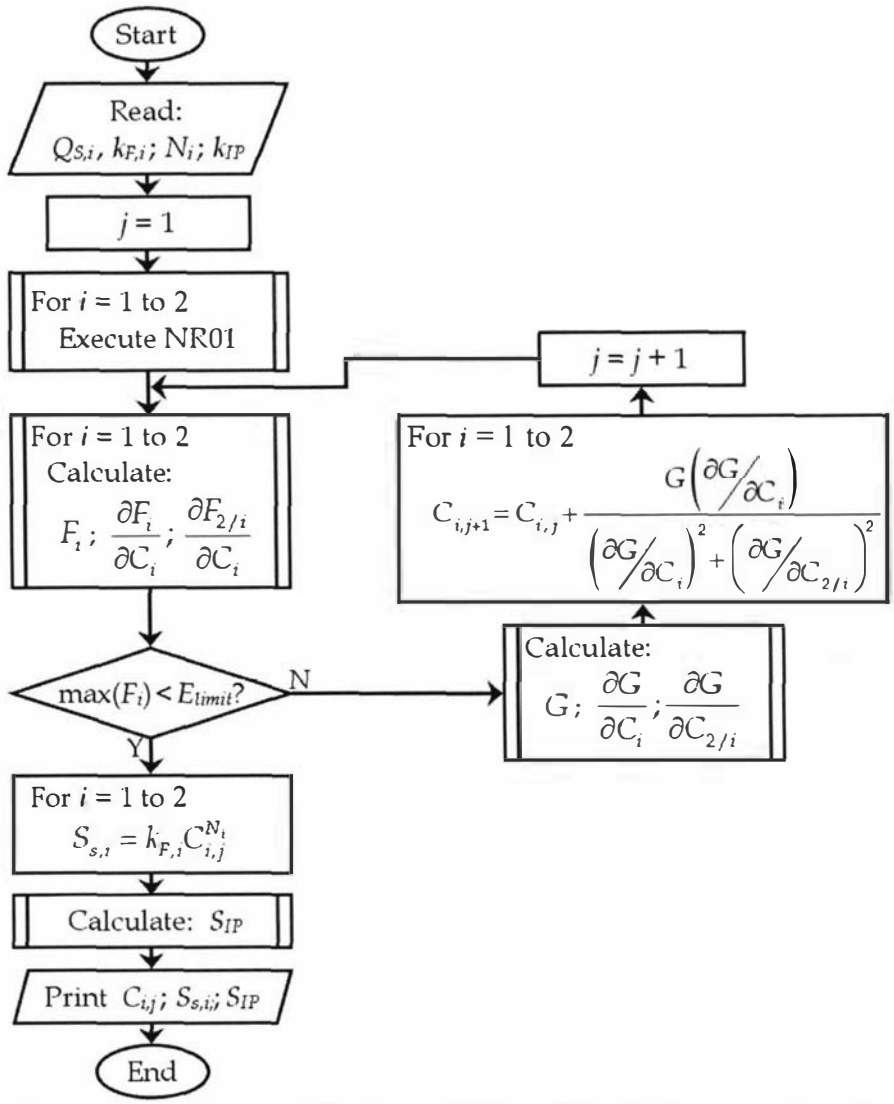


Figure B.5. Flowchart of the routine NR02 for solving the adsorption model with IPA

B.2.2.1. Solution with PGA

In this approach the ion-pair adsorption is defined by:

$$S_{IP} = k_s S_{s,i} S_{s,2/i} \qquad [B.15]$$

Therefore, $S_{s,i}$ is the best component to be used as the independent variable, and for that, Equation [B.2] has to be re-written as:

$$C_i = \left(\frac{S_{s,i}}{k_{F,i}} \right)^{\frac{1}{N_i}} \qquad [B.16]$$

And the working equation becomes:

$$F_i = \vartheta \left(\frac{S_{s,i}}{k_{F,i}} \right)^{\frac{1}{N_i}} + S_{s,i} + k_s S_{s,i} S_{s,2/i} - Q_{S,i} \qquad [B.17]$$

With the derivatives, for each solute:

$$\frac{\partial F_i}{\partial S_{s,i}} = \frac{\vartheta}{k_{F,i} N_i} \left(\frac{S_{s,i}}{k_{F,i}} \right)^{\frac{1}{N_i}-1} + 1 + k_s S_{s,2/i} \qquad [B.18]$$

$$\frac{\partial F_{2/i}}{\partial S_{s,i}} = k_s S_{s,2/i} \qquad [B.19]$$

B.2.2.2. Solution with SGA1

In this approach the ion-pair adsorption is defined by:

$$S_{IP} = \vartheta k_c C_i C_{2/i} \qquad [B.20]$$

C_i is consequently chosen to be used as the independent variable. Using this equation and Equation [B.2], the working equation can be re-written as:

$$F_i = \vartheta C_i + k_{F,i} C_i^{N_i} + \vartheta k_c C_i C_{2/i} - Q_{S,i} \qquad [B.21]$$

With the derivatives:

$$\frac{\partial F_i}{\partial C_i} = \vartheta + k_{F,i} N_i C_i^{N_i - 1} + \vartheta k_c C_{2/i} \qquad [B.22]$$

$$\frac{\partial F_{2/i}}{\partial C_i} = \vartheta k_c C_{2/i} \qquad [B.23]$$

B.2.2.3. Solution with SGA2

Now the ion-pair adsorption is described by:

$$S_{IP} = k_r \left(C_i C_{2/i} \right)^{0.5} \qquad [B.24]$$

Again, C_i is chosen as the independent variable. The working equation, using this approach and Equation [B.2], is re-written as:

$$F_i = \vartheta C_i + k_{F,i} C_i^{N_i} + k_r \left(C_i C_{2/i}\right)^{0.5} - Q_{S,i} \qquad [B.25]$$

Finally, the derivatives are:

$$\frac{\partial F_i}{\partial C_i} = \vartheta + k_{F,i} N_i C_i^{N_i - 1} + 0.5 k_r \left(\frac{C_{2/i}}{C_i}\right)^{0.5} \qquad [B.26]$$

$$\frac{\partial F_{2/i}}{\partial C_i} = 0.5 k_r \left(\frac{C_{2/i}}{C_i}\right)^{0.5} \qquad [B.27]$$

B.3. Routine for evaluating the objective function

The objective function (Φ) is a summary of the comparisons between observed and modelled data. These comparisons are done for each pair of observed values, that is, the adsorption data for sulphate and calcium. The general expression is given by:

$$\Phi = \sum_{i=1}^{2} \sum_{j=1}^{n_D} \frac{1}{\sigma_i^2} \left(O_{i,j} - P_{i,j}\right)^2 \qquad [B.28]$$

where $O_{i,j}$ and $P_{i,j}$ represent the observed and the predicted data for the j equilibration (from batch experiment) of the solute i, and σ_i^2 is the variance of the observed data. As presented in Chapter 5, $P_{i,j}$ and $O_{i,j}$ can represent the values of either $C_{i,j}$ or $S_{i,j}$, accordingly to the objective function to be used (Equation [5.30] or [5.31]. In case the third function (Equation [5.32]) is chosen, Equation [B.28] is computed for both variables separately, yielding Φ_C and Φ_S respectively. The final value of Φ is then obtained by:

$$\Phi = \Phi_S + \Phi_C \vartheta^2 \qquad [B.29]$$

Because each observed data pair is contrasted to the modelled values, the computation of the objective function is coupled with the routine for

solving the adsorption model. The simplified flowchart of the procedure for computing the objective function is shown in Figure B.6.

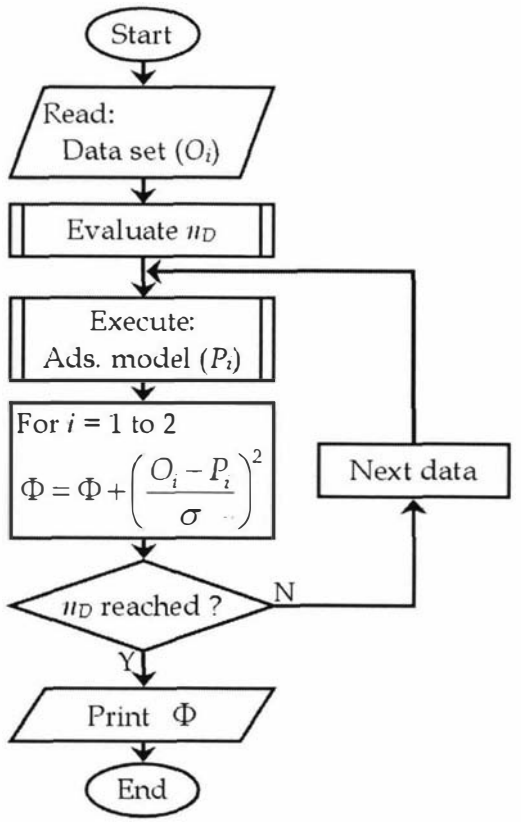


Figure B.6. Flowchart of the simplified routine for obtaining the value of the objective function (Φ).

B.4. Routines for the variation of the adsorption model parameters

Two loop routines are available for analysing the agreement between the adsorption model and the observed data set. These routines are called here replication loop and optimisation loop. As shown in Figure B.1 both loops keep calling the routine to evaluate the adsorption model and objective function until the criterion to stop is reached. Also for each loop the parameter set is changed. The criterion to stop the loop and the way the parameters are changed are the basic differences between the two loops.

B.4.1. Replication loop

This is the simplest loop, where the objective function is calculated for a predefined number of times, with no judgment on its value being done during the process. It is aimed for performing exploratory analyses of the model. The variation range for the parameters, defined by the initial and final values, as well as the increment (step) for the variation at each cycle, are set in the beginning. These values define the number of simulations, or cycles of the loop.

The parameters that are going to be varied can be chosen. If more that one is chosen the replications follow the order shown in Figure B.7. In this figure, using y as a counter (varying between 1 and 5), the initial, final, and the step values for the parameters are generalised set as $p_{\text{ini}}(y)$; $p_{\text{ini}}(y)$; and $p_{\text{step}}(y)$ respectively. The number of simulations for varying a given parameter y, can be obtained by:

$$n_{S,y} = \frac{p_{\text{end}}(y) - p_{\text{ini}}(y)}{p_{\text{step}}(y)} + 1 \qquad \text{[B.30]}$$

As all combinations of the parameter values are calculated, the number of cycles increases fast with increasing the number of parameter set to vary simultaneously. The total number of simulations is given by the product:

$$n_S = \prod_{y=1}^{5} n_{S,y} \qquad \text{[B.31]}$$

Note that, for each loop, the procedure to calculate Φ is called, which in its turn calls the adsorption model routine as many times as the number of data pairs (sulphate and calcium adsorption) in the input file. This all imply in a lot of computation effort, and consequently a lot of output data. This routine is, therefore, suited for exploratory analyses of one or two variables at a time; especially because interpreting data from a larger number of parameters would be difficult.

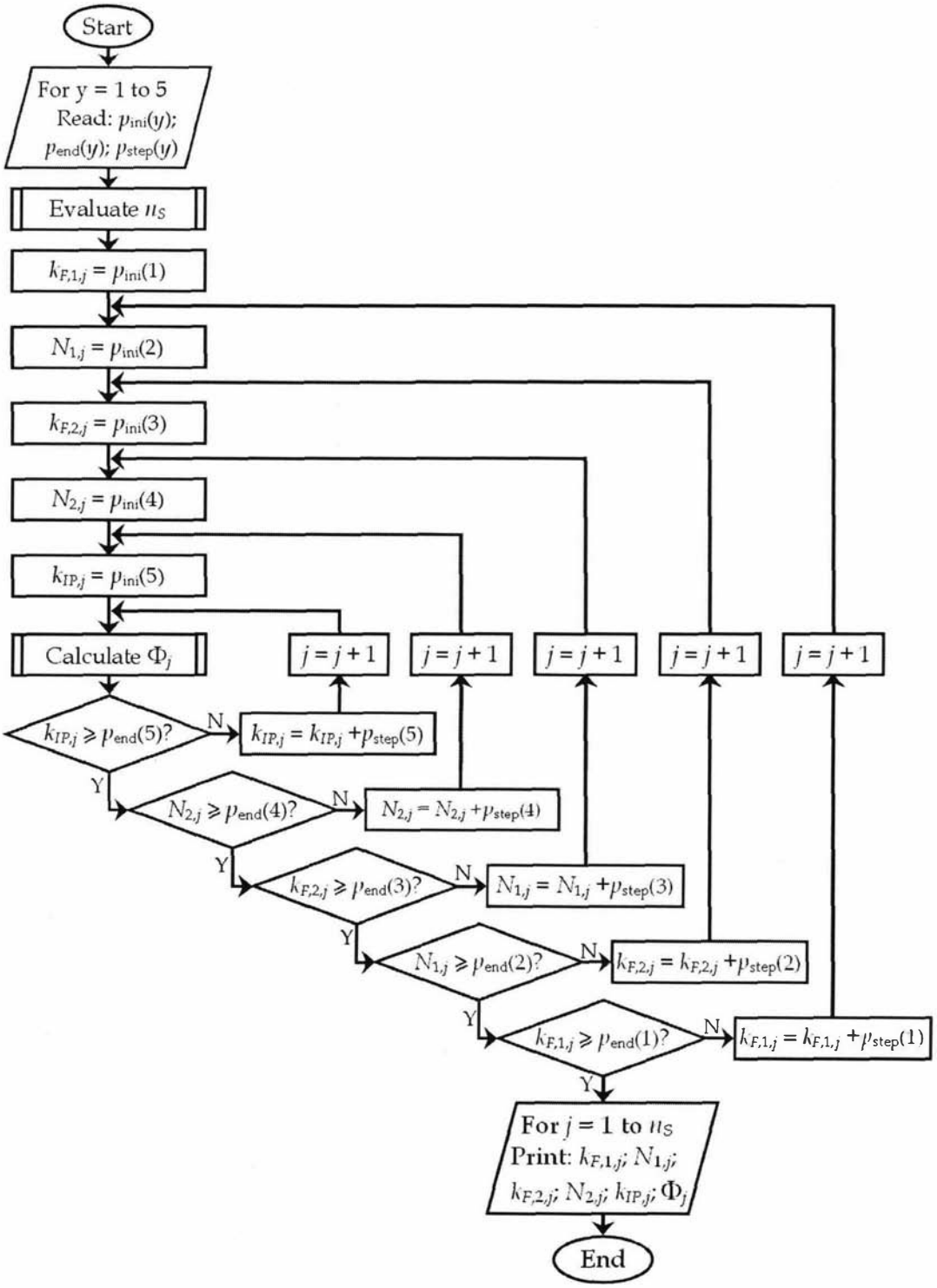


Figure B.7. Flowchart of the replication loop routine, showing the hierarchy of the parameter variation.

B.4.2. Optimisation loop

The objective of this routine is to optimise the parameter values, that is, to find the values that minimise the objective function. For this, at each loop the values of the parameters are changed based on the comparison between previous estimates of the objective function. Therefore neither the number of cycles nor the size of the increments for the parameters are predefined.

From the calculus theory, the minimum value of a function is found where its derivative is zero. In the case of the adsorption model being used here, the values of five parameters have to be optimised. This means that:

$$\frac{\partial \Phi}{\partial k_{F,i}} = \frac{\partial \Phi}{\partial N_i} = \frac{\partial \Phi}{\partial k_{F,2/i}} = \frac{\partial \Phi}{\partial N_{2/i}} = \frac{\partial \Phi}{\partial k_{IP}} = 0 \qquad [B.32]$$

where k_{IP} is a generalised IPA factor (k_s, k_c, or k_r).

The Newton-Raphson method cannot be used here because the partial derivatives of Φ (Equation [B.31]) cannot be defined. The reason for this is that the predicted value of the objective function is obtained numerically, and analytical expressions for its derivatives are not available. Besides, there are three objective functions and three IPA approaches, therefore nine combinations should be considered. Consequently the search for the best value for each parameter has to be done numerically. Another problem due to the unavailability of the derivatives is the definition of the increment for changing the parameter value at each loop.

For solving these problems this routine was devised as a series of iterative loops that attempt to find the best set of values for the selected parameters, one at a time. A major loop evaluates if the condition defined by Equation [B.31] has been reached. Within this major loop there are loops for optimising each parameter. The simplified flowchart is presented in Figure B.8. The procedure is exemplified further for a better comprehension.

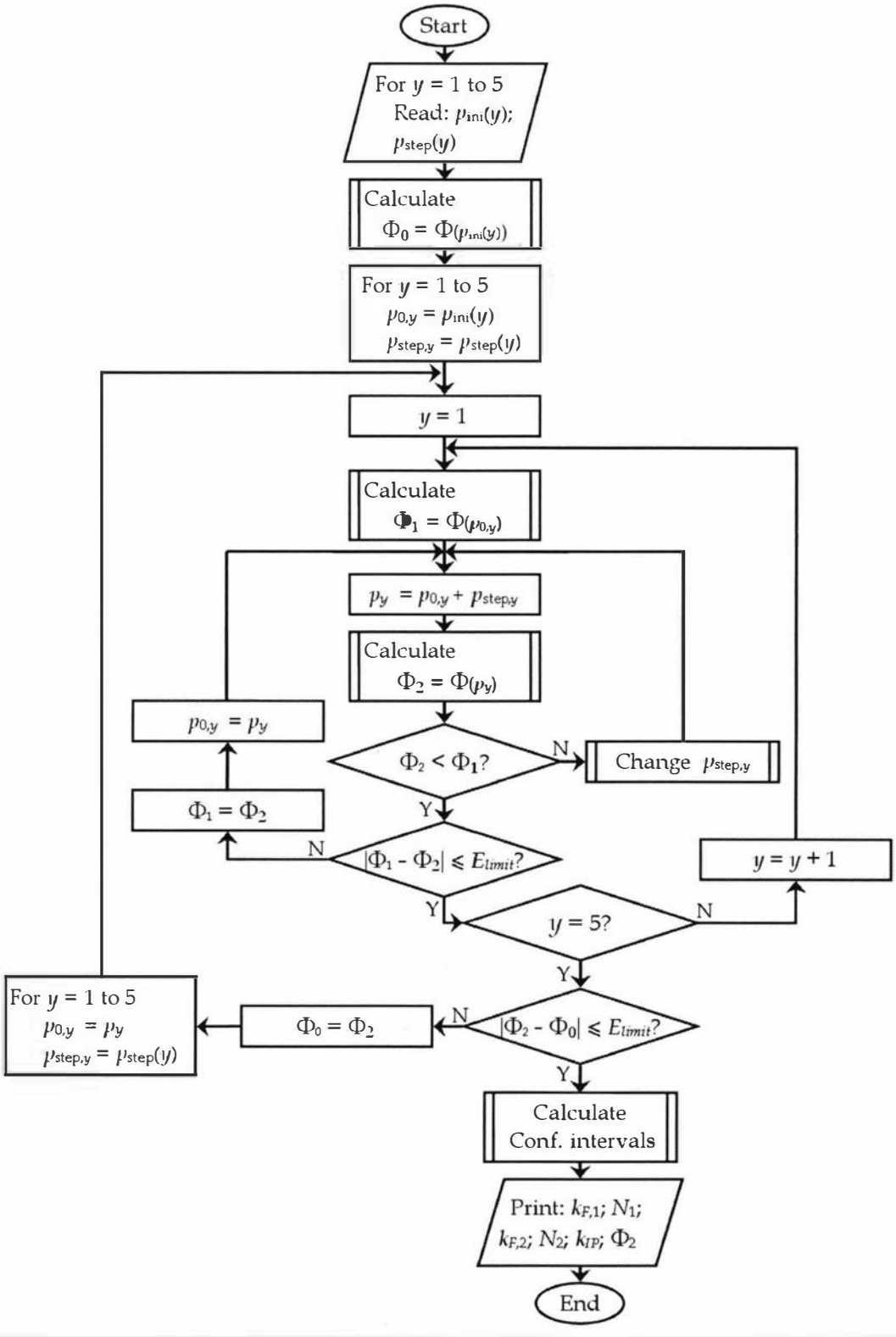


Figure B.8. Flowchart of the optimisation loop routine.

B.4.2.1. The optimisation loop at work

A simple example is presented hereafter to illustrate the procedure used for the optimisation of the adsorption model. Let's consider here a sub-set of the adsorption data from the batch experiment. This sub-set is composed by the values obtained in equilibrations with sulphate solutions without adding calcium. Thus, the optimisation is done to search only the Freundlich equation parameters. The objective function (Equation [B.28]) is used for comparing the values of S.

The general variation pattern presented by the objective function for a wide range of the parameters values is shown in Figure B.9.

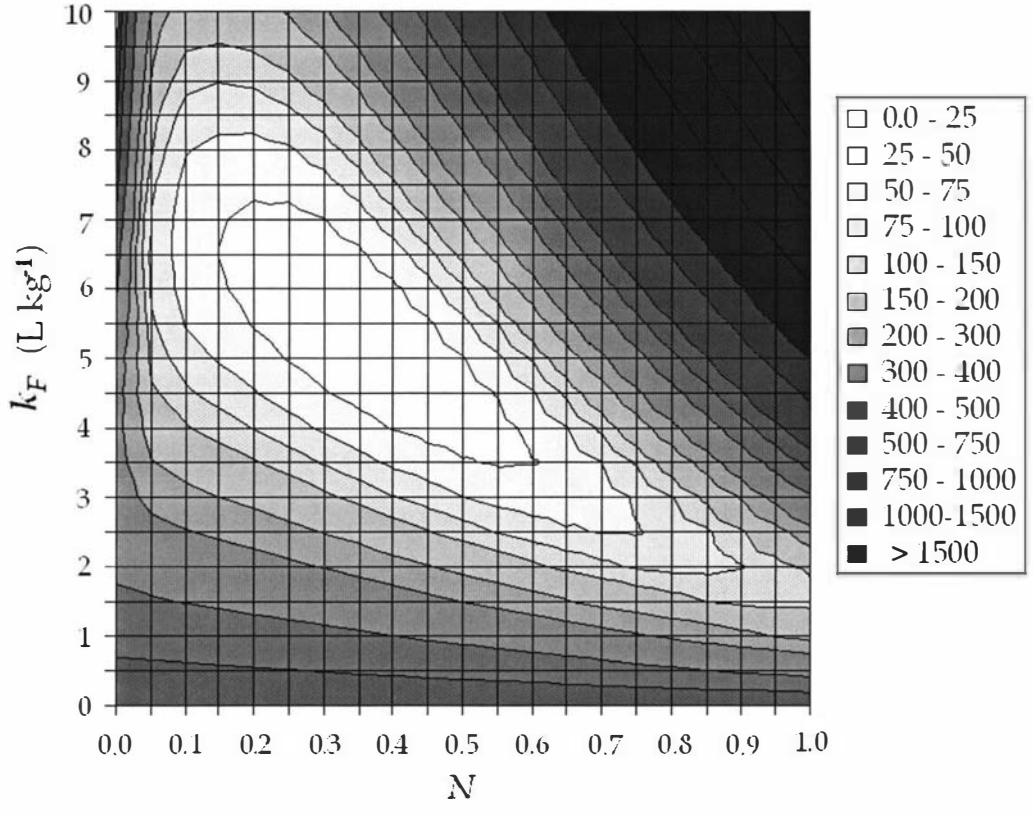


Figure B.9. Variation of the objective function (Equation [B.28], with S) for a range of values of the two Freundlich equation parameters.

The pattern shown in Figure B.9 reveal that the relation between the parameters is quite complex, even for such a simple model. The parameters

present negative correlation and variation is non-linear. The values of the objective function vary greatly in this range of parameters, reaching over 3400 in the right-upper corner, although the minimum is smaller than 25. And these variations are very different for the other directions (corners). Nonetheless the curves are concentric, indicating that a single solution does exist.

For the optimisation of the two parameters, let's assume their initial values to be 5 L kg^{-1} for k_F and 0.5 for N, and the initial increments as 0.1 and 0.01 respectively. The value of the objective function in this point is 23.25. Initially the value of k_F is optimised with N kept constant. This first step is shown Figure B.10, with its variation detached on the right-upper corner. Using the initial increment the value of k_F is changed (decreased in this case) until the variation in Φ starts to increase. Then the increment is halved and Φ is calculated until its value starts to increase, when the increment is again halved. This procedure is repeated until the increment in k_F is smaller than the limit (here $E_{limit} = 10^{-6}$). The value 4.3 L kg^{-1} for k_F is found. Then, using a similar procedure, and fixing the new value of k_F, N is optimised (Figure B.10, right-lower corner). The new value for N is 0.46. This completes one major loop, with the objective function value of 11.01. Thus, in one optimisation loop, the improvement in the model represented a decrease in Φ of 12.24. Another loop renders k_F = 4.6 L kg^{-1}, N = 0.43, and Φ = 8.28. This procedure is repeated 17 times until the difference between two consecutive values of Φ is $6.42\ 10^{-7}$. The optimum parameters values found after this are k_F = 5.37 L kg^{-1}, N = 0.354, with Φ = 5.323.

This routine is equivalent for any number of parameters, although its visualisation is not possible. A matter of concern with increasing the number of parameters is whether the procedure will converge to any value. This is a major problem for the optimisation of complex models (Hamming, 1973). In many cases the procedure may go on infinitely with the value of the objective

function decreasing and increasing cyclically. These models are known as ill-posed models, and it is not an easy task to find a solution for this. It is also important that the procedure results in the same parameter set, despite using different initial values for starting the optimisation. This problem, called non-uniqueness, is common to models with many parameters (Press *et al.*, 2002; Dubus *et al.*, 2004). For the adsorption model presented here it cannot be granted theoretically that such convergence will happen. However, tests were performed with many different initial values as well as different initial increments for the five parameters, and the procedure always converged to the same values. This indicates that the proposed procedure for optimising the adsorption model is a well posed one.

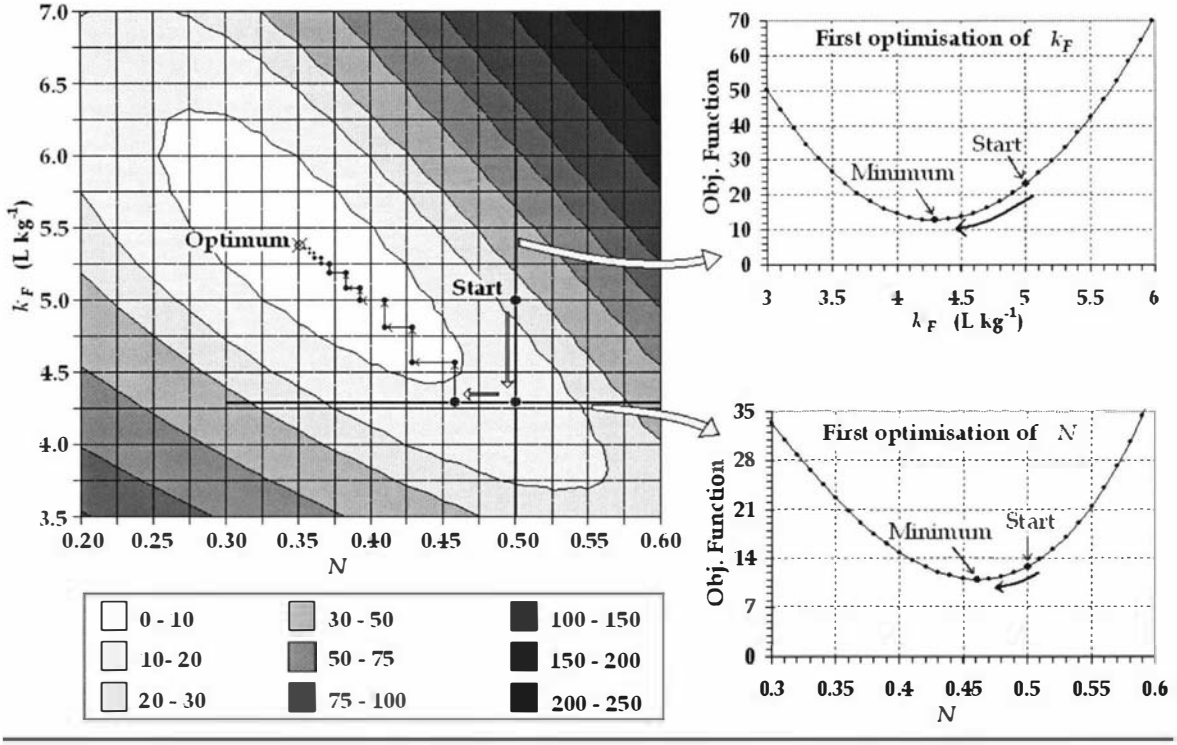


Figure B.10. Schematic of the step-by-step optimisation process. Sulphate adsorption data are used. Initial guess is k_F = 5 L kg^{-1} and N = 0.5. Optimum values are k_F = 5.35 L kg^{-1} and N = 0.354.

B.4.2.2. Computing the confidence intervals

Once the optimisation procedure has found the best set of parameters, a sub-routine for evaluating their confidence intervals is called. As explained in Chapter 5, the objective function presents a χ^2 probability distribution. So given a probability level for confidence, it is possible to define the deviation of the objective function ($\Delta\Phi$) and hence the deviations of the parameters within that confidence level. Thus, starting at the optimum value of the objective function (Φ_{opt}), the procedure searches for the parameter values that result in the given variation, that is:

$$\Phi_{opt} \pm \Phi(p) = \Delta\Phi \qquad [B.33]$$

This is done for each parameter p, with the values of the other kept constant. The flowchart is shown in Figure B.11.

If the parameters variation is linear the deviations are symmetric around the optimum value. This is seldom the case; however the differences may be small enough for accepting the assumption of linear variation. In the example given in the previous item, the variations of both parameters are non-linear (see Figure B.10). The difference between the upper and lower limits is small in this case only for k_F (Table B.1).

Table B.1. Upper and lower limits of the confidence interval for the optimisation of the Freundlich equation parameters (from B.4.2.1).

	Optimum value	Lower limit	Upper limit
k_F (L kg^{-1})	5.37	4.97	5.79
N	0.354	0.307	0.397

For the adsorption model with IPA, the differences between the maximum and minimum limits of the confidence interval were found to be dependent mainly on the objective function used, but also on the approach employed for describing IPA.

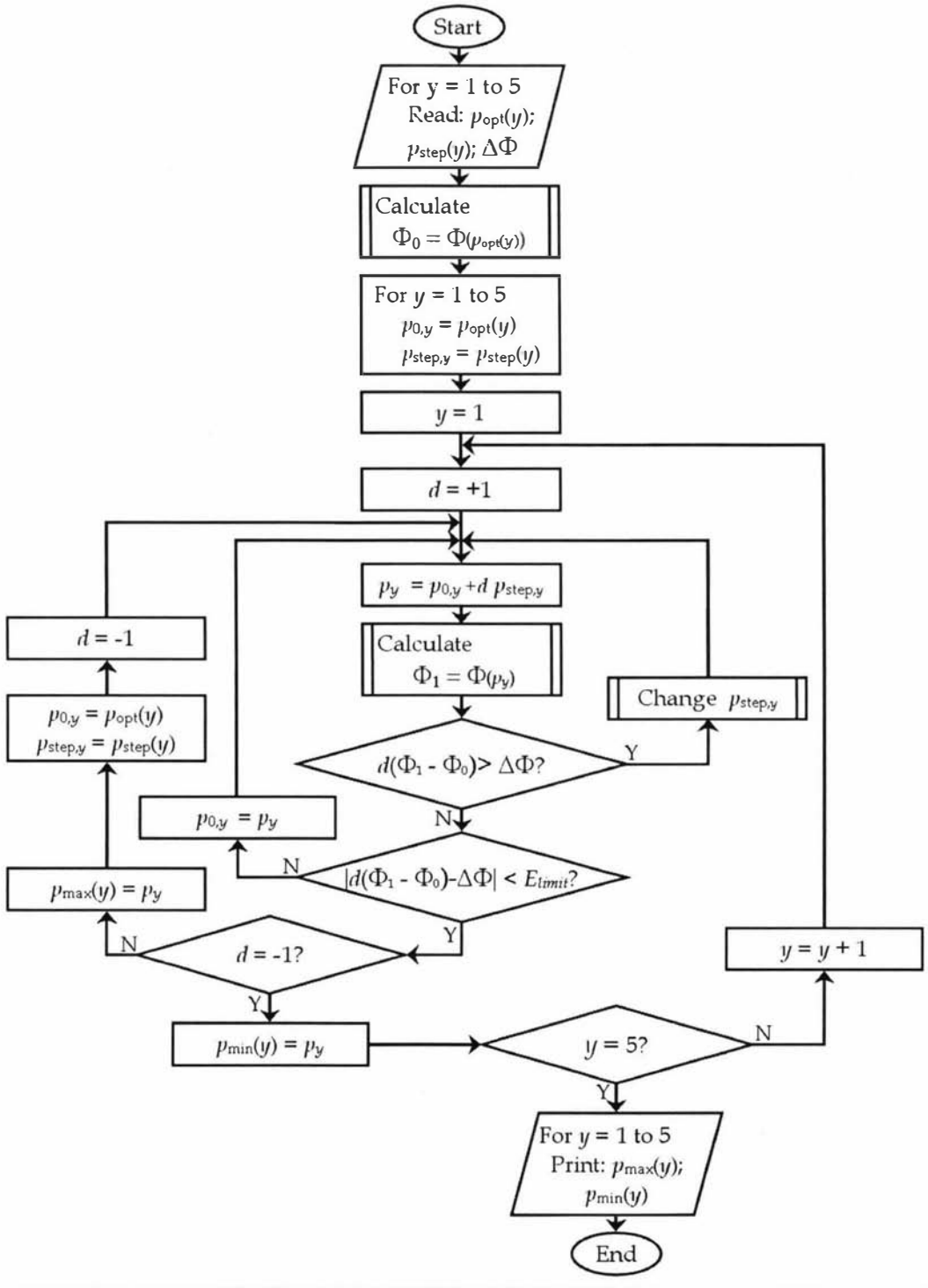


Figure B.11. Flowchart of the sub-routine for finding the confidence interval of the adsorption model parameters.

APPENDIX C

C. Describing sulphate and calcium BTCs with IPA

C.1. Introduction

In this appendix the program built for simulating the breakthrough curves (BTC) of sulphate and calcium, considering the presence of ion-pair adsorption (IPA), and for evaluating their agreement to a observed data set, is described. This program is and extension of the program described in Appendix B. Therefore the descriptions here are simplified, since many of the routines are analogous or identical to those presented in that appendix.

The general program framework here, as shown in the flowchart in Figure C.1, is different from the program of Appendix B basically only in the calculations routine, where the main feature is the solution of the solute movement using a convection-dispersion equation (CDE). The output is therefore the concentration over time of the outflow solution. Again, the two main loops, optimisation and replication, can be used for either optimising the model's parameters or for exploratory analyses. The outputs of these loops are analogous to those of the program presented in Appendix B, that is, the optimisation loop gives the optimised values for the selected parameters, while the output of the replication loop consists of the objective function's estimates at various values of the parameters. Note that now, besides the adsorption parameters ($k_{F,i}$, N_i and the IPA factor), there is an extra parameter, the hydrodynamic dispersion coefficient (D).

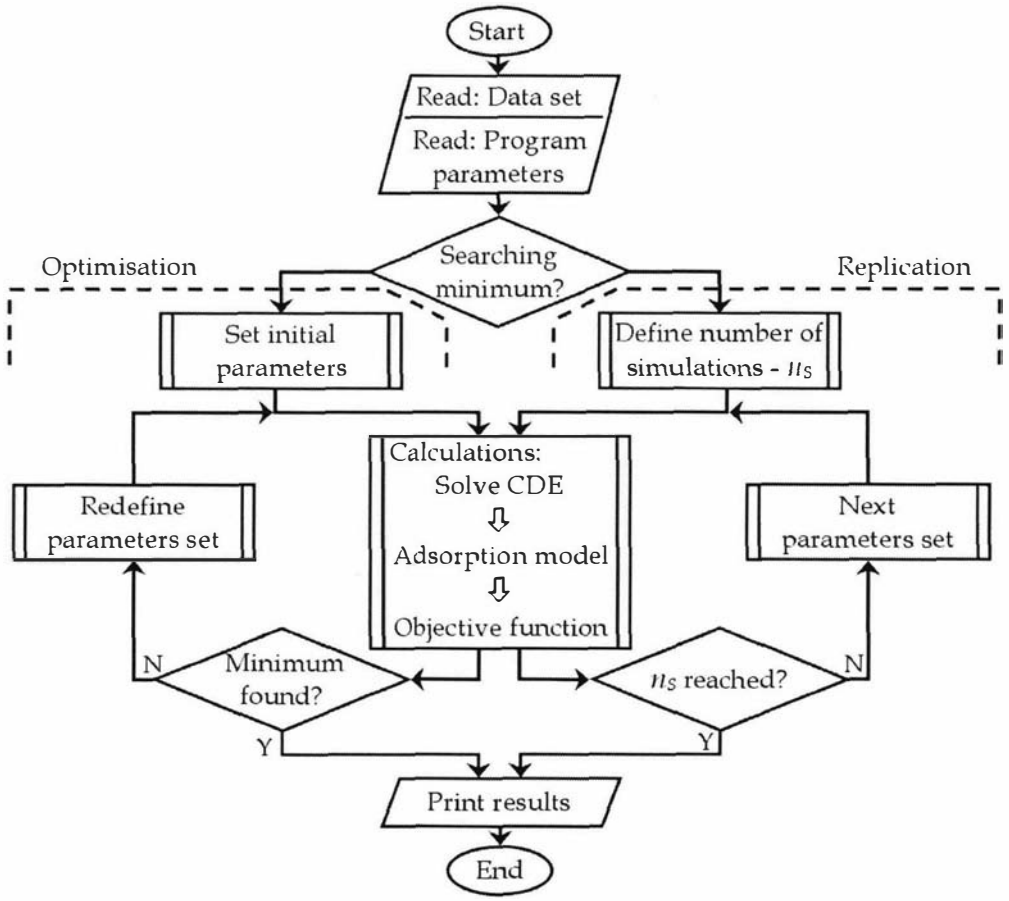


Figure C.1. Flowchart with the basic algorithm for the evaluation of BTCs using the adsorption model with IPA.

Another difference between this program and that of Appendix B refers to the evaluation of the agreement between the model's predictions and the observed data set. Here, because of the type data measured, only one type of objective function is used. This function is going to be presented later.

These differences in the input definitions for the program can be seen in the user's interface (Figure C.2).

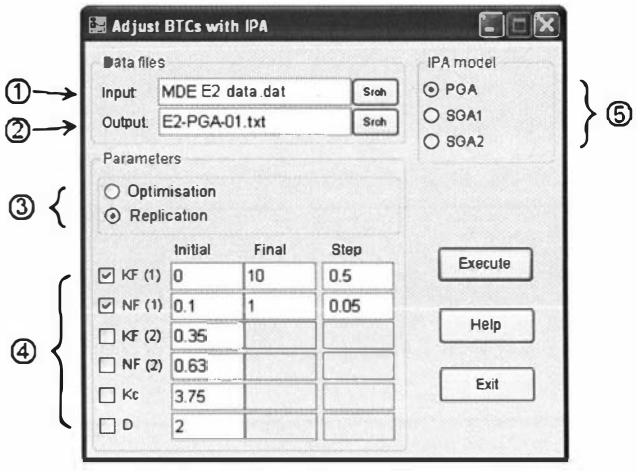


Figure C.2. User interface of the VisualBasic program built for the evaluation of BTCs using the adsorption model with IPA.

The description of the numbered fields in Figure C.2 follows:

① The file with the observed miscible displacement data;

② The file where the output is to be saved;

③ Selection of the type of parameter variation: optimisation or replication. The output values are defined accordingly to this choice, as stated before;

④ Selection of the initial values for the adsorption parameters. In the checkbox the parameters which are to be varied can be selected. If optimisation variation was selected before, here the initial value and the initial variation step are entered for the parameters to optimise. Whereas if replication was set, here the initial and final values, as well as the variation step are defined;

⑤ Selection of the proposed IPA approach to be used for solving the adsorption model;

The data set to be read consists of measurements of the sulphate and calcium concentrations in the outflow solution over the time. These

measurements are referenced to time by the number of leached water filled pore volumes (PV). An estimate of the measurements variance is also read. Note that these estimates were not available for the data set presented in this thesis. For modelling the solute movement the CDE model is used, with the assumption of a constant water flux density (q_w). This imply in a constant soil water content (θ), and therefore in a single value for the water-to-soil ratio (ϑ).

The loop routines are not going to be shown here, since they are essentially the same as presented in Appendix B. The additional parameter (D) is set as the sixth value to be optimised or replicated.

C.2. Routine for evaluating the objective function

The agreement between observed and modelled data is evaluated by the objective function (Φ). This function summarises the comparisons done for each pair of observed values, that is, the concentrations of sulphate and calcium. The general expression is given by:

$$\Phi = \sum_{i=1}^{2} \sum_{j=1}^{n_D} \frac{1}{\sigma_i^2} \left(C_{e,i,j} - \hat{C}_{e,i,j} \right)^2 \qquad [C.1]$$

where $C_{e,i,j}$ and $\hat{C}_{e,i,j}$ represent the observed and the predicted data for the j observation (a measurement of the outflow concentration) of the solute i, and σ_i^2 is the variance of the observed data.

The objective function, differently from Appendix B, is evaluated only after all the predicted data has been computed. Despite this difference the routine is called by any of the two loops and gives the output in an identical way. The flowchart with the basic algorithm of this routine is shown in Figure C.3.

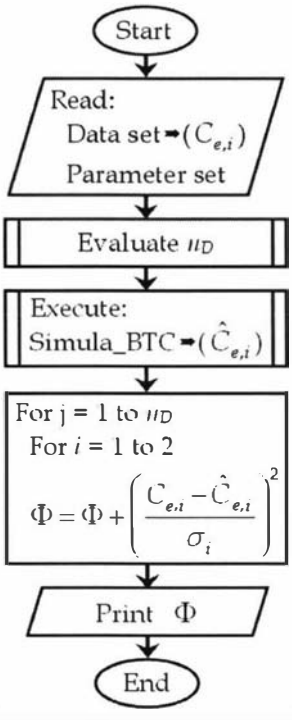


Figure C.3. Flowchart with the basic algorithm for the evaluation of the agreement between predicted and observed BTCs by means of the objective function (Φ).

C.3. Routine for solving the solute movement – Simula_BTC

This is the main routine in this program. It simulates the solute movement through a soil column employing the CDE approach coupled with the adsorption model with IPA. Basic physic-chemical parameters that define the column are given within the file with the observed data set. Only the adsorption model parameters plus D are set in the interface.

For the simulation of the solute movement a soil column is discretised. This column, with length L (m), is divided in n_L layers of thickness dz (m) as shown if Figure C.4. A numerical solution of the CDE is implemented using this schematic.

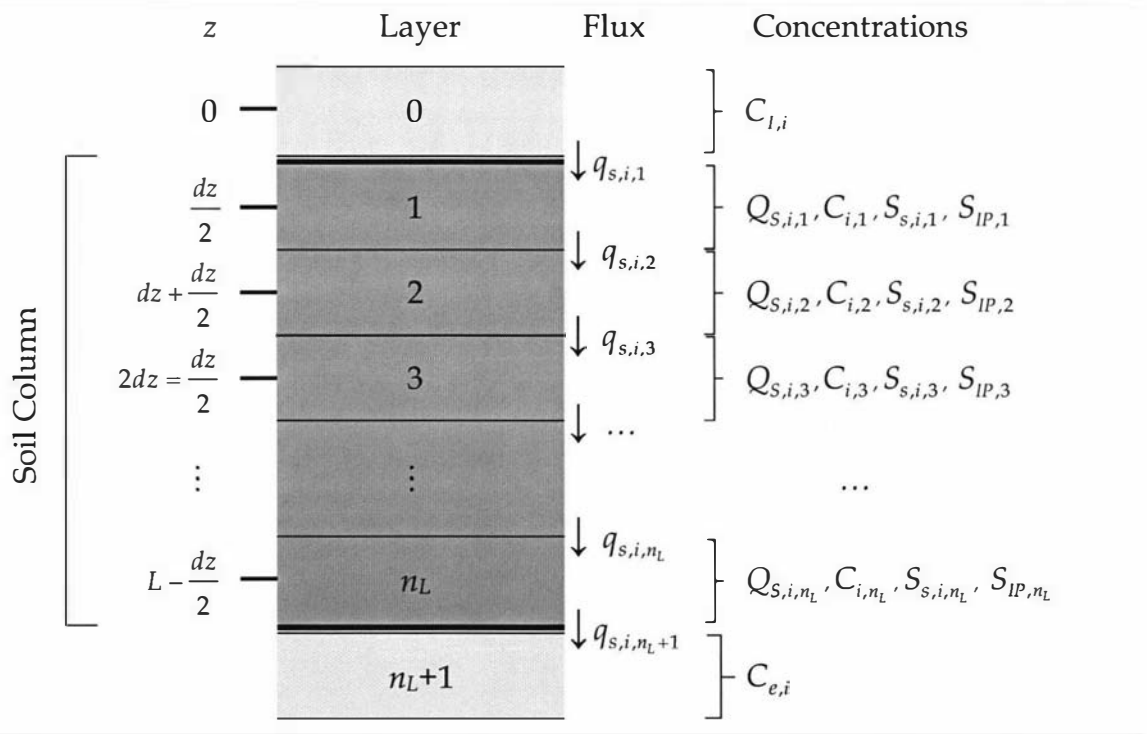


Figure C.4. Schematic of the discretisation of the soil column for the numerical calculations.

Initially the soil is considered to have a constant solute concentration, $C_{0,i}$ (mmol L^{-1}), for each solute. At $z = 0$, in the top of the column, the input solution, with concentration $C_{I,i}$ (mmol L^{-1}), is applied in unsaturated condition and at constant rate, q_w (mm s^{-1}). For each layer the total solute concentration, $Q_{S,i}$ (mmol kg^{-1}) is evaluated considering the solute flow, $q_{s,i}$ (mmol m^{-2} s^{-1}), at the upper and bottom boundaries. The values of $Q_{S,i}$ for each solute is then sent to the partition routine which resolves the values of C_i, $S_{s,i}$ and S_{IP}. The flowchart for this calculation is shown in Figure C.5.

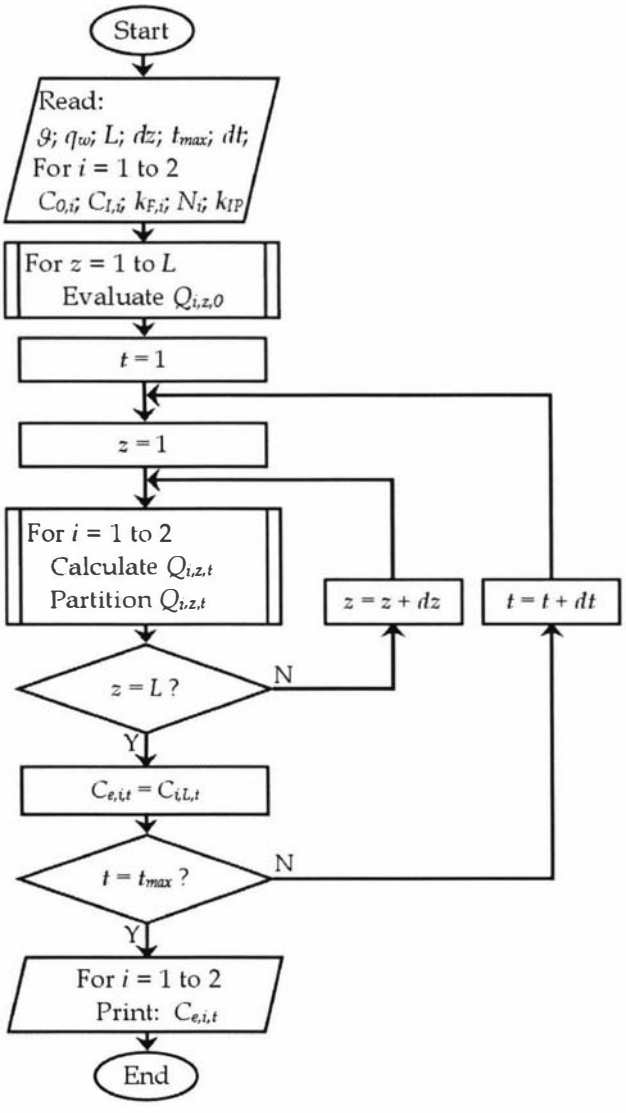


Figure C.5. Flowchart of the Simula_BTC routine, used for solving the solute movement in a soil column using CDE approach coupled with the adsorption model with IPA.

For a given solute, its flux density, using the convective-dispersive approach, can be computed by:

$$q_s = \vartheta D \frac{\partial C}{\partial z} - \frac{q_w}{\rho} C \qquad [C.2]$$

Applying Equation [C.3] to the mass conservation principle, the variation of the solute concentration in a given position in the soil can be defined by:

$$\frac{\partial Q_S}{\partial t} = \vartheta D \frac{\partial^2 C}{\partial z^2} - \frac{q_w}{\rho} \frac{\partial C}{\partial z} \qquad [C.3]$$

This is the CDE expression used to solve the solute movement for each of the two ions being considered, sulphate and calcium. Equation [C.3] is solved numerically in an explicit finite difference model (FDM), with central differences. The numeric expression for finding the values of the solute concentration, following the discretisation showed in Figure C.4 and Equation [C.3], is given by:

$$Q_{S,i,z,t} = Q_{S,i,z,t-1} + \frac{dt}{2}\left(\vartheta D \frac{C^2_{i,z+1,t-1} - 2C_{i,z,t-1} + C^2_{i,z-1,t-1}}{2dz^2} - \frac{q_w}{\rho} \frac{C_{i,z+1,t-1} - C_{i,z-1,t-1}}{dz} \right) \qquad [C.4]$$

The values of $C_{i,z,t}$ are then found using the partition routine as presented in Appendix B. The value of $C_{e,i,t}$ is computed assuming that no diffusion occurs at the bottom of the soil column.

APPENDIX D

D. The Newton-Raphson method

D.1. Introduction

The Newton-Raphson is an iterative procedure used in numerical analysis to find the root (zero) of a given function. Providing the function has only one root in the vicinity of the initial guess, the method converges very efficiently, with its precision increasing quadratically at each iteration (Hamming, 1973; Press *et al.*, 2002). The root of a function is the value of the independent variable which makes the function equal to zero. This method is used to solve many other numerical problems, such as finding the maximum or minimum of functions. This versatility makes it one of the most used optimisation algorithms.

This method was developed by Isaac Newton and Joseph Raphson in the 17th century, generalising older ideas for finding square root of numbers. It can also be seen as a first order approximation of the Taylor's series (Press *et al.*, 2002). Its concept can be easily understood for a simple equation of one independent variable, as will be shown below. However, it can be generalised to any other number of variables, although its solving procedure becomes increasingly complex. The generalised formulation is presented after the simple one-variable problem, and the solution for the 3D problem (with two variables) is further developed, as it is used to solve the adsorption model proposed in this thesis.

D.2. Method description with one variable

Let's consider a function ($F(x)$), for which the root is going to be found. Starting with an initial guess (x_0), the tangent at this point is found using the functions derivative. Then the zero of the tangent is found by elementary algebra, this value (x_1) is a better approximation for the function's root (Figure D.1). One can then use this new value to find another approximation. For an iteration j, the Newton-Raphson's method can be expressed by the equation:

$$x_{j+1} = x_j - F(x_j)\left(\frac{\partial F(x_j)}{\partial x}\right)^{-1} \qquad [D.1]$$

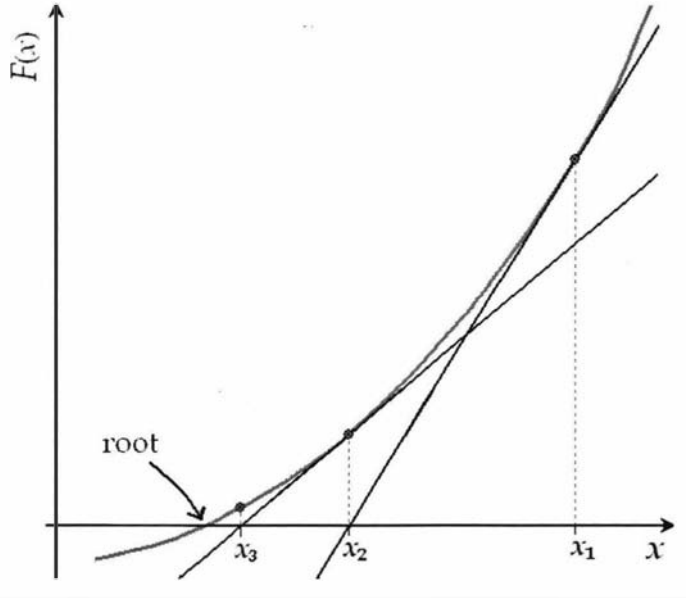


Figure D.1. Graph showing two iterations for finding the root of the function $F(x)$ using the Newton-Raphson method. The approximations start at x_1.

This process could continue infinitely until the true root would be found. The iterative procedure, however, goes only until the improvement in the approximation is smaller than a certain limit (E_{limit}), that is:

$$\left|x_{j+1} - x_j\right| < E_{limit} \qquad [D.2]$$

To use the Newton-Raphson method several aspects of the function need to be known. First it is necessary that the function is differentiable, because its derivative is used to find the approximations of the root. Approximations of the tangent using two points, also known as the secant method, may be used is some cases where the derivative is not available. Also, should the function have a root, its value should be roughly known. That is, to ensure convergence the iterative procedure should start close to the real root. This is more important the more complex the function is. When using this method for optimisation, commonly set as to find the maximum or minimum of the function (which means find the zero of its derivative), care must be taken with multiplicity of solutions. If the function has more than one minimum (or maximum) the Newton-Raphson will converge to the nearer local minimum, which may not be the absolute one. Hence the importance of having a good initial guess.

D.3. Newton-Raphson method for two variables

The same concept presented above is used to extend the Newton-Raphson method to solve equations in R^n, although in this case the handling of the tangent is more complex. Also, because the bigger the number of variables the more complex the function tends to be. This might mean having more difficulties for finding the function's derivatives and also a larger likelihood of having local minimums, therefore increasing the chances of not reaching the real solution. Still the method converges quickly if the initial guess is good.

The generalised equation for the Newton-Raphson method is given by (Press *et al.*, 2002):

$$x_{j+1} = x_j - \nabla F(x_j)\mathbf{H}^{-1}_{F(x_j)} \qquad [D.3]$$

where $\nabla F(x_j)$ is the gradient and $\mathbf{H}^{-1}_{F(x_j)}$ is the inverse of the Hessian matrix of F at x_j. The gradient of a function is the vector describing the line with largest

slope in the derivative surface. The Hessian matrix is a quadratic matrix containing the function's partial derivatives. Here a simpler presentation of Equation [D.3] will be given considering only two independent variables.

Let's consider a 3D function ($G(x,y)$), of which the values of x and y where G is equal to zero we want to find. Having (x_j,y_j) as the initial guess, the next approximation for the root can be found by:

$$\left(x_{j+1},y_{j+1}\right)=\left(x_j,y_j\right)-\frac{G(x_j,y_j)\mathbf{U}_j}{\nabla G(x_j,y_j)\cdot\mathbf{U}_j} \qquad [D.4]$$

where $\nabla G(x_j,y_j)$ is the gradient of G at (x_j,y_j), and $\mathbf{U}_j$ is the unit vector in the direction of the gradient of G. $\nabla G(x_j,y_j)$ is made up by the two partial derivatives of G:

$$\nabla G(x_j,y_j)=\left(\frac{\partial G(x_j,y_j)}{\partial x},\frac{\partial G(x_j,y_j)}{\partial y}\right) \qquad [D.5]$$

The unit vector is then given by:

$$\mathbf{U}_j=\frac{\nabla G(x_j,y_j)}{L_{0,j}} \qquad [D.6]$$

where $L_{0,j}$ is the length of the gradient at (x_j,y_j), calculated by:

$$L_{0,j}^2=\left(\frac{\partial G(x_j,y_j)}{\partial x}\right)^2+\left(\frac{\partial G(x_j,y_j)}{\partial y}\right)^2 \qquad [D.7]$$

The dot product in Equation [D.4] can be developed as

$$\nabla G(x_j,y_j)\cdot\mathbf{U}_j=\left(\frac{\partial G(x_j,y_j)}{\partial x},\frac{\partial G(x_j,y_j)}{\partial y}\right)\cdot\left(\frac{\partial G(x_j,y_j)}{L_{0,j}\partial x},\frac{\partial G(x_j,y_j)}{L_{0,j}\partial y}\right) \qquad [D.8]$$

$$\nabla G(x_j,y_j)\cdot\mathbf{U}_j=\frac{1}{L_{0,j}}\left[\left(\frac{\partial G(x_j,y_j)}{\partial x}\right)^2+\left(\frac{\partial G(x_j,y_j)}{\partial y}\right)^2\right] \qquad [D.9]$$

$$\nabla G(x_j,y_j)\cdot\mathbf{U}_j=L_{0,j} \qquad [D.10]$$

Therefore, Equation [D.4] becomes:

$$\left(x_{j+1}, y_{j+1}\right) = \left(x_j, y_j\right) - \frac{G(x_j, y_j)\mathbf{U}_j}{L_{0,j}} \qquad [D.11]$$

Considering this equation for only one of the variables, say x:

$$x_{j+1} = x_j - \frac{G(x_j, y_j)\mathbf{U}_{j,x}}{L_{0,j}} \qquad [D.12]$$

This can be developed:

$$x_{j+1} = x_j - \frac{G(x_j, y_j)\dfrac{\partial G(x_j, y_j)}{L_{0,j}\partial x}}{L_{0,j}} \qquad [D.13]$$

$$x_{j+1} = x_j - \frac{G(x_j, y_j)\dfrac{\partial G(x_j, y_j)}{\partial x}}{L_0^2} \qquad [D.14]$$

Which yields the expression for finding the next approximation of x:

$$x_{j+1} = x_j - \frac{G(x_j, y_j)\dfrac{\partial G(x_j, y_j)}{\partial x}}{\left(\dfrac{\partial G(x_j, y_j)}{\partial x}\right)^2 + \left(\dfrac{\partial G(x_j, y_j)}{\partial y}\right)^2} \qquad [D.15]$$

And analogously for y:

$$y_{j+1} = y_j - \frac{G(x_j, y_j)\dfrac{\partial G(x_j, y_j)}{\partial y}}{\left(\dfrac{\partial G(x_j, y_j)}{\partial x}\right)^2 + \left(\dfrac{\partial G(x_j, y_j)}{\partial y}\right)^2} \qquad [D.16]$$

Thus to build a routine for solving the Newton-Raphson method in 3D, the requisites are: the function, its two partial derivatives, and a good initial guess for both variables.